FRONTIERS IN BEHAVIORAL NEUROSCIENCE - EDITOR'S PICK 2021

EDITED BY: Nuno Sousa
PUBLISHED IN: Frontiers in Behavioral Neuroscience

frontiers Research Topics

frontiers

ISSN 1664-8714
ISBN 978-2-88971-056-0
DOI 10.3389/978-2-88971-056-0

About Frontiers

Frontiers is more than just an open-access publisher of scholarly articles: it is a pioneering approach to the world of academia, radically improving the way scholarly research is managed. The grand vision of Frontiers is a world where all people have an equal opportunity to seek, share and generate knowledge. Frontiers provides immediate and permanent online open access to all its publications, but this alone is not enough to realize our grand goals.

Frontiers Journal Series

The Frontiers Journal Series is a multi-tier and interdisciplinary set of open-access, online journals, promising a paradigm shift from the current review, selection and dissemination processes in academic publishing. All Frontiers journals are driven by researchers for researchers; therefore, they constitute a service to the scholarly community. At the same time, the Frontiers Journal Series operates on a revolutionary invention, the tiered publishing system, initially addressing specific communities of scholars, and gradually climbing up to broader public understanding, thus serving the interests of the lay society, too.

Dedication to Quality

Each Frontiers article is a landmark of the highest quality, thanks to genuinely collaborative interactions between authors and review editors, who include some of the world's best academicians. Research must be certified by peers before entering a stream of knowledge that may eventually reach the public - and shape society; therefore, Frontiers only applies the most rigorous and unbiased reviews.
Frontiers revolutionizes research publishing by freely delivering the most outstanding research, evaluated with no bias from both the academic and social point of view. By applying the most advanced information technologies, Frontiers is catapulting scholarly publishing into a new generation.

What are Frontiers Research Topics?

Frontiers Research Topics are very popular trademarks of the Frontiers Journals Series: they are collections of at least ten articles, all centered on a particular subject. With their unique mix of varied contributions from Original Research to Review Articles, Frontiers Research Topics unify the most influential researchers, the latest key findings and historical advances in a hot research area! Find out more on how to host your own Frontiers Research Topic or contribute to one as an author by contacting the Frontiers Editorial Office: frontiersin.org/about/contact

FRONTIERS IN BEHAVIORAL NEUROSCIENCE - EDITOR'S PICK 2021

Topic Editor:
Nuno Sousa, University of Minho, Portugal

Citation: Sousa, N., ed. (2021). Frontiers in Behavioral Neuroscience - Editor's Pick 2021. Lausanne: Frontiers Media SA. doi: 10.3389/978-2-88971-056-0

Table of Contents

frontiers in Behavioral Neuroscience

ORIGINAL RESEARCH
published: 19 March 2019
doi: 10.3389/fnbeh.2019.00052

Affiliation, Aggression, and Selectivity of Peer Relationships in Meadow and Prairie Voles

Nicole S. Lee[1], Nastacia L. Goodwin[2], Katherine E. Freitas[3] and Annaliese K. Beery[1,2,3]**

[1]Neuroscience and Behavior Program, University of Massachusetts, Amherst, MA, United States, [2]Department of Psychology, Smith College, Northampton, MA, United States, [3]Neuroscience Program, Smith College, Northampton, MA, United States

Relationships between adult peers are central to the structure of social groups. In some species, selective preferences for specific peers provide a foundation for consistent group composition. These preferences may be shaped by affiliation toward familiar individuals, and/or by aversion to unfamiliar individuals. We compared peer interactions in two vole species that form selective preferences for familiar same-sex individuals but differ in mating system. Prairie voles (*Microtus ochrogaster*) form pair bonds with mates and may reside in family groups. Meadow voles (*Microtus pennsylvanicus*) are promiscuous breeders that form communal winter groups in the wild, and exhibit greater social behavior in short day (SD) lengths in the laboratory. We characterized affiliative, anxiety-like, and aggressive interactions with familiar and novel same-sex conspecifics in meadow and prairie voles housed in summer- or winter-like photoperiods. Species differences in affective behaviors were pronounced, with prairie voles exhibiting more aggressive behavior and less anxiety-like behavior relative to meadow voles. Meadow voles housed in short (vs. long) day lengths were more affiliative and more interactive with strangers; prosocial behavior was also facilitated by a history of social housing. Prairie voles exhibited partner preferences regardless of sex or day length, indicating that selective peer preferences are the norm in prairie voles. Prairie vole females formed preferences for new same-sex social partners following re-pairing; males were often aggressive upon re-pairing. These data suggest that preferences for familiar peers in prairie voles are maintained in part by aggression toward unfamiliar individuals, as in mate partnerships. In contrast, social tolerance is an important feature of meadow vole peer affiliation, demonstrated by low aggression toward unfamiliar conspecifics, and consistent with field data on winter tolerance.

Keywords: meadow vole, prairie vole, social behavior, affiliation, aggression, partner preference

Edited by:
Etsuro Ito,
Waseda University, Japan

Reviewed by:
Karen Lisa Bales,
University of California, Davis, United States
Nancy G. Solomon,
Miami University, United States

****Correspondence:***
Nicole S. Lee
nlee@umass.edu
Annaliese K. Beery
abeery@smith.edu

Received: *08 January 2019*
Accepted: *04 March 2019*
Published: *19 March 2019*

Citation:
Lee NS, Goodwin NL, Freitas KE and Beery AK (2019) Affiliation, Aggression, and Selectivity of Peer Relationships in Meadow and Prairie Voles. Front. Behav. Neurosci. 13:52. doi: 10.3389/fnbeh.2019.00052

INTRODUCTION

Relationships between non-mate group members are the foundation of social groups for many mammals, from same-sex bachelor herds and multi-female breeding groups to mixed-sex winter huddling groups in reproductively quiescent voles (Clutton-Brock, 2016; Smith et al., 2017; Lee and Beery, 2019). Numerous studies have provided insight into pathways involved in reproductive

relationships—such as between a mother and her offspring, or between socially monogamous mates—but these pathways may or may not generalize to non-reproductive relationships between adult peers. Peer relationships themselves are not all the same. For example, they may be selective or non-selective (Lee, 1994), transient or enduring (Lidicker and Patton, 1987), and motivated or not motivated (Goodwin et al., 2018). We sought to characterize and compare the contributions of affiliation, anxiety, and aggression to selective relationships between peers, using monogamous and promiscuous vole species that both form partner preferences for a familiar same-sex peer. These studies provide a foundation for the comparison of reproductive and non-reproductive social preferences, and inform our understanding of factors shaping peer relationships.

The meadow vole (*Microtus pennsylvanicus*) is a promiscuous, uniparental vole species (Getz, 1972; Boonstra et al., 1993) that has been studied for its seasonal peer relationships (reviewed in Beery, 2019). In the summer reproductive season, meadow voles are intolerant of other individuals: females defend distinct territories, while males roam across multiple female territories. In the winter non-breeding season, meadow voles form social groups. They exhibit shared home ranges, nest with conspecifics, and are highly tolerant of one another (Madison, 1980; McShea and Madison, 1984; Ferkin and Seamon, 1987; Madison and McShea, 1987). In laboratory settings, meadow voles form selective, long-lasting preferences for known peers, demonstrated in the partner preference test (PPT)—in which animals can choose to spend time with a familiar or unfamiliar conspecific (Parker and Lee, 2003; Beery et al., 2008; Ondrasek et al., 2015). Laboratory manipulation of photoperiod from summer-like long days (LDs) to winter-like short days (SDs) drives variation in multiple social behaviors in parallel to seasonal variations in the field (Ferkin and Seamon, 1987; Ferkin and Gorman, 1992; Beery et al., 2008; Ondrasek et al., 2015).

The closely related but socially monogamous prairie vole (*Microtus ochrogaster*) has been an important study organism for research on parental behavior and pair bonding between mates (Carter, 2017; Gobrogge et al., 2017; Walum and Young, 2018). Unlike meadow voles, prairie voles in the wild form selective, long-lasting mate relationships and provide bi-parental care. From late autumn and through winter, prairie voles also display an increase in communal groups (extended family groups with unrelated adults) due to decreased dispersion by philopatric young, despite territoriality and largely exclusive male-female pairs at other times (Getz et al., 1993; Getz and Carter, 1996). Therefore, adult-adult same-sex cohabitation occurs in both species of voles under natural conditions.

In the two studies to date that assessed peer (same-sex) partner preferences in prairie voles, LD-housed prairie voles—like meadow voles—displayed partner preferences for a same-sex partner after 24 h of cohabitation (DeVries et al., 1997; Beery et al., 2018). Other studies of peer affiliation in female prairie voles have provided evidence that these peer relationships constitute social attachments by examining the effects of separation on anxiety- and depressive-like behaviors, as well as social buffering. Socially isolated female prairie voles displayed increased anxiety- and depressive-like behaviors compared to voles housed with same-sex siblings (Grippo et al., 2008). Isolation also caused neuroendocrine disturbances, changes in adult neurogenesis, and autonomic regulation of the heart (Grippo et al., 2007a,b). Furthermore, adult neurogenesis and autonomic regulation of the heart differed between socially isolated female prairie voles and voles housed with an unfamiliar female (Fowler et al., 2002; Grippo et al., 2007c). Social interactions may also buffer the experience of exogenous stressors, with male and female prairie voles displaying increased grooming of same-sex cage-mates that had undergone a stressor (Burkett et al., 2016).

The selectivity of peer relationships demonstrated in PPTs may arise from prosocial factors favoring a familiar partner, antisocial factors disfavoring unfamiliar individuals, or both. Aggression toward non-mate conspecifics is an important factor in the maintenance of pair bonds between mated prairie voles (Resendez et al., 2016), and may also play a role in shaping the specificity of affiliative peer relationships. For instance, female prairie voles become more aggressive toward other females after 8 days of cohabitation with a male, as well as during pregnancy (Bowler et al., 2002). Trios consisting of two females and a male exhibit higher female-female huddling when the two females are siblings, but higher aggression when the two females are unrelated (Firestone et al., 1991). Furthermore, both male and female prairie voles become more aggressive toward same-sex strangers after mating (Young et al., 2011). In males, upregulation of dopamine D1-like receptors in the nucleus accumbens corresponds with pair bond maintenance—specifically, with aggression toward unfamiliar females (Aragona et al., 2006). Blocking these receptors also reduced the aggressive behavior. Thus, both affiliative and aggressive interactions mediate important aspects of the social organization of prairie voles, and may shape peer interactions.

We compared characteristics of peer social relationships within and across monogamous and promiscuous vole species, focusing on affiliative, aggressive, and anxiety-like behaviors. Prior studies have demonstrated the presence of same-sex partner preferences in meadow and prairie voles, existence of sex and day length differences in meadow vole peer partner preferences, and sex differences in prairie vole peer partner preferences in LDs (DeVries et al., 1997; Beery et al., 2008, 2009; Ondrasek et al., 2015). We asked: (1) whether there are species differences (prairie vs. meadow) in affiliation and aggression toward an unfamiliar same-sex peer, or in anxiety-related behaviors (study 1a); (2) whether meadow voles exhibit photoperiodic changes in aggressive behavior related to changing seasonal social tolerance (study 1b); and (3) whether partner preferences in prairie voles are modulated by day length, as in meadow voles, and whether they can form preferences for new peer partners following separation and re-pairing (study 2). For several of these questions we had no basis for predicting a specific outcome, but based on prior work in male prairie and meadow voles, we hypothesized that female prairie voles would be less anxious than meadow voles (Stowe et al., 2005). We also expected that there would be more intraspecific aggression in meadow voles, based on data from an interspecific comparison

of voles trapped in Illinois and Michigan (Getz, 1972). Finally, we predicted that SD-housed meadow voles would likely be less aggressive than LD-housed meadow voles, consistent with increased sociality in short photoperiods and winter field conditions. We relate differences in prairie and meadow vole aggression and anxiety to differences in peer affiliation. This study lays the behavioral foundations necessary for comparative work on mechanisms underlying social behaviors in meadow and prairie voles.

MATERIALS AND METHODS

Animal Subjects

Prairie and meadow voles were bred locally at Smith College as described in Goodwin et al. (2018). Animals were group weaned at 19 ± 1 days (meadow voles) or 21 ± 1 days (prairie voles), then separated to pair-housing with either a same-sex sibling or an age-matched same-sex non-sibling (about half to each type of pairing) within 1 week. One meadow vole group was weaned into solo-housing. Voles were maintained on a LD light cycle (14 h light; 03:00–17:00 EST) or transferred to a SD light cycle (10 h light; 07:00–17:00 EST) at weaning. Voles were housed in clear plastic cages (45 × 25 × 15 cm) with aspen bedding (Envigo TekLab), nesting material (Lab Supply Enviro-dri and a nestlet), and a PVC hiding tube. Rooms were maintained at approximately 20°C, and food (Labdiet Mouse Chow 5015 for meadow voles, and 5015 mixed with Rabbit Chow 5326 for prairie voles) and water were available *ad libitum* with every-other-day supplementation of apple or carrot.

Voles were 80 ± 7 days of age at the start of testing. This study was carried out in accordance with the recommendations in the Guide for the Care and Use of Laboratory Animals published by the National Research Council. The protocol was approved by the Institutional Animal Care and Use Committee at Smith College.

Experimental Design

Study 1a: Species Differences in Novel Social Interactions, Aggression, and Anxiety

Focal voles were tested for affiliative, aggressive, and anxiety-like behaviors. Subjects were pair-housed SD meadow vole females (n = 19), and pair-housed SD prairie vole females (n = 17). At 80 ± 7 days of age, focal voles were tested for aggressive and affiliative behaviors in a social interaction test in a neutral arena with an unrelated, same-sex, novel stranger. One week later, focal voles underwent open field tests and light-dark box tests (OFTs and LDB, respectively) on consecutive days.

Study 1b: Effects of Day Length and Social History in Meadow Voles

Pair-housed SD meadow vole females from Study 1a were also compared to pair-housed LD meadow vole females (n = 19), and solo-housed SD meadow vole females (n = 16), in the social interaction test. The solo-housed LD meadow vole female group was solo-housed from weaning. At 80 ± 7 days of age, focal voles were tested for aggressive and affiliative behaviors in a social interaction test in a neutral arena with an unrelated, same-sex, novel stranger.

Study 2: Formation and Reformation of Peer Partner Preferences in Prairie Voles

A separate cohort of voles was tested for the strength of preferences for familiar same-sex social partners after cohabitation with a partner from weaning (PPT 1). A subset was re-paired with a new partner in adulthood and tested after 24 h (PPT 2).

PPT 1: subjects were pair-housed SD prairie vole males (n = 13), SD prairie vole females (n = 11), and LD prairie vole females (n = 14). At 80 ± 7 days of age, focal voles were tested for partner preference for their cage-mate since weaning, as described below. The ability to form new same-sex partner preferences in adulthood was assessed in PPT 2: eight subjects from each group were separated from their partners 24 h after PPT 1. Voles were housed alone for 8 days, after which they were cohoused with novel, unrelated, same-sex partners. Focal voles underwent partner preference testing after 24 h of cohabitation with these new partners. The male sub-group was stopped early because of a high rate of aggression upon re-pairing, and is not included in the formal analysis.

Behavioral Testing

Partner Preference Test

Peer partner preference testing was conducted in a rectangular plastic apparatus consisting of three equal-sized compartments arranged linearly (75 × 20 × 30 cm), as previously described (Anacker et al., 2016a,b; Beery et al., 2018). The cage-mate of the focal vole (the partner) was tethered at one end of the apparatus, and an age-matched, unrelated, same-sex novel vole (the stranger) was tethered at the other end. Strangers were pair-housed from weaning, and were used no more than three times over the course of Study 2. The focal vole was placed in the center chamber and allowed to move freely for the duration of the 180-min test. Tests were video recorded, and trained observers used custom software (Intervole Timer1.6.pl, AKB) to quantify the amount of time focal voles spent huddling (side-by-side or one on top of the other), duration in each chamber, and number of times the focal vole crossed between chambers. Partner preference in a group was defined as significantly more time huddling with the partner than the stranger; partner preferences in individuals were defined as twice as much huddling with the partner as with the stranger, as in prior studies (Insel et al., 1995; Beery et al., 2009). Scorers were blind to subject groups and position of the partner/stranger.

Aggression/Social Interaction Test

Interactions with an unfamiliar vole were assessed in a neutral arena. For voles, prior research has suggested that aggression is as high in a neutral arena as in home-cage tests (i.e., resident-intruder tests; Harper and Batzli, 1997). The focal vole was placed in a new cage and allowed to acclimate for 10 min. An unrelated, unfamiliar stranger of matched species, sex, day length, and housing condition was marked for identification, then introduced into the cage. The test was recorded for 10 min, or was terminated early after three significant bouts of aggression. All voles were assessed for latency to attack; a latency of 10 min (the full test duration) was recorded for voles

that never attacked. Tests were scored by an observer blind to subject condition, using JWatcher 0.9 (University of California, Los Angeles and Macquarie University, Sydney) to measure the frequency and duration of behaviors, and latency to behaviors. Aggressive behaviors quantified included lateral attack/threat, upright (boxing), chasing, and clinch (as in Koolhaas et al., 2013). Clinch refers to a behavior in which the voles scuffle but are not upright, and one vole is on the bottom belly up. Social and investigative behaviors included sniffing and social exploration, grooming, and huddling. Test scoring focused on the behavior of the focal vole.

Behavior in the meadow vole groups was quantified across the full 10-min test interval. Most prairie vole pairs reached the criterion for early separation, so for species comparisons of detailed behavior (study 1a), the first 1 min 51 s of testing were used—the longest interval that could be compared across all subjects.

Open Field/Light-Dark Box Tests

Animals were placed at the edge of the OFT and the dark portions of the LDB test, and filmed for 5 min from above. The OFT consists of a circular open arena (42 cm diameter). Behaviors assessed included time in the center of the OFT arena (≥7 cm from the edge), distance traveled, and the number of fecal boli deposited. The LDB (49 × 20.5 × 19.5 cm) consists of a black Plexiglas box attached to a clear lidless Plexiglas box. Behaviors assessed included time in the light portion of the LDB, and latency to emerge into the light.

Data Analysis

Differences between species were assessed with Student's *t*-test (study 1a). Differences between multiple groups were assessed by one-way ANOVA (study 1b and 2). Significant ANOVAs were followed by two pair-wise comparisons between groups differing in one variable (study 1b: day length or housing; study 2: species or day length) using Fisher's PLSD for normally distributed data, or Wilcoxon rank sum tests for pair-wise comparisons on data that violated normality, assessed with Shapiro-Wilk W tests. Wilcoxon matched-pairs signed rank tests were used for within-group comparisons of partner vs. stranger huddling.

Statistical analyses were performed in JMP 8.0 (SAS, Inc.) or GraphPad Prism 7. All tests were two-tailed. Results were deemed significant at $p < 0.05$.

RESULTS

Study 1a: Species Differences

Species Differences in Stranger-Directed Interactions

In social interaction tests, SD prairie vole females exhibited aggression sooner and at higher levels than SD meadow vole females. They showed significantly shorter latencies to first (**Figure 1A**), second, and third attacks compared to SD meadow vole females ($t_{(34)} = -5.15$ for first attack, $t_{(34)} = -6.72$ for second attack, $t_{(34)} = -7.91$ for third attack, $p < 0.0001$ for

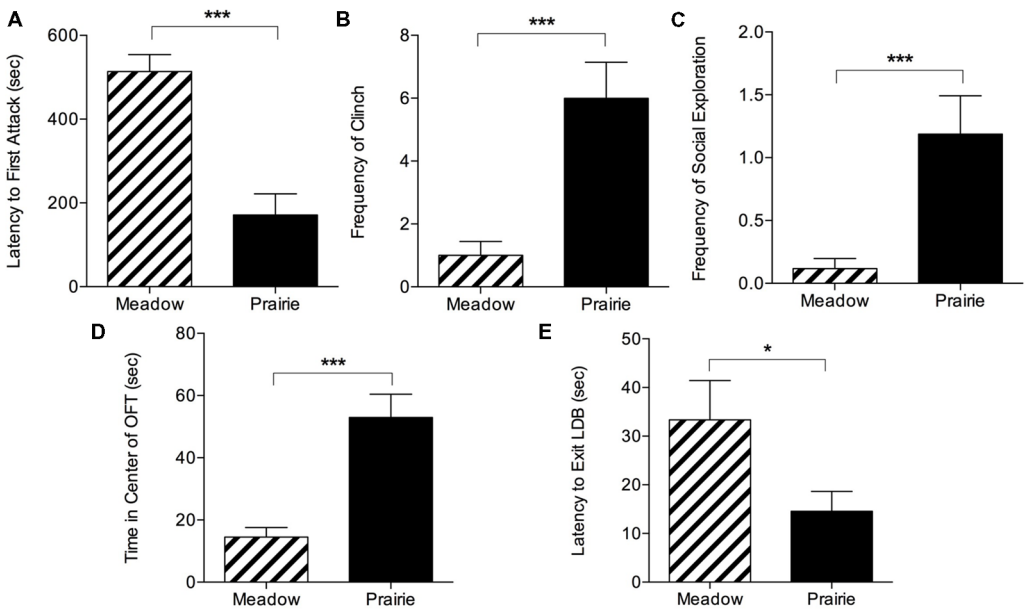

FIGURE 1 | Species differences in behavior during social interaction and anxiety tests. Top panel: in 10-min social interaction tests with a novel conspecific, prairie voles exhibited substantial aggression leading to early test termination. **(A)** Prairie voles showed significantly shorter latency to first attack than meadow voles. Voles who did not attack were given a latency of 600 s. Species comparisons in **(B,C)** were conducted on the maximum interval that included all subjects (~2 min). **(B)** Short day (SD) prairie vole females showed significantly higher frequency of clinch than SD meadow vole females. **(C)** Prairie voles showed significantly higher social exploration than meadow voles. Bottom panel: voles underwent open field tests (OFTs) and light-dark box (LDB) tests. **(D)** OFT: prairie voles spent significantly more time in the center of the open field arena than meadow voles housed in the same day length. **(E)** LDB: prairie voles exited the LDB sooner than meadow voles. $^{*}p < 0.05$, $^{***}p < 0.0005$.

all). Tests were terminated early significantly more often with prairie voles than meadow voles (12/20 vs. 4/56, $p < 0.0001$, Fisher's exact test). Because early termination led to uneven test durations, species differences in specific behaviors were assessed using the first 1:51 min of testing, the longest duration that included all tests regardless of whether they were terminated early. Within this time period, SD prairie females exhibited higher frequency of clinch ($t_{(34)} = 5.04$, $p < 0.0001$) and social exploration ($t_{(34)} = 3.90$, $p < 0.001$) compared to SD meadow females (**Figures 1B,C**).

Species Differences in Anxiety-Like Behaviors

Prairie voles exhibited less anxiety-like behavior in the OFT and LDB (**Figures 1D,E**). In the OFT, prairie voles spent significantly more time in the exposed center than did meadow voles ($t_{(35)} = 4.86$, $p < 0.0001$), and deposited somewhat fewer fecal boli during the test (Mean: 0.89 ± SEM: 0.35 vs. 3.47 ± 1.19), but this difference was not significant ($t_{(35)} = -2.03$, $p = 0.05$). There was no difference in distance traveled between prairie voles (2,181.82 ± 312.60 cm) and meadow voles (1,609.31 ± 130.91 cm; $t_{(35)} = 1.69$, $p = 0.10$). When tested in a LDB, prairie voles were faster to enter the light portion of the box than were meadow voles ($t_{(35)} = -2.04$, $p = 0.049$).

Study 1b: Effects of Day Length and Social History in Meadow Voles

Day Length Effects on Meadow Vole Social and Aggressive Behavior

Stranger-directed behaviors differed between SD- and LD-housed meadow voles in the 10-min social interaction test. SD meadow vole females displayed significantly more grooming ($t_{(34)} = 2.30$, $p = 0.027$) and pro-social contact (counts of grooming and huddling; $t_{(34)} = 2.59$, $p = 0.014$, **Figure 2A**) than did LD meadow vole females. Two conflict-related behaviors were exhibited at higher frequency in SD voles: flight (3.11 ± 0.97 vs. 0.72 ± 0.37, $t_{(34)} = 2.30$, $p = 0.028$) and lateral attack/threat (11.33 ± 2.54 vs. 2.17 ± 2.54, $Z = 2.19$, $p = 0.02$, Wilcoxon rank sum). There were no significant differences in frequency of huddling ($t_{(34)} = 2.01$, $p = 0.05$) or composite aggression score (counts of lateral attack/threat, clinch, upright, and chase; $F_{(2,48)} = 2.83$, $p = 0.07$; **Figure 2C**).

Housing Effects on Meadow Vole Stranger-Directed Interactions

SD meadow females that had been solo-housed from weaning exhibited different social and investigative behaviors than did pair-housed SD meadow females during the social interaction test. Pair-housed meadow vole females displayed significantly more sniffing ($Z = -2.41$, $p = 0.016$, Wilcoxon rank sum), grooming ($t_{(31)} = -3.32$, $p = 0.002$), huddling ($Z = -3.10$, $p = 0.002$), social score (counts of social exploration, sniffing, grooming, and huddling; $t_{(31)} = -3.51$, $p = 0.001$), and pro-social contact ($Z = -4.23$, $p < 0.0001$) than solo-housed meadow vole females (**Figures 2A,B**). Comparison of solo-housed voles to pair-housed voles also revealed significant differences in frequency of lateral attack/threat ($Z = -2.11$, $p = 0.035$) but not aggression score ($F_{(2,48)} = 2.83$, $p = 0.07$), with pair-housed voles (11.33 ± 2.54) displaying higher frequency of lateral attack/threat than solo-housed voles (3.80 ± 2.78; **Figure 2C**).

Study 2: Formation and Reformation of Peer Partner Preferences in Prairie Voles

Peer Partner Preferences After Prolonged Cohabitation (PPT 1)

All groups—female prairie voles housed in both day lengths, and males tested in SDs—exhibited partner preferences for same-sex

FIGURE 2 | Meadow vole stranger-directed behavior during 10-min social interaction tests. Cohoused SD meadow voles are the same individuals as in **Figure 1**, but analyzed for full testing intervals to compare to other meadow vole groups. **(A)** There were significant group differences in pro-social contact (one-way ANOVA, $p < 0.001$). Cohoused SD meadow voles showed higher pro-social contact than cohoused long day (LD) meadow voles. Cohoused SD meadow voles showed higher pro-social contact than solo-housed SD meadow voles. **(B)** There were significant group differences in olfactory investigation (sniffing; one-way ANOVA, $p < 0.05$). Cohoused SD meadow voles showed higher sniffing than solo-housed SD meadow voles. **(C)** There were no significant group differences in aggression score across meadow vole groups. *$p < 0.05$, ***$p < 0.0005$.

cage-mate partners from weaning, indicated by significantly more huddling with partners than strangers (**Figure 3A**; LD prairie vole females: $W = -77.00$, $p = 0.01$; SD prairie vole females: $W = -64.00$, $p = 0.002$; SD prairie vole males: $W = -91.00$, $p < 0.001$). No significant differences in partner huddling were evident across groups ($F_{(3,47)} = 1.86$, $p = 0.15$).

Peer Partner Preferences and Partner Huddling After Re-pairing (PPT 2)

Both female groups demonstrated the capacity to form preferences for new same-sex partners in adulthood in PPT 2—following 8 days of separation from the first cage-mate and re-pairing with a new cage-mate for 24 h (**Figure 3B**). Partner huddling was significantly greater than stranger huddling in both LD prairie vole females ($W = -36.00$, $p = 0.008$) and SD prairie vole females ($W = -64.00$, $p = 0.002$). LD prairie vole females huddled significantly more with their partners than did SD prairie vole females ($t_{(14)} = -2.53$, $p = 0.02$). Males were initially tested for the capacity to form new peer partner preferences in adulthood, but the same-sex re-pairing of males was discontinued following the observation of aggression and injuries in the home cage.

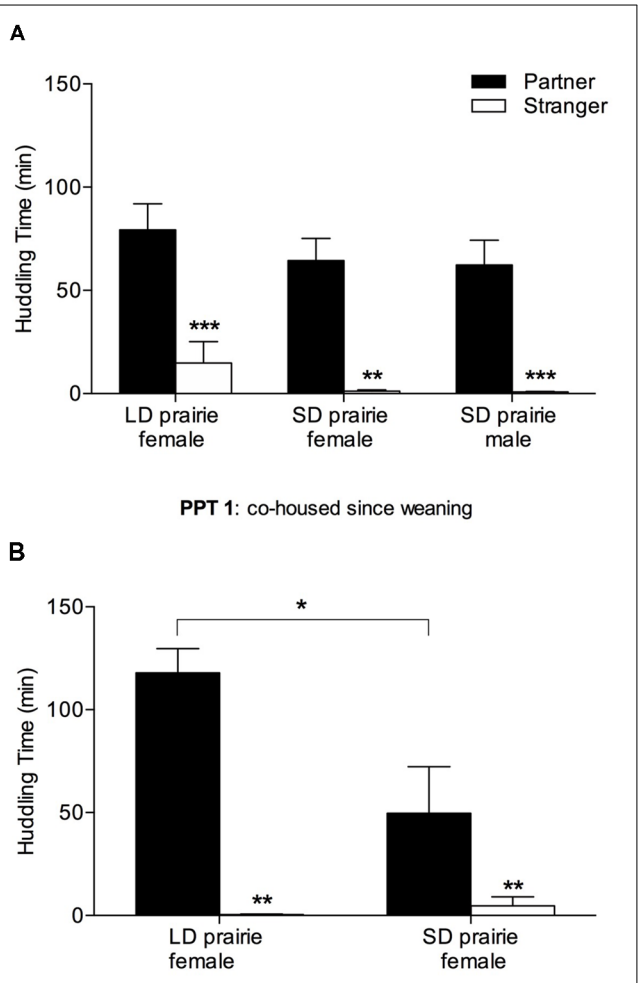

FIGURE 3 | Prairie vole partner preference for stable and new partners. **(A)** Partner preference test 1 (PPT 1; cohoused since weaning): all prairie vole groups ($n = 11$–14) showed robust partner preference for their partners. There were no group differences in partner huddling. **(B)** PPT 2 (24 h with new same-sex partner): a subset of voles was tested for the capacity to form partner preferences for new same-sex partners. Males were not included due to high aggression upon re-pairing. Both female groups ($n = 8$ each) showed robust partner preference for their partners. LD prairie vole females huddled significantly more with their partners than did SD prairie vole females. $^{*}p < 0.05$, $^{**}p < 0.01$, $^{***}p < 0.005$.

DISCUSSION

These studies are the first to directly compare the peer interactions of meadow and prairie voles, and to consider potential effects of day length on female prairie vole peer affiliation. We also extend findings on anxiety differences between species, and describe how differences in affiliation, aggression, and anxiety may contribute to differences in social structure.

Prairie Voles Are More Aggressive Than Meadow Voles

Detailed analysis of aggressive and affiliative behavior with novel conspecifics was quantified in social interaction tests. In these tests, SD prairie vole females housed with a peer were highly aggressive toward strangers compared to SD meadow vole females housed with a peer. Social exploration was also higher in prairie voles, usually in advance of the initiation of conflict interactions. This contrasts with a previous finding that meadow voles, not prairie voles, are the more aggressive species (Getz, 1962). However, that study utilized field-caught and laboratory-bred animals which were solo-housed for 2 weeks (field-caught) or 3 months (laboratory-bred) prior to behavioral testing, whereas the longest period of solo-housing in the present study was 1 week (prior to re-pairing with a new same-sex partner in Study 2 to mitigate aggression). It has been well documented that prolonged isolation produces behavioral, physiological, and neuroendocrine changes, at least in prairie voles (Grippo et al., 2008; Lieberwirth et al., 2012).

High aggression toward unfamiliar conspecifics in prairie voles may help to maintain the high selectivity of peer bonds, as it does in pair bonds among mates (Aragona et al., 2006). In other studies of meadow voles, meadow voles have displayed little aggression and high general social contact toward novel same-sex conspecifics (Beery Lab, *unpublished data*). Interaction with strangers in SD meadow voles may be an important avenue for the addition of new members to groups that form in winter.

Prairie Voles Are Less Anxious Than Meadow Voles

There were robust species differences in anxiety-like behavior in multiple tests. Prior research has shown species differences in anxiety behavior in males (Stowe et al., 2005), which we now extend to females. SD prairie vole females

exhibited significantly less anxiety-like behavior than SD meadow vole females in the OFT and the LDB. Prairie voles also exhibited higher levels of social exploration than meadow voles in the social interaction test, consistent with lower anxiety. While used here principally to elicit affiliative and aggressive behaviors, the social interaction test is also a major means of assessing anxiety in rodents (File and Seth, 2003).

Reduced anxiety behavior may be conducive to increased social interaction. In further support of the opposing roles of anxiety and social behavior, exogenous stressors disrupt the formation of partner preferences both in meadow vole females (for peers; Anacker et al., 2016b), and prairie vole females (for mates; DeVries et al., 1996).

Day Length and Housing Affect Stranger-Directed Behaviors in Meadow Voles

SD meadow vole females displayed significantly higher frequency of social behaviors with novel peers, including grooming and social contact, than LD meadow vole females. This is consistent with higher affiliation toward strangers, expected as SD meadow vole females huddle more with both partners and strangers than LD voles (Beery et al., 2008). Unexpectedly, SD meadow voles also displayed significantly higher frequency of lateral attack/threat behaviors and flight than LD meadow voles. One possible explanation is that SD meadow voles are more willing to engage in interactions of any kind with a conspecific, and that these interactions become more social, or at least more tolerant, over a longer period of time with the conspecific. Social experience may further shape affiliative behaviors, as pair-housed meadow voles showed significantly higher sniffing, grooming, and huddling frequency compared to solo-housed meadow voles. This is consistent with past findings that developmental experiences shape adult social behavior in voles and other species (Bales et al., 2007; Curley et al., 2009; Starr-Phillips and Beery, 2014).

Prairie Voles Form Peer Partner Preferences Regardless of Day Length or Sex

While social interaction tests assessed stranger-directed behaviors, PPTs assessed affiliation for a familiar animal. All groups cohoused from weaning formed partner preferences for same-sex peers. This places vole social preferences in contrast to those of rats and mice, who do not appear to form selective preferences for familiar peers under ordinary circumstances (Harrison et al., 2016; Schweinfurth et al., 2017; Beery et al., 2018).

Twenty-four hours was sufficient for the formation of new peer partner preferences following separation from old partners in adulthood in females housed in both SD and LD (male groups were discontinued because of aggression). This is consistent with prior findings that LD prairie voles form peer partner preferences within 24 h of cohabitation (DeVries et al., 1997).

Partner huddling was higher in LD prairie vole females than SD prairie vole females in PPT 2. LD prairie vole females displayed partner preferences at consistently high levels in PPT 1 and 2, and re-paired with minimal aggression or need for separation. This supports the use of LD prairie vole females, rather than SD prairie vole females or males, in future studies of peer affiliation in prairie voles. Studying LD prairie vole females for their peer affiliation will also allow for direct comparison with previous work on pair bonding in prairie voles, which was conducted with LD-housed prairie voles.

CONCLUSIONS

Selective partner preferences for same-sex peers appear to be the norm for both prairie and meadow voles, as individuals of each species, sex, and sometimes day length tested here or previously exhibited significant preferences for cage-mates. Social selectivity thus appears to be an important characteristic of social structure in voles. Prairie voles exhibited higher aggression and lower anxiety than meadow voles, and, unlike meadow voles, did not appear to be more affiliative in SD length conditions. In meadow voles, affiliative and aggressive behaviors were altered by day length and by housing. This characterization of peer affiliation, anxiety, and aggression lays the foundations for future work on the mechanisms supporting behavior in different types of peer relationships.

DATA AVAILABILITY

The datasets generated for this study are available on request to the corresponding authors.

AUTHOR CONTRIBUTIONS

All authors designed the study. NL, NG, and KF conducted the research. NL, NG, and AB conducted statistical analyses. NL and AB wrote the manuscript. All authors critically revised the manuscript and gave approval for publication.

FUNDING

The research reported in this publication was supported by the National Institute of Mental Health of the National Institutes of Health under Award Number R15MH113085.

ACKNOWLEDGMENTS

We are grateful to Kate Shambaugh, Sarah Lopez, Katrina Blandino, Katie Moshofsky, Lydia Ross, and Jennifer Christensen for their help with behavioral testing and scoring. We would also like to thank the Smith College Animal Care Facility staff for helping maintain our animal colony.

REFERENCES

Anacker, A. M. J., Christensen, J. D., LaFlamme, E. M., Grunberg, D. M., and Beery, A. K. (2016a). Septal oxytocin administration impairs peer affiliation via V1a receptors in female meadow voles. *Psychoneuroendocrinology* 68, 156–162. doi: 10.1016/j.psyneuen.2016.02.025

Anacker, A. M. J., Reitz, K. M., Goodwin, N. L., and Beery, A. K. (2016b). Stress impairs new but not established relationships in seasonally social voles. *Horm. Behav.* 79, 52–57. doi: 10.1016/j.yhbeh.2016.01.004

Aragona, B. J., Liu, Y., Yu, Y. J., Curtis, J. T., Detwiler, J. M., Insel, T. R., et al. (2006). Nucleus accumbens dopamine differentially mediates the formation and maintenance of monogamous pair bonds. *Nat. Neurosci.* 9, 133–139. doi: 10.1038/nn1613

Bales, K. L., Lewis-Reese, A. D., Pfeifer, L. A., Kramer, K. M., and Carter, C. S. (2007). Early experience affects the traits of monogamy in a sexually dimorphic manner. *Dev. Psychobiol.* 49, 335–342. doi: 10.1002/dev.20216

Beery, A. K. (2019). Frank Beach award winner: Neuroendocrinology of group living. *Horm. Behav.* 107, 67–75. doi: 10.1016/j.yhbeh.2018.11.002

Beery, A. K., Christensen, J. D., Lee, N. S., and Blandino, K. L. (2018). Specificity in sociality: mice and prairie voles exhibit different patterns of peer affiliation. *Front. Behav. Neurosci.* 12:50. doi: 10.3389/fnbeh.2018.00050

Beery, A. K., Loo, T. J., and Zucker, I. (2008). Day length and estradiol affect same-sex affiliative behavior in the female meadow vole. *Horm. Behav.* 54, 153–159. doi: 10.1016/j.yhbeh.2008.02.007

Beery, A. K., Routman, D. M., and Zucker, I. (2009). Same-sex social behavior in meadow voles: multiple and rapid formation of attachments. *Physiol. Behav.* 97, 52–57. doi: 10.1016/j.physbeh.2009.01.020

Boonstra, R., Xia, X., and Pavone, L. (1993). Mating system of the meadow vole, *Microtus pennsylvanicus*. *Behav. Ecology* 4, 83–89. doi: 10.1093/beheco/4.1.83

Bowler, C. M., Cushing, B. S., and Carter, C. S. (2002). Social factors regulate female-female aggression and affiliation in prairie voles. *Physiol. Behav.* 76, 559–566. doi: 10.1016/s0031-9384(02)00755-2

Burkett, J. P., Andari, E., Johnson, Z. V., Curry, D. C., Waal, F. B. M., and Young, L. J. (2016). Oxytocin-dependent consolation behavior in rodents. *Science* 351, 375–378. doi: 10.1126/science.aac4785

Carter, C. S. (2017). The oxytocin- vasopressin pathway in the context of love and fear. *Front. Endocrinol.* 8:356. doi: 10.3389/fendo.2017.00356

Clutton-Brock, T. (2016). *Mammal Societies*. West Sussex, UK: John Wiley Sons

Curley, J. P., Jordan, E. R., Swaney, W. T., Izraelit, A., Kammel, S., and Champagne, F. A. (2009). The meaning of weaning: Influence of the weaning period on behavioral development in mice. *Dev. Neurosci.* 31, 318–331. doi: 10.1159/000216543

DeVries, A. C., DeVries, M. B., Taymans, S. E., and Carter, C. S. (1996). The effects of stress on social preferences are sexually dimorphic in prairie voles. *Proc. Natl. Acad. Sci. U S A* 93, 11980–11984. doi: 10.1073/pnas.93.21.11980

DeVries, A. C., Johnson, C. L., and Carter, C. S. (1997). Familiarity and gender influence social preferences in prairie voles (*Microtus ochrogaster*). *Can. J. Zool.* 75, 295–301. doi: 10.1139/z97-037

Ferkin, M. H., and Gorman, M. R. (1992). Photoperiod and gonadal hormones influence odor preferences of the male meadow vole, *Microtus pennsylvanicus*. *Physiol. Behav.* 51, 1087–1091. doi: 10.1016/0031-9384(92)90098-m

Ferkin, M. H., and Seamon, J. O. (1987). Odor preference and social behavior in meadow voles, *Microtus pennsylvanicus*: seasonal differences. *Can. J. Zool.* 65, 2931–2937. doi: 10.1139/z87-445

File, S. E., and Seth, P. (2003). A review of 25 years of the social interaction test. *Eur. J. Pharmacol.* 463, 35–53. doi: 10.1016/s0014-2999(03)01273-1

Firestone, K. B., Thompson, K. V., and Carter, C. S. (1991). Female-female interactions and social stress in prairie voles. *Behav. Neural. Biol.* 55, 31–41. doi: 10.1016/0163-1047(91)80125-x

Fowler, C. D., Liu, Y., Ouimet, C., and Wang, Z. (2002). The effects of social environment on adult neurogenesis in the female prairie vole. *J. Neurobiol.* 51, 115–128. doi: 10.1002/neu.10042

Getz, L. L. (1962). Aggressive behavior of the meadow and prairie voles. *J. Mammal.* 43, 351–358. doi: 10.2307/1376942

Getz, L. L. (1972). Social structure and aggressive behavior in a population of *Microtus pennsylvanicus*. *J. Mammal.* 53, 310–317. doi: 10.2307/1379167

Getz, L. L., and Carter, C. S. (1996). Prairie-vole partnerships. *Am. Sci.* 84, 56–62.

Getz, L. L., McGuire, B., Pizzuto, T., Hofmann, J. E., and Frase, B. (1993). Social organization of the prairie vole (*Microtus ochrogaster*). *J. Mammal.* 74, 44–58. doi: 10.2307/1381904

Gobrogge, K. L., Jia, X., Liu, Y., and Wang, Z. (2017). Neurochemical mediation of affiliation and aggression associated with pair-bonding. *Biol. Psychiatry.* 81, 231–242. doi: 10.1016/j.biopsych.2016.02.013

Goodwin, N. L., Lopez, S. A., Lee, N. S., and Beery, A. K. (2018). Comparative role of reward in long-term peer and mate relationships in voles. *Horm. Behav.* doi: 10.1016/j.yhbeh.2018.10.012 [Epub ahead of print].

Grippo, A. J., Cushing, B. S., and Carter, C. S. (2007a). Depression-like behavior and stressor-induced neuroendocrine activation in female prairie voles exposed to chronic social isolation. *Psychosom. Med.* 69, 149–157. doi: 10.1097/psy.0b013e31802f054b

Grippo, A. J., Gerena, D., Huang, J., Kumar, N., Shah, M., Ughreja, R., et al. (2007b). Social isolation induces behavioral and neuroendocrine disturbances relevant to depression in female and male prairie voles. *Psychoneuroendocrinology* 32, 966–980. doi: 10.1016/j.psyneuen.2007.07.004

Grippo, A. J., Lamb, D. G., Carter, C. S., and Porges, S. W. (2007c). Social isolation disrupts autonomic regulation of the heart and influences negative affective behaviors. *Biol. Psychiatry* 62, 1162–1170. doi: 10.1016/j.biopsych.2007.04.011

Grippo, A. J., Wu, K. D., Hassan, I., and Carter, C. S. (2008). Social isolation in prairie voles induces behaviors relevant to negative affect: toward the development of a rodent model focused on co-occurring depression and anxiety. *Depress. Anxiety* 25, E17–E26. doi: 10.1002/da.20375

Harper, S. J., and Batzli, G. O. (1997). Are staged dyadic encounters useful for studying aggressive behaviour of arvicoline rodents? *Can. J. Zool.* 75, 1051–1058. doi: 10.1139/z97-126

Harrison, N., Lopes, P. C., and König, B. (2016). Oxytocin and social preference in female house mice (*Mus musculus domesticus*). *Ethology* 122, 571–581. doi: 10.1111/eth.12505

Insel, T. R., Preston, S., and Winslow, J. T. (1995). Mating in the monogamous male: behavioral consequences. *Physiol. Behav.* 57, 615–627. doi: 10.1016/0031-9384(94)00362-9

Koolhaas, J. M., Coppens, C. M., de Boer, S. F., Buwalda, B., Meerlo, P., and Timmermans, P. J. (2013). The resident-intruder paradigm: a standardized test for aggression, violence and social stress. *J. Vis. Exp.* 77:e4367. doi: 10.3791/4367

Lee, P. C. (1994). "Social structure and evolution," in *Behaviour and Evolution*, eds P. J. B. Slater and T. R. Halliday (Cambridge, UK: Cambridge University Press).

Lee, N. S., and Beery, A. K. (2019). Neural circuits underlying rodent sociality: a comparative approach. *Curr. Top. Behav. Neurosci.* doi: 10.1007/7854_2018_77 [Epub ahead of print].

Lidicker, W. Z., and Patton, J. L. (1987). "Patterns of dispersal and genetic structure in populations of small rodents," in *Mammalian dispersal patterns: the effects of social structure on population genetics*, ed. B. D. Chepko-Sade, and Z. T. Halpin. (Chicago, FL: The University Chicago Press), 144–161.

Lieberwirth, C., Liu, Y., Jia, X., and Wang, Z. (2012). Social isolation impairs adult neurogenesis in the limbic system and alters behaviors in female prairie voles. *Horm. Behav.* 62, 357–366. doi: 10.1016/j.yhbeh.2012.03.005

Madison, D. M. (1980). Space use and social structure in meadow voles, *Microtus pennsylvanicus*. *Behav. Ecol. Sociobiol.* 7, 65–71. doi: 10.1007/bf00302520

Madison, D. M., and McShea, W. J. (1987). Seasonal changes in reproductive tolerance, spacing and social organization in meadow voles: a microtine model. *Integr. Comp. Biol.* 27, 899–908. doi: 10.1093/icb/27.3.899

McShea, W. J., and Madison, D. M. (1984). Communal nesting between reproductively active females in a spring population of *Microtus pennsylvanicus*. *Can. J. Zool.* 62, 344–346. doi: 10.1139/z84-053

Ondrasek, N. R., Wade, A., Burkhard, T., Hsu, K., Nguyen, T., Post, J., et al. (2015). Environmental modulation of same-sex affiliative behavior in female meadow voles. *Physiol. Behav.* 140, 118–126. doi: 10.1016/j.physbeh.2014.12.021

Parker, K. J., and Lee, T. M. (2003). Female meadow voles (*Microtus pennsylvanicus*) demonstrate same-sex partner preferences. *J. Comp. Psychol.* 117, 283–289. doi: 10.1037/0735-7036.117.3.283

Resendez, S. L., Keyes, P. C., Day, J. J., Hambro, C., Austin, C. J., Maina, F. K., et al. (2016). Dopamine and opioid systems interact within the nucleus accumbens to maintain monogamous pair bonds. *Elife* 5:e15325. doi: 10.7554/elife.15325

Schweinfurth, M. K., Neuenschwander, J., Engqvist, L., Schneeberger, K., Rentsch, A. K., Gygax, M., et al. (2017). Do female norway rats form social bonds? *Behav. Ecol. Sociobiol.* 71:98. doi: 10.1007/s00265-017-2324-2

Smith, J. E., Lacey, E. A., and Hayes, L. D. (2017). "Sociality in non-primate mammals," in *Comparative Social Evolution*, ed. D. R. Rubenstein (Columbia University, NY: Patrick Abbot), 284–319.

Starr-Phillips, E. J., and Beery, A. K. (2014). Natural variation in maternal care shapes adult social behavior in rats. *Dev. Psychobiol.* 56, 1017–1026. doi: 10.1002/dev.21182

Stowe, J. R., Liu, Y., Curtis, J. T., Freeman, M. E., and Wang, Z. (2005). Species differences in anxiety-related responses in male prairie and meadow voles: the effects of social isolation. *Physiol. Behav.* 86, 369–378. doi: 10.1016/j.physbeh.2005.08.007

Walum, H., and Young, L. J. (2018). The neural mechanisms and circuitry of the pair bond. *Nat. Rev. Neurosci.* 19, 643–654. doi: 10.1038/s41583-018-0072-6

Young, K. A., Gobrogge, K. L., Liu, Y., and Wang, Z. (2011). The neurobiology of pair bonding: insights from a socially monogamous rodent. *Front. Neuroendocrinol.* 32, 53–69. doi: 10.1016/j.yfrne.2010.07.006

Conflict of Interest Statement: The authors declare that the research was conducted in the absence of any commercial or financial relationships that could be construed as a potential conflict of interest.

frontiers in Behavioral Neuroscience

ORIGINAL RESEARCH
published: 17 May 2019
doi: 10.3389/fnbeh.2019.00107

Analysis of Motor Function in the Tg4-42 Mouse Model of Alzheimer's Disease

*Jannek M. Wagner[1], Marius E. Sichler[1], Eva M. Schleicher[1], Timon N. Franke[1], Caroline Irwin[1], Maximilian Johannes Löw[1], Nicola Beindorff[2], Caroline Bouter[3], Thomas A. Bayer[1] and Yvonne Bouter[1]**

[1] Division of Molecular Psychiatry, Department of Psychiatry and Psychotherapy, University Medical Center Göttingen, Georg-August-University, Göttingen, Germany, [2] Berlin Experimental Radionuclide Imaging Center, Charité – University Medicine Berlin, Berlin, Germany, [3] Department of Nuclear Medicine, University Medical Center Göttingen, Georg-August-University, Göttingen, Germany

Alzheimer's disease (AD) is a neurodegenerative disorder and the most common form of dementia. Hallmarks of AD are memory impairments and cognitive deficits, but non-cognitive impairments, especially motor dysfunctions are also associated with the disease and may even precede classic clinical symptoms. With an aging society and increasing hospitalization of the elderly, motor deficits are of major interest to improve independent activities in daily living. Consistent with clinical findings, a variety of AD mouse models develop motor deficits as well. We investigated the motor function of 3- and 7-month-old Tg4-42 mice in comparison to wild-type controls and 5XFAD mice and discuss the results in context with several other AD mouse model. Our study shows impaired balance and motor coordination in aged Tg4-42 mice in the balance beam and rotarod test, while general locomotor activity and muscle strength is not impaired at 7 months. The cerebellum is a major player in the regulation and coordination of balance and locomotion through practice. Particularly, the rotarod test is able to detect cerebellar deficits. Furthermore, supposed cerebellar impairment was verified by ^{18}F-FDG PET/MRI. Aged Tg4-42 mice showed reduced cerebellar glucose metabolism in the ^{18}F-FDG PET. Suggesting that, deficits in coordination and balance are most likely due to cerebellar impairment. In conclusion, Tg4-42 mice develop motor deficits before memory deficits, without confounding memory test. Thus, making the Tg4-42 mouse model a good model to study the effects on cognitive decline of therapies targeting motor impairments.

Keywords: motor function, cerebellum, Alzheimer, transgenic mice, behavior, FDG-PET

OPEN ACCESS

Edited by:
Ekrem Dere,
Sorbonne Universités, France

Reviewed by:
Siv Vingill,
University of Oxford, United Kingdom
Terence Y. Pang,
The Florey Institute of Neuroscience and Mental Health, Australia

****Correspondence:***
Yvonne Bouter
Yvonne.bouter@med.uni-goettingen.de

Received: *28 February 2019*
Accepted: *02 May 2019*
Published: *17 May 2019*

Citation:
Wagner JM, Sichler ME, Schleicher EM, Franke TN, Irwin C, Löw MJ, Beindorff N, Bouter C, Bayer TA and Bouter Y (2019) Analysis of Motor Function in the Tg4-42 Mouse Model of Alzheimer's Disease. Front. Behav. Neurosci. 13:107. doi: 10.3389/fnbeh.2019.00107

INTRODUCTION

Alzheimer's disease (AD) is a neurodegenerative disorder and the most common form of dementia. The main clinical symptoms of AD are memory impairments and cognitive deficits. However, non-cognitive impairments especially motor dysfunctions are also associated with the disease. The observed motor deficits range from impaired balance and gait changes to disturbed activity levels (Larson et al., 1992; O'Keeffe et al., 1996; Pettersson et al., 2002; Camicioli et al., 2006).

In AD patients, motor impairments may even precede the clinical symptoms, providing a link between motor function and the development of AD (Buchman and Bennett, 2011).

Motor signs (MOSIs) decline with age and severity of the disease. The most affected MOSIs are speech, facial expression, rigidity, posture, gait, bradykinesia, and less frequently tremor (Scarmeas et al., 2004).

From mild to moderate AD the decline in motor abilities is stronger than from moderate to severe AD and associated with an increased risk of falls (Zidan et al., 2012). Slowing in fine motor dexterity seems to depend on the severity of the disease and is associated with functional decline in the active daily living (de Paula et al., 2016). In the 'Sydney Older Persons Study' a combination of cognitive decline and motor deficits was investigated over a 6-year period. Motor slowing and gait abnormalities resulted in poorer outcome of patients with dementia. Patients with decreased motor abilities were more likely to have severe cognitive impairments and even died earlier (Waite et al., 2005). Another study showed that gait abnormalities in aged patients without the diagnosis of dementia at baseline were related to lower cognitive performance and an increased incidence of mild cognitive impairment (MCI) or dementia (Beauchet et al., 2014). Wilson et al. (2000) showed a link between progression in parkinsonism (bradykinesia, gait disorder/postural reflex impairment, rigidity, tremor) and the progression of cognitive decline in AD patients. Furthermore, rigidity has been shown to be linked to death as well and to increased hospitalization in AD patients (Lopez et al., 1997).

Consistent with clinical findings, a variety of AD mouse models develop motor deficits (Kobayashi and Chen, 2005; Wirths and Bayer, 2008) (**Table 1**). There are several well established behavioral tests to assess motor function, coordination and balance in rodents such as the rotarod test, balance beam task, string suspension task, inverted grip strength task and the Open Field task for locomotor activity (Brooks and Dunnett, 2009; Deacon, 2013).

While the exact etiology of AD is still not fully understood, considerable evidence points to amyloid-beta peptides (Aβ) as a key player in the pathogenesis of AD. According to the amyloid cascade hypothesis, Aβ-plaques seem to play a causative role in the pathogenesis of AD (Hardy and Higgins, 1992). More recent data claim that, truncated and modified Aβ variants play an important role next to full-length Aβ. Especially N-truncated forms of Aβ enhance aggregation and neurotoxicity (Pike et al., 1995; Bayer and Wirths, 2014). Among the different species, Aβ beginning with phenylalanine at position 4 is particularly abundant in the brain of AD patients (Masters et al., 1985; Portelius et al., 2010). The transgenic mouse model Tg4-42 expresses exclusively intraneuronal Aβ4-42 without human amyloid precursor protein (APP) overexpression (Bouter et al., 2013). Intracellular Aβ accumulation is accompanied by micro- and astrogliosis that is most abundant in the hippocampus of these mice. Tg4-42 mice develop severe synaptic impairments and neuron loss especially in the CA1 region of the hippocampus. Furthermore, Tg4-42 mice develop age-dependent behavior and memory deficits albeit without plaque formation (Bouter et al., 2013, 2019; Dietrich et al., 2013).

The aim of the current study was to extend previous findings on the Tg4-42 model by examining motoric abilities and compare these results with the widely used 5XFAD mouse model. We investigated mice at 3 months, with no known memory deficits in comparison with 7-month-old mice, which already present strong memory deficits. Furthermore, we discuss the results in the context of other, well-studied AD models, to facilitate model selection for further research on the causes of motor impairments related to AD and the development of possible therapies.

MATERIALS AND METHODS

Transgenic Mice

The generation of Tg4-42 mice has been described previously (Bouter et al., 2013). Briefly, Tg4-42 mice express human Aβ4-42 fused to the murine thyrotropin releasing hormone signal peptide under the control of the neuronal Thy-1 promoter. Tg4-42 mice were generated and maintained on a C57Bl/6J genetic background. Only homozygous Tg4-42 mice were used in this study.

The double transgenic 5XFAD model (Jackson Laboratories, Bar Harbor, ME, United States) over-expresses the 695 amino acids isoform of the human amyloid precursor protein (APP695) carrying the Swedish, London, and Florida mutations under the control of the murine Thy-1 promoter. In addition, human presenilin-1 (PSEN-1) carrying the M146L/L286V mutations is also expressed under the control of the murine Thy-1 promoter in 5XFAD mice (Oakley et al., 2006). 5XFAD mice used in the current study were kept on a C57Bl/6J genetic background (Jawhar et al., 2012). Wild-type littermates served as age-matched control animals. In the current study, only female mice were used.

All animals were handled according to the guidelines of the 'Society for Laboratory Animals Science' (GV-SOLAS) and the guidelines of the 'Federation of European Laboratory Animal Science Association' (FELASA). All experiments were approved by the 'Lower Saxony State Office for Consumer Protection and Food Safety' (LAVES).

Mice were kept on a 12 h/12 h inverted light cycle and behavior experiments were performed during the dark phase. Mice were subjected to a battery of behavior tests at 3 and 7 months of age to assess possible motor deficits. Weight was monitored as part of a general physical assessment.

Paw-Clasping Test

The clasping test was used to test for functional impairments (Jawhar et al., 2012). Each mouse was suspended by their tail for 30 s to provoke a clasping phenotype. Healthy mice try to escape the grip by twisting their body and kicking their paws and therefore do not show any clasping phenotype. Clasping behavior was scored on a scale from zero to three: 0 = no clasping behavior, 1 = fore paws clasping, 2 = one hind paw and fore paws clasping, 3 = clasping of all paws (Miller et al., 2008).

String Suspension

Grip strength and general motor coordination were analyzed using the string suspension task as described previously

TABLE 1 | Motor function of different AD mouse models.

Mouse model	References	Test age	Sex	Open Field	Rotarod	Balance beam walk	String susp. task	Grip strength tasks
J20 $APP_{SweK670N/M671L + IndV717F}$ (Mucke et al., 2000)	Harris et al., 2010	1) 2–3 m	♂	↑	–	–	–	–
		2) 5–7 m	♂	↑	–	–	–	–
	Chang et al., 2015	1) 5 m	–	ns	ns	–	–	–
Tg2576 $APP695_{SweK670N/M671L}$ (Hsiao et al., 1996)	King and Arendash, 2002	1) 3 m	♀♂	↑	–	↓	ns	–
		2) 9 m	♀♂	ns	–	ns	ns	–
		3) 14 m	♀♂	ns	–	↓	↓	–
		4) 19 m	♀♂	ns	–	↓	↓	–
	Dineley et al., 2002	1) 5 m	♀♂	ns	ns	–	–	–
		2) 9 m	♀♂	ns	ns	–	–	–
	Perucho et al., 2010	1) 12 m	♂	ns	ns	–	–	–
APP23 $APP751_{SweK670N/M671L}$ (Sturchler-Pierrat et al., 1997)	van Dam et al., 2003	1) 6–8w	♂	ns	ns	–	–	–
		2) 3 m	♂	ns	↓	–	–	–
		3) 6 m	♂	↓	↓	–	–	–
	Lalonde et al., 2005a	1) 24 m	♀	ns	↑	ns	↑	–
APP/PS1 $APP_{SweK670N/M671L}/PS1_{\Delta E9}$ (Jankowsky et al., 2001)	Kuwabara et al., 2014	1) 3 m	♀♂	–	↓	ns	–	–
		2) 5–6 m	♂	–	↓	ns	–	–
	Singh et al., 2017	1) 4 m	♀♂	–	ns	–	–	–
		2) 8 m	♀♂	–	ns	–	–	–
		3) 12 m	♀♂	–	ns	–	–	–
	Lalonde et al., 2004	1) 7 m	♀♂	ns	ns	ns	ns	ns
APP+PS1 $APP_{SweK670N/M671L} + PS1_{M146L}$ (Holcomb et al., 1999)	Holcomb et al., 1999	1) 3 m	♀♂	–	–	–	ns	–
		2) 6 m	♀♂	–	–	–	ns	–
		3) 9 m	♀♂	–	–	–	ns	–
	Arendash et al., 2001	1) 5–7 m	♀♂	ns	–	↓	ns	–
		2) 15–17 m	♀♂	↑	–	↓	↓	–
	Sadowski et al., 2004	1) 8 m	–	ns	–	ns	–	–
		2) 22 m	–	ns	–	ns	–	–
	Ewers et al., 2006	1) 12 m	♀♂	–	↓	–	–	–
APP/PS1KI $APP_{NLh/NLh} \times PS1_{P264L/P264L}$ (Flood et al., 2002)	Webster et al., 2013	1) 7 m	♀♂	ns	ns	ns	–	ns
		2) 11 m	♀♂	ns	ns	ns	–	ns
		3) 15 m	♀♂	ns	ns	ns	–	ns
		4) 24 m	♀♂	ns	ns	ns	–	ns
5XFAD $APP_{sweK670N/M671,FloI716V,LonV717I} + PS1_{M146/L286V}$ (Oakley et al., 2006)	Jawhar et al., 2012	1) 3 m	♀	–	–	ns	ns	–
		2) 6 m	♀	–	–	ns	ns	–
		3) 9 m	♀	ns	–	↓	↓	–
		4) 12 m	♀	ns	–	↓	↓	–
	O'Leary et al., 2018a	1) 3–4 m	♀♂	ns	ns	ns	ns	ns
		2) 6–7 m	♀♂	♀♂	ns	ns	♂↓	↓
		3) 9–10 m	♀♂	ns	↓	↓	ns	ns
		4) 12–13 m	♀♂	↓	↓	↓	♂↓	↓
		5) 15–16 m	♀♂	↓	↓	↓	↓	↓
	Shukla et al., 2013	1) 6 m	♀♂	ns	ns	–	–	–
		2) 9 m	♀♂	–	ns	–	–	–
		3) 12 m	♀♂	–	↓	–	–	–
	current study	1) 3 m	♀	ns	ns	ns	ns	ns
		2) 7 m	♀	↓	ns	ns	ns	ns

(Continued)

TABLE 1 | Continued

Mouse model	References	Test age	Sex	Open Field	Rotarod	Balance beam walk	String susp. task	Grip strength tasks
3xTg $APP_{SweK670M/N671L}$, $PS1_{M136V}$, $MAPT_{P301L}$ (Oddo et al., 2003)	Oore et al., 2013	1) 2 m	♀♂	–	↑	–	–	–
		2) 6 m	♀♂	–	↑	–	–	–
		3) 9 m	♀♂	–	↑	–	–	–
		4) 12 m	♀♂	–	↑	–	–	–
		5) 15 m	♀♂	–	↑	–	–	–
	Stover et al., 2015	1) 6 m	♀♂	–	↑	ns	ns	↓
	Garvock-de Montbrun et al., 2019	1) 16 m	♀♂	–	↑	ns	ns	ns
	Filali et al., 2012	1) 12–14 m	♀	↓	↓	–	–	–
	Gulinello et al., 2009	1) 15–18 m	♀♂	↓	–	ns	–	–
TBA 42 $A\beta_{pE3-42}$ (Wittnam et al., 2012)	Meissner et al., 2014	1) 3 m	♀♂	–	–	ns	↓	ns
		2) 6 m	♀♂	–	–	↓	↓	↓
		3) 12 m	♀♂	–	–	↓	↓	↓
	Wittnam et al., 2012	1) 3 m	♀	–	–	ns	–	–
		2) 6 m	♀	–	–	ns	–	–
		3) 12 m	♀	–	–	↓	–	–
	Lopez-Noguerola et al., 2018	1) 3–4 m	♀♂	–	–	ns	ns	ns
		2) 5–6 m	♀♂	–	–	↓	↓	↓
Tg4-42 $A\beta_{4-42}$ (Bouter et al., 2013)	Lopez-Noguerola et al., 2018	1) 3–4 m	♀♂	–	–	ns	ns	ns
		2) 5–6 m	♀♂	–	–	ns	ns	ns
	Current study	1) 3 m	♀	ns	↓	ns	ns	ns
		2) 7 m	♀	ns	↓	↓	ns	ns

w, weeks; m, months; ns, not significant.

(Jawhar et al., 2012). In brief, mice were permitted to grasp a cotton string with their fore paws and were then released. Their ability to climb across the string was assessed using a 0 to 5 rating score: 0 = falls of string; 1 = hangs onto string by fore- or hind paws; 2 = hangs onto string by fore- or hind paws and attempts to climb onto string; 3 = hangs onto string by all four paws but no lateral movement; 4 = hangs onto string using all four paws and tail and moves laterally; 5 = escapes to the edge of string and touches wooden support beam (Moran et al., 1995). Each animal performed three 60-s trials throughout 1 day with a minimum of 30 min between the trials. The average score of all three trials was taken for each mouse.

Balance Beam

Fine motor coordination and balance of mice were assessed using the balance beam test as previously described (Jawhar et al., 2012). The test essentially examines the ability of a mouse to remain upright and to walk on the relatively narrow and elevated beam to one of the platforms. During a single day of testing each mouse was given three 60-s trials with a minimum of 10 min between the trials. The average time of all three trials was taken as the score for each mouse. A test trial was given to familiarize the mouse with the beam. For each trial, the mouse was placed in the center of the beam facing one of the platforms and then released. The latency to fall from the beam was recorded. If a mouse escaped to one of the platforms or remained on the beam for the entire trial, the maximum time of 60 s was given.

Inverted Grip Task

Neuromuscular abilities and muscle strength were tested with the inverted grip test as previously described (Wirths et al., 2008). Mice were placed on a metal grid and turned upside down 30 cm elevated above a padded surface. Latency to fall within 60 s was measured in one single trial.

Rotarod

Motor performance and motor learning were tested using the rotarod (TSE Systems, Germany). Testing consists of four trials per day for two consecutive days with intertrial intervals of 10–15 min. Each mouse was placed on the rod, which accelerated from 4 to 40 rpm. over the trial time of 300 s. Trials were terminated when animals fell off or the maximum time was reached. Up to five mice were tested simultaneously, separated by black plastic walls. Mice were taken out of the apparatus when the last mouse fell. Latency to fall served as an indicator of motor coordination.

^{18}F-FDG PET/MRI

^{18}F-fluoro-deoxy-glucose positron emission tomography/magnetic resonance image (^{18}F-FDG-PET/MRI) acquisition and analysis were used to evaluate brain glucose metabolism in the cerebellum of 7-month-old Tg4-42 mice and 5XFAD mice. Female Tg4-42 (n = 5), 5XFAD (n = 3) and wild-type C57Bl/6J (n = 5) control mice were fasted overnight and blood glucose levels were measured. As previously described 9–21 MBq (mean 15.76 MBq) of ^{18}F-FDG were administered

intravenously into a tail vein with a maximum volume of 200 µl (Bouter et al., 2019). Mice were anesthetized with isoflurane supplemented with oxygen during the scans and were awake during the uptake period. After an uptake period of 45 min, PET imaging was performed on a small animal 1 Tesla nanoScan PET/MRI (Mediso, Hungary). During the scan mice were placed on a 37°C heated bed. Respiration rate was monitored constantly during the scans. PET scans were performed for 20 min. MRI-based attenuation correction was conducted (matrix 144 × 144 × 163 with a voxel size of 0.5 × 0.5 × 0.6 mm^3, TR: 15 ms, TE 2.032 ms and a flip angle of 25°) and the PET images were reconstructed with the following parameters: matrix 136 × 131 × 315 with a voxel size of 0.23 × 0.3 × 0.3 mm^3. Image analysis was performed using PMOD v3.9 (PMOD Technologies, Switzerland). A predefined mouse brain atlas template was used to analyze different brain areas including the cerebellum (Cb). Corresponding PET images were matched to the MRI and statistics within the cerebellum volume of interest (VOI) in kBq/cc were generated. Standardized uptake value (SUV) was calculated [SUV = tissue activity concentration average (KBq/cc) × body/weight (g)/injected dose (kBq)] for semi-quantitative analysis and SUV values were corrected for blood glucose levels [SUVGlc = SUV × blood glucose level (mg/dl)].

Statistical Analysis

Differences between groups were tested with one-way analysis of variance (ANOVA) or two-way ANOVA followed by analysis of Bonferroni multiple comparison indicated. All data are given as mean ± standard error of the mean (SEM). Significance levels are given as follows: $^{***}p < 0.001$; $^{**}p < 0.01$; $^{*}p < 0.05$. GraphPad Prism version 6.07 for Windows (GraphPad Software, San Diego, CA, United States) was used for all calculations.

RESULTS

Normal Body Weight of Tg4-42 and 5XFAD Mice

The body weight of all mice was taken at 3 and 7 months of age. Tg4-42 and 5XFAD mice demonstrated no altered body weight compared to wild-type mice at the tested time points [**Figure 1A**, two-way ANOVA, *genotype:* $F(2,66) = 3.744$, $p = 0.0688$]. Statistically significant was the gain of weight of Tg4-42 and 5XFAD mice, but although wild-type mice gained some weight as well, this effect was not statistically significant [**Figure 1A**, two-way ANOVA, *age:* $F(1,66) = 18.55$, $p < 0.0001$, *post hoc* analysis Tg4-42: $p < 0.01$, 5XFAD: $p < 0.05$].

Clasping Phenotype in 7-Month-Old 5XFAD Mice

At 3 months none of the tested animals showed any clasping phenotype. However, 5XFAD mice develop an age-dependent clasping phenotype [**Figure 1B**, two-way ANOVA, *age:* $F(1,66) = 10.61$, $p = 0.0019$; *genotype:* $F(2,66) = 12.12$, $p < 0.001$]. Tg4-42 mice did not show a clasping behavior at 7 months and they tried to escape the grip by twisting their body and kicking their paws similar to wild-type animals.

Impaired Sensorimotor Function in Tg4-42 Mice

Fine motor coordination and balance of mice can be assessed by the balance beam task (Hau and Schapiro, 2002; Luong et al., 2011). At the age of 3 months none of the tested animals showed impairments in the balance beam task. However, 7-month-old Tg4-42 mice spent significantly less time on the beam compared to same-aged wild-type animals [**Figure 2A**, two-way ANOVA, *genotype:* $F(2,66) = 3.702$; $p < 0.05$]. Tg4-42 mice showed an age-dependent decline in balance and motor coordination [**Figure 2A**, two-way ANOVA, Tg4-42 *age:* $F(1,66) = 5.904$, $p = 0.0178$; *post hoc* analysis Tg4-42: $p < 0.05$]. In contrast, aged 5XFAD mice performed similar to wild-type controls.

Unaltered Grip Strength in 5XFAD and Tg4-42 Mice

The string suspension task evaluates motor coordination, grip and muscle strength of mice (Hullmann et al., 2017), whereas the inverted grip task assesses muscle strength (Deacon, 2013). Neither 5XFAD, nor Tg4-42 mice showed a lower grip strength in any of these tests compared to wild-type control mice [**Figures 2B,C**, two-way ANOVA, string suspension *genotype:* $F(2,66) = 0.9058$, $p = 0.4092$, *age:* $F(1,66) = 0.450$, $p = 0.5047$; inverted grip *genotype:* $F(1,66) = 2.435$, $p = 0.1234$, *age*: $F(1,66) = 2.435$, $p = 0.1234$].

Decreased Locomotor Activity of 5XFAD, but Not Tg4-42 Mice in the Open Field Task

To measure general locomotor activity, mice were tested in an Open Field task (Seibenhener and Wooten, 2015). Tg4-42 mice traveled the same distance as wild-type controls, showing no impaired locomotor activity at any tested age. On the other hand, 5XFAD mice traveled less, showing an age-dependent decreased in locomotor activity [**Figure 2D**, two-way ANOVA, *age*: $F(1,71) = 22.33$, $p < 0.001$; *genotype*: $F(2,71) = 3.706$, $p = 0.0294$].

Impaired Motor Learning Skills in Tg4-42 Mice

The rotarod task assesses motor skill learning abilities and coordination (Buitrago et al., 2004; Deacon, 2013). Performance of 5XFAD mice did not differ from wild-type controls at 3 or 7 months of age. While young Tg4-42, 5XFAD and WT mice showed an overall improved motor learning over the training trials [**Figure 2E**, two-way ANOVA, *trials*: $F(7,210) = 20.18$, $p < 0.0001$], Tg4-42 displayed a shorter latency to fall on the last trial compared to same-aged wild-type animals [**Figure 2E**, two-way ANOVA, *genotype*: $F(2,30) = 1.114$, $p = 0.3413$; *post hoc* analysis Tg4-42 *trial 8*: $p < 0.05$]. At 7 months of age Tg4-42 mice showed decreased motor learning and performed significantly

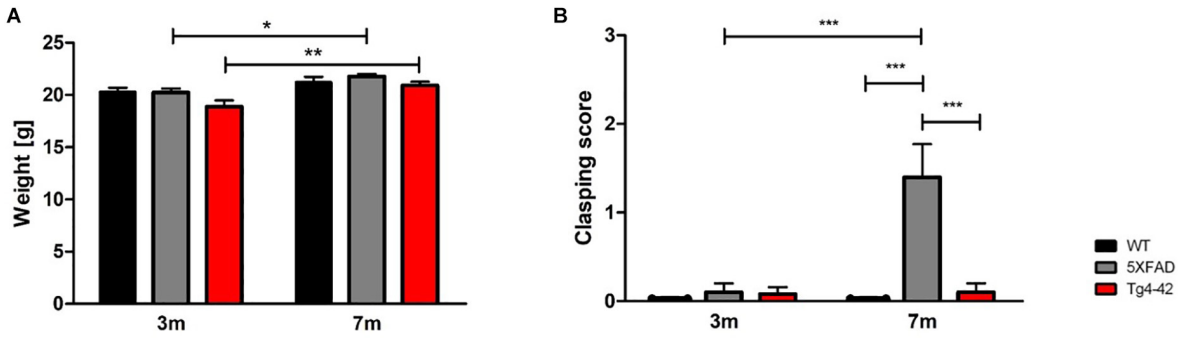

FIGURE 1 | General physical assessment of Tg4-42 and 5XFAD mice. **(A)** 3- and 7-month-old Tg4-42 and 5XFAD mice displayed normal body weight compared to aged-matched wild-type mice. **(B)** Wild-type and Tg4-42 mice showed no clasping phenotype during the tail suspension task regardless of age. 5XFAD mice showed a clasping phenotype at 7 months of age. Two-way repeated measures ANOVA, $*p < 0.05$, $**p < 0.01$, $***p < 0.001$; $n = 12$ per group; data presented as mean ± SEM; WT, wild-type; m, months.

worse than wild-type and 5XFAD animals [**Figure 2F**, two-way ANOVA, *genotype:* $F(2,41) = 33.00$, $p < 0.0001$].

Decreased Metabolic Activity in the Cerebellum of Aged Tg4-42 Mice

^{18}F-FDG-PET/MRI was used to determine cerebellar glucose metabolism. Quantitative analysis of FDG-uptake was performed using a mouse brain atlas and blood glucose corrected SUV values (SUVglc) were measured within a predefined cerebellum VOI (**Figure 3B**). Seven-month-old Tg4-42 and 5XFAD mice showed significantly decreased ^{18}F-FDG uptake in the cerebellum compared to wild-type mice [**Figures 3A,C,D**, one-way-ANOVA, $F(2,11) = 2.007$, $p = 0.0018$; *post hoc* analysis WT vs. Tg4-42: $p < 0.01$; WT vs. 5XFAD: $p < 0.05$].

DISCUSSION

Impairments of motor abilities are an important phenotype in the progression of AD. Several studies show a decline in motor function throughout the progression of the disease in patients (Zidan et al., 2012; Beauchet et al., 2014; de Paula et al., 2016). Furthermore, motor impairments can be useful in the prediction of the onset as well as the outcome of AD (Waite et al., 2005). In an aging society, maintaining motor performance in AD patients should be of major interest to help to facilitate independence in daily living and activity (Yan and Zhou, 2009). Assessing motor deficits through physical exercise in preclinical stages of AD could delay or decline the development of AD as shown previously (Larson et al., 2006). Thus, motor deficits are an important symptom to study in AD.

Similar to AD patients, most mouse models mimicking AD show motor impairments as the disease progresses. This study compared motor behavior of young and aged Tg4-42 mice with their age-matched wild-type controls and compared the results with other AD mouse models. Motoric performance of AD mice ranges from unaltered and impaired to improved motor performance. There are several tests to assess motor abilities in mice, but protocols and experimental apparatus differ highly between laboratories, complicating the comparison of results. These differences in behavior tests should always be taken into consideration (**Table 1**).

Weight can severely influence the outcome of behavior studies. Therefore, the animal's weight should always be taken into consideration especially when analyzing motor performance in mice. Previous studies showed that body weight significantly correlates with the performance of mice in the rotarod task, a test widely used to assess grip strength, motor coordination and balance (Brown and Wong, 2007; Shiotsuki et al., 2010). The weight of young and aged Tg4-42 mice was comparable to same-aged wild-type and 5XFAD mice in this study. In contrast, weight loss has previously been observed in several other AD mouse models. A reduction in the gain of body weight has been described especially in mouse models overexpressing APP (Lalonde et al., 2005a; Pugh et al., 2007; Alexandru et al., 2011). For example, 9-month-old 5XFAD mice showed a significantly reduced body weight in comparison to their wild-type littermates (Jawhar et al., 2012). Interestingly, epidemiologic studies showed that weight loss is often associated with AD and can be observed in all stages of the disease (Gillette-Guyonnet et al., 2000; Guérin et al., 2005; Cova et al., 2016). Weight loss in AD patients often correlates with a general health decline and is suggested as a clinical predictor of mortality (White et al., 1998). In mice, weight variances can also indicate poor health and a lack of body weight gain might contribute to predicting mortality.

In contrast to 5XFAD mice, Tg4-42 mice did not show a limb clasping phenotype. Aged 5XFAD mice exhibited motor abnormalities and abnormal extension reflexes by retracting their hind- and fore paws simultaneously when suspended by the tail. An abnormal clasping pattern has been observed in several mouse models including mice transgenic for human four-repeat tau and mutant human APP (Probst et al., 2000; Lalonde et al., 2012), as well as APP/PS1KI and 5XFAD mice. Interestingly, all of these mice showed signs of axonopathy (Tesseur et al., 2000; Wirths et al., 2007; Jawhar et al., 2012). But surprisingly, the number of motor neurons of 6-month-old 5XFAD mice in the cervical spinal cord was similar to wild-type littermates (Chu et al., 2017). Both

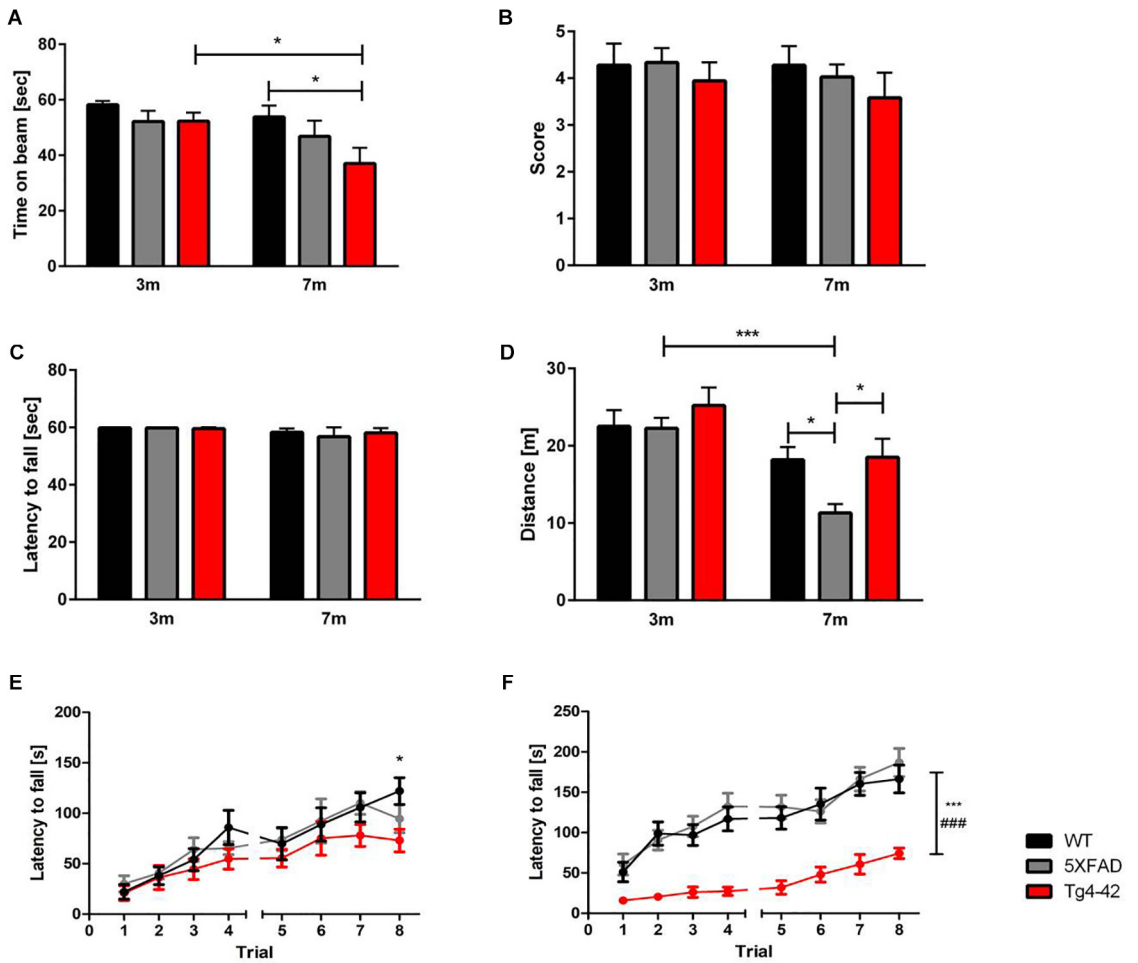

FIGURE 2 | Motor deficits in aged Tg4-42 mice. **(A)** Tg4-42 mice showed age-dependent motor deficits in the balance beam. 5XFAD mice displayed no deficits in the balance beam. Tg4-42 and 5XFAD mice performed similar to same-aged wild-type control mice in the **(B)** string suspension task and **(C)** inverted grip task. **(D)** 5XFAD mice displayed an age-dependent decreased distance traveled in the Open Field task. Seven-month-old 5XFAD mice traveled significantly less than same-aged Tg4-42 and wild-type mice. **(E)** Young Tg4-42 and 5XFAD mice showed a similar latency to fall on the accelerating rotarod on trials 1–7. On the last trial of the test Tg4-42 mice performed worse than same-aged wild-type mice. **(F)** Aged Tg4-42 mice showed a decreased performance on the accelerating rotarod compared to same-aged wild-type and 5XFAD mice. Two-way repeated measures ANOVA, vs. 5XFAD $^{###}p < 0.001$; vs. WT $^{***}p < 0.001$; $^{*}p < 0.05$; n = 9–15 per group, data presented as mean ± SEM; WT, wild-type; m, month.

Tg4-42 and 5XFAD mice show intracellular Aβ accumulation in the spinal cord, but only 5XFAD show signs of axon swelling and axonopathy (Jawhar et al., 2012; Lopez-Noguerola et al., 2018).

The Open Field locomotion test can be used to examine motor function by measuring spontaneous activity in an open arena (Lee et al., 2009). The Open Field task is an easy task to perform and measures general locomotor activity in mice (Seibenhener and Wooten, 2015). Our results show that Tg4-42 mice did not have alterations in locomotor activity. In contrast, 5XFAD mice showed lower activity levels consistent with previous studies (Sawmiller et al., 2017). Surprisingly, O'Leary et al. (2018a) found increased locomotor activity in 6- to 7-month-old female 5XFAD mice. This variation is likely due to different experimental protocols. However, in older 5XFAD mice the data is consistently showing reduced locomotor activity (Schneider et al., 2014; Griñán-Ferré et al., 2016; O'Leary et al., 2018a,b) (**Table 1**). Altered locomotor activities need to be taken into consideration when interpreting results of behavioral tests such as anxiety-related or memory-related tests (Crawley and Bailey, 2008; Brooks et al., 2012; Deacon, 2013). Nevertheless, Tg4-42 mice did not show any impairments in the Open Field that could possibly influence anxiety- and memory-related behavior. In line with these findings, general motor abilities of Tg4-42 mice have been shown to be intact in the Morris water maze as swimming speed did not differ from wild-type animals (Bouter et al., 2013, 2014, 2019; Antonios et al., 2015).

Generally speaking, APP single-transgenic mice seem to show increased locomotor activity at young ages (King and Arendash, 2002; Harris et al., 2010), whereas mouse models with multiple mutations develop impairments at an older age (Gulinello et al., 2009; Filali et al., 2012; O'Leary et al., 2018a). Similar to Tg4-42

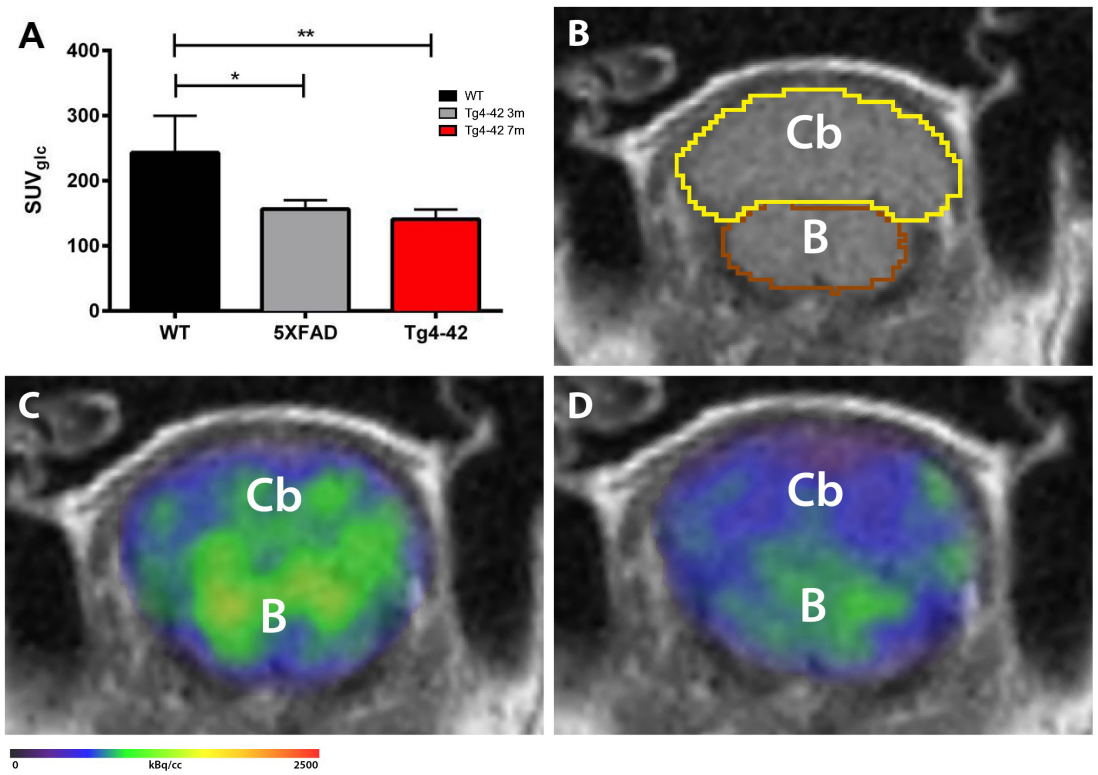

FIGURE 3 | ^{18}F-FDG-PET shows decreased metabolic activity in the cerebellum of 7-month-old Tg4-42 and 5XFAD mice. **(A)** Quantification of ^{18}F-FDG uptake in the cerebellum. ^{18}F-FDG-uptake in the cerebellum was significantly reduced in aged Tg4-42 and 5XFAD mice compared to wild-type. **(B)** Magnetic resonance image (MRI; coronal view) with volumes of interest (VOIs) of the mouse brain atlas MRIs of each mouse. **(C)** Fused ^{18}F-FDG-PET/MRI of a wild-type mouse in coronal view. **(D)** Fused ^{18}F-FDG-PET/MRI of a 7-month-old Tg4-42 mouse in coronal view with distinctly lower FDG uptake compared to the wild-type mouse. One-way-ANOVA; $^{**}p < 0.01$; $^{*}p < 0.05$; WT, wild-type; m, months; Cb, cerebellum; B, brainstem.

mice, double-transgenic mice carrying single APP and PS1 mutation are less likely to have locomotor activity impairments (Lalonde et al., 2004; Sadowski et al., 2004; Webster et al., 2013) (**Table 1**).

It has to be mentioned that the Open Field task is one of the tests with relatively high variability in experimental procedures (Walsh and Cummins, 1976). The material and the size of the arena, as well as the testing time, differ immensely between the protocols used in analyzing different AD models. For example, some mice were granted time to adapt to the apparatus (van Dam et al., 2003) and others not (Lalonde et al., 2005a; Harris et al., 2010; Jawhar et al., 2012). The amount of time tested ranged from 5 min (Arendash et al., 2001; Jawhar et al., 2012; O'Leary et al., 2018a) to 30 min (Dineley et al., 2002; Webster et al., 2013). In addition, most mice were placed into the center of the box (King and Arendash, 2002; Jawhar et al., 2012), whereas others started in the corners (van Dam et al., 2003; O'Leary et al., 2018a). While most studies use only a single trial, other groups tested the same mouse multiple times and therefore assessing habituation rather than spontaneous locomotor activity alone (Dai et al., 1995; Lalonde et al., 2005b). Furthermore, the experimental apparatus used for the Open Field often differs in size, material, form or transparency between laboratories (King and Arendash, 2002; Gulinello et al., 2009; Filali et al., 2012; Jawhar et al., 2012). These varieties need to be taken into consideration when comparing different AD mouse lines.

Several studies suggested a link between muscle strength and cognitive decline in AD patients (Boyle et al., 2009). In mice, the string suspension and grip strength test can be used to measure muscle strength (Deacon, 2013). We could show that 7-month-old Tg4-42 and 5XFAD mice did not present any impairments in muscle strength in the string suspension or grip strength tasks, consistent with previous findings for 5XFAD mice (Jawhar et al., 2012; Bhattacharya et al., 2014). However, previous studies showed a loss of muscle strength in both tests beginning at the age of 9 months (Jawhar et al., 2012). In contrast, O'Leary et al. (2018a) could show deficits already beginning from 6 to 7 months of age in 5XFAD mice. Generally speaking, a decline in muscle strength seems to be more frequent in aged AD mice (**Table 1**). Tg4-42 mice display severe memory deficits at 7 months of age and therefore mice were not tested for muscle strength at older ages, which should be investigated in upcoming studies to compare strength with other AD mouse models. The pyroglutamate Aβ3-42 expressing mouse model TBA42 showed muscle strength deficits starting with 6 months, while muscle strength declined in Tg2576 not before 14 months, preceding memory deficits

in both models (King and Arendash, 2002; Meissner et al., 2014) (**Table 1**). Interestingly, homozygous TBA42 had such severe motor deficits, that they had to be sacrificed at the age of 2 months (Lopez-Noguerola et al., 2018). APP+PS1 mice did not show signs of strength decline before 15 to 17 months of age (Holcomb et al., 1999; Arendash et al., 2001). APP+PS1 mice develop memory deficits at younger ages, similar to 5XFAD mice. Noteworthy, female and male 3xTg mice show memory impairments before the onset of motor deficits with 16 months of age (Garvock-de Montbrun et al., 2019), similar to Tg4-42 mice (**Table 1**), but memory deficits do not progress through age in 3xTg mice (Stevens and Brown, 2015). These inconsistent findings with regard to onset of memory and motor deficits should be considered when choosing a suitable mouse model for research, depending on the symptom of interest.

Motor coordination is an important aspect of AD since bradykinesia and gait disturbances are part of AD motor impairments (Scarmeas et al., 2004), correlating with a poorer outcome of patients (Waite et al., 2005).

The rotarod and balance beam test are mainly used to test motor coordination and balance in mice. Additionally, the rotarod test assesses motor learning (Hamm et al., 1994; Le Marec and Lalonde, 1997; Luong et al., 2011; Deacon, 2013).

The cerebellum as a major player of motor control is important for regulation of balance and locomotion through practice (Morton and Bastian, 2004). Especially the rotarod task is able to detect motor disturbances through cerebellar dysfunction (Shiotsuki et al., 2010).

We could show deficits in the balance beam task of aged Tg4-42 mice. In context with Lopez-Noguerola et al. (2018) who tested younger Tg4-42 mice at the age of 5 months, an age dependent decline in balance and coordination could be observed. These findings suggest an onset of this deficit in the Tg4-42 mouse model for AD at the age of 6 to 7 months.

Deterioration in the rotarod test was already observed in young Tg4-42 mice and aggravated with age. Early deficits in the rotarod have been described in male APP23 mice (van Dam et al., 2003). In contrary Tg2567 mice did not show any impairment in the rotarod (Dineley et al., 2002; King and Arendash, 2002), but the balance beam test was able to detect deficits (King and Arendash, 2002). APP/PS1 KI mice did not show any motor deterioration and were comparable to controls at even older ages (Webster et al., 2013). Strikingly, male and female 3xTg mice performed better in rotarod task than controls up to the age of 16 months (Oore et al., 2013; Stover et al., 2015; Garvock-de Montbrun et al., 2019) (**Table 1**), but performance declined with age (Garvock-de Montbrun et al., 2019). Only Filali et al. (2012) who tested only female 3xTg mice showed reduced performance in the rotarod, possibly due to protocol differences. Stover et al. (2015) suggests that tau P301L might be responsible for enhanced motor performance. Whereas other researchers found increased motor performance to be paradoxical (Filali et al., 2012), since other tau mouse models do present motor impairments in the rotarod test (Scattoni et al., 2010; Xu et al., 2010). Thus, suggesting no direct correlation between the transgene and severity of motor deficits.

Since Tg4-42 mice did not have altered muscle strength, we presumed that impairments in the balance beam task and rotarod was rather due to learning and balance, coordination impairments than muscle function. In previous studies we could show a severe learning deficit in the Morris water maze, beginning from the age of 5 months in Tg4-42 mice (Antonios et al., 2015). Interestingly, despite the massive impairments in the rotarod, the ability to swim in the Morris water maze was not altered in same-aged Tg4-42 mice (Bouter et al., 2013, 2014; Antonios et al., 2015).

The cerebellum is the center of motor function and contributes to motor learning by determining how to perform correct and accurate movements. It has been shown that cerebellar damage leads to disturbance in movements and body support (Porras-García et al., 2013) and cerebellar atrophy is characteristic for sporadic AD (Jacobs et al., 2018). Kuwabara et al. (2014) could detect relatively high levels of Aβ1-42 in cerebellar lysates and impairments in the rotarod test in 3-month-old APP/PS1 mice, but no impairments in the balance beam test.

Subsequently, we analyzed the cerebellum of Tg4-42 mice via ^{18}F-FDG-PET to detect possible synaptic dysfunctions. ^{18}F-FDG-PET, as a functional biomarker for synaptic dysfunction, confirmed findings of the behavioral tests showing reduced glucose metabolism in the cerebellum of aged Tg4-42 mice. Findings are in line with several earlier ^{18}F-FDG-PET studies showing cerebellar hypo metabolism in different transgenic mouse models of AD (Platt et al., 2011; Macdonald et al., 2014; Deleye et al., 2016; Takkinen et al., 2017; Waldron et al., 2017; Bouter et al., 2019). But furthermore, intraneuronal Aβ accumulation in the spinal cord of Tg4-42 mice have been described previously (Lopez-Noguerola et al., 2018) and may contribute to motor deficits. But since strength was not yet affected in 7-month-old Tg4-42 mice we focused on the processing and coordination of motor function by *in vivo* imaging of the cerebellum.

Interestingly, a study by Macdonald et al. (2014) using ^{18}F-FDG-PET in 2-, 5-, and 12-month-old 5XFAD mice showed decreased FDG-uptake in the cerebellum of 12-month-old 5XFAD mice while 2- and 5-month-old animals did not show significant differences to wild-type mice. In line with these findings, female 7-month-old 5XFAD performed as wild-type mice on the rotarod, while older mice display strong impairments (O'Leary et al., 2018a) (**Table 1**). However, 5XFAD mice showed decreased FDG-uptake as early as 7 months of age in our study. This seems to be an indicator of early cerebellar changes, even before motor impairments occur, as glucose metabolism is known to be an early marker of neuronal dysfunction.

Mouse models allow to investigate motor abilities and are suitable tools to analyze different aspects of AD pathologies and the effectiveness of possible therapies.

Tg4-42 displays an AD mouse model with intact general motor activity and strength, but age-dependent

motor impairments in motor coordination and balance present at the age of 7 months, most likely due to impaired cerebellar activity.

DATA AVAILABILITY

The datasets generated for this study are available on request to the corresponding author.

ETHICS STATEMENT

All animals were handled according to the guidelines of the "Society for Laboratory Animals Science" (GV-SOLAS) and the guidelines of the "Federation of European Laboratory Animal Science Association" (FELASA). All experiments were approved by the "Lower Saxony State Office for Consumer Protection and Food Safety" (LAVES).

AUTHOR CONTRIBUTIONS

JW performed the experiments, analyzed the data, and wrote the manuscript. MS performed the experiments and analyzed the data. ES, ML, TF, NB, and CI performed the experiments. CB analyzed the data and wrote the manuscript. TB participated in the discussion of the results. YB conceived and designed the project, performed the experiments, analyzed the data, and wrote the manuscript. All authors contributed to revising the manuscript and approved the final version.

FUNDING

This work was supported by the German Research Foundation (CNMPB) to YB. This study was also supported by the Jacob-Henle-Program for Experimental Medicine of the University Medicine Göttingen to JW and ML. MS was supported by Helios Kliniken GmbH. This work was supported in part by the Deutsche Forschungsgemeinschaft (DFG) for PET/MRI use (INST 335/454-1FUGG).

ACKNOWLEDGMENTS

We acknowledge the support by the Open Access Publication Funds of the Göttingen University.

REFERENCES

Alexandru, A., Jagla, W., Graubner, S., Becker, A., Bäuscher, C., Kohlmann, S., et al. (2011). Selective hippocampal neurodegeneration in transgenic mice expressing small amounts of truncated Aβ is induced by pyroglutamate-Aβ formation. *J. Neurosci.* 31, 12790–12801. doi: 10.1523/JNeurosci.1794-11.2011

Antonios, G., Borgers, H., Richard, B. C., Brauß, A., Meißner, J., Weggen, S., et al. (2015). Alzheimer therapy with an antibody against N-terminal Abeta 4-X and pyroglutamate Abeta 3-X. *Sci. Rep.* 5:17338. doi: 10.1038/srep17338

Arendash, G. W., King, D. L., Gordon, M. N., Morgan, D., Hatcher, J. M., Hope, C. E., et al. (2001). Progressive, age-related behavioral impairments in transgenic mice carrying both mutant amyloid precursor protein and presenilin-1 transgenes. *Brain Res.* 891, 42–53. doi: 10.1016/S0006-8993(00)03186-3

Bayer, T. A., and Wirths, O. (2014). Focusing the amyloid cascade hypothesis on N-truncated Abeta peptides as drug targets against Alzheimer's disease. *Acta Neuropathol.* 127, 787–801. doi: 10.1007/s00401-014-1287-x

Beauchet, O., Allali, G., Montero-Odasso, M., Sejdić, E., Fantino, B., and Annweiler, C. (2014). Motor phenotype of decline in cognitive performance among community-dwellers without dementia: population-based study and meta-analysis. *PLoS One* 9:e99318. doi: 10.1371/journal.pone.0099318

Bhattacharya, S., Haertel, C., Maelicke, A., and Montag, D. (2014). Galantamine slows down plaque formation and behavioral decline in the 5XFAD mouse model of Alzheimer's disease. *PLoS One* 9:e89454. doi: 10.1371/journal.pone.0089454

Bouter, C., Henniges, P., Franke, T. N., Irwin, C., Sahlmann, C. O., Sichler, M. E., et al. (2019). 18F-FDG-PET detects drastic changes in brain metabolism in the Tg4–42 model of Alzheimer's disease. *Front. Aging Neurosci.* 10:425. doi: 10.3389/fnagi.2018.00425

Bouter, Y., Dietrich, K., Wittnam, J., Pillot, T., Papot-Couturier, S., Lefebvre, T., et al. (2013). Tg4-42: a new mouse model of Alzheimer's disease—N-truncated amyloid β (Aβ) 4-42 induces severe neuron loss and behavioral deficits. *Alzheimers Dement.* 9, 498–499. doi: 10.1016/j.jalz.2013.05.1031

Bouter, Y., Kacprowski, T., Weissmann, R., Dietrich, K., Borgers, H., BrauÃź, A., et al. (2014). Deciphering the molecular profile of plaques, memory decline and neuron loss in two mouse models for Alzheimer's disease by deep sequencing. *Front. Aging Neurosci.* 6:75. doi: 10.3389/fnagi.2014.00075

Boyle, P. A., Buchman, A. S., Wilson, R. S., Leurgans, S. E., and Bennett, D. A. (2009). Association of muscle strength with the risk of Alzheimer disease and the rate of cognitive decline in community-dwelling older persons. *Arch. Neurol.* 66, 1339–1344. doi: 10.1001/archneurol.2009.240

Brooks, S. P., and Dunnett, S. B. (2009). Tests to assess motor phenotype in mice: a user's guide. *Nat. Rev. Neurosci.* 10, 519–529. doi: 10.1038/nrn2652

Brooks, S. P., Trueman, R. C., and Dunnett, S. B. (2012). Assessment of motor coordination and balance in mice using the rotarod, elevated bridge, and footprint tests. *Curr. Protoc. Mouse Biol.* 2, 37–53. doi: 10.1002/9780470942390.mo110165

Brown, R. E., and Wong, A. A. (2007). The influence of visual ability on learning and memory performance in 13 strains of mice. *Learn. Mem.* 14, 134–144. doi: 10.1101/lm.473907

Buchman, A. S., and Bennett, D. A. (2011). Loss of motor function in preclinical Alzheimer's disease. *Expert Rev. Neurother.* 11, 665–676. doi: 10.1586/ern.11.57

Buitrago, M. M., Schulz, J. B., Dichgans, J., and Luft, A. R. (2004). Short and long-term motor skill learning in an accelerated rotarod training paradigm. *Neurobiol. Learn. Mem.* 81, 211–216. doi: 10.1016/j.nlm.2004.01.001

Camicioli, R., Bouchard, T., and Licis, L. (2006). Dual-tasks and walking fast: relationship to extra-pyramidal signs in advanced Alzheimer disease. *J. Neurol. Sci.* 248, 205–209. doi: 10.1016/j.jns.2006.05.013

Chang, W. -H., Chen, M. C., and Cheng, I. H. (2015). Antroquinonol lowers brain amyloid-β levels and improves spatial learning and memory in a transgenic mouse model of Alzheimer's disease. *Sci. Rep.* 5:15067. doi: 10.1038/srep15067

Chu, T. H., Cummins, K., Sparling, J. S., Tsutsui, S., Brideau, C.,. Nilsson, J. T., Joseph, K. P. R., and Stys, P. K. (2017). Axonal and myelinic pathology in 5xFAD Alzheimer's mouse spinal cord. *PLoS One* 12:e0188218. doi: 10.1371/journal.pone.0188218

Cova, I., Clerici, F., Rossi, A., Cucumo, V., Ghiretti, R., Maggiore, L., et al. (2016). Weight loss predicts progression of mild cognitive impairment to Alzheimer's disease. *PLoS One* 11:e0151710. doi: 10.1371/journal.pone.0151710

Crawley, J., and Bailey, K. (2008). "Anxiety-related behaviors in mice," in *Methods of Behavior Analysis in Neuroscience*, 2nd Edn, ed. J. Buccafusco (Boca Raton, FL: CRC Press), 77–101.

Dai, H., Krost, M., and Carey, R. J. (1995). A new methodological approach to the study of habituation: the use of positive and negative behavioral indices of habituation. *J. Neurosci. Methods* 62, 169–174. doi: 10.1016/0165-0270(95)00073-9

Deacon, R. M. J. (2013). Measuring motor coordination in mice. *J. Vis. Exp.* 75:e2609. doi: 10.3791/2609

Deleye, S., Waldron, A.-M., Richardson, J. C., Schmidt, M., Langlois, X., Stroobants, S., et al. (2016). The effects of physiological and methodological determinants on 18F-FDG mouse brain imaging exemplified in a double transgenic Alzheimer model. *Mol. Imaging* 15:1536012115624919. doi: 10.1177/1536012115624919

de Paula, J. J., Albuquerque, M. R., Lage, G. M., Bicalho, M. A., Romano-Silva, M. A., and Malloy-Diniz, L. F. (2016). Impairment of fine motor dexterity in mild cognitive impairment and Alzheimer's disease dementia: association with activities of daily living. *Braz. J. Psychiatry* 38, 235–238. doi: 10.1590/1516-4446-2015-1874

Dietrich, K., Bouter, Y., Wittnam, J., Pillot, T., Papot-Couturier, S., Lefebvre, T., et al. (2013). Tg4-42: a new mouse model of Alzheimer's disease—N-truncated beta-amyloid 4-42 affects memory decline and synaptic plasticity. *Alzheimers Dement.* 9:P498. doi: 10.1016/j.jalz.2013.05.1030

Dineley, K. T., Xia, X., Bui, D., Sweatt, J. D., and Zheng, H. (2002). Accelerated plaque accumulation, associative learning deficits, and up-regulation of alpha 7 nicotinic receptor protein in transgenic mice co-expressing mutant human presenilin 1 and amyloid precursor proteins. *J. Biol. Chem.* 277, 22768–22780. doi: 10.1074/jbc.M200164200

Ewers, M., Morgan, D. G., Gordon, M. N., and Woodruff-Pak, D. S. (2006). Associative and motor learning in 12-month-old transgenic APP+PS1 mice. *Neurobiol. Aging* 27, 1118–1128. doi: 10.1016/j.neurobiolaging.2005.05.019

Filali, M., Lalonde, R., Theriault, P., Julien, C., Calon, F., and Planel, E. (2012). Cognitive and non-cognitive behaviors in the triple transgenic mouse model of Alzheimer's disease expressing mutated APP, PS1, and Mapt (3xTg-AD). *Behav. Brain Res.* 234, 334–342. doi: 10.1016/j.bbr.2012.07.004

Flood, D. G., Reaume, A. G., Dorfman, K. S., Lin, Y. G., Lang, D. M., Trusko, S. P., et al. (2002). FAD mutant PS-1 gene-targeted mice: increased A beta 42 and A beta deposition without APP overproduction. *Neurobiol. Aging* 23, 335–348.

Garvock-de Montbrun, T., Fertan, E., Stover, K., and Brown, R. E. (2019). Motor deficits in 16-month-old male and female 3xTg-AD mice. *Behav. Brain Res.* 356, 305–313. doi: 10.1016/j.bbr.2018.09.006

Gillette-Guyonnet, S., Nourhashemi, F., Andrieu, S., Glisezinski, I. de, Ousset, P. J., Riviere, D., et al. (2000). Weight loss in Alzheimer disease. *Am. J. Clin. Nutr.* 71, 637–642.

Griñán-Ferré, C., Sarroca, S., Ivanova, A., Puigoriol-Illamola, D., Aguado, F., Camins, A., et al. (2016). Epigenetic mechanisms underlying cognitive impairment and Alzheimer disease hallmarks in 5XFAD mice. *Aging* 8, 664–684. doi: 10.18632/aging.100906

Guérin, O., Andrieu, S., Schneider, S. M., Milano, M., Boulahssass, R., Brocker, P., et al. (2005). Different modes of weight loss in Alzheimer disease: a prospective study of 395 patients. *Am. J. Clin. Nutr.* 82, 435–441.

Gulinello, M., Gertner, M., Mendoza, G., Schoenfeld, B. P., Oddo, S., LaFerla, F., et al. (2009). Validation of a 2-day water maze protocol in mice. *Behav. Brain Res.* 196, 220–227. doi: 10.1016/j.bbr.2008.09.002

Hamm, R. J., Pike, B. R., O'Dell, D. M., Lyeth, B. G., and Jenkins, L. W. (1994). The rotarod test: an evaluation of its effectiveness in assessing motor deficits following traumatic brain injury. *J. Neurotrauma* 11, 187–196. doi: 10.1089/neu.1994.11.187

Hardy, J. A., and Higgins, G. A. (1992). Alzheimer's disease: the amyloid cascade hypothesis. *Science* 256, 184–185.

Harris, J. A., Devidze, N., Halabisky, B., Lo, I., Thwin, M. T., Yu, G.-Q., et al. (2010). Many neuronal and behavioral impairments in transgenic mouse models of Alzheimer's disease are independent of caspase cleavage of the amyloid precursor protein. *J. Neurosci.* 30, 372–381. doi: 10.1523/JNEUROSCI.5341-09.2010

Hau, J., and Schapiro, S. J. (2002). *Handbook of Laboratory Animal Science, Essential Principles and Practices*, 2nd Edn. Milton Park: Taylor & Francis.

Holcomb, L. A., Gordon, M. N., Jantzen, P., Hsiao, K., Duff, K., Morgan, D., et al. (1999). Behavioral changes in transgenic mice expressing both amyloid precursor protein and presenilin-1 mutations: lack of association with amyloid deposits. *Behav. Genet.* 29, 177–185.

Hsiao, K., Chapman, P., Nilsen, S., Eckman, C., Harigaya, Y., Younkin, S., et al. (1996). Correlative memory deficits, a elevation, and amyloid plaques in transgenic mice. *Science* 274, 99–103. doi: 10.1126/science.274.5284.99

Hullmann, M., Albrecht, C., van Berlo, D., Gerlofs-Nijland, M. E., Wahle, T., Boots, A. W., et al. (2017). Diesel engine exhaust accelerates plaque formation in a mouse model of Alzheimer's disease. *Part. Fibre Toxicol.* 14:35. doi: 10.1186/s12989-017-0213-5

Jacobs, H. I. L., Hopkins, D. A., Mayrhofer, H. C., Bruner, E., van Leeuwen, F. W., Raaijmakers, W., et al. (2018). The cerebellum in Alzheimer's disease: evaluating its role in cognitive decline. *Brain* 141, 37–47. doi: 10.1093/brain/awx194

Jankowsky, J. L., Slunt, H. H., Ratovitski, T., Jenkins, N. A., Copeland, N. G., and Borchelt, D. R. (2001). Co-expression of multiple transgenes in mouse CNS: a comparison of strategies. *Biomol. Eng.* 17, 157–165.

Jawhar, S., Trawicka, A., Jenneckens, C., Bayer, T. A., and Wirths, O. (2012). Motor deficits, neuron loss, and reduced anxiety coinciding with axonal degeneration and intraneuronal Aβ aggregation in the 5XFAD mouse model of Alzheimer's disease. *Neurobiol. Aging* 33, 196.e29–196.e40. doi: 10.1016/j.neurobiolaging.2010.05.027

King, D. L., and Arendash, G. W. (2002). Behavioral characterization of the Tg2576 transgenic model of Alzheimer's disease through 19 months. *Physiol. Behav.* 75, 627–642. doi: 10.1016/S0031-9384(02)00639-X

Kobayashi, D. T., and Chen, K. S. (2005). Behavioral phenotypes of amyloid-based genetically modified mouse models of Alzheimer's disease. *Genes Brain Behav.* 4, 173–196. doi: 10.1111/j.1601-183X.2005.00124.x

Kuwabara, Y., Ishizeki, M., Watamura, N., Toba, J., Yoshii, A., Inoue, T., et al. (2014). Impairments of long-term depression induction and motor coordination precede Aβ accumulation in the cerebellum of APPswe/PS1dE9 double transgenic mice. *J. Neurochem.* 130, 432–443. doi: 10.1111/jnc.12728

Lalonde, R., Dumont, M., Staufenbiel, M., and Strazielle, C. (2005a). Neurobehavioral characterization of APP23 transgenic mice with the SHIRPA primary screen. *Behav. Brain Res.* 157, 91–98. doi: 10.1016/j.bbr.2004.06.020

Lalonde, R., Kim, H. D., Maxwell, J. A., and Fukuchi, K. (2005b). Exploratory activity and spatial learning in 12-month-old APP(695)SWE/co+PS1/DeltaE9 mice with amyloid plaques. *Neurosci. Lett.* 390, 87–92. doi: 10.1016/j.neulet.2005.08.028

Lalonde, R., Fukuchi, K.-I., and Strazielle, C. (2012). Neurologic and motor dysfunctions in APP transgenic mice. *Rev. Neurosci.* 23, 363–379. doi: 10.1515/revneuro-2012-0041

Lalonde, R., Kim, H. D., and Fukuchi, K. (2004). Exploratory activity, anxiety, and motor coordination in bigenic APPswe + PS1/DeltaE9 mice. *Neurosci. Lett.* 369, 156–161. doi: 10.1016/j.neulet.2004.07.069

Larson, E. B., Kukull, W. A., and Katzman, R. L. (1992). Cognitive impairment: dementia and Alzheimer's disease. *Annu. Rev. Public Health* 13, 431–449. doi: 10.1146/annurev.pu.13.050192.002243

Larson, B., Wang, L., Bowen, J. D., McCormick, W. C., Teri, L., Crane, P., et al. (2006). Exercise is associated with reduced risk for incident dementia among persons 65 years of age and older. *J. Cardiopulm. Rehabil.* 26, 244–245. doi: 10.1097/00008483-200607000-00008

Le Marec, N., and Lalonde, R. (1997). Sensorimotor learning and retention during equilibrium tests in Purkinje cell degeneration mutant mice. *Brain Res.* 768, 310–316. doi: 10.1016/S0006-8993(97)00666-5

Lee, H.-G., Casadesus, G., Perry, G., Bryan, K., and Smith, M. (2009). "Transgenic mouse models of Alzheimer's disease," in *Methods of Behavior analysis in Neuroscience*, ed. J. J. Buccafusco (Boca Raton, FL: CRC Press), 1–18.

Lopez, O. L., Wisnieski, S. R., Becker, J. T., Boiler, F., and DeKosky, S. T. (1997). Extrapyramidal signs in patients with probable Alzheimer disease. *Arch. Neurol.* 54, 969–975. doi: 10.1001/archneur.1997.00550200033007

Lopez-Noguerola, J. S., Giessen, N. M. E., Ueberück, M., Meißner, J. N., Pelgrim, C. E., Adams, J., et al. (2018). Synergistic effect on neurodegeneration by N-truncated Aβ4-42 and pyroglutamate Aβ3-42 in a mouse model of Alzheimer's disease. *Front. Aging Neurosci.* 10:64. doi: 10.3389/fnagi.2018.00064

Luong, T. N., Carlisle, H. J., Southwell, A., and Patterson, P. H. (2011). Assessment of motor balance and coordination in mice using the balance beam. *J. Vis. Exp.* 49:2376. doi: 10.3791/2376

Macdonald, I. R., DeBay, D. R., Reid, G. A., O'Leary, T. P., Jollymore, C. T., Mawko, G., et al. (2014). Early detection of cerebral glucose uptake changes in the 5XFAD mouse. *Curr. Alzheimer Res.* 11, 450–460. doi: 10.2174/1567205011666140505111354

Masters, C. L., Simms, G., Weinman, N. A., Multhaup, G., McDonald, B. L., and Beyreuther, K. (1985). Amyloid plaque core protein in Alzheimer disease and Down syndrome. *Proc. Natl. Acad. Sci. U.S.A.* 82, 4245–4249.

Meissner, J. N., Bouter, Y., and Bayer, T. A. (2014). Neuron loss and behavioral deficits in the TBA42 mouse model expressing N-truncated pyroglutamate amyloid-beta3-42. *J. Alzheimers Dis.* 45, 471–482. doi: 10.3233/JAD-142868

Miller, B. R., Dorner, J. L., Shou, M., Sari, Y., Barton, S. J., Sengelaub, D. R., et al. (2008). Up-regulation of GLT1 expression increases glutamate uptake and attenuates the Huntington's disease phenotype in the R6/2 mouse. *Neuroscience* 153, 329–337. doi: 10.1016/j.neuroscience.2008.02.004

Moran, P. M., Higgins, L. S., Cordell, B., and Moser, P. C. (1995). Age-related learning deficits in transgenic mice expressing the 751-amino acid isoform of human beta-amyloid precursor protein. *Proc. Natl. Acad. Sci. U.S.A.* 92, 5341–5345.

Morton, S. M., and Bastian, A. J. (2004). Cerebellar control of balance and locomotion. *Neuroscientist* 10, 247–259. doi: 10.1177/1073858404263517

Mucke, L., Masliah, E., Yu, G. -Q., Mallory, M., Rockenstein, E. M., Tatsuno, G., et al. (2000). High-level neuronal expression of Aβ 1–42 in wild-type human amyloid protein precursor transgenic mice: synaptotoxicity without plaque formation. *J. Neurosci.* 20, 4050–4058. doi: 10.1523/JNEUROSCI.20-11-04050.2000

Oakley, H., Cole, S. L., Logan, S., Maus, E., Shao, P., Craft, J., et al. (2006). Intraneuronal beta-amyloid aggregates, neurodegeneration, and neuron loss in transgenic mice with five familial Alzheimer's disease mutations: potential factors in amyloid plaque formation. *J. Neurosci.* 26, 10129–10140. doi: 10.1523/JNEUROSCI.1202-06.2006

Oddo, S., Caccamo, A., Shepherd, J. D., Murphy, M. P., Golde, T. E., Kayed, R., et al. (2003). Triple-transgenic model of Alzheimer's disease with plaques and tangles: intracellular Abeta and synaptic dysfunction. *Neuron* 39, 409–421.

O'Keeffe, S. T., Kazeem, H., Philpott, R. M., Playfer, J. R., Gosney, M., and Lye, M. (1996). Gait disturbance in Alzheimer's disease: a clinical study. *Age Ageing* 25, 313–316.

O'Leary, T. P., Mantolino, H. M., Stover, K. R., and Brown, R. E. (2018a). Age-related deterioration of motor function in male and female 5xFAD mice from 3 to 16 months of age. *Genes Brain Behav.* doi: 10.1111/gbb.12538

O'Leary, T. P., Robertson, A., Chipman, P. H., Rafuse, V. F., and Brown, R. E. (2018b). Motor function deficits in the 12 month-old female 5xFAD mouse model of Alzheimer's disease. *Behav. Brain Res.* 337, 256–263. doi: 10.1016/j.bbr.2017.09.009

Oore, J. J., Fraser, L. M., and Brown, R. E. (2013). Age-related changes in motor ability and motor learning in triple transgenic (3xTg-AD) and control (B6129SF1/J) mice on the accelerating rotarod. *Proc. N. S. Inst. Sci.* 47, 281–296. doi: 10.15273/pnsis.v47i2.4343

Perucho, J., Casarejos, M. J., Rubio, I., Rodriguez-Navarro, J. A., Gómez, A., Ampuero, I., et al. (2010). The effects of parkin suppression on the behaviour, amyloid processing, and cell survival in APP mutant transgenic mice. *Exp. Neurol.* 221, 54–67. doi: 10.1016/j.expneurol.2009.09.029

Pettersson, A. F., Engardt, M., and Wahlund, L. -O. (2002). Activity level and balance in subjects with mild Alzheimer's disease. *Dement. Geriatr. Cogn. Disord.* 13, 213–216. doi: 10.1159/000057699

Pike, C. J., Overman, M. J., and Cotman, C. W. (1995). Amino-terminal deletions enhance aggregation of beta-amyloid peptides in vitro. *J. Biol. Chem.* 270, 23895–23898.

Platt, B., Drever, B., Koss, D., Stoppelkamp, S., Jyoti, A., Plano, A., et al. (2011). Abnormal cognition, sleep, EEG and brain metabolism in a novel knock-in Alzheimer mouse, PLB1. *PLoS One* 6:e27068. doi: 10.1371/journal.pone.0027068

Porras-García, M. E., Ruiz, R., Pérez-Villegas, E. M., and Armengol, J. Á. (2013). Motor learning of mice lacking cerebellar Purkinje cells. *Front. Neuroanatomy* 7:4. doi: 10.3389/fnana.2013.00004

Portelius, E., Bogdanovic, N., Gustavsson, M. K., Volkmann, I., Brinkmalm, G., Zetterberg, H., et al. (2010). Mass spectrometric characterization of brain amyloid beta isoform signatures in familial and sporadic Alzheimer's disease. *Acta Neuropathol.* 120, 185–193. doi: 10.1007/s00401-010-0690-1

Probst, A., Gotz, J., Wiederhold, K. H., Tolnay, M., Mistl, C., Jaton, A. L., et al. (2000). Axonopathy and amyotrophy in mice transgenic for human four-repeat tau protein. *Acta Neuropathol.* 99, 469–481.

Pugh, P. L., Richardson, J. C., Bate, S. T., Upton, N., and Sunter, D. (2007). Non-cognitive behaviours in an APP/PS1 transgenic model of Alzheimer's disease. *Behav. Brain Res.* 178, 18–28. doi: 10.1016/j.bbr.2006.11.044

Sadowski, M., Pankiewicz, J., Scholtzova, H., Ji, Y., Quartermain, D., Jensen, C. H., et al. (2004). Amyloid-β deposition is associated with decreased hippocampal glucose metabolism and spatial memory impairment in APP/PS1 mice. *J. Neuropathol. Exp. Neurol.* 63, 418–428. doi: 10.1093/jnen/63.5.418

Sawmiller, D., Li, S., Mori, T., Habib, A., Rongo, D., Delic, V., et al. (2017). Beneficial effects of a pyrroloquinolinequinone-containing dietary formulation on motor deficiency, cognitive decline and mitochondrial dysfunction in a mouse model of Alzheimer's disease. *Heliyon* 3:e00279. doi: 10.1016/j.heliyon.2017.e00279

Scarmeas, N., Hadjigeorgiou, G. M., Papadimitriou, A., Dubois, B., Sarazin, M., Brandt, J., et al. (2004). Motor signs during the course of Alzheimer disease. *Neurology* 63, 975–982. doi: 10.1212/01.WNL.0000138440.39918.0C

Scattoni, M. L., Gasparini, L., Alleva, E., Goedert, M., Calamandrei, G., and Spillantini, M. G. (2010). Early behavioural markers of disease in P301S tau transgenic mice. *Behav. Brain Res.* 208, 250–257. doi: 10.1016/j.bbr.2009.12.002

Schneider, F., Baldauf, K., Wetzel, W., and Reymann, K. G. (2014). Behavioral and EEG changes in male 5xFAD mice. *Physiol. Behav.* 135, 25–33. doi: 10.1016/j.physbeh.2014.05.041

Seibenhener, M. L., and Wooten, M. C. (2015). Use of the Open Field Maze to measure locomotor and anxiety-like behavior in mice. *J. Vis. Exp.* 96:e52434. doi: 10.3791/52434

Shiotsuki, H., Yoshimi, K., Shimo, Y., Funayama, M., Takamatsu, Y., Ikeda, K., et al. (2010). A rotarod test for evaluation of motor skill learning. *J. Neurosci. Methods* 189, 180–185. doi: 10.1016/j.jneumeth.2010.03.026

Shukla, V., Zheng, Y.-L., Mishra, S. K., Amin, N. D., Steiner, J., Grant, P., et al. (2013). A truncated peptide from p35, a Cdk5 activator, prevents Alzheimer's disease phenotypes in model mice. *FASEB J.* 27, 174–186. doi: 10.1096/fj.12-217497

Singh, B. K., Vatsa, N., Kumar, V., Shekhar, S., Sharma, A., and Jana, N. R. (2017). Ube3a deficiency inhibits amyloid plaque formation in APPswe/PS1δE9 mouse model of Alzheimer's disease. *Hum. Mol. Genet.* 26, 4042–4054. doi: 10.1093/hmg/ddx295

Stevens, L. M., and Brown, R. E. (2015). Reference and working memory deficits in the 3xTg-AD mouse between 2 and 15-months of age: a cross-sectional study. *Behav. Brain Res.* 278, 496–505. doi: 10.1016/j.bbr.2014.10.033

Stover, K. R., Campbell, M. A., van Winssen, C. M., and Brown, R. E. (2015). Analysis of motor function in 6-month-old male and female 3xTg-AD mice. *Behav. Brain Res.* 281, 16–23. doi: 10.1016/j.bbr.2014.11.046

Sturchler-Pierrat, C., Abramowski, D., Duke, M., Wiederhold, K. H., Mistl, C., Rothacher, S., et al. (1997). Two amyloid precursor protein transgenic mouse models with Alzheimer disease-like pathology. *Proc. Natl. Acad. Sci. U.S.A.* 94, 13287–13292.

Takkinen, J. S., López-Picón, F. R., Al Majidi, R., Eskola, O., Krzyczmonik, A., Keller, T., et al. (2017). Brain energy metabolism and neuroinflammation in ageing APP/PS1-21 mice using longitudinal 18F-FDG and 18F-DPA-714 PET imaging. *J. Cereb. Blood Flow Metab.* 37, 2870–2882. doi: 10.1177/0271678X16677990

Tesseur, I., van Dorpe, J., Bruynseels, K., Bronfman, F., Sciot, R., van Lommel, A., et al. (2000). Prominent axonopathy and disruption of axonal transport in transgenic mice expressing human apolipoprotein E4 in neurons of brain and spinal cord. *Am. J. Pathol.* 157, 1495–1510. doi: 10.1016/S0002-9440(10)64788-8

van Dam, D., D'Hooge, R., Staufenbiel, M., van Ginneken, C., van Meir, F., and de Deyn, P. P. (2003). Age-dependent cognitive decline in the APP23 model precedes amyloid deposition. *Eur. J. Neurosci.* 17, 388–396. doi: 10.1046/j.1460-9568.2003.02444.x

Waite, L. M., Grayson, D. A., Piguet, O., Creasey, H., Bennett, H. P., and Broe, G. A. (2005). Gait slowing as a predictor of incident dementia: 6-year longitudinal data from the Sydney Older Persons Study. *J. Neurol. Sci.* 229–230, 89–93. doi: 10.1016/j.jns.2004.11.009

Waldron, A.-M., Wyffels, L., Verhaeghe, J., Richardson, J. C., Schmidt, M., Stroobants, S., et al. (2017). Longitudinal characterization of 18F-FDG and 18F-AV45 uptake in the double transgenic TASTPM mouse model. *J. Alzheimers Dis.* 55, 1537–1548. doi: 10.3233/JAD-160760

Walsh, R. N., and Cummins, R. A. (1976). The open-field test: a critical review. *Psychol. Bull.* 83, 482–504.

Webster, S. J., Bachstetter, A. D., and van Eldik, L. J. (2013). Comprehensive behavioral characterization of an APP/PS-1 double knock-in mouse model of Alzheimer's disease. *Alzheimers Res. Ther.* 5:28. doi: 10.1186/alzrt182

White, H., Pieper, C., and Schmader, K. (1998). The association of weight change in Alzheimer's disease with severity of disease and mortality: a longitudinal analysis. *J. Am. Geriatr. Soc.* 46, 1223–1227.

Wilson, R. S., Bennett, D. A., Gilley, D. W., Beckett, L. A., Schneider, J. A., and Evans, D. A. (2000). Progression of parkinsonism and loss of cognitive function in Alzheimer disease. *Arch. Neurol.* 57, 855–860. doi: 10.1001/archneur.57.6.855

Wirths, O., and Bayer, T. A. (2008). Motor impairment in Alzheimer's disease and transgenic Alzheimer's disease mouse models. *Genes Brain Behav.* 7(Suppl. 1), 1–5. doi: 10.1111/j.1601-183X.2007.00373.x

Wirths, O., Breyhan, H., Schäfer, S., Roth, C., and Bayer, T. A. (2008). Deficits in working memory and motor performance in the APP/PS1ki mouse model for Alzheimer's disease. *Neurobiol. Aging* 29, 891–901. doi: 10.1016/j.neurobiolaging.2006.12.004

Wirths, O., Weis, J., Kayed, R., Saido, T. C., and Bayer, T. A. (2007). Age-dependent axonal degeneration in an Alzheimer mouse model. *Neurobiol. Aging* 28, 1689–1699. doi: 10.1016/j.neurobiolaging.2006.07.021

Wittnam, J. L., Portelius, E., Zetterberg, H., Gustavsson, M. K., Schilling, S., Koch, B., et al. (2012). Pyroglutamate amyloid β (Aβ) aggravates behavioral deficits in transgenic amyloid mouse model for Alzheimer disease. *J. Biol. Chem.* 287, 8154–8162. doi: 10.1074/jbc.M111.308601

Xu, J., Sato, S., Okuyama, S., Swan, R. J., Jacobsen, M. T., Strunk, E., et al. (2010). Tau-tubulin kinase 1 enhances prefibrillar tau aggregation and motor neuron degeneration in P301L FTDP-17 tau-mutant mice. *FASEB J.* 24, 2904–2915. doi: 10.1096/fj.09-150144

Yan, J. H., and Zhou, C. L. (2009). Effects of motor practice on cognitive disorders in older adults. *Eur. Rev. Aging Phys. Act.* 6, 67–74. doi: 10.1007/s11556-009-0049-6

Zidan, M., Arcoverde, C., Araújo, N. B. D., Vasques, P., Rios, A., Laks, J., et al. (2012). Alterações motoras e funcionais em diferentes estágios da doença de Alzheimer. *Rev. Psiquiatr. Clín.* 39, 161–165. doi: 10.1590/S0101-60832012000500003

Conflict of Interest Statement: University Medicine Göttingen has been granted a patent on the Tg4-42 mouse model, on which TB is listed as an inventor.

The remaining authors declare that the research was conducted in the absence of any commercial or financial relationships that could be construed as a potential conflict of interest.

The reviewer SV declared a past collaboration with one of the authors TB to the handling Editor.

frontiers in Behavioral Neuroscience

ORIGINAL RESEARCH
published: 04 June 2019
doi: 10.3389/fnbeh.2019.00123

Role of Tryptophan in Microbiota-Induced Depressive-Like Behavior: Evidence From Tryptophan Depletion Study

*Iva Lukić[1], Dmitriy Getselter[1], Omry Koren[2] and Evan Elliott[1]**

[1]*Molecular and Behavioral Neuroscience, Bar-Ilan University, Safed, Israel,* [2]*Microbiome Research Laboratories, The Azrieli Faculty of Medicine, Bar-Ilan University, Safed, Israel*

During the past decade, there has been a substantial rise in the knowledge about the effects of gut microbiota on host physiology and behavior, including depressive behavior. Initial studies determined that gut microbiota can regulate host tryptophan levels, which is a main serotonin precursor. A dysfunctional serotonergic system is considered to be one of the main factors contributing to the development of depression. Therefore, we hypothesized that regulation of brain tryptophan and serotonin can explain, at least partly, the effects of microbiota on depressive behavior. To test this hypothesis, we examined depressive-like behavior and brain levels of serotonin and tryptophan, of germ free (GF) and specific-pathogen free (SPF) mice under basal conditions, or after acute tryptophan depletion (ATD) procedure, which is a method to decrease tryptophan and serotonin levels in the brain. In basal conditions, GF mice exhibited less depressive-like behavior in sucrose preference, tail-suspension and forced swim tests, compared to SPF mice. In addition, in mice that were not subjected to ATD, GF mice displayed higher levels of tryptophan, serotonin and 5-hydroxyindoleacetic acid (the main degradation product of serotonin) in medial prefrontal cortex (mPFC) and hippocampus (HIPPO), compared to SPF mice. Interestingly, ATD increased depressive-like behavior of GF, but not of SPF mice. These behavioral changes were accompanied by a stronger reduction of tryptophan, serotonin and 5-hydroxyindoleacetic acid in mPFC and HIPPO in GF mice after ATD, when compared to SPF mice. Therefore, the serotonergic system of GF mice is more vulnerable to the acute challenge of tryptophan reduction, and GF mice after tryptophan reduction behave more similarly to SPF mice. These data provide functional evidence that microbiota affects depression-like behavior through influencing brain tryptophan accessibility and the serotonergic system.

Keywords: tryptophan, serotonin, microbiota, brain, depression

OPEN ACCESS

Edited by:
Tamas Kozicz,
Mayo Clinic, United States

Reviewed by:
Lorena Coretti,
University of Malta, Malta
Maria Cecilia Giron,
University of Padova, Italy

****Correspondence:***
Evan Elliott
evanmelliott@gmail.com;
evan.elliott@biu.ac.il

Received: *13 November 2018*
Accepted: *20 May 2019*
Published: *04 June 2019*

Citation:
Lukić I, Getselter D, Koren O and Elliott E (2019) Role of Tryptophan in Microbiota-Induced Depressive-Like Behavior: Evidence From Tryptophan Depletion Study. Front. Behav. Neurosci. 13:123. doi: 10.3389/fnbeh.2019.00123

Abbreviations: ATD, acute tryptophan depletion; DRN, dorsal raphe nucleus; FST, forced swim test; GF, germ free; HIPPO, hippocampus; mPFC, medial prefrontal cortex; SPF, specific pathogen free; TRP, tryptophan; TST, tail suspension test; 5-HT, 5-hydroxytryptamine; 5-HIAA, 5-hydroxyindoleacetic acid; SERT, serotonin transporter; TPH2, tryptophan hydroxylase 2.

INTRODUCTION

Depression is one of the most common psychiatric conditions, with lifetime prevalence ranging from 6 to 18% across different populations worldwide (Kessler and Bromet, 2013). Most often it is a recurrent condition, which leads to reduced quality of life in addition to an increased risk for other medical problems, such as diabetes, heart disease, and stroke (Merikangas et al., 2007; Kessler et al., 2009; Bhattacharya et al., 2014). All these factors make depression one of the leading contributors to global chronic disease burden.

The serotonin hypothesis of depression is among the first suggested biological causes of this disorder, dating from about 50 years ago, that was based on unexpected findings regarding several drug actions (Coppen, 1967; Albert et al., 2012). Although the understanding of the complexity of brain function and etiology of depression has increased much in the past 50 years, a dysfunctional serotonergic system is still considered to be one of the main factors contributing the development of depressive symptoms (Belmaker and Agam, 2008; Albert et al., 2012; Fakhoury, 2016).

In the brain, serotonin or 5-hydroxytryptamine (5-HT) is synthetized in serotonergic neurons originating from raphe nuclei, from amino acid tryptophan (TRP; Ruddick et al., 2006; Lesch and Waider, 2012). TRP crosses blood brain barrier *via* a specific transporter, competing with other large neutral amino acids to enter the brain (Ruddick et al., 2006). The first enzyme in brain serotonin synthesis pathway is tryptophan hydroxylase 2 (TPH2; Walther et al., 2003) that is only half-saturated by normal physiological TRP concentrations, and represents a rate-limiting step of the pathway (Boadle-Biber, 1993). After the release of 5-HT, the neurotransmitter is reuptaken by a serotonin transporter (SERT), to the presynaptic terminal (Borowsky and Hoffman, 1995) and can be further metabolized to 5-hydroxyindoleacetic acid (5-HIAA), as a final product of its degradation (Jacobs and Azmitia, 1992).

Certain genetic variants of serotonin receptors (Lemonde et al., 2003), SERT (Hoefgen et al., 2005; Caspi et al., 2010), as well as TPH2 (Zill et al., 2004; Zhang et al., 2005) were associated with a higher risk of depression. In addition, decreased levels of TRP in blood (Cowen et al., 1989) and 5-HIAA in cerebrospinal fluid were reported in some depressed patients (Ashcroft et al., 1966; Dencker et al., 1966). However, some of the most consistent findings regarding the role of 5-HT in the pathophysiology of depression come from studies of acute tryptophan depletion (ATD). The procedure involves dietary manipulation in order to decrease TRP levels, and subsequently brain 5-HT synthesis. TRP depletion leads to acute mood lowering effects in patients with depression in remission, as well as in first degree relatives of depressed patents but not in healthy subjects without family history of depression (Booij et al., 2003; Ruhé et al., 2007). These data suggest that vulnerability of the serotonin system is implicated in the development of depressive episode (Jans et al., 2007).

During the past decade, there was a huge rise in knowledge about the effects of gut microbiota on host physiology and behavior, including depressive behavior. For example, germ free (GF) mice exhibit less behavioral despair compared to their conventional counterparts (De Palma et al., 2015; Campos et al., 2016). Also, patients with depression have altered gut microbiota compared to healthy subjects (Jiang et al., 2015; Kelly et al., 2016; Zheng et al., 2016).

One of the potential mechanisms through which gut microbiota could impact depressive behavior is through influence on TRP and brain 5-HT metabolism. TRP, which is an essential amino acid, is mainly supplied from ingested food and is a biosynthetic precursor of a large number of host as well as microbial metabolites (Milligan et al., 1978; Lee and Lee, 2010; Agus et al., 2018). In addition, studies have shown that gut microbiota directly regulates the blood TRP levels through stimulation of serotonin production of the gut enterochromaffin cells (Yano et al., 2015). Indeed, GF mice have higher plasma levels of TRP (Wikoff et al., 2009; Clarke et al., 2013), but lower blood levels of serotonin, compared to conventional mice. However, GF mice have higher 5-HT levels in the brain (Clarke et al., 2013). Further, some studies of gut microbiota alterations in depressed patients found increased levels of *Alistipes*, a bacterial genus that produce indole from TRP (Jiang et al., 2015). The authors suggested that its enrichment could potentially decrease TRP availability for host cells, thus impacting the balance of host brain serotonergic system. While these studies have given corroborating arguments that brain accessibility to TRP and its effect on serotonin production may partially explain the effects of microbiome on depressive-like behavior, there is yet little direct functional evidence to make this mechanistic claim.

In this study, we hypothesize that microbial influence on the availability of TRP to the brain may be a mechanism explaining, at least partly, the effects of the microbiome on depressive-like behavior. To gain evidence for this hypothesis, we performed TRP depletion in GF mice and specific-pathogen free (SPF) mice, to test if TRP reduction would attenuate the anti-depressive behavior of GF animals. Indeed, we determined that in basal conditions GF mice exhibit less depressive-like behavior compared to SPF mice. However, their serotonergic system is more vulnerable to the acute challenge of TRP reduction, leading to that GF mice act more similarly to SPF mice after TRP reduction. Therefore, these data provide direct functional evidence that microbial effects on depression-like behavior can be mediated through its effects on brain TRP accessibility and consequently serotonergic system.

MATERIALS AND METHODS

Mice

All animals used in the study were bred and maintained in animal facilities at our research institute. SPF Swiss Webster male mice were housed in SPF vivarium with 12 h light/12 h dark cycle, at 22°C, with food and water available *ad libitum*. GF Swiss Webster male mice were housed in semi-solid GF isolators, also under a 12 h light/12 h dark cycle, at 22°C, with autoclaved food and water available *ad libitum*. Three to five mice were housed per cage and the experiment was

carried out at 8–10 weeks of age. In the study of behavioral differences between GF and SPF animals, a total of 20 mice was used (10 mice per group). In the study of the effects of ATD on both GF and SPF animals, a total of 44 mice were used (11 mice per group). All experimental protocols were approved by the Animal Care and Use Committee of Bar-Ilan University.

Behavioral Testing

Behavioral tests, except sucrose preference, were performed during the light phase of the diurnal cycle, between 12 a.m. and 16 p.m. On the day of behavioral testing, SPF as well as GF mice were brought to the behavioral room in the SPF facility, at least 1 h before the test, for acclimatization.

Sucrose preference test (SPT) was used to assess anhedonic behavior in mice. The test was carried out in home cages, while mice were single-housed by dividers. Each of the mouse was presented with two pipettes to choose freely: one containing drinking water and the other 0.5% sucrose solution. The position of pippets was switched every 24 h to eliminate side preference as a confounder. The test lasted 5 days, with the 1st day considered as habituation, while the next 4 days were considered as the test. During that time consumption of water and sucrose solution was measured and sucrose preference was calculated as a percentage of the volume of sucrose solution intake divided by the volume of total fluid intake.

Tail suspension test (TST) was performed by suspending mice by their tail for 6 mins, with the tape applied about 1 cm from the tip of their tail, under low light conditions (25 lux). Behavior other than trying vigorously to escape was scored as immobility, and considered as an indicator of depressive-like behavior (i.e., small movements with only front legs as well as swinging were not considered as mobility; Can et al., 2011b). The maze was cleaned with 10% alcohol after testing of each mouse. All testing was recorded by a video camera, and scoring was done manually.

Forced swim test (FST) was performed using modified procedure with pre-test 24 h before the test day (Dulawa et al., 2004). Both pre-test and test lasted 6 min and were conducted in plastic buckets 21 cm in diameter and filled with 24 ± 1°C water 15 cm from the bottom, under low light conditions (25 lux). After testing, mice were dried, and then returned to their home cages. Immobility, defined as the absence of active swimming with all four paws and tail moving, was scored during all 6 mins on the test day as a sign of depression-like behavior (Dulawa et al., 2004; Can et al., 2011a). All experiments were recorded by a video camera, and scoring was done manually.

Experimental Procedures

Characterization of Behavioral and Gene Expression Differences Between SPF and GF Mice

After SPT was done, TST and FST were performed on the next three consequent days. In the case of GF mice, they were taken out from the isolators before TST test, and till the end of behavioral experiments, they were housed in the SPF facility.

Separate cohorts of GF and SPF mice were used for analyses of dorsal raphe nucleus (DRN) gene expression. GF mice used for these analyses were sacrificed 1 h after being taken out from the isolator.

Acute TRP Depletion in SPF and GF Mice

Prior to TRP depletion procedure, mice were handled for 3 days and once gavaged with protein-carbohydrate mixture with TRP, in order to habituate to the procedure. On the experimental day, mice were food deprived for 5 h in order to avoid the effects of TRP available in regular chow. After starvation, mice were gavaged with protein-carbohydrate mixture containing TRP (TRP^+ group, 0.28% TRP of the total protein amount) or without TRP (TRP^- group). The composition of the given protein-carbohydrate mixture is shown in **Table 1**. Carbohydrates are added to the mixture in order to stimulate protein synthesis, leading to an optimal decrease of TRP levels relative to other large amino acids, which is the major factor determining TRP accessibility to the bran (Fernstrom and Wurtman, 1997; van Donkelaar et al., 2011). Mice were assigned to groups randomly and received two doses of 10 ml/kg of the corresponding mixtures, within 30 min interval. The behavioral testing or sacrifice was performed 2 h after application of the first dose. This treatment regime was chosen according to the previous study showing that it can efficiently reduce TRP levels in the blood, compared to all other large neutral amino acids, in Swiss Webster mice (van Donkelaar et al., 2010).

The schedule of the treatment and subsequent tests and sacrifices was as follows. Food deprivation started at 7 a.m., the first dose of the corresponding mixtures was given at 12 p.m., and behavioral testing or euthanasia started at 14 p.m. First, TST was performed, and after 1 day of rest, FST was performed on the next two consecutive days. At the end of each testing day, mice

TABLE 1 | Composition of protein-carbohydrate mixture and amino acid content in gelatine-based protein.

Substance	Amount in 10 ml water (g)
Protein	10
Alanin	1.10
Arginine	0.93
Aspartic acid	0.67
Cystein	0.01
Glutamic acid	1.14
Glycin	2.90
Histidin	0.10
Hydroxylysine	1.45
Hydroxiproline	0.12
Isoleucin	0.18
Leucine	0.34
Lysin	0.45
Methionin	0.10
Phenylalanin	0.26
Proline	1.76
Serine	0.38
Threonin	0.22
Tryptophan	0.00
Thyrosin	0.10
Valiun	0.33
Glucose	10
KCl	0.095
$CaCl_2{}^*2H_2O$	2.32
L-Tryptophan (TRP^+ group)	0.28
L-Tryptophan (TRP^- group)	0

were returned to their home cages and had access to the food *ad libitum*. All the procedures were done in behavioral room in the SPF animal facility. GF mice were taken out from the isolators 1 day before the 1st day of testing and placed in isocages. On the days of testing, they were brought to the behavioral room of the SPF facility, and after the tests, they were returned to isocages. Two days after completing behavioral experimentation, mice were euthanized and brains extracted.

Brain Tissue Collection

Mice were rapidly decapitated and their brains were quickly removed. The medial prefrontal cortices (mPFC), the hippocampi (HIPPO) and dorsal rapeh nucleus (DRN) were isolated using brain matrix and gauge 13 (for mPFC and HIPPO) or 14 (for DRN). Brain tissues were immediately frozen on dry ice and stored at −80°C until further application.

Neurochemical Analyses

After weighting, the desired tissue was homogenized with lysis buffer containing 1.8% perchloric acid and 10 mM ascorbic acid. After 15 min incubation on ice, the homogenates were centrifuged for 30 min 20,000x *g*, at 4°C and the supernatants were used for subsequent measurements according to Yamaguchi et al. (1981). The HPLC analyses were performed using C18 reversed-phase column (InfinityLab Poroshell 120 EC-C18, Agilent), and Agilent 1260 Infinity II system. The mobile phase was 10 mM potassium phosphate buffer with 5% methanol (pH 5.0) and the flow rate was 1 ml/min. TRP, 5-HT and 5-HIAA were identified by fluorescence detector, with wavelength set at 285 nm for excitation, and at 345 nm for emotion. During the HPLC procedure, all samples and standards were kept at 4°C and protected from light. The desired compounds were identified according to their retention times, and their amounts were calculated according to the standard curves prepared with different concentrations of the corresponding standards. The final tissue amounts of TRP, 5-HT and 5-HIAA were expressed in pg per mg of the tissue.

Gene Expression Analyses

Total RNA was extracted by PureLink RNA Mini Kit (Invitrogen, Carlsbad, CA, USA) according to the manufacturer's protocol. High Capacity cDNA Reverse Transcription kit (Life Technologies, Carlsbad, CA, USA) was used for the synthesis of cDNA, from 400 ng of total RNA from DRN extracts.

Quantitative real-time PCR was performed using Fast Start Universal SYBR Green Master (Rox; Roche) and ViiA^{TM}7 Real-Time PCR System (Life Technologies, Carlsbad, CA, USA). Relative quantification by ddCt method was used for analyses of gene expression. Primer sequences of analyzed genes: TPH2, serotonin autoreceptor (5-HT1A) and SERT, as well as housekeeping gene (actin; ACTB) are listed in the **Supplementary Table S1**.

Statistical Analyses

Statistical analyses were done by SPSS. Data from GF and SPF mice were compared using two-tailed *t*-test. The effects of mice microbiological status and TRP depletion were analyzed by two-way analysis of variance (ANOVA), followed by LSD *post hoc* test for evaluating differences between specific groups. Values that fell out of the range mean ± 2 SD were considered as outliers and excluded from the analyses. The level of significance was set at $p < 0.05$. As a measure of the effect size of ATD in GF and SPF mice, *Cohen's d* was used.

RESULTS

GF Mice Show Less Depressive-Like Behavior Compared to SPF

First, we characterized the depressive-like behavior of GF mice compared to SPF. In the SPT, an established test of anhedonia, GF mice showed a greater preference for 0.5% sucrose compared to SPF ($t = 2.34$, $p < 0.05$, **Figure 1A**). Since we proposed that GF mice are hyperhedonic, we chose 0.5% sucrose according to our pilot experiment (**Supplementary Figure S1**), showing that SPF mice drink this percentage of sucrose solution significantly less than 1% or 2% solution of sucrose.

In tests of behavioral despair, GF mice were less immobile in both TST ($t = -3.76$, $p = 0.001$, **Figure 1B**) and FST ($t = -4.40$, $p < 0.001$, **Figure 1C**), in comparison to SPF. Altogether, GF mice exhibited less depressive-like behavior paralleled to their SPF counterparts.

GF Mice Have Higher Expression of TPH2, SERT and 5-HTR1A in DRN

With the aim to obtain further insight into differences of serotonergic system of GF mice, and their depressive behavior, we assessed expression levels of TPH2, 5-HTR1A and SERT in DRN, being that it is the major source of serotonergic neurons projecting to the forebrain, involved in regulation of depressive behavior (Lesch and Waider, 2012).

The expression of TPH2 was two times higher in GF mice compared to SPF ($t = 2.50$, $p < 0.05$, **Figure 2A**). Further, the expression of 5-HTR1A was three times higher ($t = 4.16$, $p < 0.001$, **Figure 2B**), while the SERT levels of mRNA were twice higher in GF mice than in SPF ($t = 3.87$, $p < 0.01$, **Figure 2C**). Therefore, the expression of genes regulating serotonin production and firing rate of serotonergic neurons, differed in GF mice, compared to SPF.

GF Mice Are More Sensitive to TRP Depletion Than SPF

In the next set of experiments, we examined whether GF mice respond differently to the acute challenge of TRP deprivation compared to SPF, being that it is known their nervous system develops in conditions of high availability of TRP from their blood (Wikoff et al., 2009; Clarke et al., 2013). For that purpose, we performed ATD procedure.

Assessment of Depressive-Like Behavior

First, we determined how ATD affected depressive-like behavior of SPF and GF mice. In TST (**Figure 3A**), ANOVA showed a significant effect of both TRP depletion ($F = 5.26$, $p < 0.05$) and microbial status ($F = 15.82$, $p < 0.001$) of mice. However, SPF mice that underwent ATD did not significantly differ from mice receiving full amino acid mixture ($p > 0.05$, *Cohen's d* = 0.41,

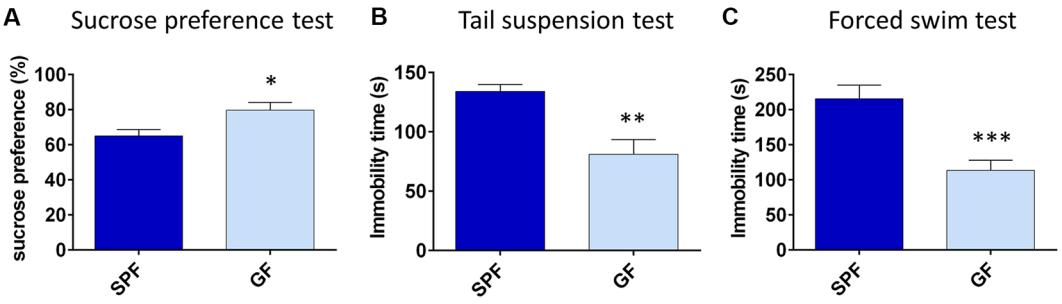

FIGURE 1 | Germ free (GF) mice exhibit less depressive-like behavior than specific pathogen free (SPF) mice. GF mice have higher preference for 0.5% sucrose **(A)**, show less immobility time in tail suspension test **(B)** and forced swim test **(C)** compared to SPF mice. $^{*}p < 0.05$, $^{**}p < 0.01$, $^{***}p < 0.001$, two-tailed *t*-test, $N = 10$ mice per group.

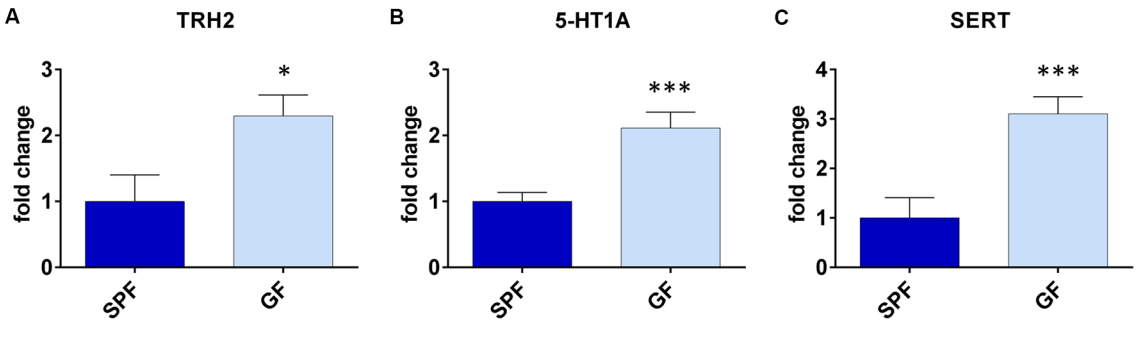

FIGURE 2 | Germ free (GF) mice exhibit different gene expressions in dorsal raphe nucleus (DRN) compared to specific pathogen free (SPF) mice. GF mice have higher expression of tryptophan hydroxilase 2 (TPH2; **A**), serotonin autoreceptor 5-HT1A **(B)** and serotonin transporter (SERT; **C**) compared to SPF mice. $^{*}p < 0.05$, $^{***}p < 0.001$, two-tailed *t*-test, $N = 10$ mice per group.

Figure 3A). On the other hand, TRP depletion led to a strong increase of immobility in GF mice in comparison to control mixture ($p < 0.05$, *Cohen's d* = 1.01, **Figure 3A**). Therefore, acute depletion of TRP from the diet had a stronger effect on GF mice than on SPF in TST.

Similarly, in FST (**Figure 3B**) the effect of ATD was significant ($F = 4.94$, $p < 0.05$), while the effect of microbial status was close to significant ($F = 3.22$, $p = 0.08$). Also, no significant differences were observed in SPF mice between TRP+ and TRP− groups ($p > 0.05$, *Cohen's d* = 0.318, **Figure 3B**), while GF TRP− group showed increased immobility time compared to GF TRP+ group ($p < 0.05$, *Cohen's d* = 0.94, **Figure 3B**). Therefore, acute depletion of TRP from diet had a stronger effect on GF mice than on SPF in FST as well.

Altogether, TRP depletion led to increased depressive-like behavior with larger effect size in GF mice compared to SPF.

Levels of TRP, 5-HT and 5-HIAA in mPFC

To gain insight into the mechanism of higher sensitivity of GF mice to ATD, we examined the levels of TRP, 5-HT and 5-HIAA in the brains of GF and SPF animals after ATD.

In mPFC, the brain region involved in coordination and control of depressive behavior (Drevets, 2000; Liu et al., 2017), levels of TRP were influenced by both TRP depletion ($F = 99.32$, $p < 0.001$) and GF state ($F = 31.14$, $p < 0.001$; **Figure 4A**). In mice not treated with TRP depletion, GF mice had higher TRP levels than SPF mice ($p < 0.001$, **Figure 4A**). In TRP depleted mice, TRP levels were significantly decreased, as expected. However, the effect of TRP depletion was much more pronounced in GF mice ($p < 0.001$, *Cohen's d* = 4.47, **Figure 4A**) than in SPF mice ($p < 0.001$, *Cohen's d* = 1.75, **Figure 4A**). Further, ANOVA showed a significant interaction between factors of ATD and microbial status ($F_{ATDxGF} = 21.33$, $p < 0.001$).

The levels of 5-HT (**Figure 4B**), as well as 5-HIAA (**Figure 4C**), which is the final product of 5-HT degradation, were also affected by both ATD (5-HT: $F = 14.09$, $p < 0.001$; 5-HIAA: $F = 12.74$, $p = 0.001$) and microbiota status (5-HT: $F = 9.41$, $p < 0.01$; 5-HIAA: $F = 5.23$, $p < 0.05$). In mice with no TRP depletion, GF mice had higher 5-HT and 5-HIAA levels compared to SPF (5-HT: $p < 0.01$, **Figure 4B**; 5-HIAA: $p < 0.01$, **Figure 4C**). After TRP depletion, levels of 5-HT and 5-HIAA were decreased only in GF mice (5-HT: $p < 0.001$, *Cohen's d* = 1.65, **Figure 4B**; 5-HIAA: $p < 0.001$, *Cohen's d* = 1.37, **Figure 4C**), and not in SPF mice (5-HT: $p > 0.05$, *Cohen's d* = 0.32; 5-HIAA: $p > 0.05$, *Cohen's d* = 0.84). The interactions of ATD and GF status at the levels of 5-HT and 5-HIAA were also close to significance (5-HT: $F_{ATDxGF} = 3.16$, $p = 0.08$; 5-HIAA: $F_{ATDxGF} = 3.80$, $p = 0.06$).

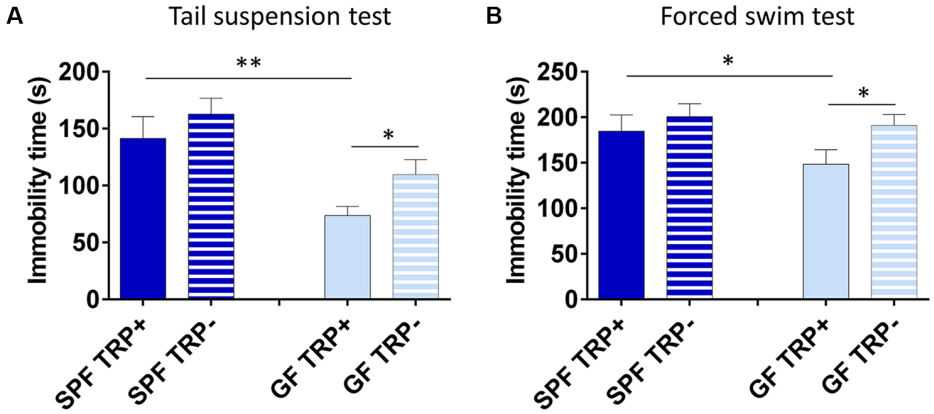

FIGURE 3 | Effects of acute tryptophan depletion (ATD) on depressive-like behavior in germ free (GF) and specific pathogen free (SPF) mice. Changes in immobility time in tail suspension test **(A)** and forced swim test **(B)** after ATD in GF and SPF mice. **TRP^{+}** - group receiving control amino acid mixture with tryptophan, **TRP^{-}** - group receiving amino acid mixture without tryptophan. *$p < 0.05$, **$p < 0.01$, LSD *post hoc* test, $N = 11$ mice per group.

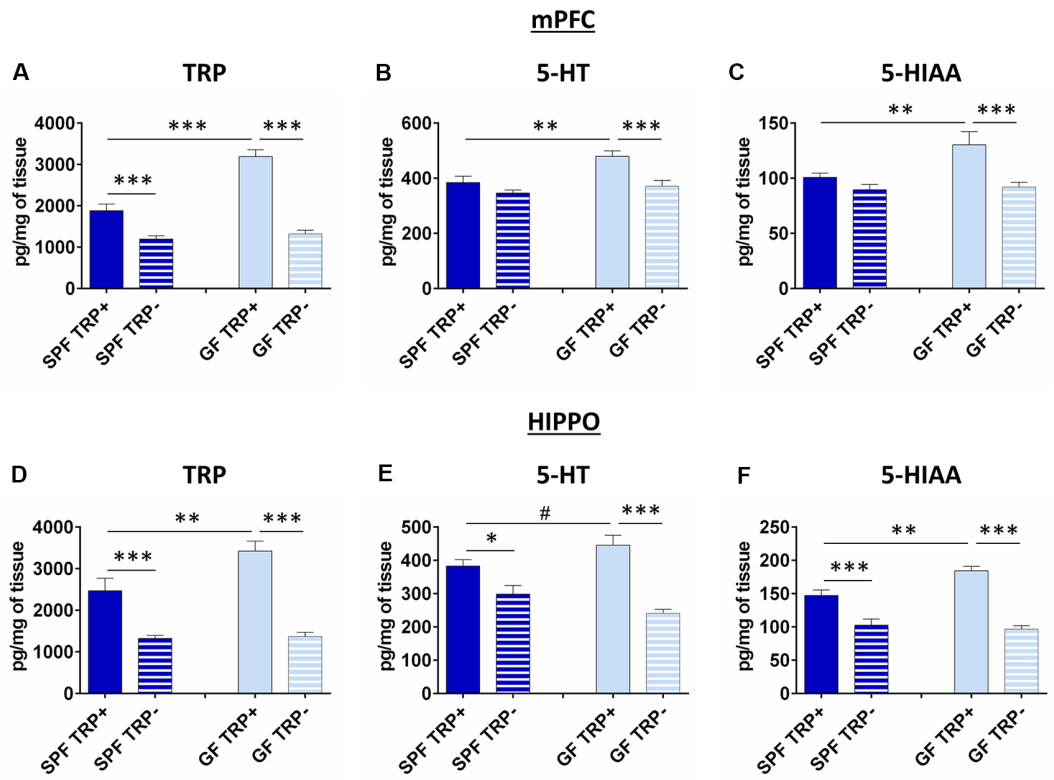

FIGURE 4 | Effects of ATD on tryptophan, serotonin and its metabolite in the brain of GF and SPF mice. Changes in the levels of tryptophan (TRP; **A**), serotonin (5-HT; **B**) and the main serotonin metabolite (5-HIAA) in medial prefrontal cortex (mPFC) after ATD in GF and SPF mice. Changes in levels of TRP **(D)** serotonin **(E)** and 5-HIAA **(F)** in hippocampus (HIPPO) after ATD in GF and SPF mice. TRP^{+} - group receiving control amino acid mixture with tryptophan, TRP^{-} - group receiving amino acid mixture without tryptophan. $^{\#}1 > p > 0.05$, *$p < 0.05$, **$p < 0.01$, ***$p < 0.01$, LSD *post hoc* test, $N = 10$ mice per group.

The ratio of 5-HT/5-HIAA, as a measure of 5-HT turnover, was not affected by any of the treatments (data not shown).

Therefore, GF mice had more 5-HT in the mPFC, but their 5-HT system showed higher vulnerability to ATD challenge, compared to SPF.

Levels of TRP, 5-HT and 5-HIAA in HIPPO

In HIPPO, a brain region also involved pathophysiology of depression (Campbell and Macqueen, 2004; Liu et al., 2017), the levels of TRP were affected by both TRP depletion ($F = 64.48$, $p < 0.001$) and GF status ($F = 6.31$, $p < 0.05$; **Figure 4D**), similarly

to mPFC. In mice not subjected to TRP depletion, SPF group had lower levels of TRP compared to GF mice ($p < 0.01$, **Figure 4D**). ATD lead to TRP decrease in both SPF ($p < 0.001$, *Cohen's d* = 1.66, **Figure 4D**) and GF mice ($p < 0.001$, *Cohen's d* = 3.63, **Figure 4D**), as expected, but the effect was greater in GF animals. There was also a significant interaction of TRP depletion and microbiota status ($F_{ATDxGF} = 5.16$, $p < 0.05$).

Serotonin levels in HIPPO (**Figure 4E**) were affected by ATD treatment ($F = 41.03$, $p < 0.001$) but not by the absence of microbiota. There was a tendency of increased 5-HT levels in SPF mice compared to GF control mice ($p = 0.058$, **Figure 4D**). After TRP depletion, 5-HT levels dropped in both SPF ($p < 0.05$, *Cohen's d* = 1.18, **Figure 4D**) and GF ($p < 0.001$, *Cohen's d* = 2.88, **Figure 4D**) mice, but the effect was stronger in GF animals. Additionally, the interaction of TRP depletion and microbiota presence was significant ($F_{ATDxGF} = 7.12$, $p < 0.05$).

The levels of 5-HIAA (**Figure 4F**) were affected by both ATD procedure ($F = 80.83$, $p < 0.001$) and GF status ($F = 4.84$, $p < 0.05$). In mice not subjected to TRP depletion, GF had higher 5-HIAA levels compared to SPF ($p < 0.01$, **Figure 4F**). However, the decrease in 5-HIAA was higher in GF TRP− compared to GF TRP+ mice ($p < 0.001$, *Cohen's d* = 4.55, **Figure 4F**), than in SPF TRP− compared to SPF TRP+ mice ($p < 0.001$, *Cohen's d* = 1.60, **Figure 4F**). Also, the significant interaction of ATD and GF status was detected ($F_{ATDxGF} = 8.99$, $p < 0.01$).

There were no differences between groups in 5-HT turnover (data not shown).

In conclusion, 5-HT system in HIPPO, as in mPFC, was affected more strongly in GF mice than in SPF.

DISCUSSION

There is an increasing interest in dysbiosis of gut microbiota and its role in the development of various psychiatric problems, including depression. Our results show that GF mice exhibit less depressive-like phenotype, but they are more sensitive to acute TRP depletion challenge. These results give direct evidence that TRP availability to the brain and its subsequent regulation of serotonin levels is one mechanism through which gut microbiota may affect depression behavior.

We first characterized the depressive-like behavior of GF animals, compared to their counterparts with normal nonpathogenic commensal microbiota. Indeed, it was already reported that GF mice exhibit different behavior compared to control mice: they are less anxious, with altered social behavior, and impaired memory. Our results are in concert with previous data showing that GF mice display reduced immobility in tests of behavioral despair, TST (De Palma et al., 2015) and FST (Campos et al., 2016). However, contrary to recent data where the authors reported no difference in sucrose preference (Campos et al., 2016), our results showed that GF mice are also hyperhedonic compared to SPF mice. The reason for this discrepancy could be due to the fact that we used 0.5% of sucrose in the test of anhedonia, while Campos et al. (2016) used 2% sucrose solution for the test. Therefore, using a lower concentration of sucrose, we were able to detect an increased preference of GF mice for sucrose solution. Altogether, GF mice exhibit a strong reduction of depressive-like behavior.

To start revealing molecular mechanisms underlying these differences in depressive behavior, we evaluated levels of genes related to serotonin metabolism in DRN, the largest nucleus with serotonergic neurons projecting to the forebrain (Jacobs and Azmitia, 1992). We found increased levels of TPH2, the rate-limiting enzyme responsible for serotonin synthesis. The previous study of serotonin system in GF mice did not find differences in TPH2 in HIPPO (Clarke et al., 2013). However, since the DRN is the major site of serotonin synthesis, our results indicate that production of serotonin is increased in GF mice, as indeed was confirmed by HPLC analyses (discussed below). The expression of 5-HT1A autoreceptor and SERT were also increased in DRN of GF mice. In DRN, 5-HT1A is a somatodendric autoreceptor, a part of negative feedback loop, sensing the serotonin release and inhibiting further serotonin release, while SERT plays a role of serotonin clearance from the synaptic cleft (Jacobs and Azmitia, 1992). Therefore, an increased expression of these two components of serotonergic system in DRN could indicate that the firing rate of serotonin neurons is decreased. However, it could be also an adaptation mechanism to the high availability of TRP in GF animals, and consequently, high serotonin synthesis, leading to actually decreased depressive-like behavior in GF mice compared to SPF.

To further evaluate the role of microbiota in shaping serotonergic system and depressive behavior of the host organism, we used TRP depletion procedure, known to be a good indicator of vulnerability of brain serotonin system and predisposition to depression (Jans et al., 2007). In humans, TRP depletion induces a decrease in mood in depressive patients or healthy subjects with a family history of depression, but not in euthymic controls (Booij et al., 2003; Ruhé et al., 2007). Effects of ATD on anxiety and depression-like behavior in animal studies are mixed, likely reflecting variation in vulnerability of different rodent strains to serotonin system manipulation (Blokland et al., 2002; Jans et al., 2007, 2010; van Donkelaar et al., 2010; Biskup et al., 2012). In our study, GF mice, despite showing reduced basal levels of depression, were more sensitive to acute TRP reduction, i.e., exacerbation of their depression-like behavior was much stronger than in SPF mice. In fact, GF mice after TRP reduction displayed similar depressive-like behavior to SPF mice. The fact that ATD did not affect depressive-like behavior of control SPF Swiss Webster mice is in line with previous studies demonstrating that ATD did not change anxiety and depression-like behavior of SPF C57 mice (van Donkelaar et al., 2010) or Brown Norway rats (Jans et al., 2010). However, the same procedure augmented depressive-like behavior of GF mice. Therefore, our results indicate that the presence of microbiota can protect mice from the behavioral consequences of TRP depletion.

GF mice had higher TRP concentration in the brain than SPF mice, which is in accordance with previous data showing that GF mice have elevated plasma TRP levels (Wikoff et al., 2009; Clarke et al., 2013). Accordingly, levels of serotonin were also

elevated, with a more pronounced increase in mPFC than in HIPPO. Indeed, expression of TPH2 in DRN, the major enzyme involved in the synthesis of brain serotonin, was two times higher in GF mice compared to SPF. The levels of 5-HIAA, a major metabolite of serotonin, was also increased in brains of GF mice receiving control amino acid mixture, while 5-HIAA/5-HT levels did not differ compared to SPF mice fed with control amino acid mixture. Therefore, it seems that in GF conditions, brain serotonin synthesis is increased, as so is its release and degradation, resulting in no change in its turnover. The higher levels of serotonin and 5-HIAA have already been reported in HIPPO of GF mice (Clarke et al., 2013). However, our data indicate that the elevation was more pronounced in mPFC than in HIPPO. Also, this increase of brain serotonin levels, especially in the mPFC, was parallel to the less depressive-like phenotype of GF mice.

After TRP depletion, the decrease of brain TRP was much more pronounced in GF mice than in SPF. This TRP reduction resulted in decreased serotonin levels in mPFC of GF mice but not SPF mice. In HIPPO, after ATD, serotonin levels were lower in both GF and SPF mice, but the decrease was more prominent in GF mice. Therefore, the stronger effect of TRP depletion on brain serotonin reduction in GF mice was in concordance with their increased depressive-like behavior after ATD.

There are several possible explanations of why SPF mice are less vulnerable to ATD, both at the molecular and behavioral levels, compared to GF mice. First, microbiota induces the production of serotonin from TRP in gut enterochromaffin cells (Yano et al., 2015), therefore decreasing the availability of dietary TRP to enter the bloodstream and brain, and to be converted to serotonin in the brain. In GF animals, in contrast, the ingested TRP will be more readily available to enter the brain, induce serotonin production, and have behavioral effects. Therefore, the action of enterochromaffin cells may attenuate the effects of ATD in SPF mice. In other words, in such way, SPF mice can be less vulnerable to the acute effects of dietary fluctuation in TRP levels. Second, there is also a possibility that TRP and serotonin produced by gut bacteria (Priya et al., 2014; Roshchina, 2016) may be supplementing the brain of SPF mice, therefore attenuating the effect of ATD. However, this is a more controversial claim. Namely, although there are some data showing that bacteria can produce TRP (Priya et al., 2014), it is still regarded that the main source of TRP for mammals is supplied by ingested food (Agus et al., 2018). Then, it is considered that most brain serotonin is produced in specific neurons of the brainstem and it does not cross the blood brain barrier (Ruddick et al., 2006; El-Merahbi et al., 2015). However, there is some evidence that brain endothelial cells express SERT, opening a possibility that blood can provide the brain with serotonin (Brust et al., 2000; Wakayama et al., 2002) which could certainly be an intriguing topic for further research. Finally, microbiota can be an important factor in the shaping of brain serotonergic system as also observed in our data by increased expression of TPH2, 5-HT1A and SERT in DRN of GF mice (Clarke et al., 2013; O'Mahony et al., 2015), and in such way it can possibly influence on the sensitivity of the serotonergic system to acute TRP deficits as well.

Overall, we have found that the presence of microbiota in mice is accompanied by lower serotonin levels and higher levels of depressive-like behavior. In contrast, the presence of microbiota can provide a better resistance to mood lowering effect induced by acute depletion of brain TRP. Therefore, this suggests that microbiota regulation of depressive behavior is complex, and may be disadvantageous or beneficial, dependent on the environmental conditions (i.e., baseline or conditions of reduced TRP brain levels), which is also in line with previous data. For example, it was shown that GF mice, despite exhibiting anxiolytic and anti-depressive phenotype, have more exaggerated rise of corticosterone, in a response to restrained stress (Sudo et al., 2004; Diaz Heijtz et al., 2011; Neufeld et al., 2011; Clarke et al., 2013), which is related to increased predisposition for depression (de Kloet et al., 2005). On the other hand, GF mice showed hypo-responsiveness to LPS challenge as well as maternal separation (De Palma et al., 2015; Campos et al., 2016). Namely, in the absence of microbiota, mice were resistant to LPS-induced depressive-like changes in behavior (Campos et al., 2016). In a separate study, examining the effects of early life stress, gut microbiota was shown to be an important factor driving depressive and anxiety-like phenotype later in the adult life, while GF mice were resilient to such experience (De Palma et al., 2015). Therefore, normal gut microbiota could be protective to some vulnerability factors towards developing depression, while mediating unfavorable effects of some other depression vulnerability factors. Which particular bacterial groups are involved in these effects is an avenue for future research.

In conclusion, our data revealed anti-depressive effect of microbiota absence, but also higher sensitivity of GF mice in response to the challenge of TRP depletion. These results suggest that microbiota, through affecting brain TRP availability, affects the brain serotonergic system of the host, and can influence the vulnerability to depression.

ETHICS STATEMENT

The study was carried out in accordance with the recommendations of the Institutional Animal Care and Use Committee of Bar Ilan University Faculty of Medicine and the protocol for this project was approved by the Institutional Animal Care and Use Committee of Bar Ilan University Faculty of Medicine.

AUTHOR CONTRIBUTIONS

IL took part in designing the study, conducted experimental work, analyzed the data, and wrote the manuscript. DG helped in conducting the experimental work. OK took part in analyzing the results and revised the manuscript. EE designed the study, discussed results and revised the manuscript.

FUNDING

This work was supported by a donation from Teva Pharmaceuticals as part of their support for the Azrieli

Faculty of Medicine of Bar Ilan University. This work was also supported by the Israel Science Foundation (grant number 898/17).

ACKNOWLEDGMENTS

We thank Roey Lahav, the manager of animal facilities at The Azrieli Faculty of Medicine, for handling of germ free mice in isolators. We thank Dr Nir Quit and Michal Leshem, from Chemistry and Biology of Protein-Protein Interactions Laboratory at The Azrieli Faculty of Medicine, for help during HPLC analyses.

SUPPLEMENTARY MATERIAL

The Supplementary Material for this article can be found online at: https://www.frontiersin.org/articles/10.3389/fnbeh.2019.00123/full#supplementary-material

REFERENCES

Agus, A., Planchais, J., and Sokol, H. (2018). Gut microbiota regulation of tryptophan metabolism in health and disease. *Cell Host Microbe* 23, 716–724. doi: 10.1016/j.chom.2018.05.003

Albert, P. R., Benkelfat, C., and Descarries, L. (2012). The neurobiology of depression--revisiting the serotonin hypothesis. I. Cellular and molecular mechanisms. *Philos. Trans. R. Soc. Lond. B Biol. Sci.* 367, 2378–2381. doi: 10.1098/rstb.2012.0190

Ashcroft, G. W., Crawford, T. B. B., Eccleston, D., Sharman, D. F., Macdougall, E., Stanton, J. B., et al. (1966). 5-hydroxyindole compounds in the cerebrospinal fluid of patients with psychiatric or neurological diseases. *Lancet* 288, 1049–1052. doi: 10.1016/s0140-6736(66)92028-9

Belmaker, R. H., and Agam, G. (2008). Major depressive disorder. *N. Engl. J. Med.* 358, 55–68. doi: 10.1056/NEJMra073096

Bhattacharya, R., Shen, C., and Sambamoorthi, U. (2014). Excess risk of chronic physical conditions associated with depression and anxiety. *BMC Psychiatry* 14:10. doi: 10.1186/1471-244x-14-10

Biskup, C. S., Sánchez, C. L., Arrant, A., Van Swearingen, A. E. D., Kuhn, C., and Zepf, F. D. (2012). Effects of acute tryptophan depletion on brain serotonin function and concentrations of dopamine and norepinephrine in C57BL/6J and BALB/cJ mice. *PLoS One* 7:e35916. doi: 10.1371/journal.pone.0035916

Blokland, A., Lieben, C., and Deutz, N. E. P. (2002). Anxiogenic and depressive-like effects, but no cognitive deficits, after repeated moderate tryptophan depletion in the rat. *J. Psychopharmacol.* 16, 39–49. doi: 10.1177/026988110201600112

Boadle-Biber, M. C. (1993). Regulation of serotonin synthesis. *Prog. Biophys. Mol. Biol.* 60, 1–15. doi: 10.1016/0079-6107(93)90009-9

Booij, L., Van der Does, A. J. W., and Riedel, W. J. (2003). Monoamine depletion in psychiatric and healthy populations: review. *Mol. Psychiatry* 8, 951–973. doi: 10.1038/sj.mp.4001423

Borowsky, B., and Hoffman, B. J. (1995). Neurotransmitter transporters: molecular biology, function and regulation. *Int. Rev. Neurobiol.* 38, 139–199. doi: 10.1016/s0074-7742(08)60526-7

Brust, P., Friedrich, A., Krizbai, I. A., Bergmann, R., Roux, F., Ganapathy, V., et al. (2000). Functional expression of the serotonin transporter in immortalized rat brain microvessel endothelial cells. *J. Neurochem.* 74, 1241–1248. doi: 10.1046/j.1471-4159.2000.741241.x

Campbell, S., and Macqueen, G. (2004). The role of the hippocampus in the pathophysiology of major depression. *J. Psychiatry Neurosci.* 29, 417–426.

Campos, A. C., Rocha, N. P., Nicoli, J. R., Vieira, L. Q., Teixeira, M. M., and Teixeira, A. L. (2016). Absence of gut microbiota influences lipopolysaccharide-induced behavioral changes in mice. *Behav. Brain Res.* 312, 186–194. doi: 10.1016/j.bbr.2016.06.027

Can, A., Dao, D. T., Arad, M., Terrillion, C. E., Piantadosi, S. C., and Gould, T. D. (2011a). The mouse forced swim test. *J. Vis. Exp.* 59:e3638. doi: 10.3791/3638

Can, A., Dao, D. T., Terrillion, C. E., Piantadosi, S. C., Bhat, S., and Gould, T. D. (2011b). The tail suspension test. *J. Vis. Exp.* 59:e3769. doi: 10.3791/3769

Caspi, A., Hariri, A. R., Holmes, A., Uher, R., and Moffitt, T. E. (2010). Genetic sensitivity to the environment: the case of the serotonin transporter gene and its implications for studying complex diseases and traits. *Focus* 8, 398–416. doi: 10.1176/foc.8.3.foc398

Clarke, G., Grenham, S., Scully, P., Fitzgerald, P., Moloney, R. D., Shanahan, F., et al. (2013). The microbiome-gut-brain axis during early life regulates the hippocampal serotonergic system in a sex-dependent manner. *Mol. Psychiatry* 18, 666–673. doi: 10.1038/mp.2012.77

Coppen, A. (1967). The biochemistry of affective disorders. *Br. J. Psychiatry* 113, 1237–1264. doi: 10.1192/bjp.113.504.1237

Cowen, P. J., Parry-Billings, M., and Newsholme, E. A. (1989). Decreased plasma tryptophan levels in major depression. *J. Affect. Disord.* 16, 27–31. doi: 10.1016/0165-0327(89)90051-7

de Kloet, E., Joëls, M., and Holsboer, F. (2005). Stress and the brain: from adaptation to disease. *Nat. Rev. Neurosci.* 6, 463–475. doi: 10.1038/nrn1683

Dencker, S. J., Malm, U., Roos, B.-E., and Werdinius, B. (1966). Acid monoamine metabolites of cerebrospinal fluid in mental depression and mania. *J. Neurochem.* 13, 1545–1548. doi: 10.1111/j.1471-4159.1966.tb04320.x

De Palma, G., Blennerhassett, P., Lu, J., Deng, Y., Park, A. J., Green, W., et al. (2015). Microbiota and host determinants of behavioural phenotype in maternally separated mice. *Nat. Commun.* 6:7735. doi: 10.1038/ncomms8735

Diaz Heijtz, R., Wang, S., Anuar, F., Qian, Y., Björkholm, B., Samuelsson, A., et al. (2011). Normal gut microbiota modulates brain development and behavior. *Proc. Natl. Acad. Sci. U S A* 108, 3047–3052. doi: 10.1073/pnas.1010529108

Drevets, W. C. (2000). Functional anatomical abnormalities in limbic and prefrontal cortical structures in major depression. *Prog. Brain Res.* 126, 413–431. doi: 10.1016/S0079-6123(00)26027-5

Dulawa, S. C., Holick, K. A., Gundersen, B., and Hen, R. (2004). Effects of chronic fluoxetine in animal models of anxiety and depression. *Neuropsychopharmacology* 29, 1321–1330. doi: 10.1038/sj.npp.1300433

El-Merahbi, R., Löffler, M., Mayer, A., and Sumara, G. (2015). The roles of peripheral serotonin in metabolic homeostasis. *FEBS Lett.* 589, 1728–1734. doi: 10.1016/j.febslet.2015.05.054

Fakhoury, M. (2016). Revisiting the serotonin hypothesis: implications for major depressive disorders. *Mol. Neurobiol.* 53, 2778–2786. doi: 10.1007/s12035-015-9152-z

Fernstrom, J. D., and Wurtman, R. J. (1997). Brain serotonin content: physiological regulation by plasma neutral amino acids. *Obes. Res.* 5, 377–380. doi: 10.1002/j.1550-8528.1997.tb00567.x

Hoefgen, B., Schulze, T. G., Ohlraun, S., von Widdern, O., Höfels, S., Gross, M., et al. (2005). The power of sample size and homogenous sampling: association between the 5-HTTLPR serotonin transporter polymorphism and major depressive disorder. *Biol. Psychiatry* 57, 247–251. doi: 10.1016/j.biopsych.2004.11.027

Jacobs, B. L., and Azmitia, E. C. (1992). Structure and function of the brain serotonin system. *Physiol. Rev.* 72, 165–229. doi: 10.1152/physrev.1992.72.1.165

Jans, L., Korte-Bouws, G., Korte, S., and Blokland, A. (2010). The effects of acute tryptophan depletion on affective behaviour and cognition in Brown Norway and Sprague Dawley rats. *J. Psychopharmacol.* 24, 605–614. doi: 10.1177/0269881108099424

Jans, L. A. W., Riedel, W. J., Markus, C. R., and Blokland, A. (2007). Serotonergic vulnerability and depression: assumptions, experimental evidence and implications. *Mol. Psychiatry* 12, 522–543. doi: 10.1038/sj.mp.4001920

Jiang, H., Ling, Z., Zhang, Y., Mao, H., Ma, Z., Yin, Y., et al. (2015). Altered fecal microbiota composition in patients with major depressive disorder. *Brain Behav. Immun.* 48, 186–194. doi: 10.1016/j.bbi.2015.03.016

Kelly, J. R., Borre, Y., O' Brien, C., Patterson, E., El Aidy, S., Deane, J., et al. (2016). Transferring the blues: depression-associated gut microbiota induces neurobehavioural changes in the rat. *J. Psychiatr. Res.* 82, 109–118. doi: 10.1016/j.jpsychires.2016.07.019

Kessler, R. C., Aguilar-Gaxiola, S., Alonso, J., Chatterji, S., Lee, S., Ormel, J., et al. (2009). The global burden of mental disorders: an update from the WHO World Mental Health (WMH) surveys. *Epidemiol. Psichiatr. Soc.* 18, 23–33. doi: 10.1017/s1121189x00001421

Kessler, R. C., and Bromet, E. J. (2013). The epidemiology of depression across cultures. *Annu. Rev. Public Health* 34, 119–138. doi: 10.1146/annurev-publhealth-031912-114409

Lee, J.-H., and Lee, J. (2010). Indole as an intercellular signal in microbial communities. *FEMS Microbiol. Rev.* 34, 426–444. doi: 10.1111/j.1574-6976.2009.00204.x

Lemonde, S., Turecki, G., Bakish, D., Du, L., Hrdina, P. D., Bown, C. D., et al. (2003). Impaired repression at a 5-hydroxytryptamine 1A receptor gene polymorphism associated with major depression and suicide. *J. Neurosci.* 23, 8788–8799. doi: 10.1523/jneurosci.23-25-08788.2003

Lesch, K.-P., and Waider, J. (2012). Serotonin in the modulation of neural plasticity and networks: implications for neurodevelopmental disorders. *Neuron* 76, 175–191. doi: 10.1016/j.neuron.2012.09.013

Liu, W., Ge, T., Leng, Y., Pan, Z., Fan, J., Yang, W., et al. (2017). The role of neural plasticity in depression: from hippocampus to prefrontal cortex. *Neural Plast.* 2017:6871089. doi: 10.1155/2017/6871089

Merikangas, K. R., Ames, M., Cui, L., Stang, P. E., Ustun, T. B., Von Korff, M., et al. (2007). The impact of comorbidity of mental and physical conditions on role disability in the US adult household population. *Arch. Gen. Psychiatry* 64, 1180–1188. doi: 10.1001/archpsyc.64.10.1180

Milligan, T. W., Doran, T. I., Straus, D. C., and Mattingly, S. J. (1978). Growth and amino acid requirements of various strains of group B streptococci. *J. Clin. Microbiol.* 7, 28–33.

Neufeld, K. M., Kang, N., Bienenstock, J., and Foster, J. A. (2011). Reduced anxiety-like behavior and central neurochemical change in germ-free mice. *Neurogastroenterol. Motil.* 23: 255–e119. doi: 10.1111/j.1365-2982.2010.01620.x

O'Mahony, S. M., Clarke, G., Borre, Y. E., Dinan, T. G., and Cryan, J. F. (2015). Serotonin, tryptophan metabolism and the brain-gut-microbiome axis. *Behav. Brain Res.* 277, 32–48. doi: 10.1016/j.bbr.2014.07.027

Priya, V. K., Sarkar, S., and Sinha, S. (2014). Evolution of tryptophan biosynthetic pathway in microbial genomes: a comparative genetic study. *Syst. Synth. Biol.* 8, 59–72. doi: 10.1007/s11693-013-9127-1

Roshchina, V. V. (2016). New trends and perspectives in the evolution of neurotransmitters in microbial, plant and animal cells. *Adv. Exp. Med. Biol.* 874, 25–77. doi: 10.1007/978-3-319-20215-0_2

Ruddick, J. P., Evans, A. K., Nutt, D. J., Lightman, S. L., Rook, G. A., and Lowry, C. A. (2006). Tryptophan metabolism in the central nervous system: medical implications. *Expert Rev. Mol. Med.* 8, 1–27. doi: 10.1017/S1462399406000068

Ruhé, H. G., Mason, N. S., and Schene, A. H. (2007). Mood is indirectly related to serotonin, norepinephrine and dopamine levels in humans: a meta-analysis of monoamine depletion studies. *Mol. Psychiatry* 12, 331–359. doi: 10.1038/sj.mp.4001949

Sudo, N., Chida, Y., Aiba, Y., Sonoda, J., Oyama, N., Yu, X.-N., et al. (2004). Postnatal microbial colonization programs the hypothalamic-pituitary-adrenal system for stress response in mice. *J. Physiol.* 558, 263–275. doi: 10.1113/jphysiol.2004.063388

van Donkelaar, E. L., Blokland, A., Ferrington, L., Kelly, P. A. T., Steinbusch, H. W. M., and Prickaerts, J. (2011). Mechanism of acute tryptophan depletion: is it only serotonin? *Mol. Psychiatry* 16, 695–713. doi: 10.1038/mp.2011.9

van Donkelaar, E. L., Blokland, A., Lieben, C. K. J., Kenis, G., Ferrington, L., Kelly, P. A. T., et al. (2010). Acute tryptophan depletion in C57BL/6 mice does not induce central serotonin reduction or affective behavioural changes. *Neurochem. Int.* 56, 21–34. doi: 10.1016/j.neuint.2009.08.010

Wakayama, K., Ohtsuki, S., Takanaga, H., Hosoya, K., and Terasaki, T. (2002). Localization of norepinephrine and serotonin transporter in mouse brain capillary endothelial cells. *Neurosci. Res.* 44, 173–180. doi: 10.1016/s0168-0102(02)00120-7

Walther, D. J., Peter, J.-U., Bashammakh, S., Hörtnagl, H., Voits, M., Fink, H., et al. (2003). Synthesis of serotonin by a second tryptophan hydroxylase isoform. *Science* 299:76. doi: 10.1126/science.1078197

Wikoff, W. R., Anfora, A. T., Liu, J., Schultz, P. G., Lesley, S. A., Peters, E. C., et al. (2009). Metabolomics analysis reveals large effects of gut microflora on mammalian blood metabolites. *Proc. Natl. Acad. Sci. U S A* 106, 3698–3703. doi: 10.1073/pnas.0812874106

Yamaguchi, T., Sawada, M., Kato, T., and Nagatsu, T. (1981). Demonstration of tryptophan 5-monooxygenase activity in human-brain by highly sensitive high-performance liquid-chromatography with fluorometric detection. *Biochem. Int.* 2, 295–303.

Yano, J. M., Yu, K., Donaldson, G. P., Shastri, G. G., Ann, P., Ma, L., et al. (2015). Indigenous bacteria from the gut microbiota regulate host serotonin biosynthesis. *Cell* 161, 264–276. doi: 10.1016/j.cell.2015.02.047

Zhang, X., Gainetdinov, R. R., Beaulieu, J.-M., Sotnikova, T. D., Burch, L. H., Williams, R. B., et al. (2005). Loss-of-Function mutation in tryptophan hydroxylase-2 identified in unipolar major depression. *Neuron* 45, 11–16. doi: 10.1016/j.neuron.2004.12.014

Zheng, P., Zeng, B., Zhou, C., Liu, M., Fang, Z., Xu, X., et al. (2016). Gut microbiome remodeling induces depressive-like behaviors through a pathway mediated by the host's metabolism. *Mol. Psychiatry* 21, 786–796. doi: 10.1038/mp.2016.44

Zill, P., Baghai, T. C., Zwanzger, P., Schüle, C., Eser, D., Rupprecht, R., et al. (2004). SNP and haplotype analysis of a novel tryptophan hydroxylase isoform (TPH2) gene provide evidence for association with major depression. *Mol. Psychiatry* 9, 1030–1036. doi: 10.1038/sj.mp.4001525

Conflict of Interest Statement: The authors declare that the research was conducted in the absence of any commercial or financial relationships that could be construed as a potential conflict of interest.

frontiers in Behavioral Neuroscience

ORIGINAL RESEARCH
published: 18 June 2019
doi: 10.3389/fnbeh.2019.00126

Prophylactic Effects of *Bifidobacterium adolescentis* on Anxiety and Depression-Like Phenotypes After Chronic Stress: A Role of the Gut Microbiota-Inflammation Axis

Ying Guo[1,2,3,4], Jian-Ping Xie[5], Ke Deng[1,4], Xia Li[3], Yun Yuan[3], Qun Xuan[3], Jing Xie[1], Xiao-Ming He[1], Qian Wang[3], Juan-Juan Li[3] and Huai-Rong Luo[1,2,4]**

[1]State Key Laboratory of Phytochemistry and Plant Resources in West China, Yunnan Key Laboratory of Natural Medicinal Chemistry, Kunming Institute of Botany, Chinese Academy of Sciences, Kunming, China, [2]Key Laboratory for Aging and Regenerative Medicine, Department of Pharmacology, School of Pharmacy, Southwest Medical University, Luzhou, China, [3]School of Basic Medical Sciences, Kunming Medical University, Kunming, China, [4]University of Chinese Academy of Sciences, Beijing, China, [5]Library, Yunnan Minzu University, Kunming, China

Stress disturbs the balance of the gut microbiota and stimulates inflammation-to-brain mechanisms. Moreover, stress leads to anxiety and depressive disorders. *Bifidobacterium adolescentis* displays distinct anti-inflammatory effects. However, no report has focused on the anxiolytic and antidepressant effects of *B. adolescentis* related to the gut microbiome and the inflammation on chronic restraint stress (CRS) in mice. We found that pretreatment with *B. adolescentis* increased the time spent in the center of the open field apparatus, increased the percentage of entries into the open arms of the elevated plus-maze (EPM) and the percentage of time spent in the open arms of the EPM, and decreased the immobility duration in the tail suspension test as well as the forced swimming test (FST). Moreover, *B. adolescentis* increased the sequence proportion of *Lactobacillus* and reduced the sequence proportion of *Bacteroides* in feces. Furthermore, *B. adolescentis* markedly reduced the protein expression of interleukin-1β (IL-1β), tumor necrosis factor α (TNF-α), p-nuclear factor-kappa B (NF-κB) p65 and Iba1 and elevated brain derived neurotrophic factor (BDNF) expression in the hippocampus. We conclude that the anxiolytic and antidepressant effects of *B. adolescentis* are related to reducing inflammatory cytokines and rebalancing the gut microbiota.

Keywords: *Bifidobacterium adolescentis*, antidepressant, chronic restraint stress, gut microbiota, inflammation

OPEN ACCESS

Edited by:
Jee Hyun Kim,
Florey Institute of Neuroscience and Mental Health, Australia

Reviewed by:
Kenji Hashimoto,
Chiba University, Japan
Caitlin Cowan,
University College Cork, Ireland

****Correspondence:***
Ying Guo
guoying1@mail.kib.ac.cn
Huai-Rong Luo
luohuairong@mail.kib.ac.cn

Received: *04 February 2019*
Accepted: *24 May 2019*
Published: *18 June 2019*

Citation:
Guo Y, Xie J-P, Deng K, Li X, Yuan Y, Xuan Q, Xie J, He X-M, Wang Q, Li J-J and Luo H-R (2019) Prophylactic Effects of Bifidobacterium adolescentis on Anxiety and Depression-Like Phenotypes After Chronic Stress: A Role of the Gut Microbiota-Inflammation Axis. Front. Behav. Neurosci. 13:126. doi: 10.3389/fnbeh.2019.00126

INTRODUCTION

With high mortality and morbidity, depression is a common and recurrent mood disorder accompanied by behavioral deficits (McKeever et al., 2017). Evidence shows that response to the first-line treatment of depression is 40%–60%, while remission following antidepressant treatment is 30%–45% (Trivedi et al., 2006). Thus, our efforts have focused on developing better antidepressant drugs.

In recent years, emerging evidence has suggested an involvement of the gut microbiota in inflammation, brain development and behavior (Evrensel and Ceylan, 2015). The relationship between microbiota and anxiety/depression has been studied by the chronic restraint stress (CRS) model, in which the gut microbiota, specifically the abundance of *Allobaculum*, *Bifidobacterium*, *Turicibacter* and *Clostridium*, is altered (Wong et al., 2016). It is becoming apparent that probiotics induce substantial impacts on the health of the host. The absence of probiotic bacteria in the gut is implicated in the etiology of depression (Desbonnet et al., 2008), and additionally, the prolonged intake of probiotics (*Lactobacillus helveticus* R0052 and *Bifidobacterium longum* R0175) has favorable effects on anxiety- and depression-related behaviors without the presence of any adverse events (Messaoudi et al., 2011). Studies have found that *Bifidobacterium* has positive effects on stress-related diseases (Meyer and Vassar, 2018), and furthermore, the probiotic *Bifidobacterium infantis* may possess antidepressant properties (Desbonnet et al., 2008). However, the exact mechanisms underlying the antidepressant effect of *Bifidobacterium* in connection with the brain-gut axis remain poorly understood.

Inflammatory mechanisms mediate increased stress responsiveness and depression susceptibility (Hennessy et al., 2019). The increased release of peripheral cytokines exacerbates anxiety- and depression-like behaviors in stressed animals (Hodes et al., 2014). In addition, interleukin (IL)-1β is pivotal to the acquisition of depressive phenotypes in stressed animals (Maes et al., 2012). Antidepressant effects occur when the interleukin-1β (IL-1β) level is decreased (Zhang et al., 2015). The data from a clinical study suggest that plasma tumor necrosis factor (TNF)-α is also correlated with depression severity (Oglodek et al., 2017), and anti-TNF-α treatment alleviates depressive mood (Krishnan et al., 2007). In chronic stress models, microglial activation is significantly increased in the cingulate and medial orbital cortices, nucleus accumbens, caudate putamen, amygdala and hippocampus in the mouse brain (Farooq et al., 2012), and furthermore, the levels of IL-1β, IL-6 and tumor necrosis factor α (TNF-α) are increased in the substantia nigra (de Pablos et al., 2014). Stress can disturb the balance of the gut microbiota, stimulate inflammation-to-brain mechanisms, and lead to microglia activation in depressive disorders (Maes, 2008). Nuclear factor κB (NF-κB) is one of the major transcription factors that mediate inflammatory responses, and the activation of NF-κB in HT-29 cells can be inhibited by pre-incubation with *Bifidobacterium adolescentis* NCC251 (Riedel et al., 2006). *B. adolescentis* IM38 can regulate the *Proteobacteria* to *Bacteroidetes* ratio in the gut microbiota and inhibit NF-κB activation in the colon (Lim and Kim, 2017). *B. adolescentis* NK98 can suppress the occurrence and development of anxiety/depression, the infiltration of activated microglia into the hippocampus, and hippocampal NF-κB activation caused by acute immobilization stress (Jang et al., 2019). However, for CRS, the underlying connection between the anxiolytic and antidepressant effects of *B. adolescentis*, the gut microbiota, and inflammation are still unclear.

In this study, we investigated the anxiolytic and antidepressant effects of *B. adolescentis* related to the gut microbiota, inflammation, and behavior in CRS mice to evaluate the gut microbiota and inflammation as potential therapeutic targets in anxiety and depression.

MATERIALS AND METHODS

Animals

Male ICR mice (6 weeks old) were purchased from Kunming Medical University. The mice were housed in groups of 4–5 per cage (290 mm × 178 mm × 150 mm) in a room under normal conditions (22 ± 1°C, 50 ± 2% humidity, and a 12-h light/12-h dark cycle) with free access to food and water. The animals were adapted to the laboratory conditions for 1 week before the experiment. The procedures were approved by the Institutional Animal Care and Use Committee of Kunming Medical University and were performed in accordance with the Guide for the Care and Use of Laboratory Animals.

Experimental Design and Sample Collection

Experiment 1

The mice were randomly divided into five groups: the Con group, which received 10 mL/kg distilled water; the Ami group, which received 10 mg/kg amitriptyline (the dose was determined by our preliminary experiments and the references; Manning et al., 2014; Sanna et al., 2017); the Bif 0.25 (Bif) group, which received 0.25×10^9 CFU/kg *B. adolescentis*; the Bif 0.5 group, which received 0.5×10^9 CFU/kg *B. adolescentis*; and the Bif 1 group, which received 1×10^9 CFU/kg *B. adolescentis*. Each experimental group consisted of ten mice. The mice were treated with distilled water, amitriptyline (dissolved in distilled water), or *B. adolescentis* (dissolved in distilled water) by gavage for 21 days depending on the group. After 21 days, all mice underwent a behavioral test for three consecutive days (**Figure 1**).

Experiment 2

The mice were randomly allocated into three groups: the Con group, which received 10 mL/kg distilled water; the CRS group, which was subjected to the CRS procedure and received 10 mL/kg distilled water; and the Bif+CRS group, which was subjected to the CRS procedure and received 0.25×10^9 CFU/kg *B. adolescentis*. Each group consisted of twelve mice. The mice were treated with distilled water or *B. adolescentis* by gavage for 21 days depending on the group. For the CRS procedure, the mice were placed in a 50-mL tube for 4 h for 21 consecutive days. The behavioral test procedure was performed as reported previously with few modifications (Yang et al., 2015). After 21 days, all mice underwent a behavioral test for four consecutive days (**Figure 2**). One day after the completion of the behavioral test, six mice from each group were anesthetized (6% sodium pentobarbital, intraperitoneally) and subsequently sacrificed by decapitation. The whole hippocampus was quickly dissected and frozen in liquid nitrogen and stored at −80°C for Western blotting (**Figure 5**). The cecal contents were collected and used for 16S

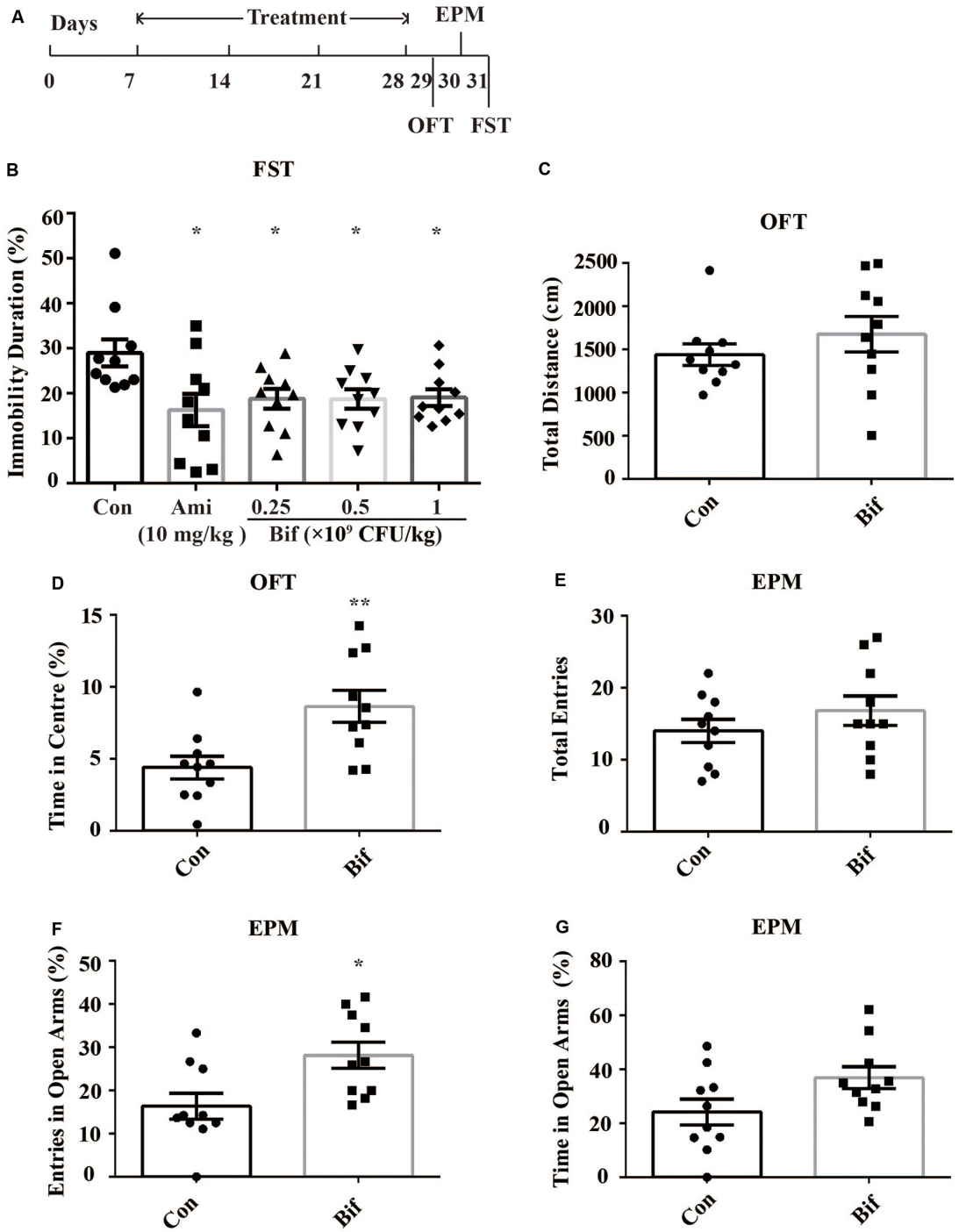

FIGURE 1 | Potential anxiolytic and antidepressant effects of *B. adolescentis*. The mice in the Con, Ami (10 mg/kg), Bif (0.25×10^9 CFU/kg), Bif (0.5×10^9 CFU/kg), and Bif (1×10^9 CFU/kg) groups were treated with 10 mL/kg distilled water, 10 mg/kg amitriptyline, 0.25×10^9 CFU/kg *B. adolescentis*, 0.5×10^9 CFU/kg *B. adolescentis*, and 1×10^9 CFU/kg *B. adolescentis*, respectively, by gavage for 21 days. **(A)** The timeline of Experiment 1. **(B)** The results of the FST showed that the immobility duration was significantly decreased in the Ami (10 mg/kg), Bif (0.25×10^9 CFU/kg), Bif (0.5×10^9 CFU/kg), and Bif (1×10^9 CFU/kg) groups. **(C)** The OFT showed no significant difference between the control group and the Bif (0.25×10^9 CFU/kg) group in the total distance traveled. **(D)** The OFT showed that the time spent in the center was significantly increased in the Bif (0.25×10^9 CFU/kg) group. **(E)** The EPM test showed no significant difference between the control group and the Bif (0.25×10^9 CFU/kg) group in the total number of entries. **(F)** The number of entries into the open arms of the EPM was significantly increased in the Bif (0.25×10^9 CFU/kg) group. **(G)** The EPM test showed no significant difference between the control group and the Bif (0.25×10^9 CFU/kg) group in time spent in the open arms. The data are shown as the mean ± SEM. Student's *t*-test was used. $^*p < 0.05$ and $^{**}p < 0.01$ vs. control. Con, Control; Bif, *B. adolescentis*; FST, forced swimming test; OFT, open field test; EPM, elevated plus-maze.

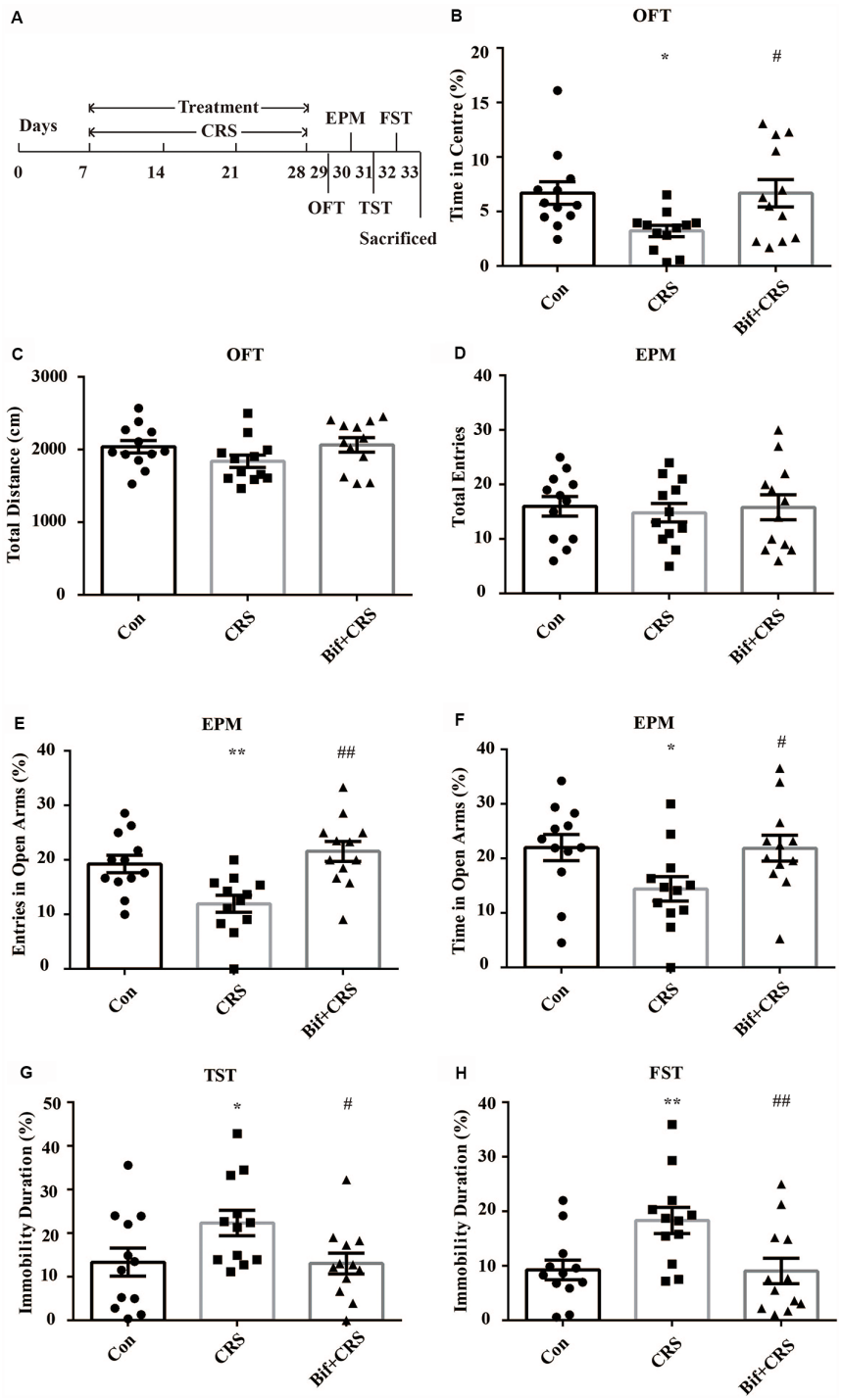

FIGURE 2 | Anxiolytic and antidepressant effects of *B. adolescentis* in chronic restraint stress (CRS) mice. The mice in the Con, CRS, and Bif+CRS groups were treated with 10 mL/kg distilled water, 10 mL/kg distilled water, and 0.25×10^9 CFU/kg *B. adolescentis*, respectively, by gavage for 21 days. **(A)** The schedules show the establishment of the CRS model, treatment, and behavioral tests. **(B)** The OFT showed that the time spent in the center was significantly decreased in the CRS group, and the change in the time spent in the center induced by CRS was reversed by *B. adolescentis*. **(C)** The OFT showed no significant difference among the three groups in the total distance traveled. **(D)** The EPM test showed no significant difference in the total number of entries induced by *B. adolescentis*. **(E)** The number of entries into the open arms of the EPM was significantly increased in the *B. adolescentis* group. **(F)** The time spent in the open arms of the EPM was significantly increased in the *B. adolescentis* group. **(G)** The TST showed that the immobility duration was significantly increased in the CRS group; the change in the immobility duration induced by CRS was reversed by *B. adolescentis*. **(H)** The FST showed that the immobility duration was significantly increased in the CRS group;

(*Continued*)

FIGURE 2 | Continued
the change in the immobility duration induced by CRS was reversed by *B. adolescentis*. The data are shown as the mean ± SEM. One-way analysis of variance (ANOVA) followed by the Student-Newman-Keuls test was used. $^{*}p < 0.05$ and $^{**}p < 0.01$ vs. the control; $^{\#}p < 0.05$ and $^{\#\#}p < 0.01$ vs. the CRS group; $n = 12$ per group. Con, Control; CRS, chronic restraint stress; Bif+CRS, *B. adolescentis* + chronic restraint stress; OFT, open field test; EPM, elevated plus-maze; TST, tail suspension test; FST, forced swimming test.

rRNA sequence analysis (**Figures 3**, **4**). After deep anesthesia with 6% sodium pentobarbital, six mice from each group were perfused with 4% paraformaldehyde for immunofluorescence labeling (**Figure 6**).

CRS

To establish the CRS model, the mice were placed in a horizontal resting position inside a well-ventilated (12 holes and 0.5 mm in diameter) 50-mL tube for 4 h for 21 consecutive days (Wong et al., 2016).

ANTIBODIES AND REAGENTS

Rabbit anti-brain-derived neurotrophic factor (BDNF) antibody, rabbit anti-ionized calcium binding adapter molecule 1 (Iba1) antibody, and rabbit anti-IL-1β antibody were acquired from Abcam (Shanghai, China). Rabbit anti-TNF-α, rabbit anti-p-NFκBp65, rabbit anti-NFκBp65, β-actin, and horseradish peroxidase (HRP)-conjugated anti-rabbit IgG antibodies were obtained from Cell Signaling Technology (Boston, MA, USA). An E.Z.N.A. Stool DNA Kit was acquired from Omega Bio-Tek (Norcross, GA, USA). An AxyPrep DNA Gel Extraction Kit was obtained from Axygen Biosciences (Union City, CA, USA). Live *B. adolescentis* AY240946 was purchased from Lizhu Pharmaceutical Factory (Guangdong, China).

Behavioral Tests

The illumination in the testing room was controlled, providing 60 lux inside the apparatus. Thirty minutes before the tests, each mouse was brought into the testing laboratory. The behavioral tests were carried out between 9:00 and 13:00.

Open Field Test (OFT)

The open field apparatus was a box (50 × 50 × 28 cm) with a floor divided into 25 squares. The nine central squares were defined as the center. On the day of the OFT, each mouse was gently placed in the center of the open field, and its movements were digitally recorded by video tracking software Smart V3.0 (Panlab, Spain) over a 6-min trial.

Elevated Plus-Maze (EPM) Test

On the day of the EPM test, each mouse was gently placed in the center of the EPM. The EPM was elevated 50 cm above the floor and consisted of two open arms (31 × 7.8 cm), two enclosed arms (31 × 6.5 × 11 cm) with walls, and a central area (7.8 × 6.5 cm). Movements were measured over a 6-min trial by Smart V3.0.

Tail Suspension Test (TST)

On the day of the tail suspension test, the mice were suspended upside down by their tails 40 cm above the floor, and an adhesive tape was placed 1 cm from the tail tip. The testing period was 6 min long, and the immobility time was analyzed over the last 4 min by Smart V3.0.

Forced Swimming Test (FST)

On the day of the FST, the mice were placed in a vertical transparent cylinder (30 cm in height and 12 cm in diameter) containing tap water at 25 ± 1°C and 20 cm in depth. The testing period was 6 min long, and the immobility time of each mouse was scored over the last 4 min by Smart V3.0.

Analysis of Cecal Microflora Community Diversity

Previously described procedures (Ravel et al., 2011) were used. For 16S rRNA sequence analysis, DNA was extracted and then amplified to target the V1-V3 region with indexes and the adaptor-linked universal primers 27F (5′-AGAGTTTGATCCTGGCTCAG-3′) and 533R (5′-TTACCGCGGCTGCTGGCAC-3′). Amplicons were extracted, purified, and quantified by QuantiFluor-ST (Promega, San Luis Obispo, CA, USA). The purified amplicons were tagged with nucleotide barcodes, pooled in equimolar quantities and paired-end sequenced (2 × 300 bp) on an Illumina MiSeq platform. The raw fastq files were de-multiplexed, quality-filtered with Trimmomatic (Version 3.29), and merged with FLASH (version 1.2.7). Operational taxonomic units (OTUs) were collected with a 97% similarity cut-off by UPARSE (version 7.1[1]), and chimeric sequences were identified and removed by UCHIME. The taxonomy of each 16S rRNA gene sequence was analyzed by the RDP Classifier algorithm[2] against the Silva (SSU128) 16S rRNA database with a confidence threshold of 70%. The data were analyzed on the free online platform called Majorbio I-Sanger Cloud Platform[3].

Western Blotting of the Hippocampus (Yuan et al., 2014)

Samples were homogenized with a protein extraction reagent containing protease inhibitors, and the concentrations of the proteins were determined using a BCA protein concentration assay kit. The proteins were separated by sodium dodecyl sulfate poly-acrylamide gel electrophoresis in a Mini-Protein II apparatus (Bio-Rad, CA, USA). The protein bands were electro-blotted onto a polyvinylidene fluoride membrane, and the membranes were blocked. The membranes were incubated with primary antibodies against BDNF (1:1,000), IL-1β (1:1,000), Iba1 (1:1,000), TNF-α (1:1,000), p-NF-κB p65 (1:1,000), and NF-κB p65 (1:1,000) overnight at 4°C. They were further incubated with a HRP-conjugated anti-rabbit IgG (1:5,000) antibody and then developed with ECL reagents. The different blots were incubated with different antibodies. As much of the proteins, which had different molecular weights, as possible were transferred to a single membrane, and then the blots were cut at different molecular weights and incubated with different antibodies according to the

[1]http://drive5.com/uparse/
[2]http://rdp.cme.msu.edu/
[3]www.i-sanger.com

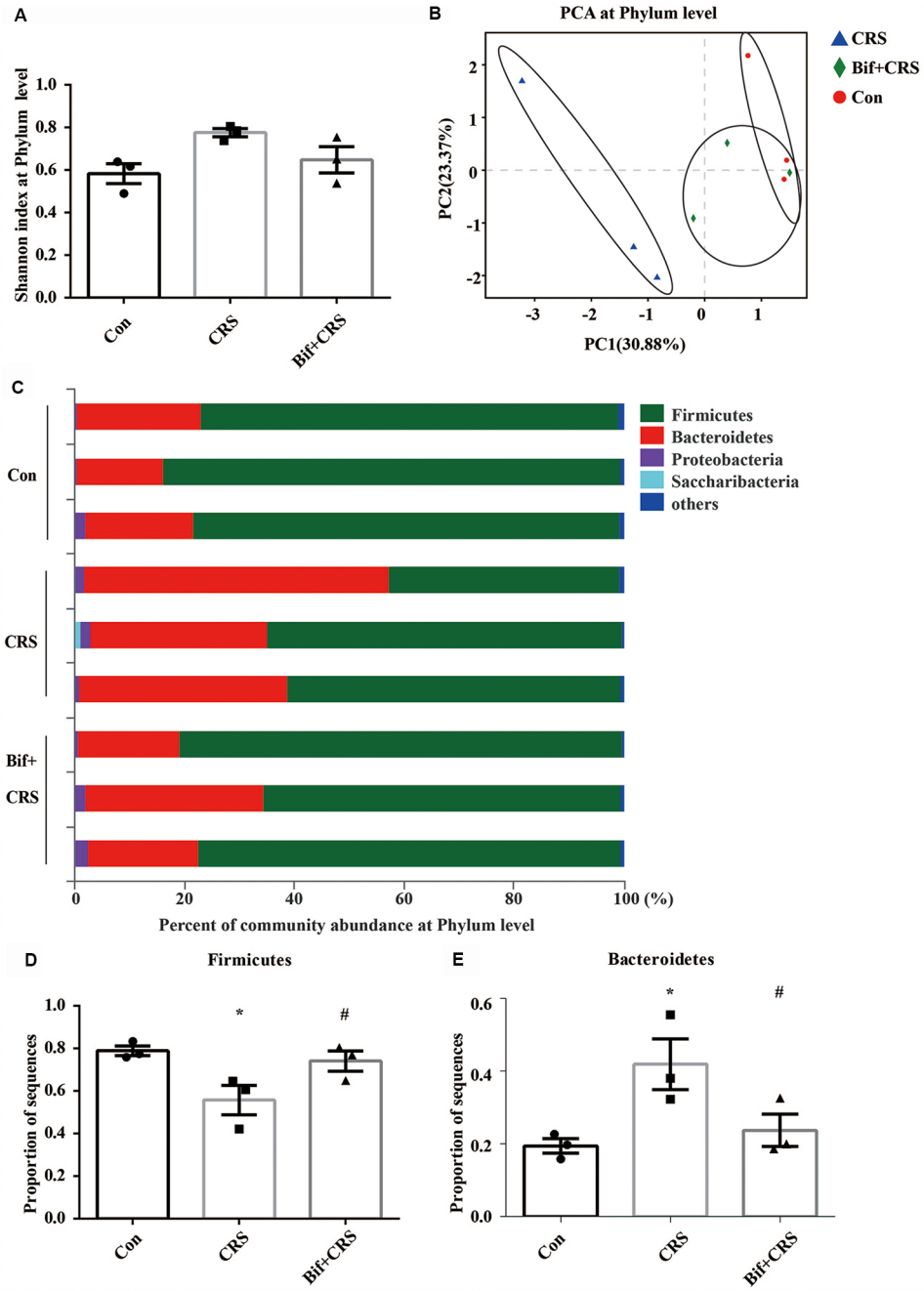

FIGURE 3 | *B. adolescentis* reversed the imbalance of the intestinal microflora induced by CRS at the phylum level. The mice in the Con, CRS, and Bif+CRS groups were given 10 mL/kg distilled water, 10 mL/kg distilled water, and 0.25 × 10^9 CFU/kg *B. adolescentis*, respectively, by gavage for 21 days. **(A)** There was no significant difference in the Shannon index at the phylum level induced by *B. adolescentis*. **(B)** The principal component analysis (PCA) results showed no significant difference in the microbial community composition. **(C)** Community barplot analysis showed the community composition and species abundance in the three groups. **(D)** The decrease in *Firmicutes* abundance in the CRS group was enhanced by *B. adolescentis*. **(E)** The increased *Bacteroidetes* abundance in the CRS group was decreased by *B. adolescentis*. The data are shown as the mean ± SEM. One-way ANOVA followed by the Student-Newman-Keuls test was used. $^*p < 0.05$ vs. the control; $^{\#}p < 0.05$ vs. the CRS group; $n = 3$ per group. Con, Control; CRS, chronic restraint stress; Bif+CRS, *B. adolescentis* + chronic restraint stress.

molecular weight of the target proteins. The target protein band was compared with the β-actin band on the same membrane. The chemiluminescence signal was imaged using a ChemiDoc XRS system (Bio-Rad) and the protein band signals were measured using ImageJ 1.4.3.67 software. The signal intensities of the individual protein bands were normalized to the β-actin band intensity and were represented by arbitrary units.

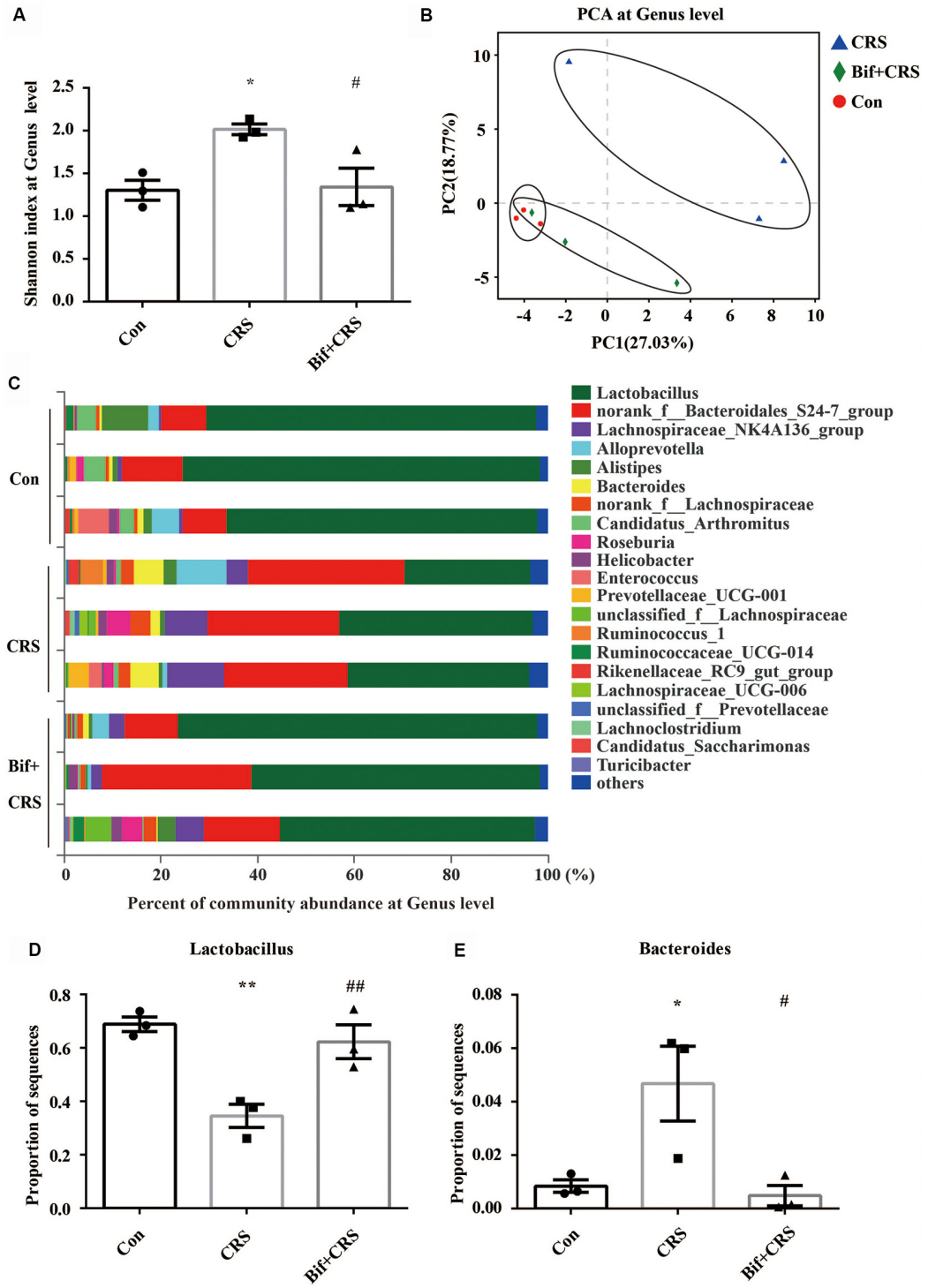

FIGURE 4 | *B. adolescentis* reversed the imbalance of the intestinal microflora induced by CRS at the genus level. The mice in the Con, CRS, and Bif+CRS groups were treated with 10 mL/kg distilled water, 10 mL/kg distilled water, and 0.25 × 10^9 CFU/kg *B. adolescentis*, respectively, by gavage for 21 days. **(A)** An increased Shannon index was observed in the CRS group compared with the control group, and the increase in the index was attenuated by *B. adolescentis*. **(B)** PCA revealed that the microbial community composition in the *B. adolescentis* group was more similar to that in the control than that in the CRS group, as shown by the clustering of the samples in the plots. **(C)** Community barplot analysis is shown. **(D)** The decrease in the *Lactobacillus* abundance in the CRS group was increased by *B. adolescentis*. **(E)** The enhanced *Bacteroides* abundance in the CRS group was reversed by *B. adolescentis*. The data are shown as the mean ± SEM. One-way ANOVA followed by the Student-Newman-Keuls test was used. $^{*}p < 0.05$ and $^{**}p < 0.01$ vs. the control; $^{\#}p < 0.05$ and $^{\#\#}p < 0.01$ vs. the CRS group; $n = 3$ per group. Con, Control; CRS, chronic restraint stress; Bif+CRS, *B. adolescentis* + chronic restraint stress.

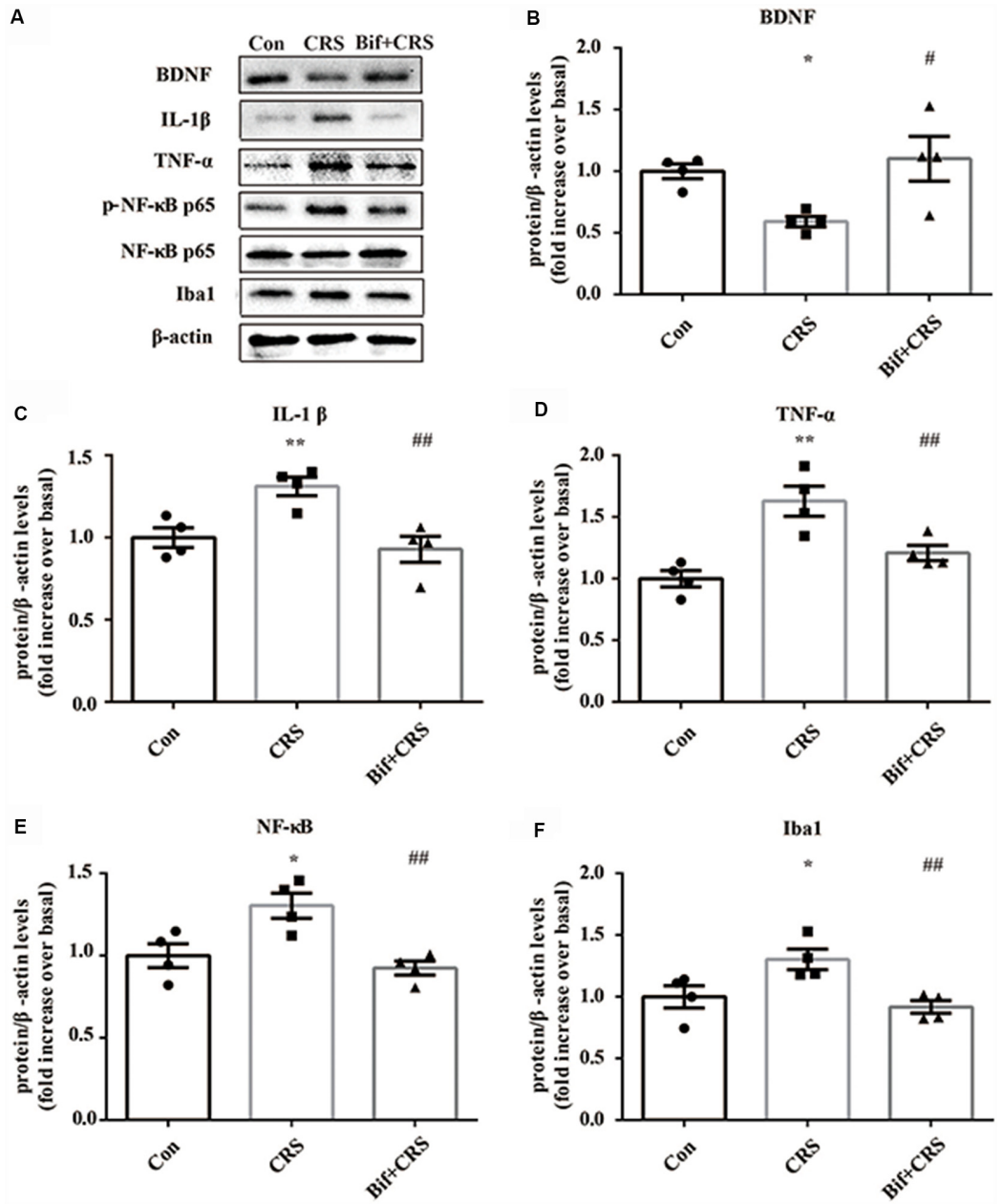

FIGURE 5 | Changes in the protein expression of BDNF, IL-1β, TNF-α, p-NF-κB p65 and Iba1 in the hippocampus induced by pretreatment with *B. adolescentis*. The mice in the Con, CRS, and Bif+CRS groups were treated with 10 mL/kg distilled water, 10 mL/kg distilled water, and 0.25×10^9 CFU/kg *B. adolescentis*, respectively, by gavage for 21 days. **(A)** Western blotting showed that **(B)** the protein level of BDNF was upregulated by *B. adolescentis*, and the protein levels of **(C)** IL-1β, **(D)** TNF-α, **(E)** p-NF-κB p65 and **(F)** Iba1 in the hippocampus were obviously suppressed by *B. adolescentis*. The data are shown as the mean ± SEM. One-way ANOVA followed by the Student-Newman-Keuls test was used. $^*p < 0.05$ and $^{**}p < 0.01$ vs. the control; $^{\#}p < 0.05$ and $^{\#\#}p < 0.01$ vs. the CRS group; $n = 4$ per group. Con, Control; CRS, chronic restraint stress; Bif+CRS, *B. adolescentis* + chronic restraint stress; BDNF, brain derived neurotrophic factor; IL-1β, interleukin-1β; TNF-α, tumor necrosis factor α; NF-κB, nuclear factor-kappa B; Iba1, ionized calcium binding adapter molecule 1.

Immunofluorescence Labeling in the Hippocampus (Fang et al., 2015)

The brains were removed and embedded in paraffin. Coronal sections of 7 μm thickness were cut using a microtome (Model: CUT5062; Mainz, SLEE, Germany), and the sections were blocked in 5% goat serum for 1 h at room temperature (22–24°C). After the serum was discarded, the sections were incubated with primary antibodies against BDNF (1:100), TNF-α (1:100), IL-1β (1:100), and Iba1 (1:100) overnight at 4°C. The sections were incubated with a Cy3-conjugated secondary antibody (1:200) for 1 h at room temperature and then mounted with a fluorescent mounting medium containing 4′,6-diamidino-2-phenylindole

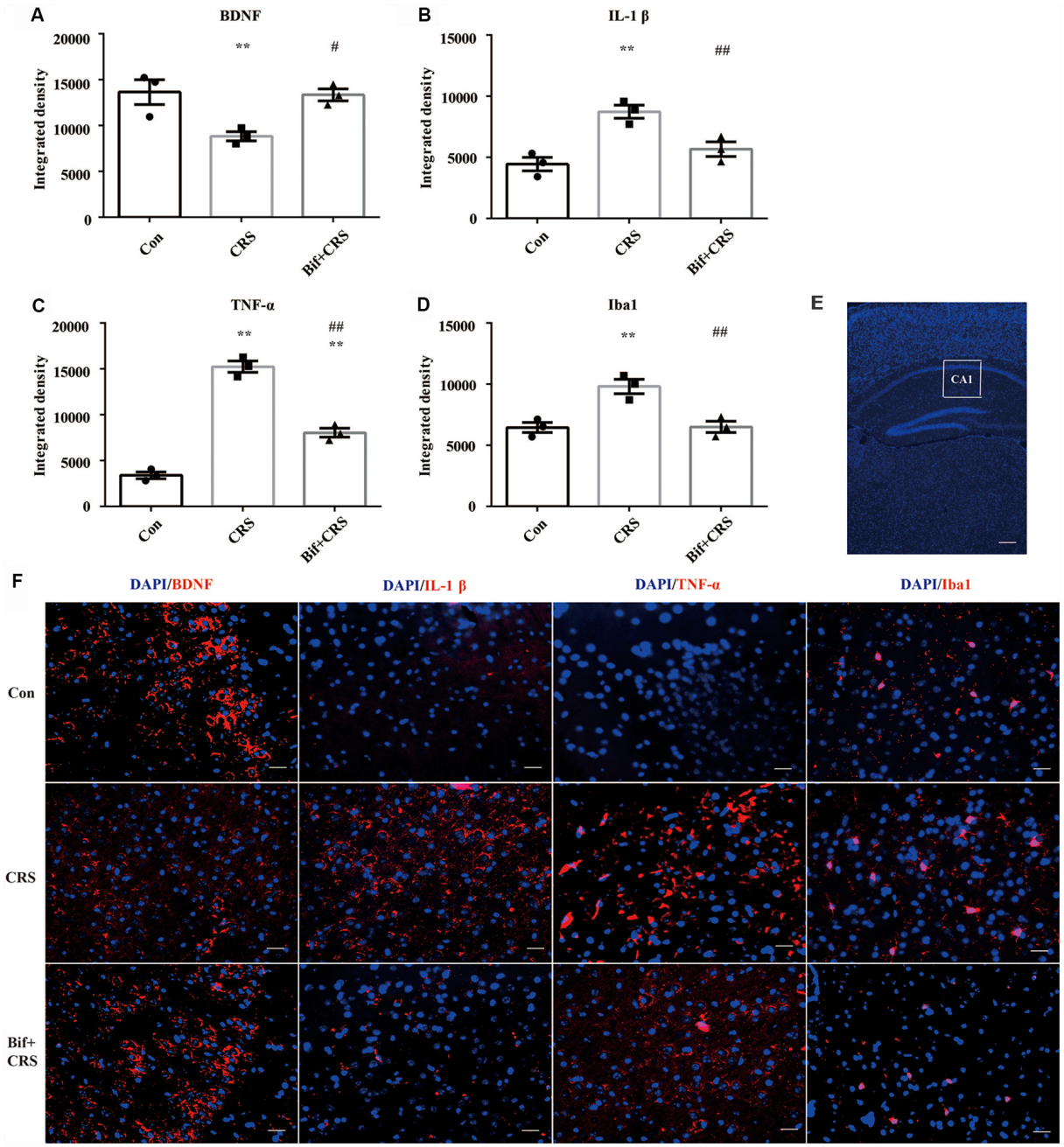

FIGURE 6 | Changes in the protein expression of BDNF, IL-1β, TNF-α, and Iba1 in the CA1 region of the hippocampus induced by pretreatment with *B. adolescentis*. Immunofluorescence analysis showed that **(A)** the protein level of BDNF was upregulated by *B. adolescentis*, and the protein levels of **(B)** IL-1β, **(C)** TNF-α, and **(D)** Iba1 in the CA1 region of the hippocampus were obviously suppressed by *B. adolescentis*. The data are shown as the mean ± SEM. One-way ANOVA followed by the Student-Newman-Keuls test was used. $^{**}p < 0.01$ vs. the control; $^{\#}p < 0.05$ and $^{\#\#}p < 0.01$ vs. the CRS group; $n = 3$ per group. **(E)** The CA1 region was identified as shown in the box. Scale bar = 200 μm. **(F)** Immunofluorescence was performed and subsequently visualized with Cy3 (red)-labeled secondary antibodies. DAPI (blue) was used as a nuclear stain. Scale bar = 20 μm. Con, Control; CRS, chronic restraint stress; Bif+CRS, *B. adolescentis* + chronic restraint stress; BDNF, brain derived neurotrophic factor; IL-1β, interleukin-1β; TNF-α, tumor necrosis factor α; Iba1, ionized calcium binding adapter molecule 1.

(DAPI). Eight successive slices from each mouse were used for immunofluorescence, and four successive slices (two arrays) were allocated for incubation with the different antibodies. The sections were subsequently observed by an inverted fluorescence microscope (Axio Observer. Z1, Zeiss, Germany). The CA1 region was assessed in the immunofluorescence and was represented on the template coronal slices from 1.70 mm to 1.94 mm inclusive, anterior to the bregma. The quantification

of immunofluorescence intensity in the fluorescence images was expressed as integrated density, which was quantified using ImageJ software.

Statistical Analysis

All data are presented as the mean ± standard error of mean (SEM). Statistical analyses were performed using a two-tailed Student's *t*-test or one-way analysis of variance (ANOVA) followed by a Student-Newman-Keuls *post hoc* test using SPSS 19.0 (SPSS Inc., Chicago, IL, USA). For the microbiota, the Adonis test was used to analyze the ß diversity in principal component analysis (PCA), and False Discovery Rate (FDR) was used to correct for multiple testing of the comparisons of specific genera. A p-value < 0.05 was considered statistically significant.

RESULTS

Potential Anxiolytic and Antidepressant Effects of *B. adolescentis*

To preliminarily investigate the antidepressant effects of *B. adolescentis*, the FST was used. The immobility duration ($t_{18} = 2.698$, $p = 0.015$; $t_{18} = 2.741$, $p = 0.013$; $t_{18} = 2.794$, $p = 0.012$; $t_{18} = 2.824$, $p = 0.011$; **Figure 1B**) was decreased significantly by amitriptyline (10 mg/kg) and *B. adolescentis* (0.25×10^9 CFU/kg, 0.5×10^9 CFU/kg, and 1×10^9 CFU/kg). The OFT and the EPM were used to evaluate spontaneous activity and the anxiolytic effects of *B. adolescentis*. The total distance traveled in the OFT ($t_{18} = -0.995$, $p = 0.333$, **Figure 1C**) did not significantly differ between the control group and the *B. adolescentis*-treated (0.25×10^9 CFU/kg) group, and the time spent in the center of the OFT apparatus ($t_{18} = -3.11$, $p = 0.006$, **Figure 1D**) was increased by *B. adolescentis* (0.25×10^9 CFU/kg). Moreover, the total number of entries into the arms of the EPM ($t_{18} = -1.087$, $p = 0.292$, **Figure 1E**) did not differ between the control group and the *B. adolescentis*-treated (0.25×10^9 CFU/kg) group. *B. adolescentis* (0.25×10^9 CFU/kg) increased the percentage of entries into the open arms of the EPM ($t_{18} = -2.768$, $p = 0.013$, **Figure 1F**). However, *B. adolescentis* (0.25×10^9 CFU/kg) did not increase the percentage of time spent in the open arms of EPM ($t_{18} = -2.018$, $p = 0.059$, **Figure 1G**). These data (**Table 1**) indicate the potential anxiolytic and antidepressant effects of *B. adolescentis*.

Anxiolytic and Antidepressant Effects of *B. adolescentis* in CRS Mice

To further investigate the anxiolytic and antidepressant effects of *B. adolescentis*, a CRS model was used, as shown in the schedule (**Figure 2A**). There was a significant difference in the time spent in the center of the OFT apparatus ($F_{(2,33)} = 4.183$, $p = 0.024$, **Figure 2B**). The time spent in the center of the OFT apparatus was decreased in the CRS group compared with the control group ($p < 0.05$), and the *B. adolescentis* group spent a significantly longer time in the center than that spent by the CRS group ($p < 0.05$). There were no remarkable changes among the three groups in the total distance traveled in the OFT ($F_{(2,33)} = 1.875$, $p = 0.169$, **Figure 2C**). The EPM test showed no significant difference between the two groups in the total number of entries ($F_{(2,33)} = 0.104$, $p = 0.901$, **Figure 2D**). *B. adolescentis* increased the percentage of entries into the open arms of the EPM ($F_{(2,33)} = 9.108$, $p = 0.001$, **Figure 2E**) and the percentage of time spent in the open arms of the EPM ($F_{(2,33)} = 3.465$, $p = 0.043$, **Figure 2F**). Both the percentage of entries into the open arms of the EPM ($p < 0.01$) and the percentage of time spent in the open arms of the EPM ($p < 0.05$) were decreased in the CRS group compared with the control group. Both percentages ($p < 0.01$, $p < 0.05$) were increased in the *B. adolescentis* group compared with the CRS group. There was a significant difference in the immobility durations in the TST ($F_{(2,33)} = 3.422$, $p = 0.045$, **Figure 2G**) and the FST ($F_{(2,33)} = 5.78$, $p = 0.007$, **Figure 2H**). The results showed markedly increased immobility durations in the CRS mice in both the TST ($p < 0.05$) and the FST ($p < 0.01$). Decreased immobility durations were observed in both the TST ($p < 0.05$) and the FST ($p < 0.01$) in the *B. adolescentis* group compared with the CRS group. Altogether, these data (**Table 2**) indicate that *B. adolescentis* has anxiolytic and antidepressant effects on CRS mice in these behavioral tests.

B. adolescentis Reversed the Imbalance of Cecal Microflora Induced by CRS

To test the assumption that the anxiolytic and antidepressant effects of *B. adolescentis* are related to rebalancing the gut microbiota, cecal microflora community diversity was analyzed. There was no significant difference in the Shannon index at the phylum level ($F_{(2,6)} = 4.5$, $p = 0.064$, **Figure 3A**). PCA revealed that there was no significant difference in the microbial community composition of the three groups at the phylum level ($R^2 = 0.53264$, $p = 0.108$, **Figure 3B**). Community barplot analysis showed the community composition and species abundance in the three groups (**Figure 3C**). Further analysis showed a significant difference in the abundance of *Firmicutes* ($F_{(2,6)} = 5.946$, $p = 0.038$, **Figure 3D**) and *Bacteroidetes* ($F_{(2,6)} = 5.9$, $p = 0.038$, **Figure 3E**) at the phylum level. The decline ($p < 0.05$) in *Firmicutes* abundance in the CRS group was enhanced ($p < 0.05$) by *B. adolescentis*. Additionally, the previous increase ($p < 0.05$) in *Bacteroidetes* in the CRS group was decreased ($p < 0.05$) by *B. adolescentis* (**Table 3**).

For the further verification of cecal microflora community diversity, Shannon index, principal component and community barplot analyses were performed at the genus level. There was a significant difference in the Shannon index at the genus level ($F_{(2,6)} = 7.294$, $p = 0.025$, **Figure 4A**). An increased Shannon index ($p < 0.05$) was observed in the CRS group compared with the control group, and the increase in the index was attenuated ($p < 0.05$) by *B. adolescentis*. PCA revealed that the microbial community composition in the *B. adolescentis* group was more similar to that in the control group than that in the CRS group, as shown by the clustering of the samples in the plots ($R^2 = 0.54811$, $p = 0.008$, **Figure 4B**). Community barplot analysis is shown in **Figure 4C**. Significant differences in the abundance of *Lactobacillus* ($F_{(2,6)} = 14.997$, $p = 0.005$, **Figure 4D**) and *Bacteroides* ($F_{(2,6)} = 7.488$, $p = 0.023$, **Figure 4E**) are shown.

TABLE 1 | Potential anxiolytic and antidepressant effects of *B. adolescentis*.

B. Immobility Duration of Forced swimming test (%)					C. Total Distance of Open Field (cm)		D. Time in Center of Open Field (%)		E. Total Entries of EPM		F. Entries in Open Arms of EPM (%)		G. Time in Open Arms of EPM (%)	
Con	Ami (10 mg/kg)	Bif (0.25×10^9 CFU/kg)	Bif (0.5×10^9 CFU/kg)	Bif (1×10^9 CFU/kg)	Con	Bif (0.25×10^9 CFU/kg)	Con	Bif (0.25×10^9 CFU/kg)	Con	Bif (0.25×10^9 CFU/kg)	Con	Bif (0.25×10^9 CFU/kg)	Con	Bif (0.25×10^9 CFU/kg)
39.17	2.5	28.89	22.22	16.69	1263.21	2053.69	4.43	7.34	15	10	26.67	20.00	32.24	26.28
27.78	4.44	23.17	12.5	14.81	1595.11	2465.83	4.67	12.69	14	8	14.29	37.50	14.92	35.56
21.94	23.06	11.11	29.72	17.08	1121.71	1635.51	2.51	9.32	16	26	12.50	34.62	18.52	62.16
21.39	3.06	22.08	7.22	13.97	1242.33	2493.29	2.44	12.36	8	18	12.50	16.67	33.28	34.88
30.56	10.56	6.39	25	12.67	1382.98	504.9	5.37	8.56	19	12	0.00	41.67	0	54.24
23.06	31.11	25.83	13.06	30.67	1480.85	971.53	9.64	4.28	18	15	11.11	40.00	10.24	31.48
24.44	14.17	12.78	23.33	15.47	1577.51	1446.7	0.45	6.13	7	22	14.29	18.18	26.4	42.32
51.11	18.06	20.28	15.83	20.27	972.73	2119.14	3.35	4.21	9	27	33.33	25.93	42.52	32.76
23.06	35	18.06	18.61	26.53	2412.68	1785.53	6.4	14.25	22	15	13.64	20.00	14.72	28
27.22	21.11	19.72	20	22.42	1324.97	1272.91	4.65	7.2	12	15	25.00	26.67	48.6	20.52
compared with control *t*-test for Equality of Means					compared with control *t*-test for Equality of Means		compared with control *t*-test for Equality of Means		compared with control *t*-test for Equality of Means		compared with control *t*-test for Equality of Means		compared with control *t*-test for Equality of Means	
$p = 0.015$		0.013	0.012	0.011	$p = 0.333$		$p = 0.006$		0.292		0.013		0.059	
$df = 18$		18	18	18	$df = 18$		$df = 18$		$df = 18$		$df = 18$		$df = 18$	
$t = 2.698$		2.741	2.794	2.824	$t = -0.995$		$t = -3.11$		$t = -1.087$		$t = -2.768$		$t = -2.018$	

The mice in groups of Con, Ami (10 mg/kg), Bif(0.25×10^9 CFU/kg), Bif (0.5×10^9 CFU/kg) and Bif (1×10^9 CFU/kg) were given with distilled water (10 mL/kg), amitriptyline (10 mg/kg), B. adolescentis (0.25×10^9 CFU/kg), B. adolescentis (0.5×10^9 CFU/kg) and B. adolescentis (1×10^9 CFU/kg) respectively, by gavage for 21 days. N = 10 per group.

TABLE 2 | Anxiolytic and antidepressant effects of *B. adolescentis* in CRS mice.

B. Time in Center of Open Field (%)			C. Total Distance of Open Field (cm)			D. Total Entries of EPM			E. Entries in Open Arms of EPM (%)			F. Time in Open Arms of EPM (%)			G. Immobility Duration of Tail Suspension Test (%)			H. Immobility Duration of Forced swimming test (%)		
Con	CRS	Bif+CRS	Con	CRS	Bif+CRS	Con	CRS	Bif+CRS	Con	CRS	Bif+CRS	Con	CRS	Bif+CRS	Con	CRS	Bif+CRS	Con	CRS	Bif+CRS
5.39	0.32	2.6	1941.64	1658.32	1543.94	15	13	8	20.00	15.38	25.00	21.32	16.32	23.17	22.05	34.53	11.55	5.9	19.33	15.18
5.81	2.84	12.29	1977.99	1462.89	2161.88	19	21	14	26.32	14.29	28.57	25.44	24.48	36.54	2.82	42.82	12.15	8.31	15.45	2.22
8.02	3.78	1.7	2243.67	1696.25	2026.44	23	5	6	21.74	0.00	16.67	23.58	0	17.25	1.35	24.54	32.22	22	29.35	14.88
6.96	0.56	6.97	1854.72	1604.73	2330.81	10	8	20	20.00	12.50	20.00	21.95	15.12	18.94	14.9	22.68	17.27	6.83	35.9	1.03
7.01	3.02	5.51	1936.98	2234.28	2407.91	25	24	10	16.00	16.67	20.00	28.33	18.29	23.19	5.25	22.4	0	9.88	10.32	7.53
4.51	3.76	10.56	2572.29	1902.54	1907.05	6	15	9	16.67	6.67	33.33	22.03	10.54	34	24.03	14.9	12.77	9.62	22.03	3.63
2.46	1.46	4.62	1704.71	1608.22	2393.15	21	10	30	28.57	20.00	23.33	34.26	29.98	20.05	11.58	13.92	13.02	19.22	7.22	24.97
3.71	4.98	6.31	1965.25	1994.96	1623.36	8	22	22	12.50	13.64	9.09	9.35	14.76	5.27	13.52	11.15	6.68	0.62	18.73	7.67
16.11	3.96	2.26	2274.03	1956.94	2101.34	17	11	19	17.65	9.09	15.79	29.42	10	15.74	0.4	33.27	19.03	1.05	7.52	5.53
4.64	3.96	12.06	1529.13	1588.10	2308.45	10	18	27	10.00	11.11	18.52	4.54	11.85	19.57	5	21.32	18.25	7.03	15.78	1.7
5.6	6.53	13.08	2111.62	2502.09	2453.90	20	12	17	25.00	8.33	23.53	26	7.42	22.46	35.6	13.92	3.95	12.27	18.25	21.28
10.18	3.51	2.25	2385.22	1873.10	1532.85	18	19	8	16.67	15.79	25.00	17.55	14.11	26.57	23.95	12.72	9.65	8.64	20.33	3.08
df	*F*	*P*	*df*	*F*	*P*	*df*	*F*	*P*	*df*	*F*	*P*	*df*	*F*	*P*	*df*	*F*	*P*	*df*	*F*	*P*
2,33	4.183	0.024	2,33	1.875	0.169	2,33	0.104	0.901	2,33	9.108	0.001	2,33	3.465	0.043	2,33	3.422	0.045	2,33	5.78	0.007

The mice in groups of Con, CRS and Bif+CRS were given with distilled water (10 mL/kg), distilled water (10 mL/kg), B. adolescentis (0.25×10^9 CFU/kg) respectively, by gavage for 21 days. N = 12 per group.

TABLE 3 | *B. adolescentis* reversed the imbalance of the intestinal microflora induced by CRS at the phylum level.

A. Shannon index on Phylum level			B. PCA on Phylum level			D. Proportion of sequences on Phylum level: Firmicutes			E. Proportion of sequences on Phylum level: Bacteroidetes		
Con	**CRS**	**Bif+CRS**		**PC1**	**PC2**	**Con**	**CRS**	**Bif+CRS**	**Con**	**CRS**	**Bif+CRS**
0.618248	0.804381	0.538529	Con	1.4023	−0.1719	0.7599	0.4212	0.8048	0.2271	0.5547	0.186
0.490792	0.785661	0.652056		1.4472	0.1895	0.8335	0.646	0.6492	0.1586	0.3226	0.3261
0.639374	0.737641	0.754216		0.7645	2.1739	0.7751	0.6067	0.7693	0.1977	0.3805	0.2002
			CRS	−1.253	−1.4395						
df	*F*	*P*		−3.2233	1.7086	*df*	*F*	*P*	*df*	*F*	*P*
2,6	4.5	0.064		−0.8385	−2.0185	2,6	5.946	0.038	2,6	5.9	0.038
			Bif+CRS	1.5016	−0.047						
				−0.1986	−0.9116						
				0.3979	0.5164						
			R^2 = 0.53264, p = 0.108								

The mice in groups of Con, CRS and Bif+CRS were given with distilled water (10 mL/kg), distilled water (10 mL/kg), B. adolescentis (0.25×109 CFU/kg) respectively, by gavage for 21 days. N = 3 per group.

TABLE 4 | *B. adolescentis* reversed the imbalance of the intestinal microflora induced by CRS at the genus level.

A. Shannon index on Genus level			B. PCA on Genus level			D. Proportion of sequences on Genus level: Lactobacillus			E. Proportion of sequences on Genus level: Bacteroides		
Con	**CRS**	**Bif+CRS**		**NMDS1**	**NMDS2**	**Con**	**CRS**	**Bif+CRS**	**Con**	**CRS**	**Bif+CRS**
1.29678	2.136918	1.103383	Con	−4.3868	−1.0162	0.684	0.261	0.7448	0.0057	0.0618	0.0125
1.106301	1.925281	1.781085		−3.218	−1.3881	0.7375	0.4001	0.5294	0.0065	0.0188	0.0016
1.511226	1.984399	1.145668		−4.0307	−0.46	0.6449	0.3768	0.5958	0.0131	0.0598	0.0006
			CRS	−1.8479	9.6013						
df	*F*	*P*		7.3032	−0.9993	*df*	*F*	*P*	*df*	*F*	*P*
2,6	7.294	0.025		8.495	2.9059	2,6	14.997	0.005	2,6	7.488	0.023
			Bif+CRS	−3.6345	−0.6355						
				−2.0275	−2.618						
				3.3472	−5.3902						
			R^2 = 0.54811, p = 0.008								

The mice in groups of Con, CRS and Bif+CRS were given with distilled water (10 mL/kg), distilled water (10 mL/kg), B. adolescentis (0.25×109 CFU/kg) respectively, by gavage for 21 days. N = 3 per group.

TABLE 5 | Changes in the protein expression of BDNF, IL-1β, TNF-α, p-NF-κB p65 and Iba1 in the hippocampus induced by pretreatment with *B. adolescentis*.

	B. Western blotting analysis for BDNF, IL-1β, TNF-α, p-NF-κ B p65 and Iba1 expression				
	BDNF	**IL-1β**	**TNF-α**	**p-NF-κB p65/ NF-κB p65**	**Iba1**
Con	1.0723	0.9218	0.9743	0.9441	1.1421
	1.0099	1.1345	0.8306	0.8215	0.7453
	1.0872	0.8812	1.0628	1.1499	1.1128
	0.8307	1.0634	1.1325	1.0852	1.0011
CRS	0.4894	1.1463	1.9127	1.1227	1.1859
	0.6007	1.3988	1.7253	1.2378	1.1808
	0.6971	1.3309	1.3475	1.4009	1.3169
	0.5803	1.3691	1.5323	1.4565	1.5296
Bif+CRS	1.5287	0.6976	1.1223	0.9601	0.8247
	1.1179	0.9694	1.3875	0.8072	1.0179
	1.1195	1.0616	1.1956	0.9221	0.9956
	0.6419	0.9869	1.1328	1.0082	0.8336
df	2,9	2,9	2,9	2,9	2,9
F	5.731	9.477	13.469	9.3	7.066
P	0.025	0.006	0.002	0.006	0.014

The mice in groups of Con, CRS and Bif+CRS were given with distilled water (10 mL/kg), distilled water (10 mL/kg), B. adolescentis (0.25×109 CFU/kg) respectively, by gavage for 21 days. N = 4 per group.

The decrease in *Lactobacillus* abundance ($p < 0.01$) in the CRS group was increased ($p < 0.01$) by *B. adolescentis*. Furthermore, the enhanced abundance of *Bacteroides* ($p < 0.05$) in the CRS group was also reversed ($p < 0.05$) by *B. adolescentis* (**Table 4**). The 16S rRNA sequencing datasets for this study were deposited at NCBI and are accessible at https://www.ncbi.nlm.nih.gov/sra/PRJNA498761.

B. adolescentis Increased BDNF Expression and Reduced the Expression of Inflammatory Cytokines in the Hippocampus of CRS Mice

To investigate the relationship between the anti-inflammatory effects and the anxiolytic/antidepressant effects of *B. adolescentis* and to verify the effects of the inflammatory conditions that are induced by chronic stress, we evaluated protein expression in the hippocampus, which is related to inflammation and chronic stress (Sathyanesan et al., 2017). Chronic stress can trigger both anxiety- and depression-like behaviors as well as reduce BDNF levels (Berry et al., 2012) and additionally, cytokines can attenuate the BDNF level in depression (Yu and Chen, 2011). There was a significant difference in BDNF expression ($F_{(2,9)} = 5.731$, $p = 0.025$, **Figure 5B**). It is striking that the decreased BDNF expression ($p < 0.05$) in the CRS treated with *B. adolescentis* showed the most drastic increase ($p < 0.05$). Western blotting analysis also showed that the protein levels of IL-1β ($F_{(2,9)} = 9.477$, $p = 0.006$, **Figure 5C**), TNF-α ($F_{(2,9)} = 13.469$, $p = 0.002$, **Figure 5D**), p-NF-κB p65 ($F_{(2,9)} = 9.3$, $p = 0.006$, **Figure 5E**) and Iba1 ($F_{(2,9)} = 7.066$, $p = 0.014$, **Figure 5F**) in the hippocampus were significantly different. The increases ($p < 0.01$, $p < 0.01$, $p < 0.05$, $p < 0.05$) were clearly suppressed ($p < 0.01$, $p < 0.01$, $p < 0.01$, $p < 0.01$) in the *B. adolescentis*-treated mice compared with the CRS mice (**Table 5**). To further explore the correlation between anxiety/depression and inflammation, the protein expression of BDNF, IL-1β, TNF-α and Iba1 were examined in the CA1 region (Berkiks et al., 2018) of the hippocampus, as shown in **Figure 6E**. The protein expression of BDNF ($F_{(2,6)} = 8.868$, $p = 0.016$, **Figure 6A**), IL-1β ($F_{(2,6)} = 15.471$, $p = 0.004$, **Figure 6B**), TNF-α ($F_{(2,6)} = 143.837$, $p = 0$, **Figure 6C**) and Iba1 ($F_{(2,6)} = 15.24$, $p = 0.004$, **Figure 6D**) was verified by immunofluorescence (**Figure 6F**). The integrated density results showed that decreased BDNF expression ($p < 0.01$) was increased by *B. adolescentis* ($p < 0.05$), and the enhanced expression of IL-1β ($p < 0.01$), TNF-α ($p < 0.01$) and Iba1 ($p < 0.01$) was reduced ($p < 0.01$, $p < 0.01$, $p < 0.01$) by *B. adolescentis* (**Table 6**). The results imply that *B. adolescentis* increases BDNF expression under CRS conditions related to its anti-inflammatory effects in the hippocampus.

DISCUSSION

Here, we present novel evidence that *B. adolescentis* prevents the development of anxiety- and depression-like behaviors caused by CRS and that the effects of *B. adolescentis* are related to reducing inflammatory cytokines and rebalancing the gut microbiota.

The gut immune system consists of 70%–80% of the body's immune cells (Furness et al., 1999). Injury to the gastrointestinal tract, which is induced by CRS and related to the alteration of intestinal flora, triggers the discrimination of pathogenic and commensal microorganisms by the gut immune system and an immune response to the pathogen (Artis, 2008). The immune system is an indispensable part of central nervous system activity, including anxiety (Bercik et al., 2010) and depression (Hayley, 2011; Park et al., 2011). Additionally, intestinal flora exert substantial impacts on brain function through immune pathways by inducing the release of inflammatory cytokines into the circulatory system and then into the brain through the transport system of the blood brain barrier to directly influence brain activity and function (Pfau et al., 2018). Moreover, alterations in brain activity and function contribute to behavioral changes (Foster, 2016).

Depressed patients exhibit dysbiosis of gut bacteria or alterations in enteric microorganisms (Aizawa et al., 2016; Zheng et al., 2016; Dinan and Cryan, 2017; Fung et al., 2017). Chronic stress and depression were found to increase both the diversity and richness of gut bacterial populations (Naseribafrouei et al., 2014; Jiang et al., 2015; Li et al., 2018), but this result is in contrast to others (Kelly et al., 2016; Bharwani et al., 2017). In our study, an increase in gut bacterial α-diversity (Shannon index) was found in the CRS group, indicating that it is possible that CRS triggers an increase in the diversity of microbiota similar to dysbiosis induced by depression in patients.

Furthermore, *Lactobacillus* was reduced in the CRS group compared with the control group. Women who receive *Lactobacillus rhamnosus* HN001 have significantly lower depression and anxiety scores in the postpartum period, and appropriate intervention with *Lactobacillus* is beneficial for depressive patients (Slykerman et al., 2017). Our data reinforce the essential link between anxiety/depression and the abundance of *Lactobacillus*. The data showed an increase in

TABLE 6 | Changes in the protein expression of BDNF, IL-1β, TNF-α and Iba1 in the CA1 region of the hippocampus induced by pretreatment with *B. adolescentis*.

	Con			CRS			Bif+CRS			*df*	*F*	*P*
BDNF	14,751	10,982	15,237	8,019	9,727	8,762	13,296	14,505	12,274	2,6	8.868	0.016
IL-1β	3,433	4,576	5,334	8,892	7,734	9,565	4,654	5,672	6,708	2,6	15.471	0.004
TNF-α	2,829	4,075	3,323	15,288	14,169	16,283	7,956	8,932	7,249	2,6	143.837	0
Iba1	6,533	7,142	5,706	10,026	8,717	10,696	5,719	6,477	7,329	2,6	15.24	0.004

The mice in groups of Con, CRS and Bif+CRS were given with distilled water (10 mL/kg), distilled water (10 mL/kg), B. adolescentis (0.25 × 109 CFU/kg), respectively, by gavage for 21 days. N = 3 per group.

Lactobacillus in the CRS plus *B. adolescentis* group, verifying that the *Lactobacillus* increase was probably a major factor in preventing anxiety and depression. Consistent with the previous study, this study presumes that highly diverse bacterial communities, which are likely included in the pathogenesis of stress-induced behavioral deficits, are related to decreased *Lactobacillus* abundance (Li et al., 2018). The recovery of intestinal *Lactobacillus* levels is effective in improving behavioral deficits. Host kynurenine metabolism may be suppressed by reactive oxygen species derived by *Lactobacillus via* inhibiting the metabolizing enzyme IDO1 in the intestine (Marin et al., 2017).

It has been reported that 80% of patients with depression have a high proportion of *Bacteroides* in the fecal microbiota (Liu et al., 2016). As our study showed, the increased *Bacteroides* proportion in the CRS group was reversed by pretreatment with *B. adolescentis*, and at the same time, the decreased *Firmicutes* proportion in the CRS group was reversed by pretreatment with *B. adolescentis*. However, another controversial report showed that (R)-ketamine significantly increases the levels of Bacteroidales in susceptible mice after chronic social defeat stress (CSDS; Qu et al., 2017). The difference between the trends of Bacteroidales and *Bacteroides* may result from the different models, drugs and drug doses. The antidepressant effects of (R)-ketamine in a CSDS model may be regulated by the rebalancing of the intestinal microbiota to some extent, and (R)-ketamine can reduce the level of *Butyricimonas* in susceptible mice (Yang et al., 2017b). Moreover, *Clostridium butyricum*, a probiotic, augments 5-HT and BDNF expression, and its antidepressant effects in mice exposed to chronic unpredictable mild stress are partly due to the stimulation of intestinal glucagon-like peptide-1 secretion (Sun et al., 2018). The distinct appearance of *Bifidobacterium* is discovered in unsusceptible (resilient) mice and additionally, the administration of *Bifidobacterium* may confer resilience against CSDS (Yang et al., 2017a). Together, these findings show that the antidepressant mechanisms of *Bifidobacterium* related to the intestinal flora are complicated and require further investigation.

Gut microbiota can influence peripheral inflammation or CNS processes and subsequent behavioral responses to stress through cytokine-mediated immune signaling pathways, such as by increasing TNF-α (Ren et al., 2018), IL-1β (Grenham et al., 2011), and NF-κB (Wang et al., 2016), which is consistent with our data. Gut microbiota analysis shows that an anti-mouse IL-6 receptor antibody significantly improves the decreased *Firmicutes*/*Bacteroidetes* ratio in susceptible mice in a CSDS model (Zhang et al., 2017). It is possible that the increased *Firmicutes* and decreased *Bacteroidetes* levels induced by *B. adolescentis* are related to blockade of the IL-6 receptor. The gene expression of IL-1β in bone marrow-derived macrophage cells is increased after treatment with an isolate of *Bacteroides fragilis* (Deng et al., 2016). The bacterial flora of neonatal necrotizing enterocolitis patients contain significantly higher amounts of *Bacteroides*, which is accompanied by an enhancement of TNF-α (Hui et al., 2017), and *Bacteroides vulgatus* induces NF-κB activation and pro-inflammatory gene expression in intestinal epithelial cells (Haller et al., 2003). These studies show that *Bacteroides* is positively correlated with inflammatory factors, including IL-1β, TNF-α, and NF-κB. Additionally, a study demonstrated that the anxiolytic effect of *B. adolescentis* IM38 in mice may occur *via* reducing the blood IL-6 and TNF-α levels (Jang et al., 2018). Our data also showed an increase in *Bacteroides* and inflammatory cytokines, including IL-1β, TNF-α and NF-κB, in the CRS group, and the downregulation of these cytokines after pretreatment with *B. adolescentis*, confirming that a decreased *Bacteroides* level may be a vital element in the anti-inflammatory effects of *B. adolescentis*.

Lactobacillus brevis 23017 relieves colon toxicity by modulating oxidative stress and inflammation through NF-κB signaling cascades (Jiang et al., 2018). Additionally, our data demonstrate a reduction in *Lactobacillus* in the CRS group and the upregulation of *Lactobacillus* after pretreatment with *B. adolescentis*, verifying that an increase in *Lactobacillus* may be another key factor in the anti-inflammatory actions of *B. adolescentis*.

Microglia, which participate in synaptic pruning, promoting tissue repair, and recruiting peripheral leukocytes to sites of inflammation, have been observed in brain regions such as the hippocampus, amygdala, and prefrontal cortex (Wohleb, 2016; Ménard et al., 2017). *B. adolescentis* NK98 can inhibit the infiltration of Iba1 into the hippocampus caused by the acute immobilization stress (Jang et al., 2019). In our study, the *B. adolescentis*-pretreated group showed reduced Iba1 levels following CRS, which is in agreement with previously published studies that have highlighted the potential therapeutic efficacy of targeting central inflammatory processes, particularly those mediated by microglia, in depression (Alcocer-Gómez et al., 2016).

This study has a few limitations. First, in the preliminary efficacy screening experiment, *B. adolescentis* showed anxiolytic and antidepressant effects, then the mice were divided into a control group and a *B. adolescentis*-treated group. In our subsequent experiment, to study the anxiolytic and antidepressant mechanisms of *B. adolescentis*, we established a

B. adolescentis treatment plus CRS group, but we did not use a *B. adolescentis*-treated group as a control. Second, our current analyses of the gut microbiota and the brain were obtained from three or four samples per group; therefore, a large sample size may be needed in future studies to improve our understanding of the mechanisms underlying the relationship between the gut microbiota and inflammation. Third, the current study is correlational in nature, so no conclusions can be drawn about whether the inflammatory effects are the mechanism for the treatment effect on behavior. It could equally be the case that there is some other mechanism and the inflammatory findings are merely tangential.

CONCLUSION

In conclusion, we found that *B. adolescentis* increases the sequence proportion of *Lactobacillus* and reduces the sequence proportion of *Bacteroides* in feces. Moreover, *B. adolescentis* decreases IL-1β, TNF-α, NF-κB, and Iba1 protein expression and increases BDNF protein expression in the hippocampus of CRS mice. *B. adolescentis* has anxiolytic and antidepressant effects on behavioral performance in mice exposed to CRS. Thus, we conclude that the anxiolytic and antidepressant effects of *B. adolescentis* are related to reducing inflammatory cytokines and rebalancing the gut microbiota. Our data will contribute to the understanding of anti-inflammatory effects and the rebalancing of the gut microbiota as possible essential experimental therapeutic strategies for anxiety and depression.

ETHICS STATEMENT

Male ICR mice were purchased from Kunming Medical University. The procedures were approved by the Institutional Animal Care and Use Committee of Kunming Medical University, and were performed in accordance with the Guide for the Care and Use of Laboratory Animals.

AUTHOR CONTRIBUTIONS

YG and J-PX: conceptualization. KD, X-MH, QW and J-JL: data curation. XL, YY, QX and JX: formal analysis. YG, YY and QW: funding acquisition. H-RL: methodology and writing—review and editing. YG: writing—original draft.

FUNDING

This work was supported by the National Natural Science Foundation of China (31760297; YY), Applied Basic Research Foundation of Yunnan Province (2017FE467-160; YG) and Yunnan Provincial Department of Education Foundation (601160911; QW). This work was supported by the key project of Applied Bascic Research Foundation of Yunnan Province (Study on the antidepressant active components and mechanism of rosemary), and the cultivation object of Yunnan innovation team (Kunming Medical University innovation team for the discovery and utilization of the active ingredients of toxic medicinal plants).

REFERENCES

Aizawa, E., Tsuji, H., Asahara, T., Takahashi, T., Teraishi, T., Yoshida, S., et al. (2016). Possible association of *Bifidobacterium* and *Lactobacillus* in the gut microbiota of patients with major depressive disorder. *J. Affect. Disord.* 202, 254–257. doi: 10.1016/j.jad.2016.05.038

Alcocer-Gómez, E., Ulecia-Morón, C., Marín-Aguilar, F., Rybkina, T., Casas-Barquero, N., Ruiz-Cabello, J., et al. (2016). Stress-induced depressive behaviors require a functional NLRP3 inflammasome. *Mol. Neurobiol.* 53, 4874–4882. doi: 10.1007/s12035-015-9408-7

Artis, D. (2008). Epithelial-cell recognition of commensal bacteria and maintenance of immune homeostasis in the gut. *Nat. Rev. Immunol.* 8, 411–420. doi: 10.1038/nri2316

Bercik, P., Verdu, E. F., Foster, J. A., Macri, J., Potter, M., Huang, X., et al. (2010). Chronic gastrointestinal inflammation induces anxiety-like behavior and alters central nervous system biochemistry in mice. *Gastroenterology* 139, 2102.e1–2112.e1. doi: 10.1053/j.gastro.2010.06.063

Berkiks, I., Boulbaroud, S., Garcia-Segura, L. M., Mesfioui, A., Ouichou, A., Mouden, S., et al. (2018). Thymelaea lythroides extract attenuates microglial activation and depressive-like behavior in LPS-induced inflammation in adult male rats. *Biomed. Pharmacother.* 99, 655–663. doi: 10.1016/j.biopha.2018.01.125

Berry, A., Bellisario, V., Capoccia, S., Tirassa, P., Calza, A., Alleva, E., et al. (2012). Social deprivation stress is a triggering factor for the emergence of anxiety- and depression-like behaviours and leads to reduced brain BDNF levels in C57BL/6J mice. *Psychoneuroendocrinology* 37, 762–772. doi: 10.1016/j.psyneuen.2011.09.007

Bharwani, A., Mian, M. F., Surette, M. G., Bienenstock, J., and Forsythe, P. (2017). Oral treatment with *Lactobacillus* rhamnosus attenuates behavioural deficits and immune changes in chronic social stress. *BMC Med.* 15:7. doi: 10.1186/s12916-016-0771-7

de Pablos, R. M., Herrera, A. J., Espinosa-Oliva, A. M., Sarmiento, M., Muñoz, M. F., Machado, A., et al. (2014). Chronic stress enhances microglia activation and exacerbates death of nigral dopaminergic neurons under conditions of inflammation. *J. Neuroinflammation* 11:34. doi: 10.1186/1742-2094-11-34

Deng, H., Li, Z., Tan, Y., Guo, Z., Liu, Y., Wang, Y., et al. (2016). A novel strain of *Bacteroides* fragilis enhances phagocytosis and polarises M1 macrophages. *Sci. Rep.* 6:29401. doi: 10.1038/srep29401

Desbonnet, L., Garrett, L., Clarke, G., Bienenstock, J., and Dinan, T. G. (2008). The probiotic Bifidobacteria infantis: an assessment of potential antidepressant properties in the rat. *J. Psychiatr. Res.* 43, 164–174. doi: 10.1016/j.jpsychires.2008.03.009

Dinan, T. G., and Cryan, J. F. (2017). Microbes, immunity, and behavior: psychoneuroimmunology meets the microbiome. *Neuropsychopharmacology* 42, 178–192. doi: 10.1038/npp.2016.103

Evrensel, A., and Ceylan, M. E. (2015). The gut-brain axis: the missing link in depression. *Clin. Psychopharmacol. Neurosci.* 13, 239–244. doi: 10.9758/cpn.2015.13.3.239

Fang, M., Yuan, Y., Rangarajan, P., Lu, J., Wu, Y., Wang, H., et al. (2015). Scutellarin regulates microglia-mediated TNC1 astrocytic reaction and astrogliosis in cerebral ischemia in the adult rats. *BMC Neurosci.* 16:84. doi: 10.1186/s12868-015-0219-6

Farooq, R. K., Isingrini, E., Tanti, A., Le Guisquet, A. M., Arlicot, N., Minier, F., et al. (2012). Is unpredictable chronic mild stress (UCMS) a reliable model to study depression-induced neuroinflammation? *Behav. Brain Res.* 231, 130–137. doi: 10.1016/j.bbr.2012.03.020

Foster, J. A. (2016). Gut microbiome and behavior: focus on neuroimmune interactions. *Int. Rev. Neurobiol.* 131, 49–65. doi: 10.1016/bs.irn.2016.07.005

Fung, T. C., Olson, C. A., and Hsiao, E. Y. (2017). Interactions between the microbiota, immune and nervous systems in health and disease. *Nat. Neurosci.* 20, 145–155. doi: 10.1038/nn.4476

Furness, J. B., Kunze, W. A., and Clerc, N. (1999). Nutrient tasting and signaling mechanisms in the gut. II. The intestine as a sensory organ: neural, endocrine, and immune responses. *Am. J. Physiol.* 277, G922–G928. doi: 10.1152/ajpgi.1999.277.5.g922

Grenham, S., Clarke, G., Cryan, J. F., and Dinan, T. G. (2011). Brain-gut-microbe communication in health and disease. *Front. Physiol.* 2:94. doi: 10.3389/fphys.2011.00094

Haller, D., Holt, L., Kim, S. C., Schwabe, R. F., Sartor, R. B., and Jobin, C. (2003). Transforming growth factor-β 1 inhibits non-pathogenic Gram negative bacteria-induced NF-κB recruitment to the interleukin-6 gene promoter in intestinal epithelial cells through modulation of histone acetylation. *J. Biol. Chem.* 278, 23851–23860. doi: 10.1074/jbc.M300075200

Hayley, S. (2011). Toward an anti-inflammatory strategy for depression. *Front. Behav. Neurosci.* 5:19. doi: 10.3389/fnbeh.2011.00019

Hennessy, M. B., Schiml, P. A., Berberich, K., Beasley, N. L., and Deak, T. (2019). Early attachment disruption, inflammation, and vulnerability for depression in rodent and primate models. *Front. Behav. Neurosci.* 12:314. doi: 10.3389/fnbeh.2018.00314

Hodes, G. E., Pfau, M. L., Leboeuf, M., Golden, S. A., Christoffel, D. J., Bregman, D., et al. (2014). Individual differences in the peripheral immune system promote resilience versus susceptibility to social stress. *Proc. Natl. Acad. Sci. U S A* 111, 16136–16141. doi: 10.1073/pnas.1415191111

Hui, L., Dai, Y., Guo, Z., Zhang, J., Zheng, F., Bian, X., et al. (2017). Immunoregulation effects of different γδT cells and toll-like receptor signaling pathways in neonatal necrotizing enterocolitis. *Medicine* 96:e6077. doi: 10.1097/md.0000000000006077

Jang, H. M., Jang, S. E., Han, M. J., and Kim, D. H. (2018). Anxiolytic-like effect of *Bifidobacterium adolescentis* IM38 in mice with or without immobilisation stress. *Stress* 9, 123–132. doi: 10.3920/bm2016.0226

Jang, H. M., Lee, K. E., and Kim, D. H. (2019). The preventive and curative effects of *lactobacillus* reuteri NK33 and *Bifidobacterium adolescentis* NK98 on immobilization stress-induced anxiety/depression and colitis in mice. *Nutrients* 11:E819. doi: 10.3390/nu11040819

Jiang, X., Gu, S., Liu, D., Zhao, L., Xia, S., He, X., et al. (2018). *Lactobacillus brevis* 23017 relieves mercury toxicity in the colon by modulation of oxidative stress and inflammation through the interplay of MAPK and NF-κB signaling cascades. *Front. Microbiol.* 9:2425. doi: 10.3389/fmicb.2018.02425

Jiang, H., Ling, Z., Zhang, Y., Mao, H., Ma, Z., Yin, Y., et al. (2015). Altered fecal microbiota composition in patients with major depressive disorder. *Brain Behav. Immun.* 48, 186–194. doi: 10.1016/j.bbi.2015.03.016

Kelly, J. R., Borre, Y., O'Brien, C., Patterson, E., El Aidy, S., Deane, J., et al. (2016). Transferring the blues: depression-associated gut microbiota induces neurobehavioural changes in the rat. *J. Psychiatr. Res.* 82, 109–118. doi: 10.1016/j.jpsychires.2016.07.019

Krishnan, R., Cella, D., Leonardi, C., Papp, K., Gottlieb, A. B., Dunn, M., et al. (2007). Effects of etanercept therapy on fatigue and symptoms of depression in subjects treated for moderate to severe plaque psoriasis for up to 96 weeks. *Br. J. Dermatol.* 157, 1275–1277. doi: 10.1111/j.1365-2133.2007.08205.x

Li, N., Wang, Q., Wang, Y., Sun, A., Lin, Y., Jin, Y., et al. (2018). Oral probiotics ameliorate the behavioral deficits induced by chronic mild stress in mice via the gut microbiota-inflammation axis. *Front. Behav. Neurosci.* 12:266. doi: 10.3389/fnbeh.2018.00266

Lim, S. M., and Kim, D. H. (2017). *Bifidobacterium adolescentis* IM38 ameliorates high-fat diet-induced colitis in mice by inhibiting NF-κB activation and lipopolysaccharide production by gut microbiota. *Nutr. Res.* 41, 86–96. doi: 10.1016/j.nutres.2017.04.003

Liu, Y., Zhang, L., Wang, X., Wang, Z., Zhang, J., Jiang, R., et al. (2016). Similar fecal microbiota signatures in patients with diarrhea-predominant irritable bowel syndrome and patients with depression. *Clin. Gastroenterol. Hepatol.* 14, 1602.e5–1611.e5. doi: 10.1016/j.cgh.2016.05.033

Maes, M. (2008). The cytokine hypothesis of depression: inflammation, oxidative & nitrosative stress (IO&NS) and leaky gut as new targets for adjunctive treatments in depression. *Neuro Endocrinol. Lett.* 29, 287–291.

Maes, M., Song, C., and Yirmiya, R. (2012). Targeting IL-1 in depression. *Expert Opin. Ther. Targets* 16, 1097–1112. doi: 10.1517/14728222.2012.718331

Manning, J., Kulbida, R., Rai, P., Jensen, L., Bouma, J., Singh, S. P., et al. (2014). Amitriptyline is efficacious in ameliorating muscle inflammation and depressive symptoms in the mdx mouse model of Duchenne muscular dystrophy. *Exp. Physiol.* 99, 1370–1386. doi: 10.1113/expphysiol.2014.079475

Marin, I. A., Goertz, J. E., Ren, T., Rich, S. S., Onengut-Gumuscu, S., Farber, E., et al. (2017). Microbiota alteration is associated with the development of stress-induced despair behavior. *Sci. Rep.* 7:43859. doi: 10.1038/srep43859

McKeever, A., Agius, M., and Mohr, P. (2017). A review of the epidemiology of major depressive disorder and of its consequences for society and the individual. *Psychiatr. Danub.* 29, 222–231.

Ménard, C., Pfau, M. L., Hodes, G. E., and Russo, S. J. (2017). Immune and neuroendocrine mechanisms of stress vulnerability and resilience. *Neuropsychopharmacology* 42, 62–80. doi: 10.1038/npp.2016.90

Messaoudi, M., Lalonde, R., Violle, N., Javelot, H., Desor, D., Nejdi, A., et al. (2011). Assessment of psychotropic-like properties of a probiotic formulation (*Lactobacillus helveticus* R0052 and *Bifidobacterium* longum R0175) in rats and human subjects. *Br. J. Nutr.* 105, 755–764. doi: 10.1017/s0007114510004319

Meyer, C., and Vassar, M. (2018). The fragility of probiotic *Bifidobacterium* longum NCC3001 use for depression in patients with irritable bowel syndrome. *Gastroenterology* 154:764. doi: 10.1053/j.gastro.2017.09.055

Naseribafrouei, A., Hestad, K., Avershina, E., Sekelja, M., Linløkken, A., Wilson, R., et al. (2014). Correlation between the human fecal microbiota and depression. *Neurogastroenterol. Motil.* 26, 1155–1162. doi: 10.1111/nmo.12378

Oglodek, E. A., Just, M. J., Szromek, A. R., and Araszkiewicz, A. (2017). Assessing the serum concentration levels of NT-4/5, GPX-1, TNF-α, and l-arginine as biomediators of depression severity in first depressive episode patients with and without posttraumatic stress disorder. *Pharmacol. Rep.* 69, 1049–1058. doi: 10.1016/j.pharep.2017.04.013

Park, S. E., Dantzer, R., Kelley, K. W., and McCusker, R. H. (2011). Central administration of insulin-like growth factor-I decreases depressive-like behavior and brain cytokine expression in mice. *J. Neuroinflammation* 8:12. doi: 10.1186/1742-2094-8-12

Pfau, M. L., Ménard, C., and Russo, S. J. (2018). Inflammatory mediators in mood disorders: therapeutic opportunities. *Annu. Rev. Pharmacol. Toxicol.* 58, 411–428. doi: 10.1146/annurev-pharmtox-010617-052823

Qu, Y., Yang, C., Ren, Q., Ma, M., Dong, C., and Hashimoto, K. (2017). Comparison of (R)-ketamine and lanicemine on depression-like phenotype and abnormal composition of gut microbiota in a social defeat stress model. *Sci. Rep.* 7:15725. doi: 10.1038/s41598-017-16060-7

Ravel, J., Gajer, P., Abdo, Z., Schneider, G. M., Koenig, S. S., McCulle, S. L., et al. (2011). Vaginal microbiome of reproductive-age women. *Proc. Natl. Acad. Sci. U S A* 108, 4680–4687. doi: 10.1073/pnas.1002611107

Ren, Y., Geng, Y., Du, Y., Li, W., Lu, Z. M., Xu, H. Y., et al. (2018). Polysaccharide of Hericium erinaceus attenuates colitis in C57BL/6 mice via regulation of oxidative stress, inflammation-related signaling pathways and modulating the composition of the gut microbiota. *J. Nutr. Biochem.* 57, 67–76. doi: 10.1016/j.jnutbio.2018.03.005

Riedel, C. U., Foata, F., Philippe, D., Adolfsson, O., Eikmanns, B. J., and Blum, S. (2006). Anti-inflammatory effects of bifidobacteria by inhibition of LPS-induced NF-κB activation. *World J. Gastroenterol.* 12, 3729–3735. doi: 10.3748/wjg.v12.i23.3729

Sanna, M. D., Ghelardini, C., and Galeotti, N. (2017). Effect of amitriptyline treatment on neurofilament-H protein in an experimental model of depression. *Brain Res. Bull.* 128, 1–6. doi: 10.1016/j.brainresbull.2016.11.001

Sathyanesan, M., Haiar, J. M., Watt, M. J., and Newton, S. S. (2017). Restraint stress differentially regulates inflammation and glutamate receptor gene expression in the hippocampus of C57BL/6 and BALB/c mice. *Stress* 20, 197–204. doi: 10.1080/10253890.2017.1298587

Slykerman, R. F., Hood, F., Wickens, K., Thompson, J. M. D., Barthow, C., Murphy, R., et al. (2017). Effect of *lactobacillus rhamnosus* HN001 in pregnancy on postpartum symptoms of depression and anxiety: a randomised double-blind placebo-controlled trial. *EBioMedicine* 24, 159–165. doi: 10.1016/j.ebiom.2017.09.013

Sun, J., Wang, F., Hu, X., Yang, C., Xu, H., Yao, Y., et al. (2018). *Clostridium butyricum* attenuates chronic unpredictable mild stress-induced depressive-like behavior in mice via the gut-brain axis. *J. Agric. Food Chem.* 66, 8415–8421. doi: 10.1021/acs.jafc.8b02462

Trivedi, M. H., Greer, T. L., Grannemann, B. D., Chambliss, H. O., and Jordan, A. N. (2006). Exercise as an augmentation strategy for treatment of major depression. *J. Psychiatr. Pract.* 12, 205–213. doi: 10.1097/00131746-200607000-00002

Wang, W., Li, Z., Han, Q., Guo, Y., Zhang, B., and D'Inca, R. (2016). Dietary live yeast and mannan-oligosaccharide supplementation attenuate intestinal inflammation and barrier dysfunction induced by Escherichia coli in broilers. *Br. J. Nutr.* 116, 1878–1888. doi: 10.1017/s0007114516004116

Wohleb, E. S. (2016). Neuron-microglia interactions in mental health disorders: "for better, and for worse". *Front. Immunol.* 7:544. doi: 10.3389/fimmu.2016.00544

Wong, M. L., Inserra, A., Lewis, M. D., Mastronardi, C. A., Leong, L., Choo, J., et al. (2016). Inflammasome signaling affects anxiety- and depressive-like behavior and gut microbiome composition. *Mol. Psychiatry* 21, 797–805. doi: 10.1038/mp.2016.46

Yang, C., Fujita, Y., Ren, Q., Ma, M., Dong, C., and Hashimoto, K. (2017a). *Bifidobacterium* in the gut microbiota confer resilience to chronic social defeat stress in mice. *Sci. Rep.* 7:45942. doi: 10.1038/srep45942

Yang, C., Qu, Y., Fujita, Y., Ren, Q., Ma, M., Dong, C., et al. (2017b). Possible role of the gut microbiota-brain axis in the antidepressant effects of (R)-ketamine in a social defeat stress model. *Transl. Psychiatry* 7:1294. doi: 10.1038/s41398-017-0031-4

Yang, L. P., Jiang, F. J., Wu, G. S., Deng, K., Wen, M., Zhou, X., et al. (2015). Acute treatment with a novel TRPC4/C5 channel inhibitor produces antidepressant and anxiolytic-like effects in mice. *PLoS One* 10:e0136255. doi: 10.1371/journal.pone.0136255

Yu, H., and Chen, Z. Y. (2011). The role of BDNF in depression on the basis of its location in the neural circuitry. *Acta Pharmacol. Sin.* 32, 3–11. doi: 10.1038/aps.2010.184

Yuan, Y., Zha, H., Rangarajan, P., Ling, E. A., and Wu, C. (2014). Anti-inflammatory effects of Edaravone and Scutellarin in activated microglia in experimentally induced ischemia injury in rats and in BV-2 microglia. *BMC Neurosci.* 15:125. doi: 10.1186/s12868-014-0125-3

Zhang, Y., Liu, L., Liu, Y. Z., Shen, X. L., Wu, T. Y., Zhang, T., et al. (2015). NLRP3 inflammasome mediates chronic mild stress-induced depression in mice via neuroinflammation. *Int. J. Neuropsychopharmacol.* 18:pyv006. doi: 10.1093/ijnp/pyv006

Zhang, J. C., Yao, W., Dong, C., Yang, C., Ren, Q., Ma, M., et al. (2017). Blockade of interleukin-6 receptor in the periphery promotes rapid and sustained antidepressant actions: a possible role of gut-microbiota-brain axis. *Transl. Psychiatry* 7:e1138. doi: 10.1038/tp.2017.112

Zheng, P., Zeng, B., Zhou, C., Liu, M., Fang, Z., Xu, X., et al. (2016). Gut microbiome remodeling induces depressive-like behaviors through a pathway mediated by the host's metabolism. *Mol. Psychiatry* 21, 786–796. doi: 10.1038/mp.2016.44

Conflict of Interest Statement: The authors declare that the research was conducted in the absence of any commercial or financial relationships that could be construed as a potential conflict of interest.

frontiers in Behavioral Neuroscience

ORIGINAL RESEARCH
published: 06 September 2019
doi: 10.3389/fnbeh.2019.00204

The Cognitive, Behavioral, and Emotional Aspects of Eating Habits and Association With Impulsivity, Chronotype, Anxiety, and Depression: A Cross-Sectional Study

Carla Aoun[1,2], *Lynn Nassar*[1,2], *Stéphanie Soumi*[1,2], *Nada El Osta*[3,4], *Tatiana Papazian*[1,2] *and Lydia Rabbaa Khabbaz*[1,2]*

[1] Laboratoire de Pharmacologie, Pharmacie Clinique et Contrôle de qualité des médicaments, Faculty of pharmacy, Saint-Joseph University of Beirut, Beirut, Lebanon, [2] Department of Nutrition, Faculty of Pharmacy, Saint-Joseph University of Beirut, Beirut, Lebanon, [3] Department of Public Health, Faculty of Medicine, Saint-Joseph University, Beirut, Lebanon, [4] Department of Prosthodontics, Faculty of Dental Medicine, Saint-Joseph University, Beirut, Lebanon

OPEN ACCESS

Edited by:
Walter Adriani,
Istituto Superiore di Sanità (ISS), Italy

Reviewed by:
Terence Y. Pang,
Florey Institute of Neuroscience and Mental Health, Australia
Giulia Ballarotto,
Sapienza University of Rome, Italy

***Correspondence:**
Lydia Rabbaa Khabbaz
lydia.khabbaz@usj.edu.lb

Specialty section:
This article was submitted to Motivation and Reward, a section of the journal Frontiers in Behavioral Neuroscience

Received: *09 April 2019*
Accepted: *20 August 2019*
Published: *06 September 2019*

Citation:
Aoun C, Nassar L, Soumi S, El Osta N, Papazian T and Rabbaa Khabbaz L (2019) The Cognitive, Behavioral, and Emotional Aspects of Eating Habits and Association With Impulsivity, Chronotype, Anxiety, and Depression: A Cross-Sectional Study. Front. Behav. Neurosci. 13:204. doi: 10.3389/fnbeh.2019.00204

Background and objectives: Understanding behavioral issues associated with eating would provide important insight into obesity development and possibly procure ways to prevent its occurrence or to treat it. This study's objectives were to examine links between cognitive, behavioral, and emotional aspects of eating habits and chronotype, impulsivity, anxiety, and depression among university students.

Subjects and methods: The following questionnaires were used: TFEQ-R 18, UPPS-short, HADS, and MEQ. All participants gave their informed written consent prior to enrolment.

Results: Among females, increased BMI was associated to uncontrolled eating and emotional eating, while in males, BMI was associated to emotional eating only. In males, no associations of BMI with impulsivity were found while in females they were present. Chronotype scores were positively correlated to cognitive restraint and negatively to uncontrolled eating among males. No associations were found for females. CR was lower among females with higher depression scores, while higher anxiety scores were associated to UE among males.

Conclusions: This was a cross-sectional study of three cognitive and emotional domains related to eating habits among university students (young adults). Results showed significant correlations between BMI, TFEQ-R18 scores, impulsivity and anxiety or depression. Future studies should replicate findings in samples of individuals with different aspects of eating disorders such as binge eating disorder, food addiction or bulimia nervosa.

Keywords: eating habits, cognitive restraint, uncontrolled eating, emotional eating, impulsivity, chronotype, anxiety, university students

INTRODUCTION

Obesity is one of the most prevalent public health problems but is often ignored (Singh et al., 2017). Numerous factors at the individual, interpersonal, environmental, and macrosystem levels contribute to obesity (Banna et al., 2018). Understanding behavioral eating issues would provide important insight into obesity development and possibly procure ways to prevent its occurrence or to treat it. One of the tools used to examine disorders in eating behaviors related to development of obesity is the Three-Factor Eating Questionnaire (TFEQ) (de Lauzon et al., 2004). It was initially developed to assess cognitive restraint, disinhibition, and susceptibility to hunger in adults (Stunkard and Messick, 1985). The TFEQ, which was first created by Stunkard and Messick (1985), is a widely used instrument in eating behavior researches all over the world. The TFEQ-R18 is a shortened, revised version of the TFEQ questionnaire with three subscales, where disinhibition and hunger scales were grouped in a single subscale and labeled as uncontrolled eating (UE); The Cognitive Restraint (CR) scale was shortened, and a third subscale was added including three items tagged as emotional eating (EE) (Provencher et al., 2003; Hays and Roberts, 2008).

CR or restricting eating to control body weight is characterized as the cognitive and self-imposed limitation of food ingestion to control weight (Preedy et al., 2011). However, disinhibited eating could happen among individuals with high cognitive restraint under stress (Zigmond and Snaith, 1983; Boutelle et al., 2010).

The UE behavior is a tendency to lose control regarding food when an individual feels hungry or when external cues (e.g., very palatable food) are present. This could happen even when physiological hunger is absent (Tholin et al., 2005). Finally, EE is the tendency to eat in response to negative mood states and emotional stress (Gibson, 2012). EE is considered a common dimension of all eating disorders (Rotella et al., 2015) and is more frequent among women than men (Kemp et al., 2011). People who present an increased CR and a decreased EE and/or UE achieve better results when following weight-loss programs (Keränen et al., 2009; Konttinen et al., 2009).

In addition to eating behavior, multiple studies shows that sleeping habits have an impact on regulation of body weight (Chaput et al., 2011). Short sleep duration and poor sleep quality are major factors linked to weight and eating pattern. A longitudinal study of a large sample of adults reported higher food consumption in the event of sleep deprivation (Chaput et al., 2011) leading to an increase in stress-related eating (Bond et al., 2001).

Chronotype is a circadian typology that splits individuals into morning, intermediate or evening types, each with its own properties and predispositions to several diseases. The disparity between chronotype groups is an important factor that affects sleep and sleep patterns (Adan et al., 2012; Song et al., 2018). Night-type individuals exhibit a social jet lag that is defined by a gap between the social clock and the endogenous circadian clock, leading to chronic sleep loss, metabolic and psychological modification, including cardiovascular diseases, type 2 diabetes, depressive symptoms, and emotional eating (Haffen, 2009; Konttinen et al., 2014). On the other hand, a positive association is shown between morning chronotype and dietary restriction (Schubert and Randler, 2008).

Another factor contributing to eating behavior is impulsivity: some dimensions of impulsivity have been implicated in binge eating and more specifically in exaggerated food consumption with loss of control (Espel et al., 2017). Impulsivity is defined as a general tendency to have rapid or even unforeseen reactions to external or internal stimuli regardless of the consequences of these actions on oneself or others (Jasinska et al., 2012). Depression, anxiety, chronotype and impulsivity are closely related (Caci et al., 2005; Moustafa et al., 2017). This study's objectives were to examine links between cognitive, behavioral, and emotional aspects of eating habits and chronotype, impulsivity, anxiety, and depression among young adults (university students). To the best of our knowledge, no previous study has assessed these associations.

MATERIALS AND METHODS

Ethical Considerations

The ethics committee of Saint-Joseph University (Ref USJ-2017-81) approved the protocol of this study. Informed written consent was obtained from all participants in the study.

Survey Procedure and Sampling

This is a cross-sectional questionnaire-based survey conducted among Lebanese university students (Grand Beirut universities: USJ, Lebanese university, USEK, ALBA, NDU, LAU, SAGESSE), from October 2017 till March 2018. Inclusion criteria were: students $\geq$18 years, willingly participating in the study. Exclusion criteria were the presence of any cognitive deficit or other chronic diseases. A random number table was used to randomly select students within each university, in order to ensure the representativeness of the sample. The random selection was proportional to students number in each university. The selected students were approached at the end of their courses, before leaving the classroom, by two trained research assistants. Out of 580 students approached (56% females−44% males), 400 agreed to participate. In the final sample, 81% of females approached agreed to participate while only 53.7% of males approached did.

Data Collection

Data were collected during a face-to-face interview, using a survey tool (self-administered and standardized) based on internationally reliable and validated questionnaires, namely the TFEQ-R 18, the UPPS-short, the HADS, and the MEQ. The duration of interviews ranged from 15 to 25 min.

Measures

Participants

Socio-demographic characteristics of the participants were collected. The crowding index (number of people living in the same house divided by the number of rooms in the house excluding the kitchen and bathrooms) was calculated. Caffeine intake was assessed with two questions: number of cups of

coffee/day and number of units of any beverage containing caffeine (mainly soft drinks containing caffeine).

Eating Habits Assessed With the Three-Factor Eating Questionnaire Revised 18-Item Version (TFEQ-R 18)

Originally consisting of 51 items, Karlsson et al. (2000) developed a reduced version of the TFEQ-R18 (Three-Factor Eating Questionnaire Revised 18-item version). The reduced version assesses three main eating behaviors: emotional eating (EE), uncontrolled eating (UE), and cognitive restraint (CR). The components of eating behavior assessed by this questionnaire are related to energy and macronutrient intake or intake of certain types of foods. It is based on a four-point answer scale (absolutely true, mostly true, absolutely wrong, and mostly false). Responses to each of the 18 points have a score range between 1 and 4 and the scores are added (de Lauzon et al., 2004). The Cronbach alpha was 0.726.

Impulsivity Assessed With the Impulsive Behavior Scale (UPPS-P Short Version)

The UPPS scale was originally developed by Whiteside and Lynam (2003). Four impulsivity traits were included in the original version of the scale: lack of premeditation, negative urgency, sensation seeking, and lack of perseverance (Jasinska et al., 2012; Booth et al., 2018). Impulsive action under extreme positive emotions were not well-conceptualized in this scale. Therefore, Cyders and colleagues created a scale of positive urgency, which was later incorporated into the UPPS-P scale and in the shorter version, the UPPS-P short version that we used in this study (Cyders et al., 2014). Higher scores indicate higher impulsivity. The Cronbach alpha was 0.843.

Evaluation of Anxiety and Depression With the Hospital Anxiety and Depression Scale (HADS)

The HADS is an effective instrument for evaluating anxiety and depressive disorders and was validated by Zigmond and Snaith (1983). Fourteen items are included in the scale. Each item is rated on a scale from 0 to 3. The HADS is divided into two subscales: HADS-A with seven items built to the clinical criteria for diagnosis of anxiety symptoms and HADS-D, with seven other items built to the clinical criteria for diagnosis of depression symptoms. Each subscale score is calculated by summing the points of the items included in the subscale and the value range is 0–21. The interpretation of the obtained score is as follows: $\leq$7: absence of anxiety/depression; 8–10: borderline abnormal; 11–21: severe anxiety/depression. A total HADS score can also be calculated. The Cronbach alpha was 0.771.

Evaluation of the Chronotype With the Morningness-Eveningness Questionnaire (MEQ)

The Morningness-Eveningness Questionnaire (MEQ) is a widely-used international questionnaire validated by Horne and Ostberg (1976). This questionnaire is composed of 19 items. It is self-administered and measures the person's peak alertness/sleepiness (morning or evening). MEQ consists of 19 questions allowing to calculate a total score between 16 and 86; scores $\leq$30 indicate definite evening type, 31–41 indicate moderate evening type, 42–58 intermediate type, 59–69 moderate morning type, and 70–86 definite morning type. The Cronbach alpha was 0.784.

TABLE 1 | Sociodemographic characteristics of the participants.

	N	Percentage
GENDER		
Male	137	34.2
Female	263	65.8
LIVING		
Alone	16	4.0
In couple	2	0.5
With family	381	95.2
Missing values	1	0.2
BMI CATEGORIZED*		
Males		
Underweight	8	5.8
Normal	86	62.8
Overweight	42	30.7
Obese	1	0.7
Females		
Underweight	42	16.1
Normal	199	76.2
Overweight	17	6.5
Obese	3	1.1
ECONOMIC STATUS OF THE STUDENT		
Not working	342	85.5
Working	55	13.7
Missing values	3	0.8
SMOKING STATUS		
No	280	70.0
Ex-smoker	21	5.2
Yes	81	20.2
Missing values	18	4.5
ALCOHOL INTAKE		
No	90	22.5
Occasionally	214	53.5
$\leq$ once per week	50	12.5
$>$ once per week	35	8.8
Missing values	11	2.8
COFFEE		
No	172	43.0
1–2 cups/day	186	46.5
$>$2 cups/day	38	9.5
Missing values	4	1.0

	N	Minimum	Maximum	Mean	Standard deviation
Age	400	18	30	20.39	1.83
Crowding index	399	0.0	4.0	0.95	0.44
BMI*	398	16.0	32	22.06	3.12
Males	137	16.1	32.2	23.78	2.99
Females	263	16.0	30.5	21.15	2.78

**Significant difference between males and females ($p < 0.001$).*

Data Analysis

Statistical analysis

The statistical analyses were performed with SPSS software for Windows (version 24.0, Chicago, IL, USA). A significance level of 0.05 was set. Means and standard deviations were calculated for continuous variables and percentages for categorical variables. The normality distribution of continuous variables was tested with Kolmogorov-Smirnov tests. Chi-square independence tests and Fisher Exact tests were used to examine the relationship between categorical variables. Pearson and Spearman correlation coefficients were used to evaluate the association between continuous variables. In step one, univariate analyses were carried out with the Student's *t*-test or its equivalent non-parametric Mann-Whitney test and analysis of variance (ANOVA) or its equivalent non-parametric Kruskal-Wallis test. Univariate followed by multivariate analyses were performed to assess the association between explanatory variables and eating habits dimensions.

Each of cognitive, behavioral and emotional eating was the dependant variables of the study. Impulsivity, anxiety and depression were the explanatory independent variables.

Candidates for the multivariate model, according to the Enter method were the independent variables that showed associations with a $p < 0.200$ in univariate analyses. Collinearity among independent variables was also examined and we excluded variables highly correlated from the model. Interaction between each component of impulsivity and anxiety/depression was also tested when introduced in the same multivariate model. The interaction results between impulsivity and anxiety/depression were not statistically significant ($p > 0.05$).

RESULTS

The socio-demographic characteristics of the participants are summarized in **Table 1**. 400 students were included (65.8% females), with a mean age of 20.39 (SD = 1.83).

BMI was analyzed in two different ways: as continuous variable and was also categorized according to the World Health Organization (WHO) cut-off points (underweight < 18.5, normal 18.5–24.9, overweight 25–29.9, and obese > 30 kg/m^2) (WHO, 1995).

The average scores relative to the questionnaires, according to gender, are summarized in **Table 2**. Among eating habits, emotional eating component was significantly different between males and females ($p = 0.038$). Impulsivity facets and chronotype did not show gender differences. Anxiety scores were significantly higher among females and depression scores higher among males ($p = 0.000$ and 0.039, respectively).

Tables 3, **4** show the correlations found between the different components of the questionnaires and the continuous sociodemographic factors among males and females. BMI was significantly correlated to cognitive restraint and emotional eating in both gender; however, no significant correlation was detected between BMI and uncontrolled eating among males. BMI was also significantly and positively correlated to lack of premeditation among males as well as to higher depression scores among females and higher anxiety scores among males.

Age was significantly and positively correlated to the chronotype score in both gender. Crowding index was significantly and positively associated several impulsivity facets. As for alcohol, increased intake was associated with higher uncontrolled eating scores among males and higher seeking sensations scores in both gender. Coffee intake was associated with higher anxiety scores as well as higher lack of premeditation, positive and negative urgency among females.

Table 5 shows the association between the three components of eating habits and categorized BMI (according to gender). **Tables 6**, **7** present the correlations between the 3 domains of the eating habits questionnaire and the other questionnaires among females and males. Multiple significant correlations were seen between the eating habits and impulsivity (especially among

TABLE 2 | Eating habits, impulsivity, chronotype, anxiety, and depression: average scores, standard deviation (SD) and percentages.

		Men	Women	Total	*p*
Eating habits (TFEQ-R 18)	Cognitive restraint	12.99 ± 3.244	13.19 ± 3.566	13.12 ± 3.456	0.596
	Uncontrolled eating	21.61 ± 5.524	20.80 ± 5.448	21.08 ± 5.481	0.164
	Emotional eating	6.62 ± 2.346	7.16 ± 2.549	6.98 ± 2.491	0.038
Impulsivity (UPPS)	Negative urgency	9.82 ± 3.001	9.91 ± 3.045	9.88 ± 3.026	0.766
	Positive urgency	10.69 ± 2.789	10.90 ± 2.730	10.82 ± 2.748	0.466
	Lack of premeditation	7.42 ± 2.637	7.36 ± 2.795	7.38 ± 2.738	0.820
	Lack of perseverance	7.42 ± 2.785	7.24 ± 3.107	7.30 ± 2.999	0.571
	Seeking sensations	11.71 ± 2.883	11.30 ± 3.212	11.44 ± 3.106	0.209
Anxiety and depression (HADS)	Anxiety	7.77 ± 3.824	9.24 ± 3.829	8.74 ± 3.886	0.000
	Depression	6.96 ± 3.705	6.24 ± 3.124	6.48 ± 3.348	0.039
	HADS	14.73 ± 6.665	15.48 ± 6.121	15.22 ± 6.314	0.263
Chronotype (MEQ)	Chronotype	47.39 ± 9.218	47.70 ± 9.306	47.60 ± 9.266	0.746
	Definite evening type	7 (5.1%)	6 (2.3%)	13 (3.2%)	
	Moderate evening type	28 (20.4%)	57 (21.7%)	85 (21.2%)	0.568
	Intermediate type	87 (63.5%)	169 (64.3%)	256 (64.0%)	
	Moderate morning type	15 (10.9%)	29 (11.0%)	44 (11.0%)	
	Definite morning type	0 (0.0%)	2 (0.8%)	2 (0.5%)	

TABLE 3 | Associations between the different components of the questionnaires and the continuous socio-demographic characteristics of male participants ($N = 400$).

		Age	Crowding index	BMI	Alcohol	Coffee
Tfeq-R 18						
Cognitive restraint	Correlation coefficient	−0.024	−0.095	**0.207**	−0.095	−0.005
	p-value	0.777	0.272	**0.015**	0.279	0.956
	N	137	136	**137**	133	137
Uncontrolled eating	Correlation coefficient	**−0.251**	−0.001	0.153	**0.177**	0.125
	p-value	**0.003**	0.990	0.074	**0.042**	0.145
	N	**137**	136	137	**133**	137
Emotional eating	Correlation coefficient	−0.024	−0.008	**0.192**	0.075	0.075
	p-value	0.781	0.927	**0.024**	0.393	0.387
	N	137	136	**137**	133	137
Upps						
Negative urgency	Correlation coefficient	0.079	0.086	0.128	0.008	−0.057
	p-value	0.357	0.322	0.136	0.924	0.510
	N	137	136	137	133	137
Positive urgency	Correlation coefficient	−0.125	0.023	0.087	−0.109	−0.036
	p-value	0.146	0.791	0.314	0.210	0.675
	N	137	136	137	133	137
Lack of premeditation	Correlation coefficient	−0.040	**0.368**	**0.194**	0.022	−0.023
	p-value	0.647	**0.000**	**0.023**	0.797	0.793
	N	137	**136**	**137**	133	137
Lack of perseverance	Correlation coefficient	−0.122	**0.334**	0.123	−0.097	−0.040
	p-value	0.157	**0.000**	0.155	0.268	0.644
	N	136	**135**	136	132	136
Seeking sensations	Correlation coefficient	−0.030	0.056	−0.065	**0.176**	0.042
	p-value	0.730	0.517	0.450	**0.042**	0.626
	N	137	136	137	**133**	137
Hads						
Anxiety	Correlation coefficient	−0.008	−0.007	**0.175**	−0.148	0.099
	p-value	0.928	0.935	**0.040**	0.089	0.252
	N	137	136	**137**	133	137
Depression	Correlation coefficient	0.049	0.015	0.074	0.078	0.130
	p-value	0.568	0.859	0.392	0.371	0.131
	N	137	136	137	133	137
HADS	Correlation coefficient	0.023	0.005	0.142	−0.043	0.129
	p-value	0.791	0.958	0.099	0.627	0.134
	N	137	136	137	133	137
Chronotype	Correlation coefficient	**0.215**	**−0.221**	0.114	−0.110	−0.060
	p-value	**0.012**	**0.010**	0.184	0.207	0.486
	N	**137**	**136**	137	133	137

Spearman and Pearson correlation was used.
Bold mean that the results are significant.

females), while anxiety was significantly associated to eating habits in males.

Multivariate Analysis (Table 8)

Among females, increased BMI was associated to uncontrolled eating and emotional eating, while in males, BMI was associated to emotional eating only. In males, no associations of BMI with impulsivity were found while in females they were present.

Chronotype scores were positively correlated to cognitive restraint and negatively to uncontrolled eating among males. No associations were found for females.

CR was lower among females with higher depression scores, while higher anxiety scores were associated to UE among males.

DISCUSSION

The results of this study showed a gender difference in the emotional eating (EE) component (higher in females). This finding confirms previously published results showing that females turn out to be more emotional eaters than males (Hantsoo and Epperson, 2017). Males resort less to emotional

TABLE 4 | Associations between the different components of the questionnaires and the continuous socio-demographic characteristics of female participants ($N = 400$).

		Age	Crowding index	BMI	Alcohol	Coffee
Tfeq-R 18						
Cognitive restraint	Correlation coefficient	0.070	−0.052	**0.170**	0.008	0.063
	p-value	0.261	0.404	**0.006**	0.898	0.316
	N	263	263	**261**	256	259
Uncontrolled eating	Correlation coefficient	0.056	−0.001	**0.184**	0.054	−0.013
	p-value	0.362	0.981	**0.003**	0.386	0.835
	N	263	263	**261**	256	259
Emotional eating	Correlation coefficient	0.098	0.100	**0.241**	0.007	−0.019
	p-value	0.111	0.106	**0.000**	0.910	0.764
	N	263	263	**261**	256	259
Upps						
Negative urgency	Correlation coefficient	0.034	0.075	0.047	−0.094	**0.148**
	p-value	0.584	0.227	0.452	0.135	**0.017**
	N	263	263	261	256	**259**
Positive urgency	Correlation coefficient	−0.006	**0.125**	−0.013	0.008	**0.126**
	p-value	0.917	**0.043**	0.837	0.898	**0.044**
	N	263	**263**	261	256	**259**
Lack of premeditation	Correlation coefficient	0.063	0.070	0.012	−0.013	**0.173**
	p-value	0.311	0.259	0.849	0.831	**0.005**
	N	263	263	261	256	**259**
Lack of perseverance	Correlation coefficient	0.000	0.055	0.038	−0.068	0.053
	p-value	0.997	0.372	0.544	0.278	0.397
	N	263	263	261	256	259
Seeking sensations	Correlation coefficient	−0.035	0.047	−0.038	**0.166**	0.035
	p-value	0.572	0.444	0.543	**0.008**	0.576
	N	263	263	261	**256**	259
Hads						
Anxiety	Correlation coefficient	**0.161**	0.053	0.102	−0.038	**0.213**
	p-value	**0.009**	0.393	0.102	0.541	**0.001**
	N	**263**	263	261	256	**259**
Depression	Correlation coefficient	0.061	0.067	**0.128**	−0.029	0.003
	p-value	0.322	0.279	**0.039**	0.643	0.965
	N	263	263	**261**	256	259
HADS	Correlation coefficient	**0.132**	0.067	**0.129**	−0.039	**0.134**
	p-value	**0.033**	0.277	**0.038**	0.536	**0.031**
	N	**263**	263	**261**	256	**259**
Chronotype						
Chronotype	Correlation coefficient	**0.121**	**0.147**	0.040	**−0.193**	0.052
	p-value	**0.049**	**0.017**	0.520	**0.002**	0.402
	N	**263**	**263**	261	**256**	259

Spearman and Pearson correlation was used.
Bold mean that the results are significant.

eating to overcome their negative feelings, they rather resort to other ways of coping such as gambling, alcohol drinking or internet addiction (Asarian and Geary, 2013).

Significant associations between two dimensions of eating habits (uncontrolled eating UE and EE) and BMI were observed. Thus, an increased BMI was associated to emotional eating in both genders. This result was further supported by the finding that emotional eating scores increased steadily from underweight to obese categories (in both genders).

For UE, it was associated to increased BMI only in females and when BMI was analyzed as a continuous variable, not as categorized. The findings show that UE and EE may be correlated to an increase in BMI was already reported in previous studies. What was interesting in this study were the gender specificities observed highlighting EE as principal component related to BMI in both genders while UE association to BMI was only significant in females. CR was not significantly associated to BMI in our study (analyzed as continuous variable). The only

TABLE 5 | Association between eating habits and categorized BMI in males and females.

		Underweight	Normal	Overweight	Obese	*p*-value
Cognitive restraint						
	Male	12.75 ± 3.808	12.62 ± 3.444	13.88 ± 2.549	10.00	0.157
	Female	12.17 ± 3.499	13.48 ± 3.614	12.47 ± 2.787	11.00 ± 2.000	**0.038**
Uncontrolled eating						
	Male	18.62 ± 3.021	21.50 ± 5.710	22.19 ± 5.316	30.00	0.162
	Female	19.64 ± 4.089	20.81 ± 5.558	23.53 ± 6.336	23.33 ± 7.234	0.079
Emotional eating						
	Male	5.38 ± 1.408	6.57 ± 2.262	6.83 ± 2.498	12.00	**0.046**
	Female	6.57 ± 2.539	7.16 ± 2.487	8.53 ± 2.809	8.67 ± 2.517	**0.041**

Bold mean that the results are significant.

significance observed was among females after categorizing the BMI: normal weight females scored the highest on cognitive restraint component. Cognitive restraint (CR) is the intention to control food intake in order to maintain or lose weight (Hofmann et al., 2014; Julien Sweerts et al., 2019). The impact of CR on weight is very controversial; Many studies have shown a correlation between weight or body mass index (BMI) and CR, either negative (de Lauzon-Guillain et al., 2017; Singh et al., 2017) or positive (Banna et al., 2018).

UE was inversely associated to age and positively to alcohol intake among males, highlighting the fact that when age increases, uncontrolled eating decreases and that participants with larger alcohol intake had also higher UE behavior.

Interestingly, impulsivity was intimately associated to eating habits in females as well as depression to lower cognitive restraint while chronotype and anxiety were two factors associated to eating habits domains in males. Higher negative urgency and lack of perseverance were associated to lower CR among females while UE and EE were both associated to higher negative urgency. High impulsivity was already reported to be associated with personality disorders in bulimia nervosa and the inverse was observed in anorexia nervosa (Cassin and von Ranson, 2005). In addition, previous studies have pointed to similarities between addictive behaviors and eating disorders and both individuals with addiction and restrained eating behavior presented higher impulsivity (Jansen et al., 1989). Negative urgency is defined as the propensity to act out when experiencing negative emotions and it was already linked to substance use disorders and eating disorders (Owens et al., 2018). It could be a positive moderator of reactivity to stressful situations (Owens et al., 2018). Negative urgency was associated with eating concern and frequency of loss of control over eating (Lavender et al., 2017) and predicted binge eating and weight and shape concerns (Stojek et al., 2014). This is the first study showing that eating behavior in females, impulsivity in general and negative urgency in particular are significantly associated. These associations were not significant among males.

Another novel finding in this study was the association between eating habits and the chronotype among males: morning type individuals had higher CR and lower UE. A single precedent study found a positive association between morningness and dietary restraint (Schubert and Randler, 2008). More is known about links between food addiction and evening type individuals who seem more likely to exhibit food addiction than the morning types (Kandeger et al., 2018).

Finally, correlations between eating habits and anxiety or depression show gender differences. While depression scores were inversely associated to CR among females (an increase in depression score was associated to lower CR), anxiety increases in parallel to UE among males.

Depression was previously reported to be a major consequence of being overweight (Barnes et al., 2015). In addition, anxiety and depression can lead to an overconsumption of food as means to cope, leading to food consumption (Yau and Potenza, 2013), mostly comfort food (Andersen et al., 2010; Boutelle et al., 2010). Our study cannot establish a causal relationship between depression or anxiety and eating behavior because of the cross-sectional design.

Our finding that anxiety is associated to UE among males confirms previous results that uncontrolled eating (but not emotional eating or cognitive restraint) significantly mediated a relationship between certain type of anxiety and BMI (Wilkinson et al., 2019). Previous studies revealed that depression history and severity were associated with less cognitive restrained eating (Paans et al., 2018), which is similar to our results. However, gender differences were not reported before.

Our findings should take into account the study's design and limitations. The results were obtained through self-reported questionnaires. Even though self-reporting questionnaires are widely used in community surveys (NIMH; Ciarma and Mathew, 2017), the self-report methods reflect the participant's own perspective, and could lead to bias due to forgetting or not willing to disclose information sometimes. The questionnaires were formulated as scales or multiple-choice to make it easier to respond and to shorten the interview duration as much as possible, thus avoiding to disturb the students. The simplicity of the questionnaire makes it somewhat easy for the participants to give accurate information. Another limitation is that neither insomnia nor sleep quality have been examined and thus need to be explored in future studies since they are important determinant of eating habits. Chronic disease and chronic medications were among the exclusion criteria, therefore, the impact of comorbidities or the use of drugs were not examined. Another limitation is that the sample is imbalanced for male

TABLE 6 | Correlations observed between the three aspects of eating habits and impulsivity, chronotype, anxiety, and depression among male participants.

		CR	UE	EE	Negative urgency	Positive urgency	Lack of premeditation	Lack of perseverance	Seeking sensation	Anxiety	Depression	HADS
Negative urgency	Coefficient	0.048	0.110	**0.188**	1							
	p-value	0.576	0.202	**0.028**								
	N	137	137	**137**	137							
Positive urgency	Coefficient	0.024	0.063	**0.174**	**0.431**	1						
	p-value	0.780	0.468	**0.042**	**0.000**							
	N	137	137	**137**	**137**	137						
Lack of premeditation	Coefficient	−0.093	0.102	−0.032	**0.461**	**0.252**	1					
	p-value	0.278	0.234	0.710	**0.000**	**0.003**						
	N	137	137	137	**137**	**137**	137					
Lack of perseverance	Coefficient	−0.105	0.076	−0.053	**0.316**	0.033	**0.624**	1				
	p-value	0.223	0.378	0.542	**0.000**	0.704	**0.000**					
	N	136	136	136	**136**	136	**136**	136				
Seeking sensations	Coefficient	−0.079	0.141	0.069	0.109	**0.178**	0.035	−0.058	1			
	p-value	0.360	0.099	0.420	0.203	**0.038**	0.687	0.501				
	N	137	137	137	137	**137**	137	136	137			
Anxiety	Coefficient	**0.180**	**0.193**	**0.181**	**0.327**	**0.259**	**0.316**	**0.206**	−0.038	1		
	p-value	**0.035**	**0.024**	**0.034**	**0.000**	**0.002**	**0.000**	**0.016**	0.657			
	N	**137**	**137**	**137**	**137**	**137**	**137**	**136**	137	137		
Depression	Coefficient	0.061	0.095	0.043	**0.279**	0.097	**0.370**	**0.332**	0.139	**0.567**	1	
	p-value	0.482	0.270	0.616	**0.001**	0.259	**0.000**	**0.000**	0.104	**0.000**		
	N	137	137	137	**137**	137	**137**	**136**	137	**137**	137	
HADS	Coefficient	0.137	**0.204**	0.128	**0.342**	**0.202**	**0.387**	**0.270**	0.056	**0.889**	**0.881**	1
	p-value	0.110	**0.017**	0.136	**0.000**	**0.018**	**0.000**	**0.001**	0.519	**0.000**	**0.000**	
	N	137	**137**	137	**137**	**137**	**137**	**136**	137	**137**	**137**	137
Chronotype	Coefficient	**0.201**	**−0.224**	−0.084	−0.056	**−0.239**	**−0.171**	−0.134	−0.086	0.086	0.077	0.092
	p-value	**0.019**	**0.008**	0.329	0.518	**0.005**	**0.046**	0.120	0.320	0.315	0.372	0.283
	N	**137**	**137**	137	137	**137**	**137**	136	137	137	137	137

CR, cognitive restraint; UE, uncontrolled eating; EE, emotional eating. Spearman and Pearson tests were used.
Bold mean that the results are significant.

TABLE 7 | Correlations observed between the three aspects of eating habits and impulsivity, chronotype, anxiety, and depression among female participants.

		CR	UE	EE	Negative urgency	Positive urgency	Lack of premeditation	Lack of perseverance	Seeking sensation	Anxiety	Depression	HADS
Negative urgency	Coefficient	**−0.205**	**0.280**	**0.322**	1							
	p-value	**0.001**	**0.000**	**0.000**								
	N	**263**	**263**	**263**	263							
Positive urgency	Coefficient	**−0.260**	**0.176**	**0.246**	**0.608**	1						
	p-value	**0.000**	**0.004**	**0.000**	**0.000**							
	N	**263**	**263**	**263**	**263**	263						
Lack of premeditation	Coefficient	**−0.196**	**0.147**	**0.159**	**0.428**	**0.401**	1					
	p-value	**0.001**	**0.017**	**0.010**	**0.000**	**0.000**						
	N	**263**	**263**	**263**	**263**	**263**	263					
Lack of perseverance	Coefficient	**−0.162**	0.051	0.045	**0.215**	0.114	**0.520**	1				
	p-value	**0.008**	0.408	0.471	**0.000**	0.066	**0.000**					
	N	**263**	263	263	**263**	263	**263**	263				
Seeking sensations	Coefficient	0.048	0.097	**0.137**	**0.174**	**0.290**	0.064	**−0.163**	1			
	p-value	0.437	0.115	**0.026**	**0.005**	**0.000**	0.302	**0.008**				
	N	263	263	**263**	**263**	**263**	263	**263**	263			
Anxiety	Coefficient	−0.108	0.036	0.023	**0.274**	**0.238**	**0.163**	**0.149**	−0.032	1		
	p-value	0.080	0.560	0.706	**0.000**	**0.000**	**0.008**	**0.016**	0.610			
	N	263	263	263	**263**	**263**	**263**	**263**	263	263		
Depression	Coefficient	**−0.144**	0.095	0.071	**0.174**	0.119	**0.189**	**0.267**	**−0.124**	**0.545**	1	
	p-value	**0.019**	0.124	0.249	**0.005**	0.053	**0.002**	**0.000**	**0.044**	**0.000**		
	N	**263**	263	263	**263**	263	**263**	**263**	**263**	**263**	263	
HADS	Coefficient	**−0.141**	0.071	0.051	**0.260**	**0.210**	**0.199**	**0.208**	−0.079	**0.904**	**0.851**	1
	p-value	**0.022**	0.250	0.410	**0.000**	**0.001**	**0.001**	**0.001**	0.203	**0.000**	**0.000**	
	N	**263**	263	263	**263**	**263**	**263**	**263**	263	**263**	**263**	263
Chronotype	Coefficient	0.099	−0.061	**0.122**	0.008	0.038	−0.112	−0.012	−0.018	0.013	−0.041	−0.013
	p-value	0.111	0.327	**0.049**	0.903	0.544	0.071	0.844	0.775	0.835	0.504	0.833
	N	263	263	**263**	263	263	263	263	263	263	263	263

CR, cognitive restraint; UE, uncontrolled eating; EE, emotional eating. Spearman and Pearson tests were used.
Bold mean that the results are significant.

TABLE 8 | Multivariate analysis: factors significantly correlated to the three domains of the eating habits questionnaire.

	Cognitive restraint	**Non-standardized coefficients**		**Standardized coefficients**	***T***	***p*-value**	**Correlation**
		B	**Standard error**	**Beta**			
Females	BMI	0.145	0.078	0.114	1.873	0.062	0.117
	Negative urgency	−0.164	0.079	−0.138	−2.076	0.039	−0.129
	Lack of perseverance	−0.194	0.080	−0.151	−2.429	0.016	−0.150
	Depression	−0.144	0.071	−0.126	−2.036	0.043	−0.126
	Chronotype	0.032	0.023	0.085	1.396	0.164	0.087
	Depression*negative urgency	0.044	0.216	0.013	0.206	0.837	0.013
	Depression*lack of perseverance	0.126	0.223	0.035	0.566	0.572	0.035
Males	BMI	0.102	0.092	0.094	1.104	0.271	0.096
	Coffee	0.323	0.254	0.107	1.274	0.205	0.110
	Anxiety	0.117	0.072	0.138	1.619	0.108	0.140
	Chronotype	0.061	0.030	0.174	2.078	0.040	0.178
	Uncontrolled eating	**Non-standardized coefficients**		**Standardized coefficients**	***T***	***p*-value**	**Correlation**
		B	**Standard error**	**Beta**			
Females	BMI	0.337	0.117	0.172	2.891	0.004	0.178
	Negative urgency	0.445	0.120	0.244	3.700	0.000	0.226
	Lack of premeditation	0.077	0.129	0.039	0.594	0.553	0.037
	Seeking sensations	0.099	0.106	0.056	0.936	0.350	0.059
	Depression	0.025	0.109	0.014	0.226	0.822	0.014
	Depression*negative urgency	0.329	0.368	0.063	0.893	0.373	0.056
	Depression*lack of premeditation	0.181	0.326	0.038	0.556	0.579	0.035
	Depression*seeking sensation	−0.016	0.332	−0.003	−0.047	0.962	−0.003
Males	Age	−0.650	0.253	−0.213	−2.570	0.011	−0.224
	BMI	0.259	0.148	0.145	1.757	0.081	0.155
	Alcohol	0.993	0.503	0.166	1.975	0.050	0.173
	Coffee	0.529	0.666	0.066	0.794	0.429	0.071
	Seeking sensations	0.174	0.152	0.093	1.142	0.256	0.102
	Anxiety	0.293	0.117	0.207	2.492	0.014	0.218
	Chronotype	−0.101	0.049	−0.172	−2.075	0.040	−0.182
	Anxiety*seeking sensations	−0.686	0.538	−0.123	−1.276	0.204	−0.110
	Emotional eating	**Non-standardized coefficients**		**Standardized coefficients**	***t***	***p***	**Correlation**
		B	**Standard error**	**Beta**			
Females	Age	0.109	0.081	0.078	1.341	0.181	0.084
	CI	0.516	0.370	0.081	1.395	0.164	0.087
	BMI	0.205	0.053	0.225	3.904	0.000	0.238
	Negative urgency	0.229	0.054	0.270	4.253	0.000	0.258
	Lack of premeditation	0.023	0.058	0.025	0.391	0.696	0.025
	Sensation seeking	0.083	0.047	0.101	1.749	0.082	0.109
	Chronotype	0.016	0.016	0.058	0.986	0.325	0.062
Males	BMI	0.134	0.066	0.171	2.032	0.044	0.173
	Negative urgency	0.103	0.069	0.131	1.484	0.140	0.128
	Anxiety	0.068	0.055	0.111	1.241	0.217	0.107
	Anxiety* Negative urgency	0.084	0.134	0.037	0.628	0.530	0.026

**Means interaction (statistical interaction between both variables).*
Gray mean that the results are significant.

and female ratio; even though the ratio was balanced during the random selection (56% females vs. 44% males, similar to the gender distribution of the university students), 81% of the females approached agreed to participate vs. only 53.7% of the males that we approached. This limitation was taken into account in part by separating females' data from males.

Finally, our study cannot establish a causal relationship between impulsivity, depression or anxiety and eating behavior because of the cross-sectional design. Other, prospective longitudinal studies are needed to establish causality with eating behavior.

Despite the limitations, several findings observed in this study are of major importance in explaining eating habits and their relation to BMI and warrant further future investigations.

To the best of our knowledge, this study was the first to assess the relationships between four different neuropsychiatric aspects, i.e., impulsivity, chronotype, anxiety, and depression, and eating habits among young adults. Even though some findings were already reported in other countries, our results are very informative for the Lebanese population.

In conclusion, this was a cross-sectional study of three cognitive and emotional domains related to eating habits among university students (young adults). We surveyed chronotype, impulsivity and affective scores (depression/anxiety). Results showed significant correlations between BMI, TFEQ-R18 scores, impulsivity and anxiety or depression. There was a significant association between two dimensions of eating habits (UE and EE) and BMI. Significant correlations between eating habits and impulsivity domains or depression were observed among females. Among males, chronotype and anxiety seem to play a key role. Future studies should replicate findings in samples of individuals with different aspects of eating disorders such as binge eating disorder, food addiction or bulimia nervosa.

DATA AVAILABILITY

The raw data supporting the conclusions of this manuscript will be made available by the authors, without undue reservation, to any qualified researcher.

ETHICS STATEMENT

The protocol of the study was approved by the ethics committee of Saint-Joseph University (Ref USJ-2017-81). Informed written consent was obtained from all individuals participating in the study.

AUTHOR CONTRIBUTIONS

CA, LN, and SS: field work, entering results, double checking data. NE: statistical analysis. TP: writing the manuscript draft. LR: supervising the study and writing the final version of the manuscript.

ACKNOWLEDGMENTS

The authors would like to thank Drs. Joelle Najem and Maroun Saber as well as the students who participated and they also would like to thank the Saint-Joseph University research council for the research grant.

REFERENCES

Adan, A., Archer, S. N., Hidalgo, M. P., Di Milia, L., Natale, V., and Randler, C. (2012). Circadian typology: a comprehensive review. *Chronobiol. Int.* 29, 1153–1175. doi: 10.3109/07420528.2012.719971

Andersen, J. R., Aasprang, A., Bergsholm, P., Sletteskog, N., Våge, V., and Natvig, G. K. (2010). Anxiety and depression in association with morbid obesity: changes with improved physical health after duodenal switch. *Health Qual. Life Outcomes* 8:52. doi: 10.1186/1477-7525-8-52

Asarian, L., and Geary, N. (2013). Sex differences in the physiology of eating. *Am. J. Physiol. Regul. Integr. Comp. Physiol.* 305, R1215–R1267 doi: 10.1152/ajpregu.00446.2012

Banna, J. C., Panizza, C. E., Boushey, C. J., Delp, E. J., and Lim, E. (2018). Association between cognitive restraint, uncontrolled eating, emotional eating and BMI and the amount of food wasted in early adolescent girls. *Nutrients* 10:E1279. doi: 10.3390/nu10091279

Barnes, E. R., Theeke, L., Minchau, E., Mallow, J., Lucke-Wold, N., and Wampler, J. (2015). Relationships between obesity management and depression management in a university-based family medicine center. *J. Am. Assoc. Nurse Pract.* 27, 256–261. doi: 10.1002/2327-6924.12174

Bond, M. J., McDowell, A. J., and Wilkinson, J. Y. (2001). The measurement of dietary restraint, disinhibition and hunger: an examination of the factor structure of the Three Factor Eating Questionnaire (TFEQ). *Int. J. Obes. Relat. Metab. Disord.* 25, 900–906. doi: 10.1038/sj.ijo.0801611

Booth, C., Spronk, D., Grol, M., and Fox, E. (2018). Uncontrolled eating in adolescents: the role of impulsivity and automatic approach bias for food. *Appetite* 120, 636–643. doi: 10.1016/j.appet.2017.10.024

Boutelle, K. N., Hannan, P., Fulkerson, J. A., Crow, S. J., and Stice, E. (2010). Obesity as a prospective predictor of depression in adolescent females. *Health Psychol.* 29, 293–298. doi: 10.1037/a0018645

Caci, H., Mattei, V., Baylé, F. J., Nadalet, L., Dossios, C., Robert, P., et al. (2005). Impulsivity but not venturesomeness is related to morningness. *Psychiatry Res.* 134, 259–265. doi: 10.1016/j.psychres.2004.02.019

Cassin, S. E., and von Ranson, K. M. (2005). Personality and eating disorders: a decade in review. *Clin. Psychol. Rev.* 25, 895–916. doi: 10.1016/j.cpr.2005.04.012

Chaput, J.-P., Després, J.-P., Bouchard, C., and Tremblay, A. (2011). The association between short sleep duration and weight gain is dependent on disinhibited eating behavior in adults. *Sleep* 34, 1291–1297. doi: 10.5665/SLEEP.1264

Ciarma, J. L., and Mathew, J. M. (2017). Social anxiety and disordered eating: the influence of stress reactivity and self-esteem. *Eat. Behav.* 26, 177–181. doi: 10.1016/j.eatbeh.2017.03.011

Cyders, M. A., Littlefield, A. K., Coffey, S., and Karyadi, K. A. (2014). Examination of a short English version of the UPPS-P impulsive behavior scale. *Addict. Behav.* 39, 1372–1376. doi: 10.1016/j.addbeh.2014.02.013

de Lauzon, B., Romon, M., Deschamps, V., Lafay, L., Borys, J.-M., Karlsson, J., et al. (2004). The three-factor eating questionnaire-R18 is able to distinguish among different eating patterns in a general population. *J. Nutr.* 134, 2372–2380. doi: 10.1093/jn/134.9.2372

de Lauzon-Guillain, B., Clifton, E. A., Day, F. R., Clément, K., Brage, S., Forouhi, N. G., et al. (2017). Mediation and modification of genetic susceptibility to obesity by eating behaviors. *Am. J. Clin. Nutr.* 106, 996–1004. doi: 10.3945/ajcn.117.157396

Espel, H. M., Muratore, A. F., and Lowe, M. R. (2017). An investigation of two dimensions of impulsivity as predictors of loss-of-control eating severity and frequency. *Appetite* 117, 9–16. doi: 10.1016/j.appet.2017.06.004

Gibson, E. L. (2012). The psychobiology of comfort eating: implications for neuropharmacological interventions. *Behav. Pharmacol.* 23, 442–460. doi: 10.1097/FBP.0b013e328357bd4e

Haffen, E. (2009). Measuring circadian rhythm. *L'Encephale* 35(Suppl. 2), S63–67. doi: 10.1016/S0013-7006(09)75536-8

Hantsoo, L., and Epperson, C. N. (2017). Anxiety disorders among women: a female lifespan approach. *Focus* 15, 162–172. doi: 10.1176/appi.focus.20160042

Hays, N. P., and Roberts, S. B. (2008). Aspects of eating behaviors "disinhibition" and "restraint" are related to weight gain and BMI in women. *Obes. (Silver Spring)* 16, 52–58. doi: 10.1038/oby.2007.12

Hofmann, W., Adriaanse, M., Vohs, K. D., and Baumeister, R. F. (2014). Dieting and the self-control of eating in everyday environments: an experience sampling study. *Br. J. Health Psychol.* 19, 523–539. doi: 10.1111/bjhp.12053

Horne, J. A., and Ostberg, O. (1976). A self-assessment questionnaire to determine morningness-eveningness in human circadian rhythms. *Int. J. Chronobiol.* 4, 97–110.

Jansen, A., Klaver, J., Merckelbach, H., and van den Hout, M. (1989). Restrained eaters are rapidly habituating sensation seekers. *Behav. Res. Ther.* 27, 247–252. doi: 10.1016/0005-7967(89)90043-0

Jasinska, A. J., Yasuda, M., Burant, C. F., Gregor, N., Khatri, S., Sweet, M., et al. (2012). Impulsivity and inhibitory control deficits are associated with unhealthy eating in young adults. *Appetite* 59, 738–747. doi: 10.1016/j.appet.2012.08.001

Julien Sweerts, S., Apfeldorfer, G., Kureta-Vanoli, K., and Romo, L. (2019). Emotional therapies for overweight or obesity. *Encephale.* 45, 263–270. doi: 10.1016/j.encep.2019.02.009

Kandeger, A., Selvi, Y., and Tanyer, D. K. (2018). The effects of individual circadian rhythm differences on insomnia, impulsivity, and food addiction. *Eat Weight. Disord.* 1–9. doi: 10.1007/s40519-018-0518-x

Karlsson, J., Persson, L. O., Sjöström, L., and Sullivan, M. (2000). Psychometric properties and factor structure of the Three-Factor Eating Questionnaire (TFEQ) in obese men and women. Results from the Swedish Obese Subjects (SOS) study. *Int. J. Obes. Relat. Metab. Disord.* 24, 1715–1725. doi: 10.1038/sj.ijo.0801442

Kemp, E., Bui, M., and Grier, S. (2011). Eating their feelings: examining emotional eating in at-risk groups in the United States. *J. Consum. Policy* 34, 211–229. doi: 10.1007/s10603-010-9149-y

Keränen, A.-M., Savolainen, M. J., Reponen, A. H., Kujari, M.-L., Lindeman, S. M., Bloigu, R. S., et al. (2009). The effect of eating behavior on weight loss and maintenance during a lifestyle intervention. *Prev. Med.* 49, 32–38. doi: 10.1016/j.ypmed.2009.04.011

Konttinen, H., Haukkala, A., Sarlio-Lähteenkorva, S., Silventoinen, K., and Jousilahti, P. (2009). Eating styles, self-control and obesity indicators. The moderating role of obesity status and dieting history on restrained eating. *Appetite* 53, 131–134. doi: 10.1016/j.appet.2009.05.001

Konttinen, H., Kronholm, E., Partonen, T., Kanerva, N., Männistö, S., and Haukkala, A. (2014). Morningness-eveningness, depressive symptoms, and emotional eating: a population-based study. *Chronobiol. Int.* 31, 554–563. doi: 10.3109/07420528.2013.877922

Lavender, J. M., Goodman, E. L., Culbert, K. M., Wonderlich, S. A., Crosby, R. D., Engel, S. G., et al. (2017). Facets of impulsivity and compulsivity in women with anorexia nervosa. *Eur. Eat. Disord. Rev.* 25, 309–313. doi: 10.1002/erv.2516

Moustafa, A. A., Tindle, R., Frydecka, D., and Misiak, B. (2017). Impulsivity and its relationship with anxiety, depression and stress. *Compr. Psychiatry* 74, 173–179. doi: 10.1016/j.comppsych.2017.01.013

NIMH (2016). *Social Anxiety Disorder: More Than Just Shyness.* Available online at: https://www.nimh.nih.gov/health/publications/social-anxiety-disorder-more-than-just-shyness/index.shtml (accessed October 16, 2018).

Owens, M. M., Amlung, M. T., Stojek, M., and MacKillop, J. (2018). Negative urgency moderates reactivity to laboratory stress inductions. *J. Abnorm. Psychol.* 127, 385–393. doi: 10.1037/abn0000350

Paans, N. P. G., Bot, M., Brouwer, I. A., Visser, M., Roca, M., Kohls, E., et al. (2018). The association between depression and eating styles in four European countries: The MooDFOOD prevention study. *J. Psychosom. Res.* 108, 85–92. doi: 10.1016/j.jpsychores.2018.03.003

Preedy, V. R., Watson, R. R., and Martin, C. R. (eds). (2011). *Handbook of Behavior, Food and Nutrition.* New York, NY: Springer-Verlag. Available online at: https://www.springer.com/gp/book/9780387922706 (accessed February 20, 2019).

Provencher, V., Drapeau, V., Tremblay, A., Després, J.-P., and Lemieux, S. (2003). Eating behaviors and indexes of body composition in men and women from the Québec family study. *Obes. Res.* 11, 783–792. doi: 10.1038/oby.2003.109

Rotella, F., Fioravanti, G., Godini, L., Mannucci, E., Faravelli, C., and Ricca, V. (2015). Temperament and emotional eating: a crucial relationship in eating disorders. *Psychiatry Res.* 225, 452–457. doi: 10.1016/j.psychres.2014.11.068

Schubert, E., and Randler, C. (2008). Association between chronotype and the constructs of the Three-Factor-Eating-Questionnaire. *Appetite* 51, 501–505. doi: 10.1016/j.appet.2008.03.018

Singh, A., Bains, K., and Kaur, H. (2017). Relationship of eating behaviors with age, anthropometric measurements, and body composition parameters among professional Indian women. *Ecol. Food Nutr.* 56, 411–423. doi: 10.1080/03670244.2017.1366317

Song, J., Feng, P., Zhao, X., Xu, W., Xiao, L., Zhou, J., et al. (2018). Chronotype regulates the neural basis of response inhibition during the daytime. *Chronobiol. Int.* 35, 208–218. doi: 10.1080/07420528.2017.1392550

Stojek, M. M., Fischer, S., Murphy, C. M., and MacKillop, J. (2014). The role of impulsivity traits and delayed reward discounting in dysregulated eating and drinking among heavy drinkers. *Appetite* 80, 81–88. doi: 10.1016/j.appet.2014.05.004

Stunkard, A. J., and Messick, S. (1985). The three-factor eating questionnaire to measure dietary restraint, disinhibition and hunger. *J. Psychosom. Res.* 29, 71–83. doi: 10.1016/0022-3999(85)90010-8

Tholin, S., Rasmussen, F., Tynelius, P., and Karlsson, J. (2005). Genetic and environmental influences on eating behavior: the Swedish Young Male Twins Study. *Am. J. Clin. Nutr.* 81, 564–569. doi: 10.1093/ajcn/81.3.564

Whiteside, S. P., and Lynam, D. R. (2003). Understanding the role of impulsivity and externalizing psychopathology in alcohol abuse: application of the UPPS impulsive behavior scale. *Exp. Clin. Psychopharmacol.* 11, 210–217.

WHO (1995). Physical status: the use and interpretation of anthropometry. Report of a WHO Expert Committee. *World Health Organ Technical Report Series* 854, 1–452.

Wilkinson, L. L., Rowe, A. C., and Millings, A. (2019). Disorganized attachment predicts body mass index via uncontrolled eating. *Int. J. Obes.* 1, 431–439. doi: 10.1038/s41366-019-0378-0

Yau, Y. H. C., and Potenza, M. N. (2013). Stress and eating behaviors. *Minerva Endocrinol.* 38, 255–267.

Zigmond, A. S., and Snaith, R. P. (1983). The hospital anxiety and depression scale. *Acta Psychiatr. Scand.* 67, 361–370. doi: 10.1111/j.1600-0447.1983.tb09716.x

Conflict of Interest Statement: The authors declare that the research was conducted in the absence of any commercial or financial relationships that could be construed as a potential conflict of interest.

frontiers in Behavioral Neuroscience

ORIGINAL RESEARCH
published: 08 January 2020
doi: 10.3389/fnbeh.2019.00272

Chronic Jet Lag Simulation Decreases Hippocampal Neurogenesis and Enhances Depressive Behaviors and Cognitive Deficits in Adult Male Rats

*Emily A. Horsey†, Teresa Maletta†, Holly Turner, Chantel Cole, Hugo Lehmann and Neil M. Fournier**

Department of Psychology, Trent University, Peterborough, ON, Canada

There is a long history that protracted periods of circadian disruption, such as through frequent transmeridian travel or rotating shift work, can have a significant impact on brain function and health. In addition, several studies have shown that chronic periods of circadian misalignment can be a significant risk factor for the development of depression and anxiety in some individuals with a history of psychiatric illness. In animal models, circadian disruption can be introduced through either phase advances or delays in the light–dark cycle. However, the impact of chronic phase shifts on affective behavior in rats has not been well-studied. In the present study, male rats were subjected to either weekly 6 h phase advances (e.g., traveling eastbound from New York to Paris) or 6 h phase delays (e.g., traveling westbound from New York to Hawaii) in their light/dark cycle for 8 weeks. The effect of chronic phase shifts was then examined on a range of emotional and cognitive behaviors. We found that rats exposed to frequent phase advances, which mirror conditions of chronic jet lag in humans, exhibited impairments in object recognition memory and showed signature symptoms of depression, including anhedonia, increased anxiety behavior, and higher levels of immobility in the forced swim test. In addition, rats housed on the phase advance schedule also had lower levels of hippocampal neurogenesis and immature neurons showed reduced dendritic complexity compared to controls. These behavioral and neurogenic changes were direction-specific and were not observed after frequent phase delays. Taken together, these findings support the view that circadian disruption through chronic jet lag exposure can suppress hippocampal neurogenesis, which can have a significant impact on memory and mood-related behaviors.

Keywords: circadian disruption, depression, anhedonia, learning and memory, anxiety, emotionality, neurogenesis, hippocampus

OPEN ACCESS

Edited by:
Nuno Sousa,
University of Minho, Portugal

Reviewed by:
Frederic Levy,
Institut National de la Recherche Agronomique (INRA), France
Ayanabha Chakraborti,
The University of Alabama at Birmingham, United States

***Correspondence:**
Neil M. Fournier
neilfournier@trentu.ca

†These authors have contributed equally to this work

Specialty section:
This article was submitted to Emotion Regulation and Processing, a section of the journal Frontiers in Behavioral Neuroscience

Received: *24 August 2019*
Accepted: *29 November 2019*
Published: *08 January 2020*

Citation:
Horsey EA, Maletta T, Turner H, Cole C, Lehmann H and Fournier NM (2020) Chronic Jet Lag Simulation Decreases Hippocampal Neurogenesis and Enhances Depressive Behaviors and Cognitive Deficits in Adult Male Rats. Front. Behav. Neurosci. 13:272. doi: 10.3389/fnbeh.2019.00272

INTRODUCTION

Proper circadian rhythms are an important feature of normal health enabling organisms to adapt to daily changes in their environment. Frequent transmeridian travel and rotating shift work are well-known disruptors of this internal timing system in humans (Waterhouse et al., 2007). In some individuals, short-term misalignment between the endogenous circadian clock and the

desired destination sleep/wake schedule can produce a temporary "*jet lag*" disorder, which is associated with symptoms of fatigue, gastrointestinal distress, reduced psychomotor coordination, and diminished cognition and mood. These symptoms generally dissipate as the circadian clock gradually entrains to the new destinations' time. However, with sustained periods of circadian disruption, a host of adverse health outcomes and clinical pathologies can occur, including a higher incidence of cancer, diabetes, obesity, cardiovascular diseases, and early mortality (Ekstrand et al., 1996; Maywood et al., 2006; Greene, 2012; Mota et al., 2017; Gotlieb et al., 2018; Lin and Farkas, 2018).

Long-term, repeated disturbances of the internal circadian system has been documented to adversely impact the brain (for review, see, Hastings et al., 2003). For example, flight attendants who had experienced repeated jet lag with limited recovery period between flights were found to have reduced temporal lobe volume and exhibited spatial learning deficits when compared to a ground crew control group (Cho, 2001). Interestingly, these cognitive deficits were long lasting—extending for several years—and were associated with elevated levels of the stress hormone cortisol (Cho et al., 2000), a key component of the hypothalamic-pituitary-adrenal stress axis (Sapolsky, 2015). In addition, chronic sleep disturbances have been associated with reduced cortical gray matter volume in several brain regions, including the prefrontal cortex (Altena et al., 2010; Sexton et al., 2014) and hippocampus (Joo et al., 2014). These findings underscore that structural and functional brain adaptations can be downstream effects associated with frequent episodes of circadian dysrhythmia and sleep loss.

Experimental conditions of jet lag can be simulated in rodents through either advancing or delaying the onset of when housing lights are turned off. Using this approach, there is clear evidence that repeated phase shifts of the light/dark (LD) cycle can produce disruptions to learning and memory processes in rats with phase advances typically inducing the greatest impairment (Tapp and Holloway, 1981; Fekete et al., 1985; Devan et al., 2001; Craig and Mcdonald, 2008; Loh et al., 2010; Phan et al., 2011). While the adverse effect of chronic circadian disruption on cognition in rodents and humans is clear, the impact of these changes on affective behaviors is less known. Nonetheless, there is a long history demonstrating that repeated periods of circadian misalignment can contribute to the etiology of mood and anxiety disorders (Vadnie and Mcclung, 2017). For instance, jet lag was found to be a significant precipitator of depressive symptoms in some individuals with a history of psychiatric illness (Tec, 1981; Jauhar and Weller, 1982; Young, 1995; Katz et al., 2002). In rodents, disruption of the natural circadian rhythm by constant lighting increases anxiety-like and depressive-like behavior (Tapia-Osorio et al., 2013). Furthermore, mice with mutations of circadian clock genes show abnormal emotional behaviors (Roybal et al., 2007; Kovanen et al., 2013; Landgraf et al., 2016a). These findings suggest that the proper entrainment of circadian rhythms is necessary for normal functioning of neural circuits that control emotion and regulate stress reactivity (Bedrosian and Nelson, 2017).

Despite the increasing awareness of the health risks associated with chronic jet lag, the neurobiological factors that underlie the accompanied changes in mood and cognitive behavior remain poorly understood. To address this, we exposed adult male rats to 8-weeks of frequent (6-h) phase delays or phase advances to the LD cycle to investigate the impact of chronic circadian disruption on behavioral measures related to cognitive and affective behavior. This procedure has been used extensively to simulate conditions of experimental "jet lag" in rodents (Filipski et al., 2004; Davidson et al., 2006; Craig and Mcdonald, 2008; Gibson et al., 2010; Kott et al., 2012). In addition, we examined whether chronic jet lag conditions could alter levels of hippocampal neurogenesis. Our findings demonstrate that chronic phase advancements of the LD cycle produce clear impairments in object recognition memory along with increases emotional responses, and that disruption in neurogenic processes in the hippocampus may contribute to the changes in affective and cognitive behavior associated with chronic jet lag conditions.

MATERIALS AND METHODS

Male Sprague Dawley rats, weighing between 200 and 220 g, were purchased from Charles River Laboratories (Montreal, QC, Canada). Upon arrival, rats were acclimated to the housing facility and were single housed in standard polypropylene cages with corn bedding. Rats were given free access to food and water for the duration of the study unless otherwise noted. Ambient temperature in the housing rooms was maintained between 21 ± 1°C. All experimental procedures were approved by Trent University Animal Care Committee and were in accordance with the Canadian Council on Animal Care (CCAC). Efforts were made to minimize the number of experimental animals used.

Experimental Groups

All rats were initially maintained on a standard 12:12 h LD cycle with lights on at 0700 h and off at 1900 h for 3-weeks prior to the start of the experiment. During the study, luminance was provided by a fluorescent white light (∼200–300 lux at cage level). Following acclimation to these conditions, the rats were assigned randomly to either remain under the standard LD cycle (n = 8) or placed on a chronic LD shift schedule (n = 8 per group for each of the lighting regimens, *see below*) to simulate the conditions of repeated jet lag. The procedures were carefully controlled as to match those used in a previous study (see Kott et al., 2012). The shifting protocols consisted of either shortening the light period by 6 h (phase advance – similar to the effects of eastward travel from New York To Paris) or lengthening the dark period by 6-h (phase delay – similar to the effects of westward travel from New York to Hawaii) for 8-weeks (**Figure 1**). After each 6 h phase advance or delay, the rats were left undistributed to allow adjustment until the next phase shift, which occurred 7 days later. This resulted in 8 weekly LD shifts over the course of the study. Beginning after the 8th phase advance/-delay LD shift, all rats were assessed on a battery of tests [open field test, elevated plus maze, forced swim tests (FSTs), and object recognition tests].

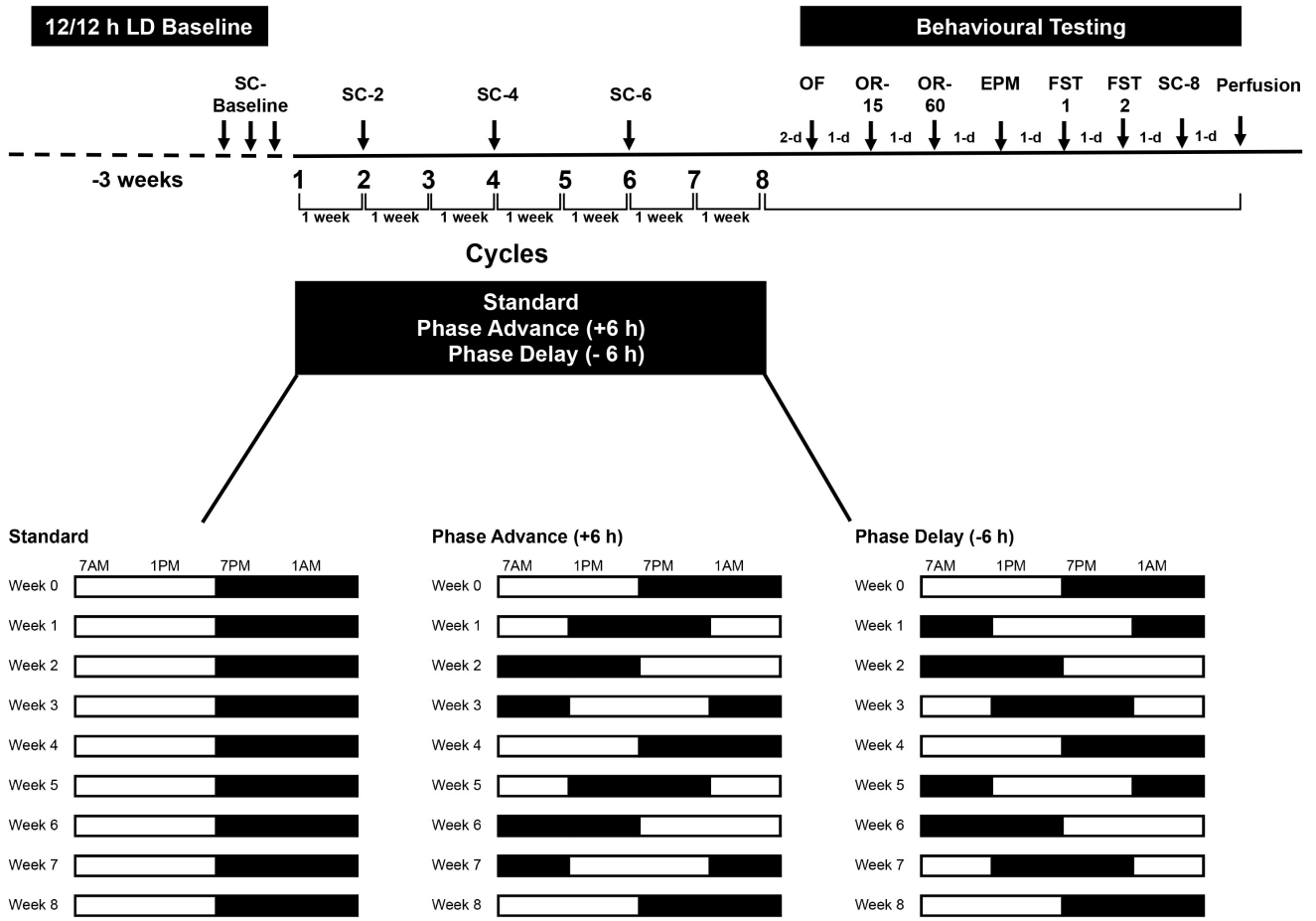

FIGURE 1 | Experimental design. Rats were housed on a standard 12/12 LD cycle for 3 weeks before the start of experiment. Rats were subjected to chronic phase advance (n = 8) or delay (n = 8) protocols, which consisted of weekly 6 h phase advances or 6 h delays of the LD cycle. A group of rats (n = 8) that remained on the standard LD cycle served as controls. All shifts took place on Monday. For 3 days prior to the first phase shift, rats were habituated to a sucrose solution (baseline sucrose consumption). Two days after the 8th final shift, rats underwent behavioral testing: open field (OF), object recognition test with 15 min retention interval (OR-15), object recognition test with 60 min retention interval (OR-60), elevated plus maze (EPM), and 2 days of forced swim test (FST1 and FST2). Rats were euthanized the day after the last sucrose consumption test. Sucrose consumption tests were conduct at the end of shifts 2, 4, 6 and at the end of behavioral testing (shift 8).

The open field test, elevated plus maze, and FSTs were used to examine changes in emotional behavior, such as anxiety and depressive-like behavior, whereas the object recognition test was used to examine learning and short-term memory. Throughout the experiment, sucrose consumption was used to assess for anhedonia, at phase shifts 2, 4, 6, and at the completion of behavior testing.

Behavioral Testing

All behavioral experiments began 48 h after the final LD cycle shift (8th cycle) and were performed during the light phase (1000 and 1600 h). The order of behavioral testing was as follows: open field test (2 habituation sessions), object recognition test 1 (retention interval: 15 min), object recognition test 2 (retention interval: 60 min), elevated plus maze, and 2 days of FST. As discussed above, sucrose consumption tests (see below) were conducted at multiple times during the experiment and on the day after the FST (please see **Figure 1** for timeline of behavioral testing).

Sucrose Consumption Tests

Anhedonic-like behavior was evaluated by monitoring of sucrose intake using a single bottle test. Rats were habituated to a 1.5% sucrose solution for 3 days prior to the first LD cycle shift. This allowed for the estimation of baseline sucrose consumption before beginning the phase advance or delay of the LD cycles. Sucrose consumption was measured after the 2nd, 4th, and 6th LD shifts, as well as after behavioral testing (i.e., end of 8th LD cycle). For the test, the rats were deprived of food and water overnight. Following overnight fluid and food deprivation, the rats were exposed to a pre-weighed 1.5% sucrose solution bottle for 1 h. The total amount of sucrose water consumed during the 1 h test was evaluated at the end of cycles 2, 4, and 6. Food and water was immediately resumed after testing before

initiating the next cycle shift. As a control, water intake was measured over a 1 h and 24 h period the day after completing a sucrose consumption test. Sucrose consumption was estimated by calculating the ratio of sucrose water consumed over tap water consumed multiplied by 100.

After completion of behavioral testing (cycle 8), a final sucrose consumption test was completed. The rats underwent a period of overnight fluid and food deprivation as described above. Following this period, the rats were exposed to a preweighed 2.0% sucrose solution bottle for 24 h. The total amount of sucrose consumption during this period was measured.

Open Field Test

Two days after the initiating the final LD cycle shift (8^{th} shift), the rats from all three groups were given two separate 10 min exposures to freely explore a novel open field arena. The arena was a stainless steel 60 cm × 60 cm × 60 cm open square box. Each arena contained a small amount of corn bedding, fully covering the flooring. During the exploration period, the distance traveled, and the time spent in the peripheral (46.6 cm × 46.6 cm) and central (24 cm × 24 cm) compartments of the arena well as the movement velocity was recorded by a video camera mounted directly above the apparatus. All behaviors were analyzed using Any-Maze software (v. 4.71, Stoelting, Co., United States). Immediately after exploration, the rat was returned to its home cage and was left undisturbed until the next exploration session. The inter-session interval was approximately 6 h. To minimize the impact of olfactory cues, the chambers were cleaned with Oxivir Five 16 concentrate (Diversey, Inc., Canada) prior to testing each rat.

Object Recognition Tests

Novel object recognition testing was carried in the same empty open field arena as described above and was completed the day after open field testing. The test consisted of two phases: a sample trial and a retention (test) phase. For the sample phase, each rat was allowed 5 min to freely explore the arena, which now contained two identical objects. The object pairs were located 15 cm from each adjacent wall. A retention test was conducted 15 min later. During this test, one of the objects previously presented was replaced by a new object. The rats were returned to the open field arena and allowed to explore for 5 min during the test phase. Object investigation was defined as sniffing (within ∼3 cm) or touching the object with the nose and/or forepaws. Turning around or sitting on the object was not considered exploratory behavior. The time spent by the rats investigating each object, familiar or novel, during the test phase was recorded by a video camera and was scored by a researcher blind to the housing condition of each subject. All object pairs as well as the position of the novel object during the test were counter-balanced across rats. A discrimination index (DI) was calculated as follows: DI = (novel object)/(novel object + familiar object) multiplied by 100, this ratio represents the time spent investigating the novel object expressed as a proportion of the total time spent investigating both objects. The open field arena was cleaned with 70% alcohol and air-dried prior to the commencement of each trial for every rat.

Twenty-four hours later, each rat was placed in the same open field arena as before, but the arena now contained a new set of objects. The rat was allowed to explore the arena and the object pairs for 5 min. A retention test was carried out 1 h later, and one of the objects presented previously was replaced by a novel object. As before, the time spent by investigating the novel and familiar objects was recorded and a discrimination index was calculated.

Elevated Plus Maze

Anxiety-like behavior was assessed using an elevated plus maze consisting of two open arms (50 cm × 10 cm) and two enclosed arms (50 cm × 10 cm × 40 cm), elevated 50 cm from the floor. The plus maze was placed in the center of a homogeneously illuminated room. Each rat was placed in intersection between the arms facing the open arm opposite to the investigator. Each session was video recorded for 5 min and the rat's position was determined by automatic video tracking (AnyMaze, Stoelting, Co.). The percentage of open arm entries, time in open arms (in seconds, s), time in closed arms (s), and time in the center square (s) was recorded.

Forced Swim Test

Behavioral despair was assessed using the FST. The rats were placed in a Plexiglas cylinder (20 cm diameter; 50 cm height) filled to a depth of 30 cm with water (23–25°C) for 15 min. The next day, the rats were re-exposed to the swim tanks for a 5 min period. Both swim sessions were video recorded. The time spent immobile was scored by an observer blind to the rat's housing history. Immobility was defined as a lack of movement but includes the presence of movements necessary to keep the head above water.

Tissue Preparation and Immunohistochemistry

The day after the last sucrose consumption test, all rats were deeply anesthetized with sodium pentobarbital (340 mg/ml; Euthansol, Merck Animal Health Canada) and then transcardially perfused with room temperature 0.1M phosphate buffered saline (PBS; pH = 7.4) followed by ice-cold 4% (w/v) formaldehyde fixative (pH = 7.4) that was freshly prepared from depolymerized paraformaldehyde. The brains were extracted and post-fixed in the same fixative overnight at 4°C. After fixation, the brains were sectioned on vibrating microtome in the coronal plane at a thickness of 40 μm. All sections were stored at −20°C in a cryoprotectant solution consisting of 30% (w/v) sucrose, 1% (w/v) polyvinylpyrrolidone, and 30% (v/v) ethylene glycol in PBS until use.

To visualize immature neurons, we used the microtubule binding protein doublecortin (DCX) (Brown et al., 2003; Spampanato et al., 2012). DCX immunohistochemistry was conducted as previously described (Fournier et al., 2010) on free-floating sections with all rinses and incubations carried out under gentle agitation. Sections were incubated for 30 min in 0.3% (v/v) H_2O_2 to quench endogenous peroxidase. Following a series of PBS rinses, sections then underwent heat-induced

epitope retrieval in sodium citrate buffer (pH = 8.5) at 85°C for 30?min and then were placed in a blocking solution containing 0.3% (v/v) Triton X-100, 5% (v/v) normal horse serum and 1% (w/v) bovine serum albumin for 1 h to reduce non-specific antibody binding. The sections were then incubated with rabbit anti-DCX polyclonal antibody (1:1000, Cell Signaling Technology) diluted in blocking solution for 48 h at 4°C. Two days later, the sections were washed several times in PBS and then incubated for 2 h at room temperature with biotinylated goat anti-rabbit IgG secondary antibody (1:500, Vector Laboratories) diluted in 0.3% Triton X-100 in PBS. The sections were then placed in avidin-biotin-peroxidase complex (1:200, 1 h, room temperature, Vectastain ABC Elite, Vector Laboratories) solution and immunolabeling was visualized using 0.02% (w/v) DAB, 2.5% (w/v) nickel ammonium sulfate, 0.083% (v/v) H_2O_2 in 0.175M sodium acetate (pH = 7.0) to yield a bluish black product. After sufficient staining, the reaction was halted by washing in PBS several times. The sections were then mounted onto glass slides and left to air-dry overnight. Slides were dehydrated through a series of alcohols, cleared in xylene, and coverslipped with Entellan (Fisher Scientific) mounting medium.

Doublecortin Stereological Quantification

The total number of DCX + immature dentate granule cells (GCs) was estimated using the unbiased optical fractionator method (West et al., 1991). Every 8th section was examined at 100X (oil immersion) magnification on Nikon Eclipse microscope equipped with a motorized stage and a computerized stereology system (Stereologer). DCX + cells were counted within the dentate granule cell layer and sub-granular zone. The total number of DCX + cells was estimated using the following formula: $N_{total} = \Sigma Q^- * 1/ssf * A(x,y\ step)/a(frame) * t/h$; where ΣQ^- is the number of counted cells; *ssf* is the section sampling fraction (1/8); *A(x,y step)* is the area associated with each x,y movement (90,000 μm^2) were used to count cells; *a(frame)* is the area of the counting frame (8,019 μm^2); *t* is the weighted average section thickness; and *h* is the height of the dissector (15 μm). A guard zone height of 2.5 μm on each side of the dissector was used during cell counting to avoid sectioning artifacts. The estimated number of cells represented the total number of cells for the combined left and right dentate gyrus. All cell counts yielded a coefficient of error that was below 0.10.

Analysis of Maturational Stage of Doublecortin Cells

For analysis of the maturation of DCX + cells, at least 8–10 images of the entire dentate gyrus were captured at 20X magnification using a Nikon TiE inverted research microscope with NIS Elements software. Images acquired were processed with ImageJ. Structural maturation of 50 DCX + cells was evaluated with a staging system based on the classifying cells into one of six stages based on the morphology, length and elaboration of the dendritic tree (Plumpe et al., 2006). Each stage was defined in the following manner: Stage 1: the DCX + cell soma was positioned in the subgranular zone and no dendritic processes were visible. Stage 2: the DCX + cell has 1–2 small short processes that stayed within the subgranular zone. Stage 3: the principal dendrite of the DCX + cell extended into the inner half of the granule cell layer. Stage 4: the leading dendrite reached the outer half of the granule cell layer. Stage 5: the leading dendrite reached the inner molecular layer. Stage 6: the leading dendrite reaches the outer molecular layer. A systematic and random sampling of the DCX + cells was accomplished by placing a 150 × 150 μm grid over the dentate gyrus and only classifying DCX + cells that resided at the points of intersections across the grid. This resulted in total 5–7 DCX + cells per section being examined across the whole hippocampus. The DCX + cells counted for each of the stages was then pooled into early (stages 1 and 2), intermediate (stages 3 and 4) and late (stages 5 and 6) stages.

Statistical Analyses

Statistical analysis was performed using Statistical Package for the Social Sciences (v. 21.0) statistical software. All data was examined for normality and homogeneity of variance. There were no violations in these parametric assumptions. One-way ANOVA with Fisher's protected least significant difference *post hoc* tests were used to determine differences between standard house and the LD shifting groups on behavioral test measures as well as DCX + cell counts. Body weight gain, sucrose consumption, and FST data were analyzed using a two-way repeated measure ANOVA with time as the within-subject factor and group as the between-subject factor. One-sample *t*-tests statistics were used to examine whether the discrimination indices calculated for each group was significantly different from chance. All data are presented as mean and standard error of the mean.

RESULTS

Effect of Chronic LD Shifting on Body Weight

All rats showed a progressive increase in body weight over the duration of the experiment. A two-way repeated measures ANOVA revealed a significant time by housing condition interaction in the relative change in body weight from baseline to the end of the behavioral testing [$F(12,126) = 2.69$, $P < 0.003$, **Figure 2A**]. The major source of the interaction was the higher change in body weight at cycles 5, 6, and 8 of the experiment for the rats housed on the phase advance schedule compared to those from the standard and phase delay groups [All *P*s < 0.05]. In addition, when examined over the entire duration of the study, the rats housed on the phase advance schedule weighed significantly more than standard ($P < 0.046$) and phase delay ($P < 0.030$) groups.

Effect of Chronic LD Shifting on Anhedonia

To assess the potential effects of chronic LD shifts on anhedonia, the rats were presented with a drinking bottle that contained 1.5% sucrose solution for a period of either 1 or 24 h. The results of

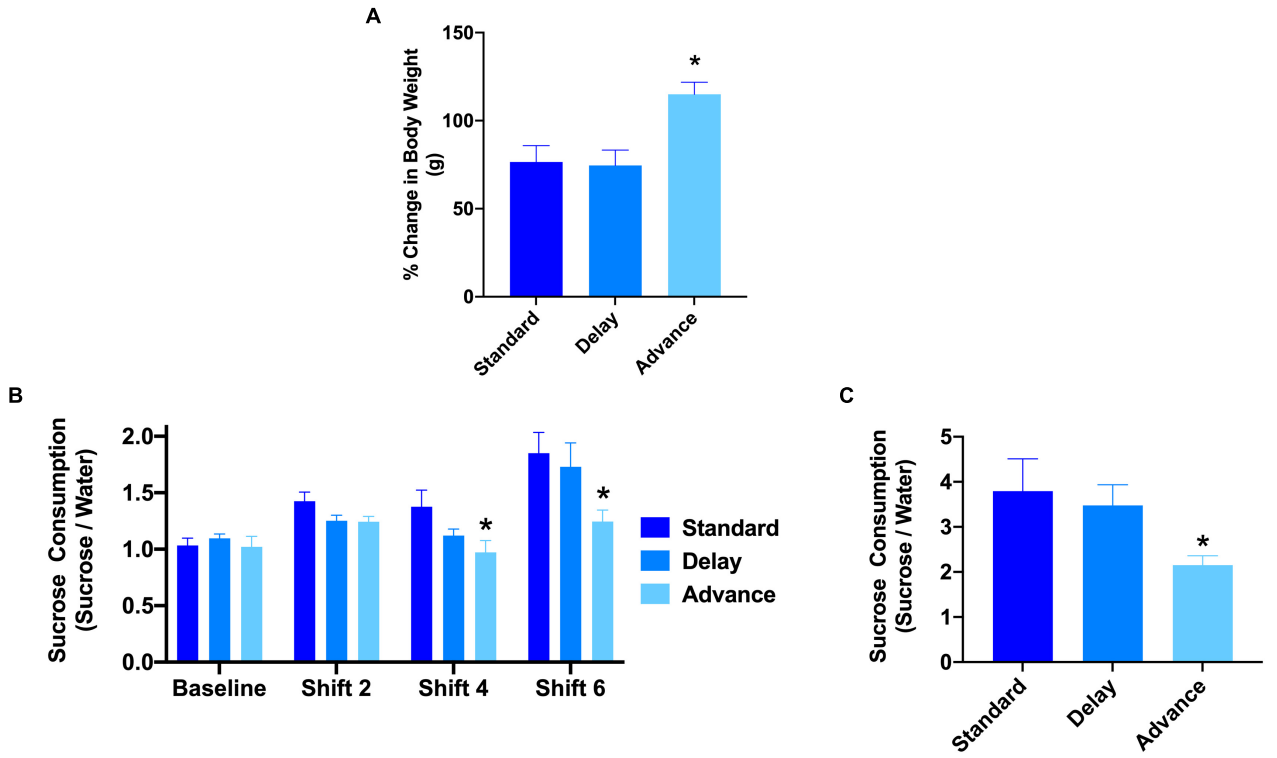

FIGURE 2 | Effect of circadian disruption on body weight and sucrose consumption. **(A)** The proposition of body weight (g) gain (from baseline) in rats housed on a standard, phase advance, or weekly 6-h phase delay LD cycle for 8 weeks. Rats housed on a chronic phase advance schedule weighed significantly more than rats housed on a standard LD cycle rats or rats housed on a chronic phase delay schedule. $^*P < 0.05$. **(B)** Sucrose consumption over a 1 h period was measured before the onset of circadian disruption (baseline) and after cycle shifts 2, 4, and 6. Rats housed on a chronic phase advance schedule consumed significantly less sucrose solution after cycle shift 4 than rats housed on the standard LD cycle. $^*P < 0.05$. **(C)** Sucrose consumption test over a 24 h period was measured after the last LD cycle shift (shift 8). Rats housed on a chronic phase advance schedule consumed significantly less sucrose solution over the 24 h period than rats housed on the standard LD cycle or rats housed on a chronic delay schedule. $^*P < 0.05$.

a repeated measures ANOVA with time (baseline, cycles 2, 4, 6) as the within-subject factor and housing condition (standard vs. advance vs. delay) revealed a significant main effect of group [$F(2,21) = 5.98$, $P < 0.008$]. The major source of the difference was the reduction in sucrose consumption during a 1 h test at cycles 4 and 6 for rats housed on a chronic phase advance schedule compared to rats maintained on a standard LD cycle (**Figure 2B**). In addition, examination of sucrose consumption over a 24 h period after the completion of behavior testing (i.e., at the end of cycle 8) further confirmed a decrease in sucrose consumption for rats maintained on the phase advance schedule (advance vs. standard: $P = 0.031$, advance vs. delay: $P = 0.077$, **Figure 2C**). There was no significant difference in general water consumption at any time point during the study (data not shown; All Ps > 0.149) suggesting that the change in sucrose preference was not related to general alterations in fluid consumption.

Effect of Chronic LD Shifting on Exploratory Behavior

The open field test and elevated plus maze test were used to evaluate the patterns of explorative behavior and anxiety. For the open field test, the rats were habituated to the open field arena twice (10 min each) on a single day (6 h between exposure). For the first session, the results of a one-way ANOVA showed a significant effect of housing condition on the time spent in the center region of the open field arena [$F(2,21) = 7.06$, $P < 0.005$, **Figure 3C**]. *Post hoc* analyses revealed that the major source of this difference was the reduced activity of the rats housed on the phase advance schedule in the center region compared to those on the phase delay [All Ps < 0.001, **Figure 3C**] or standard LD cycle [All Ps < 0.024, **Figure 3C**] groups. There was no difference across the groups with respect to the total distance traveled (**Figure 3A**) or movement velocity (**Figure 3B**). Interestingly, movement velocity in the peripheral compartment, but not center compartment, was significantly reduced for the rats housed on the phase advance schedule compared to the two other groups [$F(2,21) = 5.91$, $P < 0.009$]. For the second session, none of the behavioral parameters (e.g., time spent in center compartment, total distance traveled, movement velocity) were significantly different between groups (**Figures 3D–F**).

The results from the open field arena suggested that the initial reduction of the center compartment during the first session might have been related to increased anxiety or avoidant behaviors induced by the novelty of the environment. To explore this possibility, a second test for anxiety and exploratory behavior

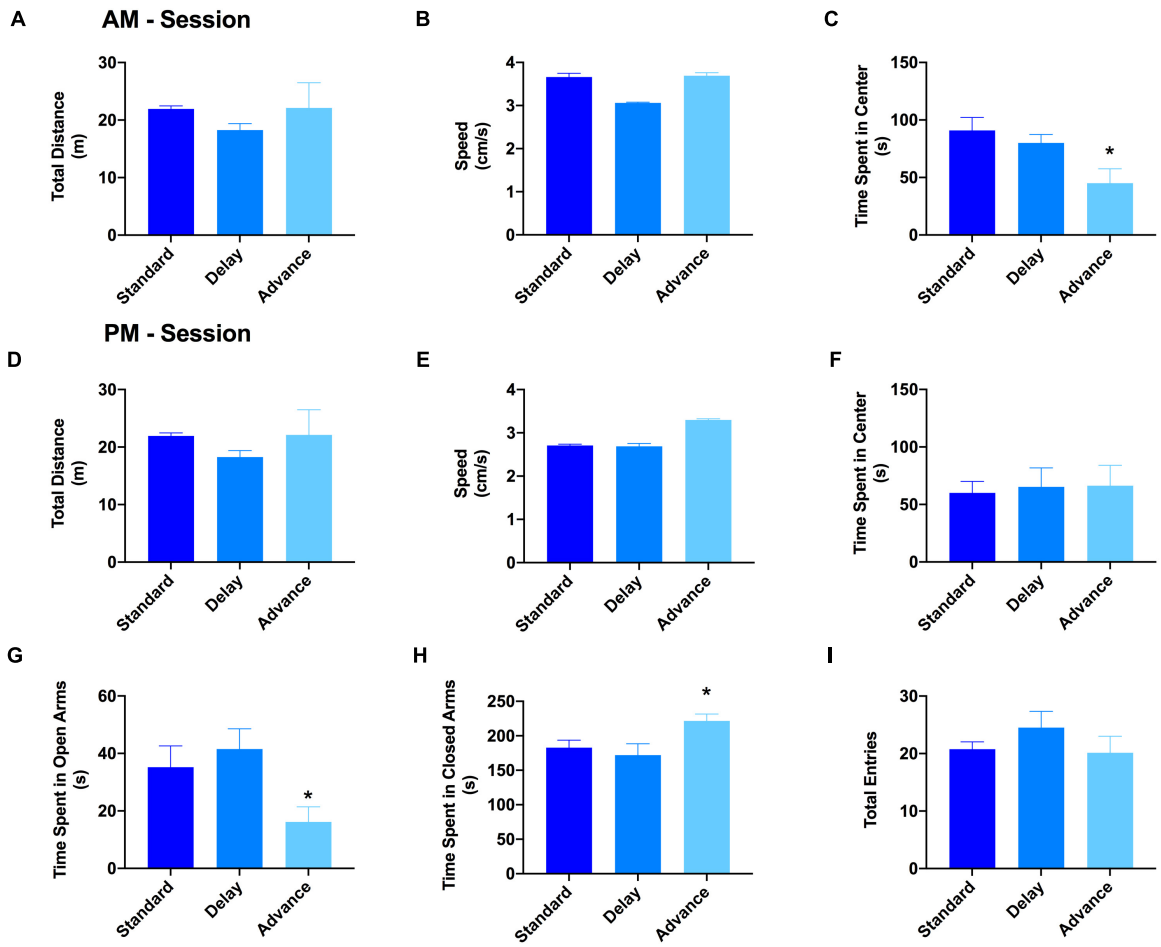

FIGURE 3 | Effect of circadian disruption on exploratory behavior. The total distance traveled **(A)**, movement velocity **(B)**, and time spent in the center **(C)** of the open field during the AM session. There was no difference in either the total distance traveled or movement velocity for rats housed on a weekly phase advance, phase delay or standard LD schedule. However, rats housed on a chronic phase advance schedule traveled and spent significantly less in the center compartment of the open field arena compared to rats housed on the standard LD cycle or rats housed on the phase delay schedule. The total distance traveled **(D)**, movement velocity **(E)**, and time spent in the center **(F)** of the open field during the PM session. There were no differences between any of the groups on these measures. Total time spent in the open **(G)** and closed **(H)** arms of the elevated plus maze. Rats chronically housed on the phase advance schedule spent significantly less time in the open arms of the elevated plus maze. **(I)** Total arm entries (open + closed arms) in the elevated plus maze. There was no significant difference in overall arm entries between groups. $^{*}P < 0.05$ from standard and phase delay groups.

was conducted using the elevated plus maze. There was a significant effect of housing condition on the time spent in the open arms of the elevated plus maze [$F(2,21) = 3.96$, $P < 0.035$]. As shown in **Figures 3G,H**, the rats housed on a chronic phase advance schedule spent significantly less time in the open arms and more time in the closed arms compared to rats maintained on a standard LD cycle [phase advance vs. standard LD controls, $P < 0.013$]. There was no significant effect for housing condition on the total number of arm entries [$F(2,21) = 0.971$, $P = 0.395$, **Figure 3I**].

Effect of Chronic LD Shifting on Recognition Memory

To examine if chronic LD shift schedules could impair cognitive function, the novel object recognition test was performed. None of the groups showed preference for either of the two identical objects presented during the sample (acquisition) phases (All Ps > 0.652). After the 15 min retention interval, a one-sample t-test was used to examine whether the discrimination index was significantly different from 50% (chance level). As shown in **Figure 4A**, all groups showed a comparable level of discrimination for the novel object after the 15 min retention interval [standard: $t(7) = 2.64$, Ps < 0.033; phase delay: $t(7) = 4.16$, $P < 0.002$; phase advance: $t(7) = 3.72$, $P < 0.007$, **Figure 4A**]. However, when the retention interval was increased to 60 min, the discrimination index for rats housed on the phase advance schedule did not differ significantly from chance [phase advance: $t(7) = 1.08$, $P = 0.315$, **Figure 4B**], whereas rats housed on either phase delay schedule or the standard condition all showed a significantly greater preference for the novel object

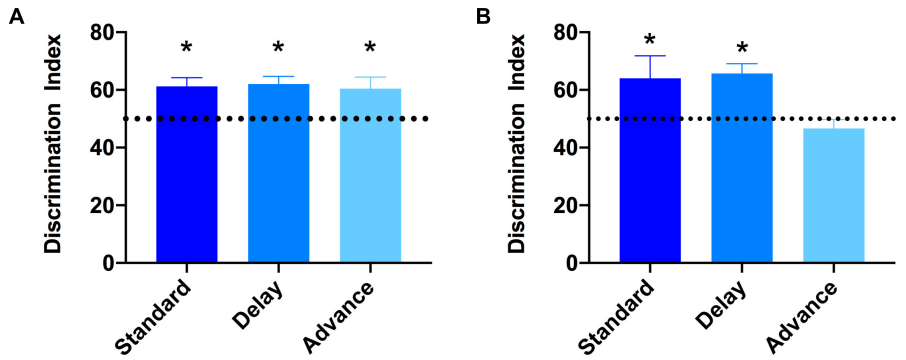

FIGURE 4 | Effect of circadian disruption on object recognition memory. **(A)** Discrimination index for the 15 min retention interval. All groups successfully discriminated the novel object over the familiar object at levels that were greater than 50% chance (*one-sampled *t*-test, $P < 0.05$). **(B)** Discrimination index for the 60 min retention interval. Rats housed on a chronic phase advance schedule did not discriminate the novel object over the familiar object at levels greater than 50% chance. *$P < 0.036$ from chance for standard and phase delay groups.

[phase delay: $t(7) = 2.60$, $P = 0.036$; standard: $t(7) = 4.56$, $P = 0.003$, **Figure 4B**].

Effect of Chronic LD Shifting on Depressive-Like Behavior

The 2-day version of the FST was used to examine whether chronic LD shifting increases responsiveness to stress (behavioral despair). The first FST session lasted for 15 min, whereas the second FST lasted for 5 min, and these two sessions were separated by 24 h. The analysis of data on the first day of the FST showed that all groups exhibited similar levels of immobility during this test [$F(2,21) = 0.223$, $P = 0.802$, **Figure 5A**]. However, for the second day of FST, rats housed on phase advance LD schedule exhibited significantly higher levels of immobility compared to the other groups [$F(2,21) = 4.39$, $P < 0.026$; phase advance vs. standard, $P < 0.016$, phase advance vs. phase delay, $P < 0.021$, **Figure 5B**]. Further analysis revealed that immobility time increased significantly beginning at the third minute of testing and persisted until the end of the session for the phase advance group [$F(8,84) = 2.24$, $P < 0.032$]. In addition, there was a tendency for rats housed on the phase advance schedule to display shorter latencies to the first episode of immobility on the second day of the FST compared to the other groups [phase advance: 24.72 ± 5.76 s vs. phase delay: 34.9 ± 5.45 s vs. standard: 35.2 ± 9.1 s], however, this difference did not reach statistical significance [$P = 0.255$].

Effect of Chronic LD Shifting on Hippocampal Neurogenesis

To measure the effects of phase shifting schedules on hippocampal neurogenesis, we quantified the number of immature GCs in the dentate gyrus using unbiased stereological procedures. A large number of DCX + cells were located in the sub-granular zone or in the inner one-third region of the dentate granule cell layer (**Figures 6A,B**). The total number of DCX + cells was decreased in the rats housed on the chronic phase advance schedule compared to the standard housed and phase delay groups [$F(2,21) = 6.90$, $P < 0.005$, **Figure 6C**].

Next, we employed a classification system to examine the degree of structural maturation of the immature dentate GC neurons (**Figure 6D**). The DCX + cells were classified according to the orientation and outgrowth of apical dendritic processes in the subgranular zone. As shown in **Figure 6E**, there was a marked shift in the distribution of DCX + cells as a function of housing condition. Rats that were chronically housed on the phase advance cycle had a greater proportion of early stage DCX + cells (stages 1, 2) then standard housed controls [$F(2,21) = 3.47$, $P < 0.05$; phase advance vs. standard, $P < 0.016$]. The soma of these DCX + cells was positioned in the sub-granular zone and these cells had either no dendritic processes or a very short dendritic process. Interestingly, the rats placed on the phase advance cycle also had a significantly lower proportion of late stage DCX + cells than the standard housed controls [$F(2,21) = 5.47$, $P < 0.012$; phase advance vs. standard, $P < 0.004$]. These DCX + cells have a leading dendrite that reached into the molecular layer and often showed branching. However, this difference did not reach statistical significance for the phase delay group [phase delay vs. phase advance, $P < 0.062$].

DISCUSSION

Our study confirms that experimental simulation of chronic jet lag in male rats can have a number of important consequences. First, we found that frequent phase advances of the LD cycle disrupted the retention of object recognition memory, but only after an interval of 1 h. Second, we found that rats exposed to the phase advance schedule exhibited signature symptoms of depression observed in animal models, including changes in body weight, anhedonia, altered exploratory behavior in a novel environment, and increased immobility in the FST. Third, we showed that rats exposed to the phase advance schedule have lower levels of hippocampal neurogenesis and reduced dendritic

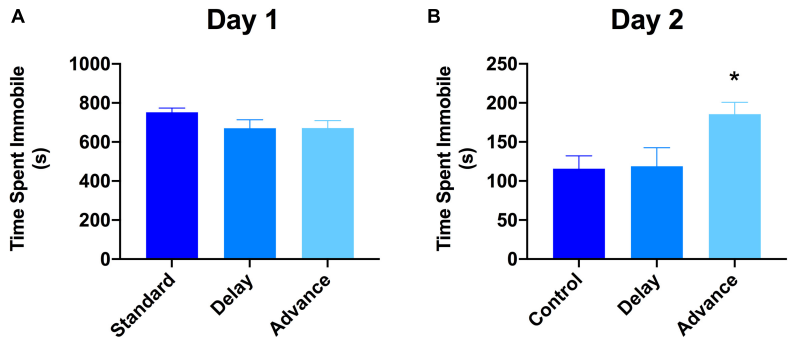

FIGURE 5 | Effect of circadian disruption on FST. **(A)** Total time spent immobile on day 1 of a 15 min FST. **(B)** Total time spent immobile on day 2 of a 5 min FST. Rats that were chronically housed on a weekly phase advance schedule spent significant more time immobile than all other groups on day 2 of the FST. *$P < 0.05$ from standard and phase delay group.

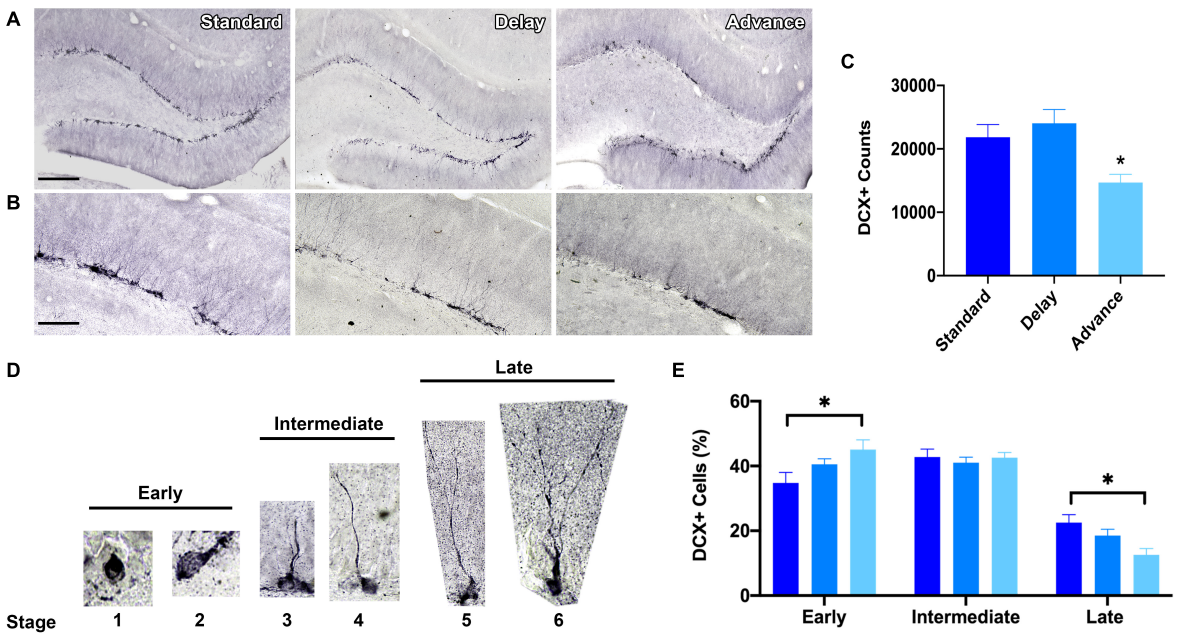

FIGURE 6 | Effect of circadian disruption on hippocampal neurogenesis. **(A)** Representative (10x) photomicrographs of doublecortin (DCX) immunolabeling in the adult dentate gyrus of a rat in each housing condition: standard housing, weekly 6 h phase delay schedule, or weekly 6 h phase advance schedule. Scale bar: 300 μm. **(B)** Representative (20x) photomicrographs of DCX immunolabeling in the adult dentate gyrus of a rats in each housing condition: standard housing, weekly 6 h phase delay schedule, or weekly 6 h phase advance schedule. Scale bar: 100 μm. **(C)** Quantitative stereological estimates at the number of immature DCX + cells in the dentate subgranular zone. Rats housed on a chronic 6 h weekly phase advance schedule had significantly less DCX + cells in the dentate subgranular zone than rats housed on a standard LD cycle, or rats housed on a chronic 6 h weekly phase delay schedule. **(D)** Immature adult born DCX + GCs were classified into three distinct stages according to the degree of their structural maturation (i.e., orientation, outgrowth of dendritic processes in the dentate subgranular zone). DCX + cells were considered to be in the early stage (stage 1 and stage 2) when the soma was positioned in the subgranular zone (SGZ) and no dendritic processes were visible (stage 1) or when the cell displayed short processes that were located within the SGZ (stage 2); DCX + cells were considered to be in the intermediate stage (stages 3 and 4) when the principal dendritic process projected into the inner half of the granule cell layer (stage 3) or when the leading dendrite reached the outer half of the GCL (stage 4); DCX + cells were considered to be in the late stage (stage 5 and stage 6) when the leading dendrite extended into the inner molecular layer (stage 5) or when the leading dendrite reached the outer molecular layer (stage 6). **(E)** Classification of adult-born DCX + cells into early, intermediate and late stages revealed a marked shift in stage distribution. Rats housed on the weekly phase advance schedule had a higher proportion of early stage DCX + cells and a reduction in late stage DCX + cells compared to rats placed on a standard LD cycle or rats housed on a weekly phase delay schedule. *$P < 0.05$.

complexity of immature dentate GCs compared to controls. And lastly, while phase advances of the LD cycle were found to be disruptive across all measures examined, phase delays had little to no effect. Taken together, these results confirm and extend past findings (Gibson et al., 2010; Fonken et al., 2012; Kott et al., 2012; Ikeno et al., 2016) that repeated phase advances of the LD cycle disrupt neurogenic processes in the hippocampus and produce clear impairments in memory function as well as increases in anxiety and depressive behavior underscoring the

importance of proper circadian alignment in regulating normal affect and cognition.

Chronic Jet Lag Disrupts Memory

Frequent episodes of circadian disruption have well-documented effects on learning and memory. Cho and colleagues observed spatial learning deficits in a group of flight attendants who had experienced repeated exposure to jet lag from working transmeridian flights for more than 3 years (Cho et al., 2000). Similar findings involving cognitive performance deficits have also been reported in industrial workers who had been exposed to frequent shift work (Rouch et al., 2005; Marquie et al., 2015). In rodents, performance on several behavioral tasks were shown to be impaired after chronic jet lag, including the Morris water maze, radial arm, and active/passive avoidance learning (Devan et al., 2001; Loh et al., 2010; Zelinski et al., 2014). In the present study, we found that repeated phase advances to the LD cycles, which can evoke symptoms of chronic jet lag in rodents (Filipski et al., 2004; Davidson et al., 2006; Craig and Mcdonald, 2008; Gibson et al., 2010; Kott et al., 2012), produced impairments in object recognition memory. This effect was observed only after a 1-h delay interval between the sample and test phases suggesting that chronic phase advances might impair consolidative processes involved in either maintaining or stabilizing new memories. At the cellular level, changes in synaptic efficacy and membrane excitability are thought to be critical events in the formation of new memories (Bliss and Collingridge, 1993), and there have been some suggestion that these neuronal properties can be altered during periods of sleep and by sleep disruption (Prince and Abel, 2013). Indeed, multiple studies have shown that sleep deprivation can alter neuronal excitability as well as reduce the strength of long-term potentiation, a cellular marker of memory, induced in hippocampal slices from sleep-deprived rats (Mcdermott et al., 2003; Marks and Wayner, 2005).

Chronic Jet Lag Increases Anxiety and Depressive-Like Behaviors

In addition to cognitive effects, evidence supporting an association between circadian rhythm disruptions and changes in mood and anxiety has been slowly accumulating (Bedrosian and Nelson, 2017). Modifications in lighting conditions and aberrant LD cycles can affect mood-like behavior in rodents. For example, anxious- and depressive-like behavior is evident in mice exposed to dim light during nocturnal periods (Bedrosian et al., 2011, 2013; Fonken and Nelson, 2013). Furthermore, short photoperiods are associated with elevated depression in diurnal rodents (Ashkenazy et al., 2009; Ashkenazy-Frolinger et al., 2015) and in some nocturnal rodent species (Prendergast and Nelson, 2005; Prendergast and Kay, 2008; Monje et al., 2011). While these findings clearly show that alterations in day length and light intensity can have an influence on affective states, the impact of chronic LD phase shifts is less clear.

The present study used multiple behavioral measures to examine the impact of chronic phase shifts on depression and anxiety. Anhedonia (i.e., diminished interest or pleasure in all or most activity most of the day) is a core diagnostic symptom of depression and can be readily modeled in rodents using the sucrose consumption test (Scheggi et al., 2018). Reduced sucrose consumption is taken as a measure of anhedonia; an interpretation validated by the demonstration that the same rats do not exhibit reduced consumption to water (Papp et al., 1991; Matthews et al., 1995). Consistent with this idea, we found that rats subjected to weekly phase advances consumed less sucrose than rats housed on a standard LD cycle or those placed on a weekly phase delay schedule. Decreased sucrose consumption was apparent after cycle 4 and persisted at each time point of assessment until the end of the study. Importantly, there was no difference in water consumption between the groups at any phase of the study arguing against the possibility that alterations in sucrose intake reflect a tendency toward reduced thirst. Next, we examined the effect of chronic jet lag on behavioral responses in the FST—a widely utilized rodent model of behavioral despair (Kara et al., 2018; Molendijk and De Kloet, 2019). Rats repeatedly exposed to phase advances engaged in more immobility during the second FST than all other groups. Finally, rats placed on the phase advance schedule also engaged in less time exploring the center portion of a novel open field arena and spent less time in the open arms of the elevated plus maze. Decreased exploration of these regions is widely accepted to reflect higher levels of anxiety behaviors in rodents (Belzung and Griebel, 2001; Walf and Frye, 2007).

Our findings also suggest a specific impact of the direction of phase shifts of the LD cycle on affective behaviors, namely that chronic phase advances induce higher levels of depression and anxiety in rats than phase delays. This is in line with evidence in both human (Aschoff et al., 1975) and rodents (Zee et al., 1992; Gibson et al., 2010; Kott et al., 2012; Zelinski et al., 2014) that phase advances of the LD cycle are typically more disruptive to physiological and behavioral processes than phase delays. Indeed, previous work has shown that reentrainment to a 6 h phase delay in mice occurs within a couple of days, whereas reentrainment to a phase advance takes at least 5 to 6 days to occur (Reddy et al., 2002). Anyan et al. (2017) found that the rate of reentrainment after a 6 h phase advance was associated with higher levels of anxiety behavior in rats, reflected as less time in the center of an activity box and reduced time spent in the open arms of the plus maze, a finding that mirrors our own. While the effect of acute circadian shifts on emotional behavior is clear, research on the impact of chronic jet lag on the development of mood disorder has been limited. However, several studies have shown that acute episodes of jet lag can exacerbate depressive and anxiety symptoms in clinically depressed patients (Tec, 1981; Jauhar and Weller, 1982; Young, 1995; Inder et al., 2016). Our findings are consistent with this observation and further suggest that chronic circadian disruption after repeated phase advancements can impact the function of neural circuits important in mood regulation and anxiety behavior. Finally, the impact of chronic jet lag on female heath has been increasingly recognized (Logan and Mcclung, 2019). While our study only examined the effect of

jet lag simulation in male rats, we predict that repeated phase advances of the LD cycle could exert greater effects in females particularly regarding emotional behaviors. Indeed, female flight attendants are 2 to 5.7 times more likely to develop depression and anxiety disorders than the general population (Mcneely et al., 2014). Nonetheless, additional work will be necessary to determine whether sex differences may exist in the behavioral and cellular responses to chronic circadian disruptions that simulate conditions of jet lag.

Impact of Chronic Jet Lag on Hippocampal Neurogenesis

Although the functional role of adult hippocampal neurogenesis is still unclear, increasing evidence has highlighted an important contribution of ongoing neurogenesis in learning and plasticity, as well in mood and stress reactivity (Cameron and Glover, 2015; Kropff et al., 2015). In rodents, exposure to chronic stress and behavioral models that induce depressive-like behavior are well-known disruptors of hippocampal neurogenesis leading to the idea that impaired neurogenesis might play as a role in the development of depression and other affective disorders (Fournier and Duman, 2012). Given our finding that chronic phase advances of the LD disrupted recognition memory and increased depressive-like behaviors, we considered that chronic phase advances might act as a stressor that could impact levels of hippocampal neurogenesis. In support of this, we found that the total number of DCX + cells was significantly reduced in rats repeatedly exposed to phase advances of the LD cycle compared to those housed on a chronic phase delay cycle or those who remained on a constant 12/12 h LD cycle. These findings are in accordance with the conclusions reached from two independent studies demonstrating that circadian disruptions mimicking jet lag conditions can reduce levels of neurogenesis (Gibson et al., 2010), and that the severity of the neurogenic deficits appear to be direction-dependent with repeated advancements of the LD cycle producing a higher suppression in cell proliferation and neurogenesis than phase delays (Kott et al., 2012).

Because DCX is expressed not only during the initial steps of neuronal differentiation but also during other periods of maturation of young neurons, such as synaptogenesis (Couillard-Despres et al., 2005; Plumpe et al., 2006), we also determined whether chronic jet lag might affect the structural maturation of immature (DCX+) neurons. We found that repeated phase advances increased the proportion of early stage post-mitotic DCX + cells (stages 1 and 2) but decreased the proportion of late stage DCX + cells (stages 5 and 6). Late stage DCX + cells are characterized by the growth of established dendritic processes that extend into the inner and outer molecular layer, and this phase of development is associated with intense spine synapse formation and circuit integration (Zhao et al., 2006, 2015; Toni and Sultan, 2011; Vivar and Van Praag, 2013; Radic et al., 2015; Beining et al., 2017; Petsophonsakul et al., 2017). The potential loss of the later stage DCX + cells, but not early stage DCX cells could suggest that chronic phase advancements might interfere with processes associated with cell maturation and/or survival as we observed a net decrease in the number of DCX + cells in this group. There is evidence that repeated phase advancements increase corticosteroid levels (Gibson et al., 2010) and can potentiate responses of the HPA axis to stress (Loh et al., 2010). Prolonged periods of stress along with aberrant glucocorticoid signaling are well-known to impair the proliferation and structural maturation of neuronal progenitors in the adult hippocampus (Wong and Herbert, 2006; Schoenfeld and Gould, 2013). Similar to our findings, Lussier et al. (2011) observed that chronic high doses of corticosterone in rats for 21 days selectively decreased the number of late phase DCX + cells and reduced dendritic complexity immature (but not mature) granule cells. Thus, it is possible that that elevated levels of GR signaling associated with frequent phase advancements might slow the maturational development of newborn neurons resulting in a decrease in late stage neural progenitors.

CONCLUSION

Chronic circadian rhythm misalignment is a core feature of many neuropsychiatric conditions, including mood and anxiety disorders, and there is increasing evidence that disrupted circadian rhythms might be involved in development of these disorders. Our findings demonstrate that chronic phase advancements of the LD cycle, an experimental model of jet lag, produce impairments in object recognition memory and increases depression and anxiety behavior in male rats. In addition, chronic phase advances also decreased levels of hippocampal neurogenesis and appeared to impair the maturation of immature neurons. In sharp contrast, chronic phase delays produced limited effects on behavior as well as levels of hippocampal neurogenesis suggesting the possibility of a direction-dependent effect of chronic jet lag conditions.

While the mechanism that mediates the adverse effect of weekly phase advances observed in this study is unclear, different responses of the circadian system to phase advances and delays have been described. For example, behavioral reentrainment in rodents takes longer after phase advances than phase delays (Reddy et al., 2002), which agrees with observations that circadian clock gene expression is more readily disrupted with phase advances of the LD cycle (Nagano et al., 2003). Indeed, the severity of jet lag symptoms is known to be influenced by the direction of travel and the number of time zones crossed with eastward flights (i.e., phase advances) taking longer to reentrain circadian processes than westward flights (i.e., phase delays) (Waterhouse et al., 2007). Phase shifts can impact glucocorticoid secretion and stress responses, however, these effects tend to be larger and more sustained with repeated phase advances (Gibson et al., 2010; Kiessling et al., 2010; Loh et al., 2010) suggesting that phase advances of the LD cycle may function as a form of chronic stress. Given the observed link between stress and circadian disruption, it is interesting to note that chronic stress can alter molecular

clock gene expression in several brain areas known to be critically involved in mood regulation and learning, such as the amygdala, nucleus accumbens, prefrontal cortex, and hippocampus (Savalli et al., 2014; Logan et al., 2015; Landgraf et al., 2016b). Interestingly, hippocampal clock gene expression can regulate the proliferation, maturation, and survival of adult-born neurons (Bouchard-Cannon et al., 2013; Malik et al., 2015) and several lines of evidence suggests that intact levels of hippocampal neurogenesis is critical for healthy mood and cognition (Fournier and Duman, 2012; Cameron and Glover, 2015). Since these behavioral processes could depend on levels of intact neurogenesis, as well as a variety of biochemical and signal transduction processes that occur across multiple brain regions (Bunney and Potkin, 2008; Vadnie and Mcclung, 2017; Snider et al., 2018), we speculate that chronic phase advances might lead to widespread disruption in circadian clock gating mechanisms thereby contributing to impaired memory and increased emotionality. In summary, our findings underscore the importance of recognizing the impact that chronic disruptions in circadian processes can have on brain function and mental health and suggests the possibility that disruptions in levels of hippocampal neurogenesis along with other neuroplastic changes might contribute to functional impairments associated with chronic jet lag.

DATA AVAILABILITY STATEMENT

The datasets generated for this study are available on request to the corresponding author.

ETHICS STATEMENT

The animal study was reviewed and approved by Trent University Animal Care and Use Committee.

AUTHOR CONTRIBUTIONS

NF designed the experiments. EH, TM, HT, and CC performed the experiments. EH, TM, CC, and NF analyzed the data. HL and NF wrote the manuscript.

FUNDING

This research was supported by a Discovery Grant (RGPIN-2015-06315) from the Natural Sciences and Engineering Research Council of Canada (NSERC) and the Canadian Foundation for Innovation (#35764, John R. Evans Leaders Fund).

REFERENCES

Altena, E., Vrenken, H., Van Der Werf, Y. D., Van Den Heuvel, O. A., and Van Someren, E. J. (2010). Reduced orbitofrontal and parietal gray matter in chronic insomnia: a voxel-based morphometric study. *Biol. Psychiatry* 67, 182–185. doi: 10.1016/j.biopsych.2009.08.003

Anyan, J., Verwey, M., and Amir, S. (2017). Individual differences in circadian locomotor parameters correlate with anxiety- and depression-like behavior. *PLoS One* 12:e0181375. doi: 10.1371/journal.pone.0181375

Aschoff, J., Hoffmann, K., Pohl, H., and Wever, R. (1975). Re-entrainment of circadian rhythms after phase-shifts of the Zeitgeber. *Chronobiologia* 2, 23–78.

Ashkenazy, T., Einat, H., and Kronfeld-Schor, N. (2009). Effects of bright light treatment on depression- and anxiety-like behaviors of diurnal rodents maintained on a short daylight schedule. *Behav. Brain Res.* 201, 343–346. doi: 10.1016/j.bbr.2009.03.005

Ashkenazy-Frolinger, T., Einat, H., and Kronfeld-Schor, N. (2015). Diurnal rodents as an advantageous model for affective disorders: novel data from diurnal degu (*Octodon degus*). *J. Neural. Transm.* 122(Suppl. 1), S35–S45. doi: 10.1007/s00702-013-1137-3

Bedrosian, T. A., Fonken, L. K., Walton, J. C., Haim, A., and Nelson, R. J. (2011). Dim light at night provokes depression-like behaviors and reduces CA1 dendritic spine density in female hamsters. *Psychoneuroendocrinology* 36, 1062–1069. doi: 10.1016/j.psyneuen.2011.01.004

Bedrosian, T. A., and Nelson, R. J. (2017). Timing of light exposure affects mood and brain circuits. *Transl. Psychiatry* 7:e1017. doi: 10.1038/tp.2016.262

Bedrosian, T. A., Weil, Z. M., and Nelson, R. J. (2013). Chronic dim light at night provokes reversible depression-like phenotype: possible role for TNF. *Mol. Psychiatry* 18, 930–936. doi: 10.1038/mp.2012.96

Beining, M., Jungenitz, T., Radic, T., Deller, T., Cuntz, H., Jedlicka, P., et al. (2017). Adult-born dentate granule cells show a critical period of dendritic reorganization and are distinct from developmentally born cells. *Brain Struct. Funct.* 222, 1427–1446. doi: 10.1007/s00429-016-1285-y

Belzung, C., and Griebel, G. (2001). Measuring normal and pathological anxiety-like behaviour in mice: a review. *Behav. Brain Res.* 125, 141–149. doi: 10.1016/s0166-4328(01)00291-1

Bliss, T. V., and Collingridge, G. L. (1993). A synaptic model of memory: long-term potentiation in the hippocampus. *Nature* 361, 31–39. doi: 10.1038/361031a0

Bouchard-Cannon, P., Mendoza-Viveros, L., Yuen, A., Kaern, M., and Cheng, H. Y. (2013). The circadian molecular clock regulates adult hippocampal neurogenesis by controlling the timing of cell-cycle entry and exit. *Cell Rep.* 5, 961–973. doi: 10.1016/j.celrep.2013.10.037

Brown, J. P., Couillard-Despres, S., Cooper-Kuhn, C. M., Winkler, J., Aigner, L., and Kuhn, H. G. (2003). Transient expression of doublecortin during adult neurogenesis. *J. Comp. Neurol.* 467, 1–10. doi: 10.1002/cne.10874

Bunney, J. N., and Potkin, S. G. (2008). Circadian abnormalities, molecular clock genes and chronobiological treatments in depression. *Br. Med. Bull.* 86, 23–32. doi: 10.1093/bmb/ldn019

Cameron, H. A., and Glover, L. R. (2015). Adult neurogenesis: beyond learning and memory. *Annu. Rev. Psychol.* 66, 53–81. doi: 10.1146/annurev-psych-010814-015006

Cho, K. (2001). Chronic 'jet lag' produces temporal lobe atrophy and spatial cognitive deficits. *Nat. Neurosci.* 4, 567–568. doi: 10.1038/88384

Cho, K., Ennaceur, A., Cole, J. C., and Suh, C. K. (2000). Chronic jet lag produces cognitive deficits. *J. Neurosci.* 20:RC66. doi: 10.1038/88384

Couillard-Despres, S., Winner, B., Schaubeck, S., Aigner, R., Vroemen, M., Weidner, N., et al. (2005). Doublecortin expression levels in adult brain reflect neurogenesis. *Eur. J. Neurosci.* 21, 1–14. doi: 10.1111/j.1460-9568.2004.03813.x

Craig, L. A., and Mcdonald, R. J. (2008). Chronic disruption of circadian rhythms impairs hippocampal memory in the rat. *Brain Res. Bull.* 76, 141–151. doi: 10.1016/j.brainresbull.2008.02.013

Davidson, A. J., Sellix, M. T., Daniel, J., Yamazaki, S., Menaker, M., and Block, G. D. (2006). Chronic jet-lag increases mortality in aged mice. *Curr. Biol.* 16, R914–R916.

Devan, B. D., Goad, E. H., Petri, H. L., Antoniadis, E. A., Hong, N. S., Ko, C. H., et al. (2001). Circadian phase-shifted rats show normal acquisition but impaired long-term retention of place information in the water task. *Neurobiol. Learn. Mem.* 75, 51–62. doi: 10.1006/nlme.1999.3957

Ekstrand, K., Bostrom, P. A., Arborelius, M., Nilsson, J. A., and Lindell, S. E. (1996). Cardiovascular risk factors in commercial flight aircrew officers compared with those in the general population. *Angiology* 47, 1089–1094. doi: 10.1177/000331979604701109

Fekete, M., Van Ree, J. M., Niesink, R. J., and De Wied, D. (1985). Disrupting circadian rhythms in rats induces retrograde amnesia. *Physiol. Behav.* 34, 883–887. doi: 10.1016/0031-9384(85)90008-3

Filipski, E., Delaunay, F., King, V. M., Wu, M. W., Claustrat, B., Grechez-Cassiau, A., et al. (2004). Effects of chronic jet lag on tumor progression in mice. *Cancer Res.* 64, 7879–7885. doi: 10.1158/0008-5472.can-04-0674

Fonken, L. K., Kitsmiller, E., Smale, L., and Nelson, R. J. (2012). Dim nighttime light impairs cognition and provokes depressive-like responses in a diurnal rodent. *J. Biol. Rhythms* 27, 319–327. doi: 10.1177/0748730412448324

Fonken, L. K., and Nelson, R. J. (2013). Dim light at night increases depressive-like responses in male C3H/HeNHsd mice. *Behav. Brain Res.* 243, 74–78. doi: 10.1016/j.bbr.2012.12.046

Fournier, N. M., Andersen, D. R., Botterill, J. J., Sterner, E. Y., Lussier, A. L., Caruncho, H. J., et al. (2010). The effect of amygdala kindling on hippocampal neurogenesis coincides with decreased reelin and DISC1 expression in the adult dentate gyrus. *Hippocampus* 20, 659–671. doi: 10.1002/hipo.20653

Fournier, N. M., and Duman, R. S. (2012). Role of vascular endothelial growth factor in adult hippocampal neurogenesis: implications for the pathophysiology and treatment of depression. *Behav. Brain Res.* 227, 440–449. doi: 10.1016/j.bbr.2011.04.022

Gibson, E. M., Wang, C., Tjho, S., Khattar, N., and Kriegsfeld, L. J. (2010). Experimental 'jet lag' inhibits adult neurogenesis and produces long-term cognitive deficits in female hamsters. *PLoS One* 5:e15267. doi: 10.1371/journal.pone.0015267

Gotlieb, N., Moeller, J., and Kriegsfeld, L. J. (2018). Circadian control of neuroendocrine function: implications for health and disease. *Curr. Opin. Physiol.* 5, 133–140. doi: 10.1016/j.cophys.2018.11.001

Greene, M. W. (2012). Circadian rhythms and tumor growth. *Cancer Lett.* 318, 115–123. doi: 10.1016/j.canlet.2012.01.001

Hastings, M. H., Reddy, A. B., and Maywood, E. S. (2003). A clockwork web: circadian timing in brain and periphery, in health and disease. *Nat. Rev. Neurosci.* 4, 649–661. doi: 10.1038/nrn1177

Ikeno, T., Deats, S. P., Soler, J., Lonstein, J. S., and Yan, L. (2016). Decreased daytime illumination leads to anxiety-like behaviors and HPA axis dysregulation in the diurnal grass rat (*Arvicanthis niloticus*). *Behav. Brain Res.* 300, 77–84. doi: 10.1016/j.bbr.2015.12.004

Inder, M. L., Crowe, M. T., and Porter, R. (2016). Effect of transmeridian travel and jetlag on mood disorders: evidence and implications. *Aust. N. Z. J. Psychiatry* 50, 220–227. doi: 10.1177/0004867415598844

Jauhar, P., and Weller, M. P. (1982). Psychiatric morbidity and time zone changes: a study of patients from Heathrow airport. *Br. J. Psychiatry* 140, 231–235. doi: 10.1192/bjp.140.3.231

Joo, E. Y., Kim, H., Suh, S., and Hong, S. B. (2014). Hippocampal substructural vulnerability to sleep disturbance and cognitive impairment in patients with chronic primary insomnia: magnetic resonance imaging morphometry. *Sleep* 37, 1189–1198. doi: 10.5665/sleep.3836

Kara, N. Z., Stukalin, Y., and Einat, H. (2018). Revisiting the validity of the mouse forced swim test: systematic review and meta-analysis of the effects of prototypic antidepressants. *Neurosci. Biobehav. Rev.* 84, 1–11. doi: 10.1016/j.neubiorev.2017.11.003

Katz, G., Knobler, H. Y., Laibel, Z., Strauss, Z., and Durst, R. (2002). Time zone change and major psychiatric morbidity: the results of a 6-year study in Jerusalem. *Comp. Psychiatry* 43, 37–40. doi: 10.1053/comp.2002.29849

Kiessling, S., Eichele, G., and Oster, H. (2010). Adrenal glucocorticoids have a key role in circadian resynchronization in a mouse model of jet lag. *J. Clin. Invest.* 120, 2600–2609. doi: 10.1172/JCI41192

Kott, J., Leach, G., and Yan, L. (2012). Direction-dependent effects of chronic "jet-lag" on hippocampal neurogenesis. *Neurosci. Lett.* 515, 177–180. doi: 10.1016/j.neulet.2012.03.048

Kovanen, L., Kaunisto, M., Donner, K., Saarikoski, S. T., and Partonen, T. (2013). CRY2 genetic variants associate with dysthymia. *PLoS One* 8:e71450. doi: 10.1371/journal.pone.0071450

Kropff, E., Yang, S. M., and Schinder, A. F. (2015). Dynamic role of adult-born dentate granule cells in memory processing. *Curr. Opin. Neurobiol.* 35, 21–26. doi: 10.1016/j.conb.2015.06.002

Landgraf, D., Long, J. E., Proulx, C. D., Barandas, R., Malinow, R., and Welsh, D. K. (2016a). Genetic disruption of circadian rhythms in the suprachiasmatic nucleus causes helplessness, behavioral despair, and anxiety-like behavior in mice. *Biol. Psychiatry* 80, 827–835. doi: 10.1016/j.biopsych.2016.03.1050

Landgraf, D., Long, J. E., and Welsh, D. K. (2016b). Depression-like behaviour in mice is associated with disrupted circadian rhythms in nucleus accumbens and periaqueductal grey. *Eur. J. Neurosci.* 43, 1309–1320. doi: 10.1111/ejn.13085

Lin, H. H., and Farkas, M. E. (2018). Altered circadian rhythms and breast cancer: from the human to the molecular level. *Front. Endocrinol.* 9:219. doi: 10.3389/fendo.2018.00219

Logan, R. W., Edgar, N., Gillman, A. G., Hoffman, D., Zhu, X., and Mcclung, C. A. (2015). Chronic stress induces brain region-specific alterations of molecular rhythms that correlate with depression-like behavior in mice. *Biol. Psychiatry* 78, 249–258. doi: 10.1016/j.biopsych.2015.01.011

Logan, R. W., and Mcclung, C. A. (2019). Rhythms of life: circadian disruption and brain disorders across the lifespan. *Nat. Rev. Neurosci.* 20, 49–65. doi: 10.1038/s41583-018-0088-y

Loh, D. H., Navarro, J., Hagopian, A., Wang, L. M., Deboer, T., and Colwell, C. S. (2010). Rapid changes in the light/dark cycle disrupt memory of conditioned fear in mice. *PLoS One* 5:e12546. doi: 10.1371/journal.pone.0012546

Lussier, A. L., Romay-Tallon, R., Kalynchuk, L. E., and Caruncho, H. J. (2011). Reelin as a putative vulnerability factor for depression: examining the depressogenic effects of repeated corticosterone in heterozygous reeler mice. *Neuropharmacology* 60, 1064–1074. doi: 10.1016/j.neuropharm.2010.09.007

Malik, A., Kondratov, R. V., Jamasbi, R. J., and Geusz, M. E. (2015). Circadian clock genes are essential for normal adult neurogenesis, differentiation, and fate determination. *PLoS One* 10:e0139655. doi: 10.1371/journal.pone.0139655

Marks, C. A., and Wayner, M. J. (2005). Effects of sleep disruption on rat dentate granule cell LTP *in vivo*. *Brain Res. Bull.* 66, 114–119. doi: 10.1016/j.brainresbull.2005.03.018

Marquie, J. C., Tucker, P., Folkard, S., Gentil, C., and Ansiau, D. (2015). Chronic effects of shift work on cognition: findings from the VISAT longitudinal study. *Occup. Environ. Med.* 72, 258–264. doi: 10.1136/oemed-2013-101993

Matthews, K., Forbes, N., and Reid, I. C. (1995). Sucrose consumption as an hedonic measure following chronic unpredictable mild stress. *Physiol. Behav.* 57, 241–248. doi: 10.1016/0031-9384(94)00286-e

Maywood, E. S., O'neill, J., Wong, G. K., Reddy, A. B., and Hastings, M. H. (2006). Circadian timing in health and disease. *Prog. Brain Res.* 153, 253–269.

Mcdermott, C. M., Lahoste, G. J., Chen, C., Musto, A., Bazan, N. G., and Magee, J. C. (2003). Sleep deprivation causes behavioral, synaptic, and membrane excitability alterations in hippocampal neurons. *J. Neurosci.* 23, 9687–9695. doi: 10.1523/jneurosci.23-29-09687.2003

Mcneely, E., Gale, S., Tager, I., Kincl, L., Bradley, J., Coull, B., et al. (2014). The self-reported health of U.S. flight attendants compared to the general population. *Environ. Health* 13:13.

Molendijk, M. L., and De Kloet, E. R. (2019). Coping with the forced swim stressor: current state-of-the-art. *Behav. Brain Res.* 364, 1–10. doi: 10.1016/j.bbr.2019.02.005

Monje, F. J., Cabatic, M., Divisch, I., Kim, E. J., Herkner, K. R., Binder, B. R., et al. (2011). Constant darkness induces IL-6-dependent depression-like behavior through the NF-kappaB signaling pathway. *J. Neurosci.* 31, 9075–9083. doi: 10.1523/JNEUROSCI.1537-11.2011

Mota, M. C., Silva, C. M., Balieiro, L. C. T., Fahmy, W. M., and Crispim, C. A. (2017). Social jetlag and metabolic control in non-communicable chronic diseases: a study addressing different obesity statuses. *Sci. Rep.* 7:6358. doi: 10.1038/s41598-017-06723-w

Nagano, M., Adachi, A., Nakahama, K., Nakamura, T., Tamada, M., Meyer-Bernstein, E., et al. (2003). An abrupt shift in the day/night cycle causes desynchrony in the mammalian circadian center. *J. Neurosci.* 23, 6141–6151. doi: 10.1523/jneurosci.23-14-06141.2003

Papp, M., Willner, P., and Muscat, R. (1991). An animal model of anhedonia: attenuation of sucrose consumption and place preference conditioning by chronic unpredictable mild stress. *Psychopharmacology* 104, 255–259. doi: 10.1007/bf02244188

Petsophonsakul, P., Richetin, K., Andraini, T., Roybon, L., and Rampon, C. (2017). Memory formation orchestrates the wiring of adult-born hippocampal neurons into brain circuits. *Brain Struct. Funct.* 222, 2585–2601. doi: 10.1007/s00429-016-1359-x

Phan, T. X., Chan, G. C., Sindreu, C. B., Eckel-Mahan, K. L., and Storm, D. R. (2011). The diurnal oscillation of MAP (mitogen-activated protein) kinase and

adenylyl cyclase activities in the hippocampus depends on the suprachiasmatic nucleus. *J. Neurosci.* 31, 10640–10647. doi: 10.1523/JNEUROSCI.6535-10.2011

Plumpe, T., Ehninger, D., Steiner, B., Klempin, F., Jessberger, S., Brandt, M., et al. (2006). Variability of doublecortin-associated dendrite maturation in adult hippocampal neurogenesis is independent of the regulation of precursor cell proliferation. *BMC Neurosci.* 7:77.

Prendergast, B. J., and Kay, L. M. (2008). Affective and adrenocorticotrophic responses to photoperiod in Wistar rats. *J. Neuroendocrinol.* 20, 261–267. doi: 10.1111/j.1365-2826.2007.01633.x

Prendergast, B. J., and Nelson, R. J. (2005). Affective responses to changes in day length in Siberian hamsters (*Phodopus sungorus*). *Psychoneuroendocrinology* 30, 438–452. doi: 10.1016/j.psyneuen.2004.08.008

Prince, T. M., and Abel, T. (2013). The impact of sleep loss on hippocampal function. *Learn. Mem.* 20, 558–569. doi: 10.1101/lm.031674.113

Radic, T., Al-Qaisi, O., Jungenitz, T., Beining, M., and Schwarzacher, S. W. (2015). Differential structural development of adult-born septal hippocampal granule cells in the Thy1-GFP mouse, nuclear size as a new index of maturation. *PLoS One* 10:e0135493. doi: 10.1371/journal.pone.0135493

Reddy, A. B., Field, M. D., Maywood, E. S., and Hastings, M. H. (2002). Differential resynchronisation of circadian clock gene expression within the suprachiasmatic nuclei of mice subjected to experimental jet lag. *J. Neurosci.* 22, 7326–7330. doi: 10.1523/jneurosci.22-17-07326.2002

Rouch, I., Wild, P., Ansiau, D., and Marquie, J. C. (2005). Shiftwork experience, age and cognitive performance. *Ergonomics* 48, 1282–1293. doi: 10.1080/00140130500241670

Roybal, K., Theobold, D., Graham, A., Dinieri, J. A., Russo, S. J., Krishnan, V., et al. (2007). Mania-like behavior induced by disruption of CLOCK. *Proc. Natl. Acad. Sci. U.S.A.* 104, 6406–6411. doi: 10.1073/pnas.0609625104

Sapolsky, R. M. (2015). Stress and the brain: individual variability and the inverted-U. *Nat. Neurosci.* 18, 1344–1346. doi: 10.1038/nn.4109

Savalli, G., Diao, W., Schulz, S., Todtova, K., and Pollak, D. D. (2014). Diurnal oscillation of amygdala clock gene expression and loss of synchrony in a mouse model of depression. *Int. J. Neuropsychopharmacol.* 18:yu095. doi: 10.1093/ijnp/pyu095

Scheggi, S., De Montis, M. G., and Gambarana, C. (2018). Making sense of rodent models of Anhedonia. *Int. J. Neuropsychopharmacol.* 21, 1049–1065. doi: 10.1093/ijnp/pyy083

Schoenfeld, T. J., and Gould, E. (2013). Differential effects of stress and glucocorticoids on adult neurogenesis. *Curr. Top. Behav. Neurosci.* 15, 139–164. doi: 10.1007/7854_2012_233

Sexton, C. E., Storsve, A. B., Walhovd, K. B., Johansen-Berg, H., and Fjell, A. M. (2014). Poor sleep quality is associated with increased cortical atrophy in community-dwelling adults. *Neurology* 83, 967–973. doi: 10.1212/WNL.0000000000000774

Snider, K. H., Sullivan, K. A., and Obrietan, K. (2018). Circadian regulation of hippocampal-dependent memory: circuits, synapses, and molecular mechanisms. *Neural. Plast* 2018:7292540. doi: 10.1155/2018/7292540

Spampanato, J., Sullivan, R. K., Turpin, F. R., Bartlett, P. F., and Sah, P. (2012). Properties of doublecortin expressing neurons in the adult mouse dentate gyrus. *PLoS One* 7:e41029. doi: 10.1371/journal.pone.0041029

Tapia-Osorio, A., Salgado-Delgado, R., Angeles-Castellanos, M., and Escobar, C. (2013). Disruption of circadian rhythms due to chronic constant light leads to depressive and anxiety-like behaviors in the rat. *Behav. Brain Res.* 252, 1–9. doi: 10.1016/j.bbr.2013.05.028

Tapp, W. N., and Holloway, F. A. (1981). Phase shifting circadian rhythms produces retrograde amnesia. *Science* 211, 1056–1058. doi: 10.1126/science.7193351

Tec, L. (1981). Depression and jet lag. *Am. J. Psychiatry* 138:858.

Toni, N., and Sultan, S. (2011). Synapse formation on adult-born hippocampal neurons. *Eur. J. Neurosci.* 33, 1062–1068. doi: 10.1111/j.1460-9568.2011.07604.x

Vadnie, C. A., and Mcclung, C. A. (2017). Circadian rhythm disturbances in mood disorders: insights into the role of the suprachiasmatic nucleus. *Neural. Plast* 2017:1504507. doi: 10.1155/2017/1504507

Vivar, C., and Van Praag, H. (2013). Functional circuits of new neurons in the dentate gyrus. *Front. Neural. Circuits* 7:15. doi: 10.3389/fncir.2013.00015

Walf, A. A., and Frye, C. A. (2007). The use of the elevated plus maze as an assay of anxiety-related behavior in rodents. *Nat. Protoc.* 2, 322–328. doi: 10.1038/nprot.2007.44

Waterhouse, J., Reilly, T., Atkinson, G., and Edwards, B. (2007). Jet lag: trends and coping strategies. *Lancet* 369, 1117–1129. doi: 10.1016/s0140-6736(07)60529-7

West, M. J., Slomianka, L., and Gundersen, H. J. (1991). Unbiased stereological estimation of the total number of neurons in thesubdivisions of the rat hippocampus using the optical fractionator. *Anat. Rec.* 231, 482–497. doi: 10.1002/ar.1092310411

Wong, E. Y., and Herbert, J. (2006). Raised circulating corticosterone inhibits neuronal differentiation of progenitor cells in the adult hippocampus. *Neuroscience* 137, 83–92. doi: 10.1016/j.neuroscience.2005.08.073

Young, D. M. (1995). Psychiatric morbidity in travelers to Honolulu, Hawaii. *Compr. Psychiatry* 36, 224–228. doi: 10.1016/0010-440x(95)90086-b

Zee, P. C., Rosenberg, R. S., and Turek, F. W. (1992). Effects of aging on entrainment and rate of resynchronization of circadian locomotor activity. *Am. J. Physiol.* 263, R1099–R1103.

Zelinski, E. L., Hong, N. S., and Mcdonald, R. J. (2014). Persistent impairments in hippocampal function following a brief series of photoperiod shifts in rats. *Anim. Cogn.* 17, 127–141. doi: 10.1007/s10071-013-0645-8

Zhao, C., Jou, J., Wolff, L. J., Sun, H., and Gage, F. H. (2015). Spine morphogenesis in newborn granule cells is differentially regulated in the outer and middle molecular layers. *J. Comp. Neurol.* 523:1588. doi: 10.1002/cne.23800

Zhao, C., Teng, E. M., Summers, R. G. Jr., Ming, G. L., and Gage, F. H. (2006). Distinct morphological stages of dentate granule neuron maturation in the adult mouse hippocampus. *J. Neurosci.* 26, 3–11. doi: 10.1523/jneurosci.3648-05.2006

Conflict of Interest: The authors declare that the research was conducted in the absence of any commercial or financial relationships that could be construed as a potential conflict of interest.

frontiers in Behavioral Neuroscience

ORIGINAL RESEARCH
published: 22 January 2020
doi: 10.3389/fnbeh.2020.00002

Can Working Memory Task-Related EEG Biomarkers Measure Fluid Intelligence and Predict Academic Achievement in Healthy Children?

*Wei Luo and Renlai Zhou**

Department of Psychology, Nanjing University, Nanjing, China

OPEN ACCESS

Edited by:
Bahar Güntekin, School of Medicine, Istanbul Medipol University, Turkey

Reviewed by:
Assunta Pompili, University of L'Aquila, Italy
Chia-Liang Tsai, National Cheng Kung University, Taiwan

***Correspondence:**
Renlai Zhou
rlzhou@nju.edu.cn

Specialty section:
This article was submitted to Learning and Memory, a section of the journal Frontiers in Behavioral Neuroscience

Received: *08 October 2019*
Accepted: *03 January 2020*
Published: *22 January 2020*

Citation:
Luo W and Zhou R (2020) Can Working Memory Task-Related EEG Biomarkers Measure Fluid Intelligence and Predict Academic Achievement in Healthy Children? Front. Behav. Neurosci. 14:2. doi: 10.3389/fnbeh.2020.00002

Background: Educational psychology research has linked fluid intelligence (Gf) with working memory (WM), but it is still dubious whether electroencephalography (EEG) markers robustly indicate Gf. This study addresses this issue and notes the relationship between WM task-related EEG markers with Gf and academic performance.

Method: A sample of 62 healthy children between the ages of 9 and 12 years was selected to perform three tasks: (1) Raven's Standard Progressive Matrices (RSPM) test to assess Gf; (2) 2-back task to assess central executive system (CES); and (3) delayed match-to-sample task to assess short-term storage. These subjects were divided into high ability (HA) and low ability (LA) groups based on their RSPM scores. Support vector machine and logistic regression were used to train the EEG candidate indicators. A multiple regression was used to predict children's academic performance using P3 amplitude, P2 latency, and θ-ERS.

Results: Behavioral results demonstrated that the correct rate of the HA group is higher than that of the LA group. The event-related potential results of the 2-back task showed that the P3 amplitude of the HA group was relatively larger and that the P2 latency was shorter than that observed in the LA group. For the delayed matching to sample task, the θ-ERS of the LA group was higher than that of the HA group. However, the area under the curve of these three indicators for Gf was < 0.75 for each and < 0.85 for the combined indicators. In predicting academic performance, only P3 amplitude showed a significant effect.

Conclusion: These results challenge previous findings, which reported that P3, P2, or theta power might be used in standard psychometric tests to assess an individual's intelligence.

Keywords: event-related potentials, event-related synchronization, fluid intelligence, academic achievement, machine learning

HIGHLIGHTS

- Both executive and storage components of working memory were considered in this research at the EEG level.
- Both logistic regression and support vector machine classifiers were applied to train the EEG data from working memory tasks to classify the fluid intelligence (Gf) of children.
- Single (area under curve [AUC] < 0.75) or combined (AUC < 0.85) indicators of three EEG signals (P3 amplitude/P2 latency/θ-event-related synchronization) all showed moderate AUC in the receiver operating characteristic analysis of Gf.
- A multiple linear regression of EEG markers to children's academic achievement showed that only the P3 amplitude exhibited an effect ($\beta = 0.017$, $p = 0.035$).

INTRODUCTION

With the development of artificial intelligence (AI), exploring the relationship between neurophysiological markers and psychological characteristics has become intensified. Especially in the fields of information engineering, facial expression recognition, and smart surgery, an integrated automatic identification system based on biomarkers is gradually being established. By collecting and analyzing the information of specific groups of index, it is possible to recognize and diagnose certain characteristics, abilities, or attributes of an organism. Relevant studies from the interdisciplinary fields of medicine and cognitive neurology have indicated that multiple brain activity markers extracted from EEG results can be good indicators of the state of consciousness or the cognitive state of human beings (Missonnier et al., 2007; Sitt et al., 2014; Engemann et al., 2018). Specially, compared with other biomarkers, EEG biomarkers have the advantages of economy, convenience, and efficiency. Combined with machine learning, EEG biomarkers can automatically identify and classify various clinical patients, so they represent the preferred clinical indicators for predicting treatment response (Engemann et al., 2018).

Fluid intelligence (Gf) has always been the focal topic in cognitive psychology, as well as in recent years. In many cases, such as career counseling or clinical application, it is necessary to assess a person's level of intelligence. However, presently, the intelligence test is still based on a pencil-and-paper test; the era of intellectualization has introduced new requirements for assessing intelligence. Intelligence scales such as Raven's and Wechsler's have demonstrated good reliability and validity; even when the testing method is relatively simple, these intelligence scales are widely used in general intelligence tests; however, when it comes to the plasticity of Gf and the evaluation of robot intelligence, these methods appear to be insufficient. How do we develop a scientific evaluation system based on neurocognition? How do we carry out targeted intelligent shaping based on the working mechanism of the brain? Obviously, to solve these problems, the neural basis of Gf warrants further clarification. In addition, with the demand of AI for intelligence shaping and people's expectations for improving Gf, the current ways of intelligence assessment are facing new challenges: "Knowing wisdom and making intelligence, knowing intelligence and making evaluation" requires cognitive neuroscience to make further breakthroughs in the understanding of Gf and develop a more reliable evaluation system. Several previous studies have applied machine learning methods to explore EEG signals that were effective in verifying Gf (Neubauer and Fink, 2009; Itthipuripat et al., 2013; Wronka et al., 2013; Amin et al., 2015; Dong et al., 2015; Qazi et al., 2017; Wongupparaj et al., 2018), and some of them revealed that individuals with different Gf levels can be well distinguished (Amin et al., 2015; Qazi et al., 2017).

Amin et al. (2015) conducted research on 34 healthy adults (ranging in age from 20 to 30 years) using the visual oddball task. An analysis of P3 component induced by the visual oddball task showed that P3 amplitude could significantly predict individual scores on Raven's Advanced Progressive Matrices with an area under the curve (AUC) reaching 0.82. Therefore, P3 amplitude could be used as a good supportive index in the standard psychological test for evaluating an individual's learning or memory ability (Amin et al., 2015). This study is the first to test the EEG effect in measuring Gf. Subsequently, Qazi et al. (2017) also used the visual oddball paradigm as a tool to examine Gf (marked by Raven's Advanced Progressive Matrices scores) and used the support vector machine (SVM) classifier to test the discriminant ability of delta band to Gf in 34 adult males. The authors showed that the statistical wavelet features and the wavelet coefficient features from the frequency bands 0.0–1.875 and 1.875–3.75 Hz resulted in 100 and 98% prediction accuracies, respectively (Qazi et al., 2017). However, the sample sizes of these studies were restricted to no more than 40, and the EEG evaluation index was limited to only one. Additionally, in the field of EEG markers of Gf, there are few comparable quantitative analysis studies, and the discriminant effect is easily affected by the discriminant method. Therefore, it is not robust enough to arrive at a conclusion; further exploration and verification are warranted. It is worth noting that while there was less discussion on the evaluation of EEG indicators in the studies of Gf, in other research fields such as mild cognitive impairment (MCI) and consciousness, the discrimination effect of EEG indicators has been discussed more fully. Missonnier et al. (2006) showed that the theta event-related synchronization (ERS) during the *n*-back working memory (WM) task can distinguish progressive MCI cases whose θ-ERS power was lower than that in the stable MCI cases, and the Area Under Curve (AUC) was 76% (Missonnier et al., 2006). While adding the event-related potential (ERP) index (P200 and N200), the combination model showed a higher AUC reaching 0.938 (Missonnier et al., 2007).

A relationship between WM and Gf has been well established. WM might be fractionated into two components: short-term memory (STM) storage and the central executive (CE). The CE is a processing component, which may be fractionated further into executive functions (EFs) like updating, inhibition, and shifting: the updating of information temporarily memorized for processing, the inhibition (or interference control) of information not or no longer relevant for the current processing step, and the shifting of the attentional focus between different task demands. Accordingly, WM-load can be differentiated into

WM storage-load and WM processing-load (i.e., demanding STM processes and demanding EFs, respectively). A typical task to induce WM storage-load is the simple digit span (Dspan) task (i.e., the short-term memorization of a sequence of digits for later recall). In contrast, complex span tasks like *N*-back ($N \geq 2$) tasks are conceptualized to induce WM processing-load (Engel De Abreu et al., 2010; Scharinger et al., 2017). Notably, even though STM and WM are theoretically distinct and sometimes assessed separately, no single task is a pure measure of either of them; even a seemingly simple task, such as Dspan, is likely to involve EFs mechanisms (Engel De Abreu et al., 2010).

The relationship between these two components of WM and Gf can be summed up using three kinds of views (mainly from the studies of structural equations and path analysis). First, STM system (the storage component of WM) has a particularly important connection with general intelligence (Colom et al., 2005; Gignac et al., 2016). Second, CE function plays a major role in Gf (Gray et al., 2017; Myers et al., 2017). Third, both STM (storage function) and WM (EF) are related to intelligence, and both components produce independent contributions to Gf, respectively (Unsworth and Engle, 2007; Unsworth et al., 2014). In all, none of them has completely denied the effect of WM processing or storage components on Gf; moreover, the relationship among them at the EEG level is still unclear. So, we assume that both the storage component (STM) and the non-storage component (EF) of WM affect Gf, and then we choose two typical representative tasks: 2-back for EF and delay match to sample (DSM) for STM in the present study.

Nevertheless, whether there exist EEG markers indicating Gf robustly is still dubious. Neural efficiency hypothesis and attentional resources allocation give cues that P3 amplitude induced by executive function task and θ-power in simple memory task may have the ability to indicate Gf. The neural efficiency hypothesis stated that brighter individuals display lower (more efficient) brain activation while performing simple cognitive tasks (Neubauer and Fink, 2009), and Julie et al. (2005) showed that the frontal midline θ-power increased as the memory load increased (Julie et al., 2005), suggesting that the frontal midline θ-power may indicate the amount of cognitive resources that need to be invested in current memory tasks, thus reflecting the subjective sense of task difficulty. Attentional resources allocation illustrated that P3 amplitude at parietal sites in the complex tasks would reflect the amount of attentional resources allocation that one person concentrates on current EF task (Polich, 2007). So, increased P3 amplitude is a manifestation of sufficient cognitive resources (Scharinger et al., 2017), and it would be accompanied by a better *N*-back performance (Tusch et al., 2016). In addition, neural speed is considered to be an evaluation index of cognitive ability, while P2 component is considered to reflect processes involved in selective attention (Wongupparaj et al., 2018) and shorter P2 latency is considered to reflect more shifting ability, which indicates more efficient use of brain resources (Lijffijt et al., 2009; Wongupparaj et al., 2018). So, we hypothesize that in the same simple memory task, children with high Gf would exhibit lower frontal midline θ-power (saving brain resources due to an easy feeling toward the task), and that in the EF task, they would exhibit larger parietal P3 amplitude (more attention resources can be focused on the task) and shorter P2 latency (more flexible) than that of children with low Gf. The present study intends to explore whether WM task-related EEG biomarkers can diagnose Gf level and predict academic achievement in healthy primary school children.

MATERIALS AND METHODS

Subject

For the experiment, a sample of 62 healthy students (28 male; all right-handed; age range, 9–12 years) were recruited from a primary school in Nanning, China. They had normal or "corrected to normal" vision and were free from medication, neurological disorders, and cognitive impairments. Their parents all signed informed consent forms before the children participated in the trials. This study was approved by the Psychology Experimental Ethics Committee of Nanjing University.

Raven's Standard Progressive Matrix (RSPM) Test

The RSPM test was performed for intelligence assessment, during which 60 items were completed within 40 min. The original scores were calculated by adding up the scores for completing 60 items, which were converted into standardized intelligence scores (RSs) ranging from 0 to 100, and according to the Intelligence Level Grading Standard, intelligence levels were classified into the following five grades: 1 (>95, very good), 2 (95–75, good), 3 (74–25, average), 4 (24–5, below average), and 5 (<5, deficit) (Wang et al., 2009).

WM Tasks

DMS task is used to assess children's ability related to encoding and storing information in STM. In general, the WM capacity of DMS paradigm is set at 4 (Zhang et al., 2016); so, the WM load in the present experiment was also 4. That is, four digits appeared each time. The task process is shown in **Figure 1** (left): First, four Arabic numerals (1,000 ms) appear on the screen. The subjects are asked to remember the four numerals. Then, a blank screen of 3,000 ms appears. Finally, a capitalized numeral appears. The subjects are asked to react immediately to determine whether the current number was contained in the four numerals that just appeared. Contained, press "F" key, while not contained, press "J" key. The task includes two blocks; each block has 20 trials, making a total of 40 trials.

The 2-back task was applied to examine the children's EF of WM. Apart from updating the WM content, when doing the task, the subjects must shift between the two subtasks and inhibit currently irrelevant information (Scharinger et al., 2017); so, it's a complex task that requires all EF subcomponents (including inhibition, updating, and shifting). The instructions are shown in **Figure 1**. After reminding the subjects with "+," an Arabic numeral in the range of 1–9 will appear randomly around the "+" for 600 ms. The subjects were required to compare whether the current number matched the number that was shown two

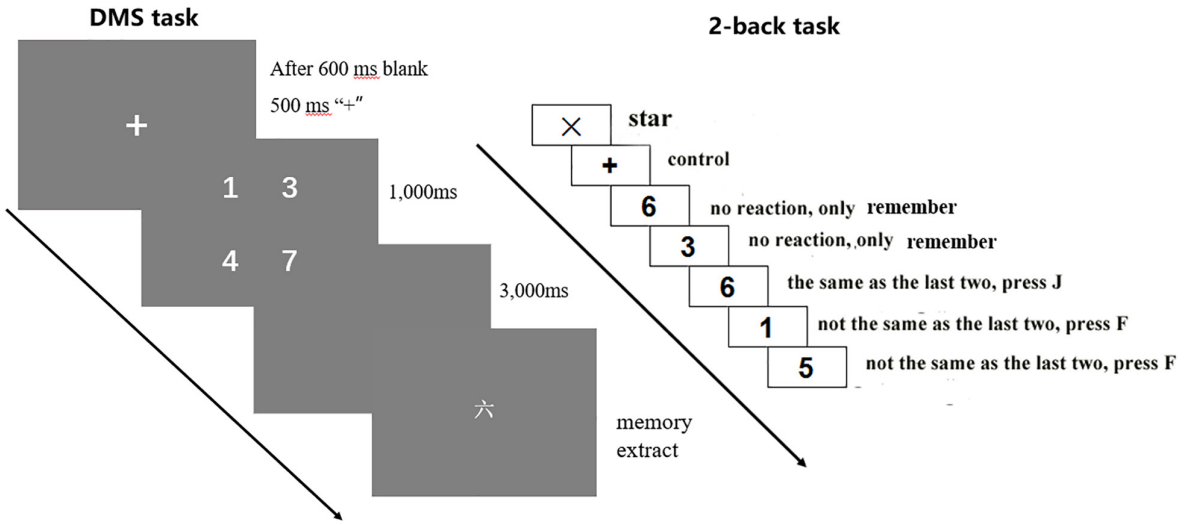

FIGURE 1 | Working memory task.

numbers prior, by pressing the "J" key for matching, or by pressing the "F" key for mismatching. Each number after the third number should be judged one by one. Matching and mismatching conditions accounted for half of the trials. In order to ensure that the subjects understand the task, an exercise session was set before they entered the formal experiment. Only those with the correct rate of exercises reaching up to 60% can enter the formal test. The exercise is set to ensure that the participants understand the task; so, if they did not pass the exercise the first time, they can get a second and even a third opportunity to exercise again (no more than three exercise in all). In this research, all of the participants got through the exercise no more than three times.

There are two blocks, 40 trials in each block, and 80 trials in total. These two tasks were all programed in E-Prime 2.0, and each task was presented on a 16-inch computer screen from a height of horizontal line of sight.

Experiment Procedure

All of the participants were informed of the schedule for data collection and, as per their availability, the experiments were arranged individually. Each subject was seated in a partially sound-attenuated room and was briefed on the procedure. Each subject was asked to perform the RSPM pencil-and-paper test first; next, each subject went to the nearby EEG room to perform the DMS task; and finally, they performed the 2-back task. The subjects had a 3-min break between tasks. During the WM time, an EEG cap was set until they completed the two computer tasks.

By the end of the next term (6 months later), the Chinese and mathematics scores of those subjects were collected as an index for academic achievement. The examinations test the students' mastery of knowledge acquired in a semester, and the items are designed by teachers who teach the corresponding curriculum. The original scores of the examinations were transformed into Z scores according to the calculating formula: $z = \frac{\text{original score} - \text{average score}}{\text{standard deviation}}$, and the average score and the standard deviation values corresponded to the subjects' grades to which they belonged.

Electrophysiological Recordings

When the participants were performing the WM tasks, the EEG data were recorded using an EEG amplifier (NuAmps 40, Compumedics Neuroscan, VIC, Australia). The sample rate was set to 1,000 Hz with a bandpass filter (0.05–100 Hz), and the reference electrode was situated on the left mastoid online, and the grounding electrode was located at the midpoint of connection between FPz and Fz (called AFz). Horizontal eye movements were recorded by electrodes positioned at the outer canthus of each eye whereas vertical eye movements were recorded by electrodes positioned above and below the left eye. The electrode impedance was maintained at <10 kΩ throughout the EEG recordings. To attenuate low- and high-frequency noise, the averaged waveforms were filtered using a 30-Hz low-pass filter and a 0.5-Hz high-pass filter in the off-line analysis.

Preprocessing

Preprocessing was conducted using Curry 7.0 (Compumedics Neuroscan), including re-reference, removing EOG artifacts, deleting bad block. and segment epoch. This procedure is described as follows:

(1) Re-reference: change the reference from left mastoid to bilateral mastoid.
(2) Remove EOG artifacts: set the removing-threshold at 150 mV, removing EOG artifacts (which are above the threshold value) from the EEG signals based on a covariance method.
(3) Delete bad block: set the delete threshold at ±100 mV to exclude the impact of bad block in the next averaged waveforms step.
(4) Segment epoch: for 2-back data, the artifact-free EEG was segmented into epochs ranging from 200 ms before

stimulus onset to 800 ms after stimulus onset, with a period of "–200 ms to 0" as baseline correction, fewer than 40 of 80 good target segments were excluded in the data analysis. For DMS data, the artifact-free EEG was segmented into epochs ranging from 500 ms before stimulus onset to 4,000 ms after stimulus onset, according to the task design; the 0–1,000 ms was coding period, 1,000–4,000 ms was delay period at each epoch, and "–500 ms to 0" was used as baseline correction. Fewer than 20 of 40 good target segments were excluded in the subsequent data analysis.

Data Analysis

Behavioral Analysis

Behavioral data were analyzed to measure performances corresponding to fluid cognitive ability as well as the WM tasks. To assess fluid cognitive ability, RSPM raw scores and standardized intelligence scores, as well as the intelligence level, were calculated for each subject. Considering that there were no children with deficits in our study sample and that the "very good" and "below average" levels were also not sufficient to form an independent group, we combined the "very good" and "good" children into the HA group and the "average" and "below average" children into the LA group. It should be noted that in similar studies by Amin et al. (2015) and Qazi et al. (2017), in which they grouped adult subjects according to the median scores of RAPM raw scores, those who scored above the median were placed in the HA group, and conversely, those who scored below the median were placed in the LA group. But in children, age is a notable factor that would affect the Raven raw scores; so, if we do like this in the present experiment, most of the older children might be grouped in the HA group. Therefore, in order to prevent this issue, we use the intelligence level that has already considered Raven's score and children's age at the same time.

For the WM tasks, each subject's performance was computed by calculating the number of correct responses (accuracy, ACC) in addition to reaction time (RT). Independent sample *t*-test was used to analyze the data with ACC and RT. A statistical analysis was performed using SPSS version 22.0 software (IBM, China).

ERP and ERS Analyses

For 2-back EEG data, a superimposed averaging process can be carried out after preprocessing; only good segments were retained in the individual averaged waveforms. In addition, to investigate whether the differences between the two groups are specific to P3 only, the P2 component was extracted and analyzed. For DMS EEG data, before obtaining the superposed average, a wavelet transform was applied to extract theta power. Both the wavelet transform and the superposed average were conducted using MATLAB R2013b, with toolbox Letswave7[1].

For ERP analysis, the waveforms and the 2-D plot of group grand average were performed before determining the time window of ERP components; the major electrodes were selected in the groups (HA vs. LA) × electrode sites (n) repeated measurements analysis of variance (ANOVA) test; both ERP amplitude and latency were extracted from the respective electrodes for each subject per group. For ERS analysis, the time-frequency map and the 3D-plot of group grand average were conducted before selecting the representative electrode sites. Also, the θ-power of the selected electrodes were analyzed by repeated measurements of variance of 2 (grouping: HA vs. LA) × n (electrode sites). Greenhouse–Geisser method was used to correct the p value while the statistical results were not satisfied with the spherical assumption, and Bonferroni method was used to correct multiple comparisons (n times) afterward. The ANOVA test was conducted using SPSS 22.0 software.

Logistic Regression and SVM

Logistic regression (LR) and SVM were two major classifiers that were applicable for non-linear discriminant analysis. The LR was based on probability theory [see Function (1), the samples that indicate $P > 0.5$ would be considered to be positive ones; a positive event here refers to LA], whereas the SVM is based on maximizing geometric interval [see Function (2)–(5)]; thus, the optimal hyperplane found by the LR model is to try to keep all of the sample points away from it, and the optimal hyperplane that the SVM is looking for is to maximize the margins (keep only the training points closest to the boundary line as far as possible). So, in the LR model, each sample data would affect the result, whereas in the SVM model, only the samples near the boundary line (that is, only those samples that support the vector) would be considered. Because of the data limitations, the *kernel* SVM was chosen as classifier instead of linear SVM. It projects implicitly the feature of low dimensionality to high dimensionality, and makes the feature disentangled in high dimensionality.

$$P(Y = 1|x) = \pi_x = \frac{e^{\beta_0+\beta_1 x}}{1 + e^{\beta_0+\beta_1 x}} \qquad \text{(Function (1))}$$

Y: intelligence group (1: LA, 0: HA); x: EEG markers; β_0: the constant; β_1: The estimated coefficient of x; $P(Y = 1|x)$: Given the x, the probability that an individual belongs to the LA group.

As described above, the hyperplane in *kernel* SVM can be described as follows:

$$f(x) = w^T \varphi(x) + b \qquad \text{(Function (2))}$$

And the radial basis function is:

$$k(x_i, x_j) = \exp\left(-\frac{|x_i - x_j|^2}{2\sigma^2}\right) \qquad \text{(Function (3))}$$

where σ is the width of kernel function; usually, $\frac{1}{2\sigma^2}$ is called gamma factor. It assumes that all of the samples are separated, and subjects to the inequation as follows:

$$y_i\left(w^T x_i + b\right) \gg 1 \qquad \text{(Function (4))}$$

In practice, not all of the samples can be separated precisely by hyperplane. In order to reduce the influence of these special undesired samples, the approach of soft margin is introduced to SVM. It allows the samples to classify the opposite category in some degree:

$$y_i\left(w^T x_i + b\right) \gg 1 - \xi_i \qquad \text{(Function (5))}$$

[1]For more details, see https://letswave.cn/index.html

where ξ_i is slack variable, representing the degree of every sample that deviates from the accurate category. In the phase of optimization, C will be introduced to control the degree of fitting.

In the present study, we used the "tune" parameter sweep tool [R coding: tune (SVM, Group∼, data = IQ_train, kernel = "radial," ranges = list (cost = c(0.001, 0.01, 0.1, 1, 10, 100, 1000)))]. A grid search was performed on seven parameter values between $C = [10^{-3}$ to $10^3]$ on the whole data. This suggested values of $C = 1$ (which let the model reach its least error: 0.27). In addition, the gamma is set to $1/N_f$ (N_f represents the feature of dimensionality). Those parameter values were used for the subsequent analysis.

In order to obtain more compelling results, We adapted fourfold cross-validation, which separated data into four segments: three for training and one for testing [75% for training and 25% for testing, leaving sufficient testing sample to ensure that it can provide useful information about accuracy rate (Stewart et al., 2014)]. Iterating through the cross-validation, each subset was used once as test data, and the score was averaged across the four splits. Additionally, to ensure comparability between these two models, an R code "set.seed(20)" was written before the cross-validation part to ensure that the division of sets was exactly the same between each model. Relatedly, the *caret*[2], *glm* and *e1071*[3] packages of the R Studio software version 1.1.456 were utilized to conduct the corresponding tests (i.e., *glm* for logistic model testing; *e1071* for SVM testing; and *caret* for cross-validation).

Besides, the receiver operating characteristic (ROC) technique was adopted for evaluating the LR and SVM models [for more details about the ROC technique, see Fawcett, 2006; Hand, 2009]. An ROC plot illustrates both sensitivity and specificity with the AUC of the ROC of 0.5 signifying random chance prediction and 1 being perfect prediction. Therefore, the closer the AUC is to 1, the greater the diagnostic value of the indicator(s). The *pROC* packages[4] of the R Studio software version 1.1.456 were utilized to plot the ROC curve.

Multiple Linear Regression (MLR) Model

The MLR is a linear statistical method, which is used for predicting the relationship of a single dependent variable (response variable: Y) with one or more independent variables (predictors: $X1$, $X2$, …, Xn). A general MLR model can be described by the following equation:

$$y = \beta_0 + \beta_1 x_1 + \beta_2 x_2 + \cdots + \beta_n x_n + \varepsilon$$

where Y represents the dependent variable, x_i indicates the i_{th} independent variable, β_i represents i_{th} predicted parameter (regression weight), and ε is the error between predicted response and observation. The regression weights (β_i) are computed in such a way that minimizes the sum of squared deviations.

In this study, the MLR analysis was performed using SPSS 22.0 with "enter" method on the selected EEG index with selected electrodes to predict academic achievement (Y). Before performing the regression, we had to decide which variable should be used in the regression model. The method included "enter," "remove," "forward," "backward," and "stepwise." We selected "enter" method to let all the Xs enter the model to test their determinant coefficients. To evaluate statistically the LR model, the following important assumptions about the residuals were considered and verified (Amin et al., 2015):

(1) The residuals should have zero mean value (Linearity).
(2) The residuals should be plotted as normal distribution (Normality).
(3) The residuals should have constant variance (Homoscedasticity).
(4) The residuals are independent (or random); otherwise, autocorrelation problem exists.
(5) The Xs are independent; otherwise, multicollinearity problem exists.

Assumption (1) is easily verified by Residual Frequency Distribution Map (see **Figure 9C** in the Results). And if a normal probability plot of the standardized residuals showed a straight line, assumption (2) is verified. Assumptions (3) and (4) can be evaluated by using scatter plots that show the relationship between standardized residuals and predicted values. Besides, the variance inflation factor (VIF) is introduced to detect the LR model collinearity with a threshold at 10 to verify assumption (5). The verification of these assumptions is given in the section "Verification of Regression Assumptions."

RESULTS

According to the participants' RSPM scores, eight subjects were rated as "very good," 34 as "good," 17 as "average," and 3 as "below average"; so, 42 children were assigned to the HA group and the rest were assigned to the LA group. Sex distribution has shown non-significant difference between the two groups ($x^2 = 1.154$, $p = 0.413$). The grouping information is presented in **Table 1**.

Behavioral Results

Behavioral data recorded during the DSM and the 2-back task were analyzed for both groups (HA and LA). As shown in **Table 2**, the HA group's accuracy (ACC) was

TABLE 1 | Grouping results (mean ± standard deviation).

	HA (*N* = 42, 17 male)	LA (*N* = 20, 11 male)	*t*	*p*
Age	10.94 ± 0.66	11.18 ± 1.07	–1.067	0.290
Raw scores of RSPM	48.29 ± 3.73	37.55 ± 5.51	9.036	<0.001

[2] Available at https://cran.r-project.org/web/packages/caret/index.html

[3] For more details, see https://cran.r-project.org/web/packages/e1071/vignettes/svmdoc.pdf

[4] Available at https://cran.r-project.org/web/packages/pROC

TABLE 2 | Working memory performance measurements (mean ± standard deviation).

	HA (*N* = 42)	LA (*N* = 20)	*t*	*p*	Effect size (Cohen's *d*)
ACC of DMS	0.90 ± 0.07	0.84 ± 0.11	2.632**	0.011	0.651
RT of DMS (ms)	832.46 ± 96.56	807.14 ± 110.57	0.921	0.361	0.244
ACC of 2-back	0.84 ± 0.10	0.78 ± 0.12	1.989*	0.051	0.543
RT of 2-back (ms)	1025.25 ± 327.33	935.72 ± 292.47	1.041	0.302	0.288

$^{*}p < 0.10$ mark; $^{**}p < 0.05$. Small effect, $0.15 \leq d < 0.40$; medium effect, $0.40 \leq d < 0.75$; large effect, $0.75 \leq d < 1.10$; very large effect, $1.10 \leq d < 1.45$; huge effect, $d > 1.45$.

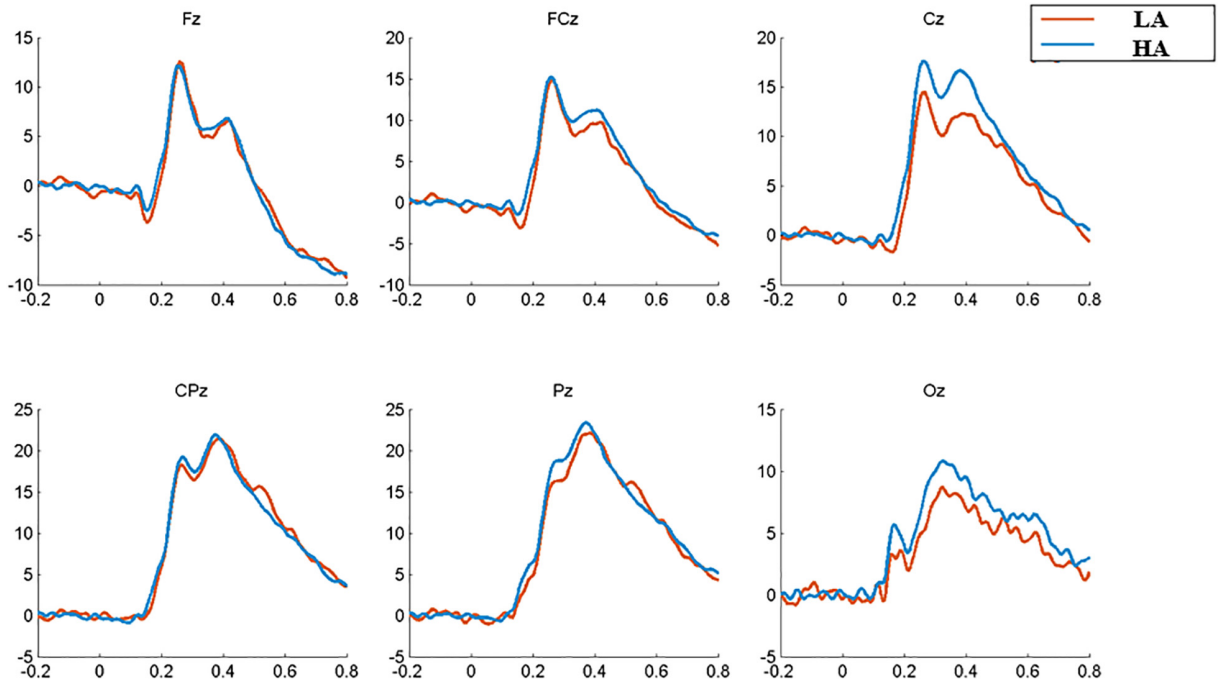

FIGURE 2 | Average ERP waveforms for 2-back task of LA (red) and HA (blue) groups.

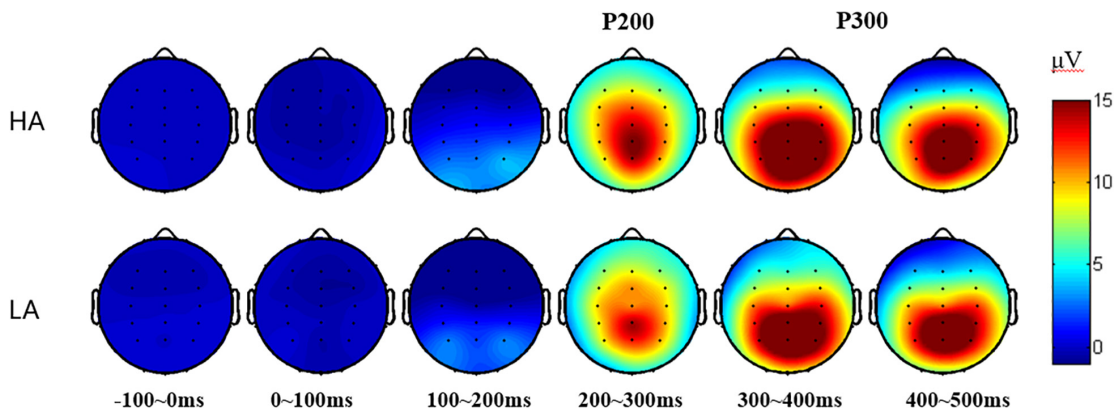

FIGURE 3 | 2-D plot of grand average ERP responses of HA and LA groups from 34 scalp locations (except for four eye electrodes and two reference sites).

significantly (or marginally significant) higher than the LA group's ACC for both tasks, while the HA group's reaction time (RT) was shorter (non-significantly) than the LA group's RT. Additionally, Cohen's *d* results (**Table 2**) indicated an intermediate effect size between the HA and the LA groups' performances for the ACC.

TABLE 3 | P200 amplitude of each group in 2-back task (μV, mean ± standard deviation).

	HA (*N* = 42)	LA (*N* = 18)
Fz	11.58 ± 5.27	12.43 ± 5.09
FCz	14.72 ± 5.67	14.81 ± 4.64
Cz	17.09 ± 5.79	14.81 ± 7.05
CPz	18.36 ± 6.22	17.89 ± 4.72
Pz	17.26 ± 7.51	15.93 ± 6.48

TABLE 4 | P300 amplitude of each group in 2-back task (μV, mean ± standard deviation).

	HA (*N* = 42)	HA (*N* = 18)
FCz	11.32 ± 6.04	9.85 ± 7.19
Cz	16.77 ± 6.20	12.87 ± 8.30
CPz	21.39 ± 6.40	18.93 ± 6.47
Pz	22.68 ± 7.36	21.04 ± 5.98
Oz	9.44 ± 7.30	7.53 ± 8.60

ERP Results

The subjects were excluded from further ERP analysis due to an insufficient number of target segments (fewer than 40 of 80 good target segments) that failed to obtain adequate "signal to noise ratio." This exclusion allowed 60 subjects for 2-back ERP analysis and excluded two subjects. With regard to waveform and 2-D topographic map (**Figures 2**, **3**), the time window of P2 is set at 220–280 ms, and P3 is set at 350–420 ms.

The analysis of latency showed that the Fz site reaches the P2-peak first (around t = 0.26 s) and that the Pz site reaches the P3-peak first (around t = 0.37 s); so, the comparison of the latency between LA and HA group is conducted for P2(Fz) and P3(Pz), respectively. The results revealed a marginally shorter (t = 1.783, p = 0.080, Cohen's d = 0.497) P2 (Fz) latency of the HA group (253.55 ± 12.75 ms) compared to that of the LA group (260.06 ± 13.43 ms). For P3(Pz) latency, a non-significant difference has been found [HA: 371.9 ± 33.0 ms; LA: 386.1 ± 38.7 ms, t = 1.492, p = 0.141, Cohen's d = 0.395].

Following previous research (Amin et al., 2015; Zhang et al., 2018) and based on our total average results (**Figure 3**), the electrode sites that show P200 or P300 component are used in further analysis (see **Tables 3**, **4**, respectively); so, a 2 (group: HA and LA) × 5 (sites: Fz, FCz, Cz, CPz, and Pz) repeated measures ANOVA was performed to analyze the average amplitude of the P200, and a 2 (group: HA and LA) × 5 (sites: FCz, Cz, CPz, Pz, and Oz) repeated measures ANOVA was performed to analyze the average amplitude of the P300.

The results of repeated measures ANOVA of P2 amplitudes between these two groups indicated a significant main effect of electrode sites [$F(4,232)$ = 19.948, p < 0.001, η^2 = 0.256], Further multiple comparisons showed that the P2 amplitude in the central-parietal region (CPz) was significantly higher than that in the frontal region (Fz, p < 0.001), frontal-central region (FCz, p < 0.001), central region (Cz, p = 0.005), and parietal region (Pz, p = 0.023); and the P2 amplitude at Fz site was significantly smaller than that at other sites ($p \leq 0.001$). The group's main effect [$F(1,58)$ = 0.196, p = 0.660, η^2 = 0.003] and the interaction effect between groups and electrode sites [$F(4,232)$ = 1.412, p = 0.231, η^2 = 0.024] were not significant.

For P3 amplitude, the statistical results showed a significant main effect of electrode sites [$F(4,232)$ = 55.074, p < 0.001, η^2 = 0.487], revealing that the P3 amplitude decreased from Pz and CPz sites to Cz, FCz, and Oz sites, respectively; and a marginally significant group main effect was found [$F(1,58)$ = 2.876, p = 0.095, η^2 = 0.047]. Further multiple comparison indicated that the P3 amplitude in the HA group was significantly higher than that in the LA group at Cz site (p = 0.049). The interaction effect between electrodes sites and groups was non-significant [$F(4,232)$ = 21.496, p = 0.702, η^2 = 0.007].

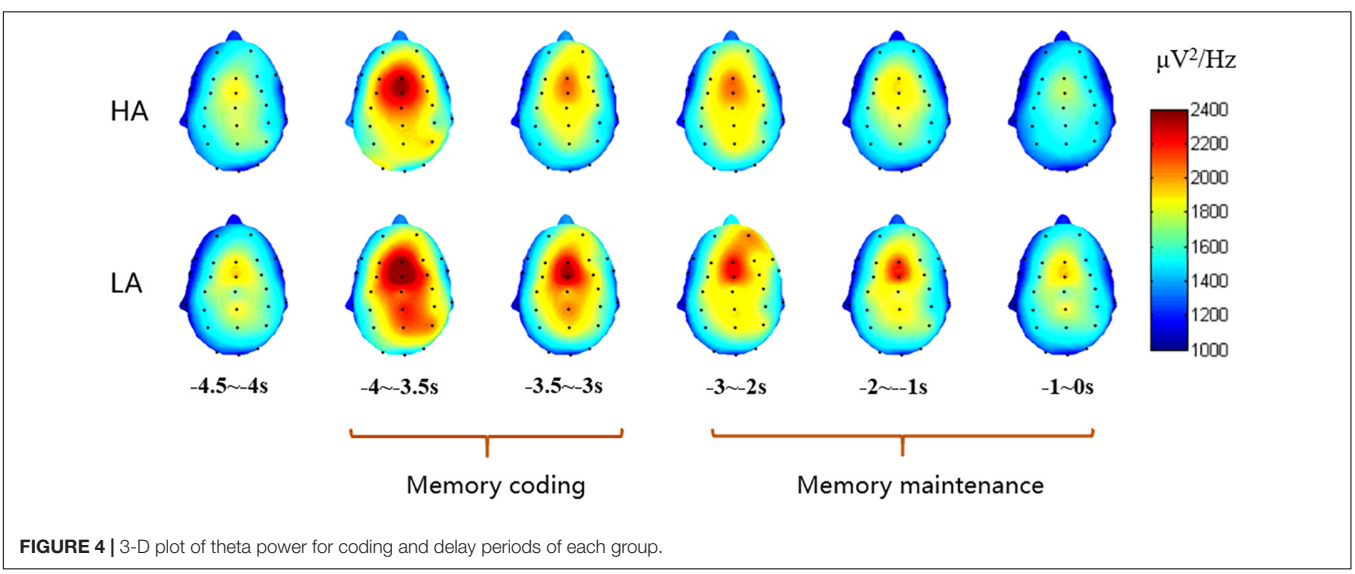

FIGURE 4 | 3-D plot of theta power for coding and delay periods of each group.

TABLE 5 | θ-ERS of each group in DSM task (Power, μV^2/Hz).

	HA (*N* = 39)		LA (*N* = 19)	
	Coding period	**Maintaining period**	**Coding period**	**Maintaining period**
F3	1885.74 ± 654.33	1656.17 ± 611.50	1901.95 ± 704.60	1697.08 ± 618.10
FZ	2216.02 ± 653.01	1876.24 ± 616.25	2386.88 ± 567.21	2086.95 ± 531.09
F4	1841.89 ± 582.67	1600.36 ± 565.92	1804.06 ± 502.64	1639.04 ± 507.29
FC3	1857.27 ± 600.07	1625.65 ± 572.07	1836.67 ± 751.88	1617.21 ± 647.29
FCZ	2196.45 ± 645.42	1876.60 ± 605.67	2518.10 ± 649.40	2123.21 ± 519.66
FC4	1850.08 ± 575.04	1639.55 ± 565.17	1988.73 ± 414.47	1735.13 ± 343.39

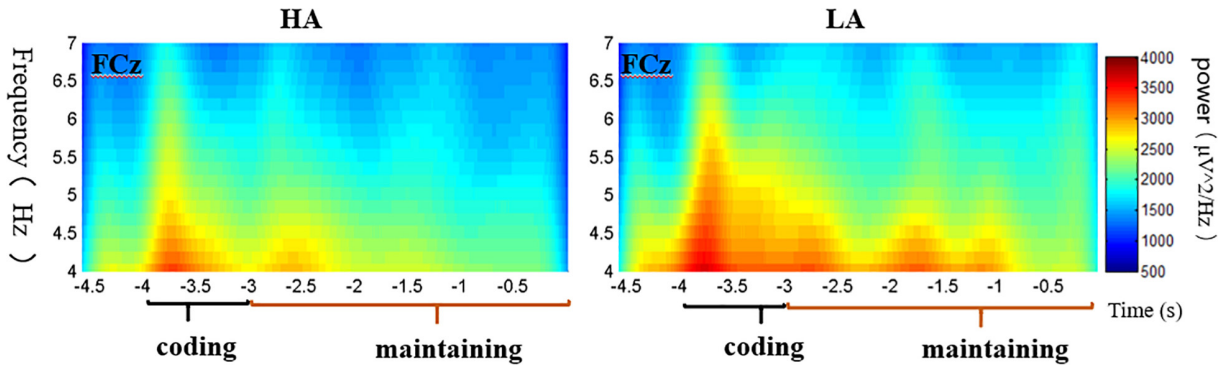

FIGURE 5 | Average spectrograms at FCz site of HA **(left)** and LA **(right)** groups.

θ-ERS Results

The subjects were excluded from further ERS analysis due to an insufficient number of target segments (fewer than 20 of 40 good target segments) that failed to obtain adequate "signal to noise ratio." This exclusion allowed 58 subjects for DMS ERS analysis and excluded four subjects. With regard to the 3-D spectrogram (**Figure 4**), the major sites with obvious activity in the theta band were included in the repeated measures ANOVA.

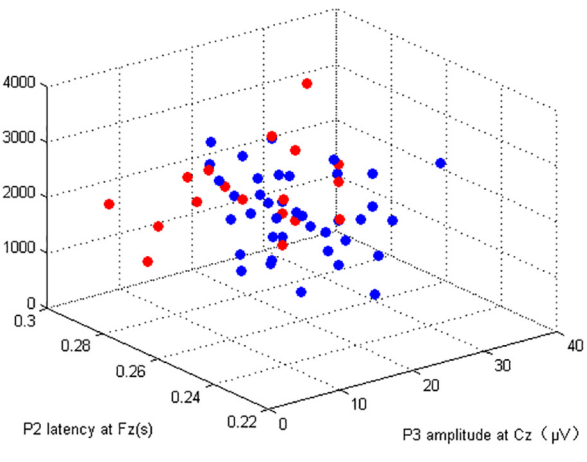

FIGURE 6 | High ability (blue) and LA (red) individual location determined by three EEG indicators.

Consistent with previous empirical studies like, Tóth et al. (2014) and Raghavachari et al. (2001), the theta band (4–7 Hz) activities were major in the frontal area. Then, a 2 (group: HA and LA) × 6 (sites: F3, Fz, F4, FC3, FCz, and FC4) repeated measures ANOVA was conducted to analyze the theta power between these two groups for coding and maintaining periods, respectively. The statistical results for coding period showed a significant main effect of electrode sites [$F(5,280) = 31.693$, $p < 0.001$, $\eta^2 = 0.361$] and a significant interaction effect between electrodes sites and groups [$F(5,280) = 2.649$, $p = 0.023$, $\eta^2 = 0.045$], while the main effect of group was non-significant [$F(1,56) = 0.407$, $p = 0.526$, $\eta^2 = 0.007$]. A further simple effect analysis shows that the

TABLE 6 | Parameters of classification (mean ± standard deviation) of testing set.

	SVM			
	P3 amplitude	**P2 latency**	**Theta ERS**	**All**
Accuracy	0.768 ± 0.107	0.696 ± 0.122	0.696 ± 0.122	0.732 ± 0.107
Sensitivity	0.217 ± 0.208	0.000 ± 0.000	0.000 ± 0.000	0.104 ± 0.125
Specificity	1.000 ± 0.000	1.000 ± 0.000	1.000 ± 0.000	1.000 ± 0.000
	LR			
	P3 amplitude	**P2 latency**	**Theta ERS**	**All**
Accuracy	0.696 ± 0.122	0.679 ± 0.092	0.679 ± 0.092	0.714 ± 0.143
Sensitivity	0.167 ± 0.236	0.000 ± 0.000	0.000 ± 0.000	0.317 ± 0.281
Specificity	0.927 ± 0.086	1.000 ± 0.000	1.000 ± 0.000	0.864 ± 0.077

theta power of the LA group was marginally higher than that of the HA group at FCz site (p = 0.081). The statistical results of delay (maintaining) period indicated a significant main effect of electrode sites [$F(5,280)$ = 21.251, p < 0.001, η^2 = 0.275], while non-significant effects of group [$F(1,56)$ = 0.522, p = 0.473, η^2 = 0.009] and the interaction of group and electrode sites [$F(5,280)$ = 1.785, p = 0.116, η^2 = 0.045] were found. The theta power of these sites for each period of two groups are presented in **Table 5**.

Taking FCz site as an example (**Figure 5**), the theta power increased at the commencement of the trial and was elevated through the memory coding period and the delay period. The average spectrograms for the LA group demonstrated more energy in the theta frequency band across the coding period.

Machine Learning Results

P3 amplitude (Cz), P2 latency (Fz) of 2-back task, and the θ-ERS (FCz) within the coding period of the DSM task were included in the machine learning analysis; the total number of subjects in this section was 56 (consider both 2-back and DSM tasks). The Gf (marked by RSPM) of our subjects was linearly inseparable by three EEG indicators (**Figure 6**). As illustrated in the section "Materials and Methods," the classification performance of fourfold cross-validation of *kernel* SVM and LR classifiers for each EEG indicator and the combination of the indicators are presented in **Table 6**. The mean was the average of the testing results of fourfold cross-validation, as well as standard deviation values. Use of a single EEG parameter permitted correct classification of 76.8% (for P3 amplitude), 69.6% (for P2 latency and theta ERS) using the SVM model, as well as a combination of these three EEG markers of 73.2%, which was lower than the P3 amplitude. For the LR model, the correct classification of P3 amplitude is 69.6%, and the classifications of both P2 latency and theta ERS are 67.9%, a combination of them is 71.4%.

The accuracy of SVM was higher than that of LR classifier for both the single or combined EEG indicators, which again verified the good generalization capabilities of SVM algorithms based on maximizing the margin that Lotte et al. (2007) had previously mentioned. But it should be noted that with respect to the AUC of ROC, the LR model showed better outcomes, especially in the regression of three comprehensive indicators, reflecting its advantages of "taking care of the overall samples" which leads to an AUC at 0.844, which is higher than that of SVM (0.792), and far higher than any single EEG indicator in the LR model (AUC all < 0.6, almost equal to 0.5, which signifies random chance prediction). Among the three single EEG indicators, P3 amplitude was by far the more suitable indicator in the discrimination of Gf because of its highest accuracy rating in both classifiers. It is worth mentioning that while the specificity was excellent in the SVM classifier (single or comprehensive

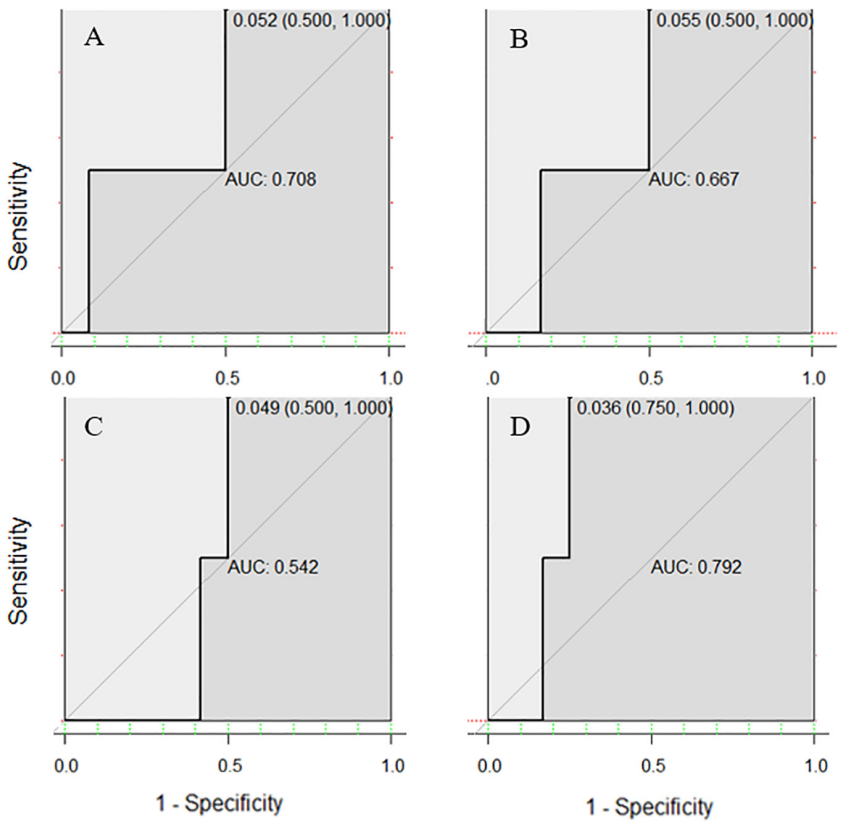

FIGURE 7 | Receiver operating characteristic curves for two-back-related frontal P3 amplitude **(A)**, P2 latency **(B)**, and DMS-related theta ERS **(C)**, and their combination based on electrode sites selected from the ANOVA test **(D)** using the SVM model.

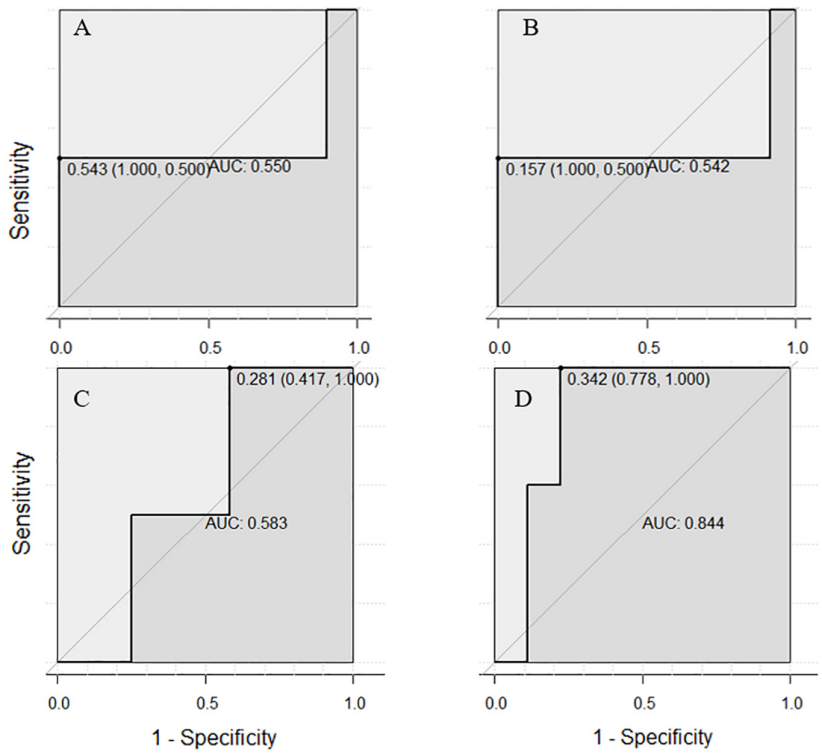

FIGURE 8 | Receiver operating characteristic curves for two-back-related frontal P3 amplitude **(A)**, P2 latency **(B)**, and DSM-related theta ERS **(C)**, and their combination based on electrode sites selected from the ANOVA test **(D)** using the LR model.

indicators have reached 1 for all four subsets), the sensitivity of diagnosing individuals with LA in both classifiers was very small, even < 0.5, indicating the limitation of those EEG signals.

The training sets that corresponded to the testing sets with the highest accuracy in both SVM and LR models were used to draw ROC curves. Interestingly, the area under the ROC curve of SVM and LR showed different styles. In the ROC curve under the SVM model (**Figure 7**), all of the best cutoff points were set at the point where sensitivity was equal to 1, and the shape of single or combined signals was similar to each other (all showed high sensitivity and low specificity). But in the ROC curve of the LR model, the combination of the three EEG indicators led to a substantial improvement of sensitivity (reach at 1.00), specificity (reach at 0.75), and proportion of correctly classified cases (**Figure 8**). Meanwhile, when the best cutoff points of P3 amplitude and P2 latency were set at the point where they had an advantage in specificity (equal to 1), the best cutoff point of θ-ERS had an advantage in sensitivity; so, it is reasonable to infer that their combination will demonstrate substantial improvement in AUC (under the LR model).

Multiple Linear Regression Results

Multiple linear regression analysis with "enter" method was performed on selected three electrodes for P3 amplitude, P2 latency, and theta ERS for predicting academic achievement (6 months later). The regression parameter was presented in **Table 7**, and the regression function was described as follows. The P3 amplitude at Cz site predicted statistically and significantly the academic achievement (total scores of Chinese and Mathematics) in this model. The explanation ratio of variance between regression and residuals was marginally significant ($F = 2.655$, $p = 0.058$).

Verification of Regression Assumptions

With regard to the regression analysis for prediction of academic scores, the mean value of the residual is about 3.82×10^{-17}, which is very close to zero (**Figure 9C**), and it also presents a normal distribution for the standardized residual; thus, the first and second regression assumption (linearity and normality) is verified. Besides, the normal probability plot of the standardized residuals shows a straight line that verifies the second assumption again (**Figure 9B**). The VIF of each independent variable is

TABLE 7 | Regression parameter of EEG signals to academic achievement.

Independent variables	*B*	Standardized β	*p*	VIF
θ ERS in coding period (FCz)	−0.000099	−0.150	0.262	1.002
P3 amplitude (Cz)	0.017**	0.285**	0.035	1.044
P2 latency (Fz)	−3.450	−0.113	0.384	1.046
Constant	1.716	7.382	0.220	–

**p < 0.10; **p < 0.05. VIF < 10 means that this variable does not have independent variable multicollinearity. The regression function: Academic Score = 1.414 − 0.000099 θ power + 0.017 P3 Amplitude − 3.540 P2 latency.*

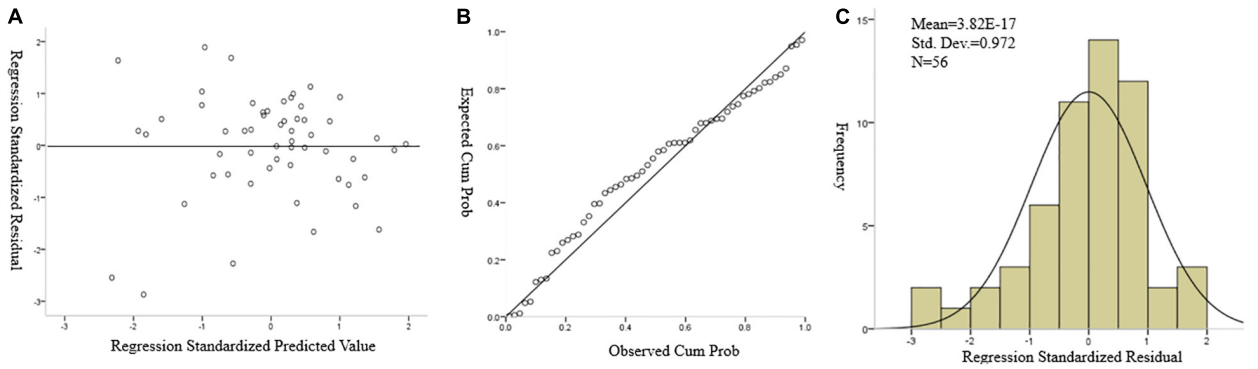

FIGURE 9 | (A) Scatter plot of regression standardized residual against the regression standardized predicted value of dependent variable (academic score). **(B)** Normal P–P plot of regression standardized residual, the plot of the residual fits the expected pattern well enough to support that the residual is normally distributed. **(C)** Normal distribution plot of regression standardized residual with zero mean value.

lower than 10, which shows that there is no multicollinearity problem in the regression model. The scatter plot of the residual against the predicted variable (**Figure 9A**) shows no specific pattern that can be observed, hence verifying the third assumption (constant variance, or homoscedasticity) and the fourth assumption (independence). Thus, the regression model assumptions are considered verified.

DISCUSSION

This study details a method for classifying Gf level in children using WM task-related EEG signals relying on machine learning. It also investigates the relationship between individual differences in WM task-related EEG signals and academic achievement. The present data suggest that P3, which reflects attentional processes involved in stimulus processing and inhibitory control, may be a biomarker for academic achievement during childhood, supporting in part what Hillman et al. (2012) had previously mentioned. To the best of our knowledge, this study is the first to apply pure EEG variables as independent variables to predict academic scores in a multiple linear regression model with verification, although the overall explanatory power is not strong (the explanation ratio of variance between regression and residuals was only 2.655); this research supplements the current literature: Although several studies demonstrated a significant connection between EEG signals measures and Gf, e.g., spectral power (Qazi et al., 2017) or P3 amplitude (Amin et al., 2015), in which the AUCs were >0.80, the present data in children could not support such connections.

The present results offer three implications: The first implication concerns experimental object. The discriminant analysis conducted in healthy people often does not demonstrate significant differentiation; not only in the results of the ROC but also in the analytical results of repeated measures ANOVA or *T*-test can we see that the differences between the HA and the LA groups of the three EEG indicators are only marginally significant. This may help to explain why some studies like the one by Covey et al. (2019), whose aim was to improve Gf in healthy groups, showed little change in the Raven's scores, while the change in EEG signals yielded a significant training effect, as reported previously in a meta-analysis by Melby-Lervåg et al. (2016). The EEG signals did not appear to be so sensitive in the assessment of Gf, especially when Gf was evaluated using the pencil-and-paper test and Raven's scores. Thus, we can infer from the present study that there may have been two possible reasons related to this phenomenon. One is that the EEG signals actually have little in common with the pencil-and-paper test; that is, the EEG signals change a lot, whereas the pencil-and-paper scores do not, or vice versa. If so, there will again be the challenge to determine what Gf is. Do the current tests based on the pencil-and-paper test really measure Gf? The other one is that in healthy samples, the difference between EEG signals and their Gf was too small to reach an acceptable sensitivity, at least based on the present method. So, if those methods were applied to the clinical samples with intellectual impairment in which the difference between positive and negative patients is large enough, the effect size would be greater.

Second, from the comparison of SVM and LR in the present study, we can summarize that while the accuracy of SVM was higher than the LR, the AUC of ROC in the LR model showed a larger AUC for the combined EEG signals, under the condition that the training and testing sets were the same between these two models. Additionally, it should be noted that although several studies have found that the indicator effect of the comprehensive indicator was better than the single indicator (Missonnier et al., 2007; Engemann et al., 2018), a counterexample appeared in this study, indicating that using one signal of P3 amplitude as input increases the classification accuracy to 76.8 from 73.2% with three complexes in the SVM model. There is speculation that the *kernel* SVM projects implicitly the feature of low dimensionality to high dimensionality and makes the feature disentangle in high dimensionality; so, adding features may cause redundancy rather than improve accuracy. In addition, every single indicator in the LR model showed only a small AUC just above chance (the AUC is close to 0.5), indicating that the LR method is sensitive to outliers; meanwhile, a complementary effect has been found between ERP and ERS in the LR model, verifying that the

selection of indicators is comprehensive and that it contributed to the improvement of the AUC in the combined indicators.

Finally, starting from the relationship between WM and Gf, this study essentially analyzes the WM task-related EEG signal and other EEG signals like resting state EEG signal (Gordon et al., 2018), functional connection signals, and other task-related EEG indicators that warrant further investigation in future studies. If there are EEG markers that can robustly indicate human Gf – no matter in what forms – current test styles for assessing intelligence could change dramatically.

Altogether, these findings extend and challenge previous findings that reported EEG signals might be used as a supporting factor in standard psychometric tests to assess an individual's IQ. We hope that the present work, as well as recent studies, will motivate researchers to further explore these important concerns.

Limitations

As we tried to control the experiment object and operation process, there are still some aspects that can be improved. First, we included children of different ages because we could not recruit a sample of children of the same age; when we grouped the children, we did consider this limitation. However, if we use a sample of children of the same age, or perhaps different age groups, the study would undoubtedly be stronger. Second, this study only focuses on three WM-related EEG candidate indicators. Although the WM is thought to be a complex system, perhaps there will be a more comprehensive EEG index system to reflect the WM in the future. Third, when we considered the predictive ability of EEG index, we only perceived it within the "WM-related" scope in the present study, but other EEG signals showed a significant correlation to academic performance, such as error-related negativity (Hirsh and Inzlicht, 2010). Therefore, future research might explore a more intense or broader scope.

DATA AVAILABILITY STATEMENT

The datasets generated for this study are available on request to the corresponding author.

ETHICS STATEMENT

The studies involving human participants were reviewed and approved by the Psychology Experimental Ethics Committee of Nanjing University. Written informed consent to participate in this study was provided by the participants' legal guardian/next of kin.

AUTHOR CONTRIBUTIONS

WL and RZ came up with the idea. RZ and WL designized the experiment and modified the final manuscript. WL collected the data and prepared the draft.

FUNDING

This work was supported, in part, by the 2019 Postgraduate Research & Practice Innovation Program of Jiangsu Province (KYCX19_0025), the Key Project of Philosophy and Social Science Research in Colleges and Universities in Jiangsu Province (2015JDXM001), and NJU National Demonstration Base for Innovation and Entrepreneurship (SCJD0406).

REFERENCES

Amin, H. U., Malik, A. S., Kamel, N., Chooi, W. T., and Hussain, M. (2015). P300 correlates with learning and memory abilities and fluid intelligence. *J. Neuroeng. Rehabil.* 12:87. doi: 10.1186/s12984-015-0077-6

Colom, R., Flores-Mendoza, C., Quiroga, M. Á, and Privado, J. (2005). Working memory and general intelligence: the role of short-term storage. *Pers. Individ. Dif.* 39, 1005–1014. doi: 10.1016/j.paid.2005.03.020

Covey, T. J., Shucard, J. L., and Shucard, D. W. (2019). Working memory training and perceptual discrimination training impact overlapping and distinct neurocognitive processes: evidence from event-related potentials and transfer of training gains. *Cognition* 182, 50–72. doi: 10.1016/j.cognition.2018.08.012

Dong, S., Reder, L. M., Yao, Y., Liu, Y., and Chen, F. (2015). Individual differences in working memory capacity are reflected in different ERP and EEG patterns to task difficulty. *Brain Res.* 1616, 146–156. doi: 10.1016/j.brainres.2015.05.003

Engel De Abreu, P. M. J., Conway, A. R. A., and Gathercole, S. E. (2010). Working memory and fluid intelligence in young children. *Intelligence* 38, 552–561. doi: 10.1016/j.intell.2010.07.003

Engemann, D. A., Raimondo, F., King, J., Rohaut, B., Louppe, G., Faugeras, F., et al. (2018). Robust EEG-based cross-site and cross-protocol classification of states of consciousness. *Brain* 141, 3179–3192. doi: 10.1093/brain/awy251

Fawcett, T. (2006). An introduction to ROC analysis. *Pattern Recognit. Lett.* 27, 861–874. doi: 10.1016/j.patrec.2005.10.010

Gignac, G. E., Shankaralingam, M., Walker, K., and Kilpatrick, P. (2016). Short-term memory for faces relates to general intelligence moderately. *Intelligence* 57, 96–104. doi: 10.1016/j.intell.2016.05.001

Gordon, S., Todder, D., Deutsch, I., Garbi, D., Getter, N., and Meiran, N. (2018). Are resting state spectral power measures related to executive functions in healthy young adults? *Neuropsychologia* 108, 61–72. doi: 10.1016/j.neuropsychologia.2017.10.031

Gray, S., Green, S., Alt, M., Hogan, T., Kuo, T., Brinkley, S., et al. (2017). The structure of working memory in young children and its relation to intelligence. *J. Mem. Lang.* 92, 183–201. doi: 10.1016/j.jml.2016.06.004

Hand, D. J. (2009). Measuring classifier performance: a coherent alternative to the area under the ROC curve. *Mach. Learn.* 77, 103–123. doi: 10.1007/s10994-009-5119-5

Hillman, C. H., Pontifex, M. B., Motl, R. W., O'Leary, K. C., Johnson, C. R., Scudder, M. R., et al. (2012). From ERPs to academics. *Dev. Cogn. Neurosci.* 2, S90–S98. doi: 10.1016/j.dcn.2011.07.004

Hirsh, J. B., and Inzlicht, M. (2010). Error−related negativity predicts academic performance. *Psychophysiology* 47, 192–196. doi: 10.1111/j.1469-8986.2009.00877.x

Itthipuripat, S., Wessel, J. R., and Aron, A. R. (2013). Frontal theta is a signature of successful working memory manipulation. *Exp. Brain Res.* 224, 255–262. doi: 10.1007/s00221-012-3305-3

Julie, O., Arnaud, D., and Scott, M. (2005). Frontal midline EEG dynamics during working memory. *NeuroImage* 27, 341–356. doi: 10.1016/j.neuroimage.2005.04.014

Lijffijt, M., Lane, S. D., Meier, S. L., Boutros, N. N., Burroughs, S., Steinberg, J. L., et al. (2009). P50, N100, and P200 sensory gating: relationships with behavioral inhibition, attention, and working memory. *Psychophysiology* 46, 1059–1068. doi: 10.1111/j.1469-8986.2009.00845.x

Lotte, F., Congedo, M., Lécuyer, A., Lamarche, F., and Arnaldi, B. (2007). A review of classification algorithms for EEG-based brain–computer interfaces. *J. Neural Eng.* 4, R1–R13. doi: 10.1088/1741-2560/4/2/R01

Melby-Lervåg, M., Redick, T. S., and Hulme, C. (2016). Working Memory training does not improve performance on measures of intelligence or other measures of "Far Transfer". *Perspect. Psychol. Sci.* 11, 512–534. doi: 10.1177/1745691616635612

Missonnier, P., Deiber, M. P., Gold, G., Herrmann, F. R., Millet, P., Michon, A., et al. (2007). Working memory load–related electroencephalographic parameters can differentiate progressive from stable mild cognitive impairment. *Neuroscience* 150, 346–356. doi: 10.1016/j.neuroscience.2007.09.009

Missonnier, P., Gold, G., Herrmann, F. R., Fazio-Costa, L., Michel, J., Deiber, M., et al. (2006). Decreased theta event-related synchronization during working memory activation is associated with progressive mild cognitive impairment. *Dement. Geriatr. Cogn. Dis.* 22, 250–259. doi: 10.1159/000094974

Myers, N. E., Stokes, M. G., and Nobre, A. C. (2017). Prioritizing Information during working memory: beyond sustained internal attention. *Trends Cogn. Sci.* 21, 449–461. doi: 10.1016/j.tics.2017.03.010

Neubauer, A. C., and Fink, A. (2009). Intelligence and neural efficiency. *Neurosci. Biobehav. Rev.* 33, 1004–1023. doi: 10.1016/j.neubiorev.2009.04.001

Polich, J. (2007). Updating P300: an integrative theory of P3a and P3b. *Clin. Neurophysiol.* 118, 2128–2148. doi: 10.1016/j.clinph.2007.04.019

Qazi, E., Hussain, M., Aboalsamh, H., Malik, A. S., Amin, H. U., and Bamatraf, S. (2017). Single trial EEG patterns for the prediction of individual differences in fluid intelligence. *Front. Hum. Neurosci.* 10:687. doi: 10.3389/fnhum.2016.00687

Raghavachari, S., Kahana, M. J., Rizzuto, D. S., Caplan, J. B., Kirschen, M. P., Bourgeois, B., et al. (2001). Gating of human theta oscillations by a working memory task. *J. Neurosci.* 21, 3175–3183. doi: 10.1523/JNEUROSCI.21-09-03175.2001

Scharinger, C., Soutschek, A., Schubert, T., and Gerjets, P. (2017). Comparison of the working memory load in n-back and working memory span tasks by means of EEG frequency band power and P300 amplitude. *Front. Hum. Neurosci.* 11:6. doi: 10.3389/fnhum.2017.00006

Sitt, J. D., King, J., El Karoui, I., Rohaut, B., Faugeras, F., Gramfort, A., et al. (2014). Large scale screening of neural signatures of consciousness in patients in a vegetative or minimally conscious state. *Brain* 137, 2258–2270. doi: 10.1093/brain/awu141

Stewart, A. X., Nuthmann, A., and Sanguinetti, G. (2014). Single-trial classification of EEG in a visual object task using ICA and machine learning. *J. Neurosci. Methods* 228, 1–14. doi: 10.1016/j.jneumeth.2014.02.014

Tóth, B., Kardos, Z., File, B., Boha, R., Stam, C. J., and Molnár, M. (2014). Frontal midline theta connectivity is related to efficiency of WM maintenance and is affected by aging. *Neurobiol. Learn. Mem.* 114, 58–69. doi: 10.1016/j.nlm.2014.04.009

Tusch, E. S., Alperin, B. R., Ryan, E., Holcomb, P. J., Mohammed, A. H., and Daffner, K. R. (2016). Changes in neural activity underlying working memory after computerized cognitive training in older adults. *Front. Aging Neurosci.* 8:225. doi: 10.3389/fnagi.2016.00255

Unsworth, N., and Engle, R. W. (2007). On the division of short-term and working memory: an examination of simple and complex span and their relation to higher order abilities. *Psychol. Bull.* 133, 1038–1066. doi: 10.1037/0033-2909.133.6.1038

Unsworth, N., Fukuda, K., Awh, E., and Vogel, E. K. (2014). Working memory and fluid intelligence: capacity, attention control, and secondary memory retrieval. *Cogn. Psychol.* 71, 1–26. doi: 10.1016/j.cogpsych.2014.01.003

Wang, Q., Zhao, H. H., Chen, J. W., Gu, K. D., Zhang, Y. Z., Zhu, Y. X., et al. (2009). Adverse health effects of lead exposure on children and exploration to internal lead indicator. *Sci. Total Environ.* 407, 5986–5992. doi: 10.1016/j.scitotenv.2009.08.038

Wongupparaj, P., Sumich, A., Wickens, M., Kumari, V., and Morris, R. G. (2018). Individual differences in working memory and general intelligence indexed by P200 and P300: a latent variable model. *Biol. Psychol.* 139, 96–105. doi: 10.1016/j.biopsycho.2018.10.009

Wronka, E., Kaiser, J., and Coenen, A. M. L. (2013). Psychometric intelligence and P3 of the event-related potentials studied with a 3-stimulus auditory oddball task. *Neurosci. Lett.* 535, 110–115. doi: 10.1016/j.neulet.2012.12.012

Zhang, D., Zhao, H., Bai, W., and Tian, X. (2016). Functional connectivity among multi-channel EEGs when working memory load reaches the capacity. *Brain Res.* 1631, 101–112. doi: 10.1016/j.brainres.2015.11.036

Zhang, H., Chang, L., Chen, X., Ma, L., and Zhou, R. (2018). Working memory updating training improves mathematics performance in middle school students with learning difficulties. *Front. Hum. Neurosci.* 12:154. doi: 10.3389/fnhum.2018.00154

Conflict of Interest: The authors declare that the research was conducted in the absence of any commercial or financial relationships that could be construed as a potential conflict of interest.

frontiers in Behavioral Neuroscience

ORIGINAL RESEARCH
published: 04 February 2020
doi: 10.3389/fnbeh.2020.00003

Effects of Limited and Extended Pavlovian Training on Devaluation Sensitivity of Sign- and Goal-Tracking Rats

Sara E. Keefer[1], *Sam Z. Bacharach*[1,2], *Daniel E. Kochli*[1], *Jules M. Chabot*[3] *and Donna J. Calu*[1,2]*

[1]Department of Anatomy and Neurobiology, University of Maryland School of Medicine, Baltimore, MD, United States, [2]Program in Neuroscience, University of Maryland School of Medicine, Baltimore, MD, United States, [3]Neuroscience and Behavior Program, Wesleyan University, Middletown, CT, United States

OPEN ACCESS

Edited by:
Jee Hyun Kim,
Florey Institute of Neuroscience and Mental Health, Australia

Reviewed by:
Paul Meyer,
University at Buffalo, United States
Laura Bradfield,
University of Technology Sydney, Australia

***Correspondence:**
Donna J. Calu
dcalu@som.umaryland.edu

Specialty section:
This article was submitted to Motivation and Reward, a section of the journal Frontiers in Behavioral Neuroscience

Received: *08 November 2019*
Accepted: *07 January 2020*
Published: *04 February 2020*

Citation:
Keefer SE, Bacharach SZ, Kochli DE, Chabot JM and Calu DJ (2020) Effects of Limited and Extended Pavlovian Training on Devaluation Sensitivity of Sign- and Goal-Tracking Rats. Front. Behav. Neurosci. 14:3. doi: 10.3389/fnbeh.2020.00003

Individual differences in Pavlovian approach predict differences in devaluation sensitivity. Recent studies indicate goal-tracking (GT) rats are sensitive to outcome devaluation while sign-tracking (ST) rats are not. With extended training in Pavlovian lever autoshaping (PLA), GT rats display more lever-directed behavior, typical of ST rats, suggesting they may become insensitive to devaluation with more Pavlovian training experience. Here, we use a within-subject satiety-induced outcome devaluation procedure to test devaluation sensitivity after limited and extended PLA training in GT and ST rats. We trained rats in PLA to determine GT and ST groups. Then, we sated rats on either the training pellets (devalued condition) or homecage chow (valued condition) prior to brief non-reinforced test sessions after limited (sessions 5/6) and extended (sessions 17/18) PLA training. GT rats decreased conditioned responding under devalued relative to valued conditions after both limited and extended training, demonstrating they are sensitive to satiety devaluation regardless of the amount of PLA training. While ST rats were insensitive to satiety devaluation after limited training, their lever directed behavior became devaluation sensitive after extended training. To determine whether sign-tracking rats also displayed sensitivity to illness-induced outcome devaluation after extended training, we trained a separate cohort of rats in extended PLA and devalued the outcome with lithium chloride injections after pellet consumption in the homecage. ST rats failed to decrease conditioned responding after illness-induced outcome devaluation, while Non-ST rats (GT and intermediates) were sensitive to illness-induced outcome devaluation after extended training. Together, our results confirm devaluation sensitivity is stable in GT rats across training and devaluation approaches. Extended training unmasks devaluation sensitivity in ST rats after satiety, but not illness-induced devaluation, suggesting ST rats respond appropriately by decreasing responding to cues during state-dependent but not inference-based devaluation.

The differences in behavioral flexibility across tracking groups and devaluation paradigms have translational relevance for the understanding state- vs. inference-based reward devaluation as it pertains to drug addiction vulnerability.

Keywords: behavioral flexibility, goal-tracking, sign-tracking, outcome devaluation, pavlovian incentive learning, reward

INTRODUCTION

Pavlovian lever autoshaping (PLA) unveils distinct sign- and goal-tracking behaviors in rats. In this task, the insertion and retraction of a Pavlovian lever cue predicts food reward delivery. Rats are not required to interact with the lever; yet, sign-tracking (ST) rats preferentially approach and interact with the lever, while goal-tracking (GT) rats approach the food cup (Hearst and Jenkins, 1974; Boakes, 1977; Flagel et al., 2007). Studies suggest that ST and GT rats vary in the extent to which they attribute incentive motivational properties of cues (Flagel and Robinson, 2017). The lever cue is more attracting and reinforcing to ST than GT, and both natural and drug-associated cues invigorate instrumental responses to a greater degree in ST than GT, resulting in greater cue-induced relapse to drug-seeking (Tomie, 1996; Robinson and Flagel, 2009; Saunders and Robinson, 2010, 2013; Meyer et al., 2012; Yager and Robinson, 2013; Yager et al., 2015; Versaggi et al., 2016; Villaruel and Chaudhri, 2016). Sign-tracking in rats also predicts heightened drug relapse despite having to traverse an electrified barrier to seek and take drugs (Saunders and Robinson, 2013). We and others have shown that even prior to the drug experience, sign-trackers are inflexible, continuing to respond to cues when associated outcomes are devalued (Morrison et al., 2015; Nasser et al., 2015; Smedley and Smith, 2018). In contrast, goal-trackers flexibly adapt after outcome devaluation and are less susceptible to drug relapse when punishment is imposed (Saunders and Robinson, 2013; Nasser et al., 2015). Sign- and goal-tracking differences in adaptive behavior evident prior to and after drug experience highlight the utility of the sign- and goal-tracking model for understanding addiction vulnerability. Despite the trait-like qualities often attributed to ST and GT, we and others have observed a shift towards lever-directed behaviors in GT rats with extended PLA training (Villaruel and Chaudhri, 2016; Bacharach et al., 2018). The increased lever approach observed in GT rats leads to our prediction that behavior of GT rats will become devaluation insensitive as they shift towards sign-tracking behaviors.

Several studies reveal a dichotomy between GT and ST behaviors in devaluation sensitivity. Outcome devaluation by lithium chloride (LiCl)-induced conditioned taste aversion (CTA) decreases conditioned responding in GT and intermediate rats, while failing to reduce conditioned responding in ST rats (Nasser et al., 2015). The failure of ST to appropriately reduce responding to cues after devaluation is evident after both after light-food and lever-food Pavlovian conditioning (Morrison et al., 2015; Nasser et al., 2015). Satiety-induced devaluation similarly results in the flexibility of goal-tracking, but not sign-tracking behaviors in rats (Patitucci et al., 2016) and humans (De Tommaso et al., 2017). In contrast, sign-tracking behaviors are sensitive to satiety and illness-induced devaluation in other studies (Cleland and Davey, 1982; Derman et al., 2018). The differences in sign-tracking devaluation sensitivity between studies may be due to differences in the amount of training prior to devaluation procedures. Insensitivity to devaluation has been observed in ST rats after limited training [<10 training sessions; (Morrison et al., 2015; Nasser et al., 2015)], and some studies using extended training prior to devaluation [>10 training sessions; (Patitucci et al., 2016; Smedley and Smith, 2018)]. Yet other studies using extended training prior to devaluation report devaluation sensitivity of lever directed behaviors generally, and in ST rats specifically (Cleland and Davey, 1982; Derman et al., 2018). Regarding goal-tracking behaviors, Pavlovian food cup directed behavior remains sensitive to devaluation, independent of the amount of training (Holland, 1998). Together, these studies suggest the observed tracking-related differences in devaluation sensitivity may be experience dependent. Here, we sought to determine how the amount of Pavlovian training influences devaluation sensitivity in sign- and goal-tracking rats.

We have previously shown GT, but not ST, rats are sensitive to LiCl-induced outcome devaluation (Nasser et al., 2015). However, this procedure results in permanent CTA, which would limit our ability to test whether extended training causes GT rats to become devaluation insensitive as they shift towards sign-tracking behaviors. Thus, in Experiment 1, we tested the same GT and ST rats on satiety-specific outcome devaluation after limited (five sessions of training) and after extended PLA (>15 sessions of training). First, we sought to determine whether sating rats on the outcome associated with the Pavlovian lever cue would also produce devaluation sensitivity in GT rats, but not ST rats, after limited training. Next, we continued to train the rats in PLA to the point that GT rats display more ST than GT behaviors. After GT rats shifted towards lever-directed behavior, we tested all rats again in satiety-specific outcome devaluation. We predicted that GT rats would be sensitive to devaluation after limited training but become devaluation insensitive after extended training when they shift towards sign-tracking behaviors. This outcome would suggest the behavioral flexibility observed in GT rats might not reflect a stable trait, instead providing evidence for experience-dependent variation in flexibility. If instead, GT and ST rats remain consistent in their devaluation sensitivity after both limited and extended training, this would suggest that behavioral flexibility differences reflect stable GT and ST trait differences.

To extend our previous study that used illness-induced outcome devaluation, and to compare the results of Experiment 1 with prior PLA devaluation studies (Cleland and Davey, 1982; Morrison et al., 2015; Nasser et al., 2015; Derman et al., 2018), in Experiment 2 we examined devaluation sensitivity using LiCl-induced outcome devaluation after extended training. Devaluation by satiation tests rats while they are in a sated state and probes approach immediately after *ad libitum* consumption of the training pellet, which requires little to no inference about the current value of the outcome. The illness-induced outcome devaluation procedure we use, instead, probes approach in a distinct context from and days after the last pairing of training pellets and illness. Thus, our illness-induced devaluation procedure requires that rats adjust responding to the lever cue based on inference about the current value of the outcome. The outcome of the two experiments allowed us to determine whether GT and ST groups differ in devaluation sensitivity based on how they respond in (1) a sated state during test and (2) an inference-based state during test, temporally and contextually distinct from taste aversion.

MATERIALS AND METHODS

Subjects

Male Long–Evans rats (Charles Rivers Laboratories, Wilmington, MA, USA; 250–275 g upon arrival; Experiment 1, n = 48 run as two separate cohorts; Experiment 2, n = 38 run as one cohort) were double housed and maintained on a 12 h light/dark cycle (lights on at 07:00). All behavioral training and testing were conducted during the light phase of the cycle. During acclimation, rats had *ad libitum* access to standard laboratory chow and water. After acclimation, rats were singly housed, food-restricted, and maintained at ∼90% of their baseline body weight throughout the experiment. All behavioral experiments were performed in accordance to the "Guide for the Care and Use of Laboratory Animals" (8th edition, 2011, US National Research Council) and were approved by the University of Maryland, School of Medicine Institutional Animal Care and Use Committee (IACUC).

Apparatus

Behavioral experiments were conducted in identical behavioral chambers (25 × 27 × 30 cm; Med Associates) located in a room different than the colony room. Each chamber was in an individual sound-attenuating cubicle with a ventilation fan. During PLA and devaluation probe tests, each chamber had one red house light (6 W) located at the top of the wall that was illuminated for the duration of each session. The opposite wall of the chamber had a recessed food cup (with photo beam detectors) located 2 cm above the grid floor. The food cup had an attached programmed pellet dispenser to deliver 45 mg food pellets (catalog# 1811155; Test Diet Purified Rodent Tablet (5TUL); protein 20.6%, fat 12.7%, carbohydrate 66.7%). One retractable lever was positioned on either side of the food cup, counterbalanced between subjects, 6 cm above the floor. Sessions began with the illumination of the red house light and lasted ∼26 min.

Experiment 1: Satiety-Induced Outcome Devaluation

Limited and Extended Pavlovian Lever Autoshaping

A summary of our experimental design can be found in **Figure 1A**. Prior to behavioral training, we exposed rats to a single 26 min magazine training session to reduce the novelty of the context and unconditioned stimuli. This session consisted of 25 trials in which two 45 mg pellets [Testdiet pellets (5TUL)] were delivered (0.5 s apart) on a VI 60 s schedule (50–70 s). The following day, we trained rats on daily, 26 min PLA sessions. Each session consisted of 25 presentations of a lever conditioned stimulus (CS+) occurring on a VI 60 s schedule (50–70 s). For each trial, the retractable lever was inserted for 10 s, then retracted, which was immediately followed with the delivery of two food pellets into the food cup, independent of contact with the lever or food cup. Following each training session, chow was provided to maintain rats at 90% of *ad libitum* body weight, and rats were transported back to the colony room.

Satiety-Induced Outcome Devaluation Procedures

As indicated in **Figure 1A**, after the 5th and 17th sessions of PLA, we gave rats two rounds of satiety-induced outcome devaluation tests. We sated half the rats by providing *ad libitum* access to the Testdiet training pellets (devalued condition), and the other half received standard chow (valued condition) in pre-habituated ceramic ramekins for 1 h in their homecage. Immediately, following consumption, we transported rats to the behavioral chambers for a 10 min lever autoshaping probe test under extinction conditions. Each probe test consisted of 10 presentations of the 10 s lever conditioned stimulus (VI 60 s, 50–70 s). After a day of rest, we retrained rats in a single reinforced PLA session. The next day we sated rats on the opposite condition (pellet or chow) prior to lever autoshaping probe test under extinction conditions. After extended PLA autoshaping (**Figure 1A**), we used identical procedures in the second round of satiety induced devaluation (pellet and chow). Notably, satiety conditions were reversed such that rats pre-fed on chow followed by pellets during limited testing received pellets followed by chow during extended testing and vice versa. This within-subject testing allowed us to measure responding in lever autoshaping during a sated state, either to the pellet outcome specifically associated with the lever (devalued) or generally sated on standard chow (valued) across conditioning.

Consumption Test of Specific Satiety

To confirm satiety was specific to the outcome on which rats were pre-fed, we gave one cohort a food choice test after all outcome devaluation testing was completed (cohort 1, n = 36; GT: n = 9; INT: n = 11; ST: n = 16). We provided rats with *ad libitum* access to either the training pellets or chow, counterbalanced for order, in ceramic ramekins for 1 h. Food was removed and replaced with two ceramic ramekins, one with 10 g of pellets and one with 10 g of chow for 30 min, after which we measured consumption of both outcomes. Two days later, we tested rats again after satiety with the opposite outcome.

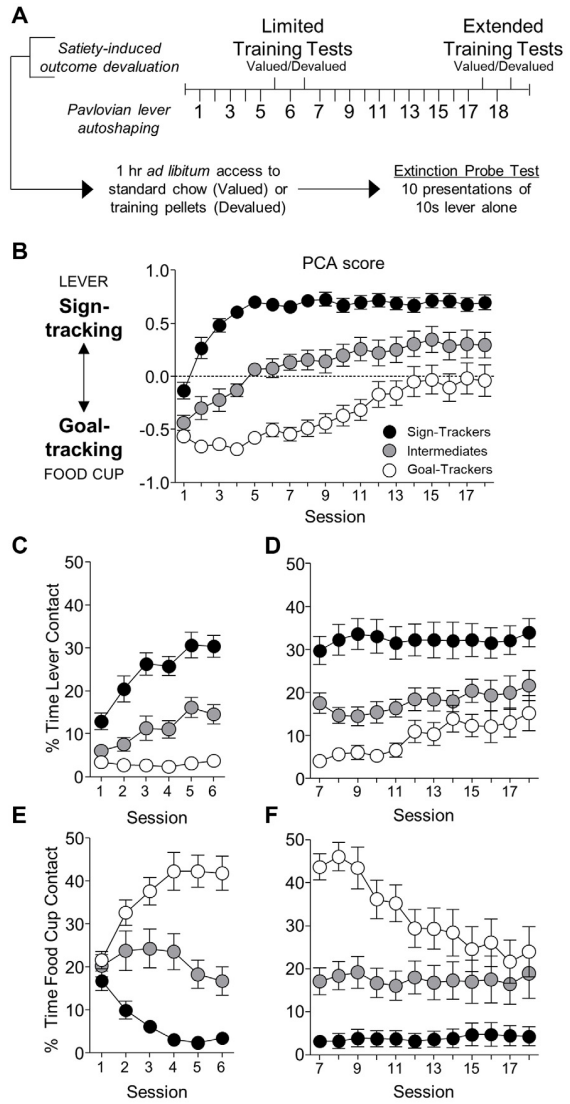

FIGURE 1 | Experiment 1: lever- and food cup-directed behaviors during Pavlovian lever autoshaping (PLA). **(A)** Experimental timeline. We trained rats for five daily reinforced PLA sessions (1–5) to determine their tracking groups. We then tested rats using a within-subject satiety-induced outcome devaluation procedure after limited training. On test days we gave rats 1 h *ad libitum* access to standard chow (valued) or training pellets (devalued), counterbalanced, prior to 10 min probe tests that consisted of 10 CS presentations under extinction conditions. Between tests, we gave one reinforced PLA session. We gave rats 11 more reinforced PLA (7–17) sessions and repeated identical satiety-induced devaluation testing after extended training. **(B–F)** Data are mean ± standard error of the mean (SEM) for Pavlovian Conditioned Approach (PCA) scores **(B)**, percentage of time contacting the lever for limited **(C)** and extended PLA **(D)**, and percentage of time contacting the food cup for limited **(E)** and extended PLA **(F)**.

Experiment 2: Illness-Induced Outcome Devaluation

Extended Pavlovian Lever Autoshaping

We trained a separate cohort of rats through extended (17 sessions) training in PLA (**Figure 4**) prior to illness-induced devaluation. Magazine training and extended autoshaping were identical to Experiment 1, except rats were tested only after extended PLA training and not after limited training.

Conditioned Taste Aversion Training

After extended PLA, we devalued the training pellets using a CTA procedure that took place in rats' homecages over 4 days. Matching groups based on rats' lever and food cup directed behavior during training, we divided rats into devalued (n = 19 pellet/LiCl paired) and valued (n = 19 pellet/LiCl unpaired) groups. Prior to the CTA procedure, we habituated all rats to the ceramic ramekins used to present the food pellets during CTA. On days 1 and 3 of CTA, we gave devalued rats 10 min access to 100 pellets in ceramic ramekins in their homecage followed immediately by lithium chloride (LiCl) injection (0.3 M, 5 ml/kg, i.p.), while we gave valued rats only the LiCl injection. On days 2 and 4, we gave valued rats 10 min access to 100 pellets in ceramic ramekins in their homecage, while devalued rats received no treatment. Across 4 days of CTA, we exposed all rats to training pellets and LiCl-induced gastric malaise; however, only the devalued group experienced pairings of training pellets with illness, while the valued group received explicit temporal separation of the training pellets and illness. We gave all rats standard homecage chow based on 90% body weight with compensation for CTA pellet consumption ∼6 h after pellet and/or injections each day to prevent association of LiCl-induced illness with homecage chow.

Outcome Devaluation Probe Test

After the last day of CTA procedure, we conducted an outcome devaluation test under extinction conditions (**Figure 4A**). This 10 min lever autoshaping probe test consisted of 10 presentations of the 10 s lever conditioned stimulus (VI 60 s, 50–70 s) with no pellet delivery, identical to the probe test in Experiment 1. Approximately 3 h after the probe test, we gave rats a pellet consumption test in the conditioning chambers to assess generalization of the CTA from the homecage to conditioning chamber. We gave rats 10 min access to 50 training pellets that were placed in the magazine of the chambers, and we recorded the number of pellets consumed. The following day we confirmed CTA to the pellets in the homecages. We gave all rats 10 min access to 100 pellets in the ramekins in their homecage and recorded the number of pellets consumed.

Behavioral Measurements

During the PLA and devaluation probe tests, we collected and recorded four behavioral measurements during the 10 s CS (lever) period. For both food cup contacts and lever contacts, the total number of contacts and total duration of response (% time) were automatically recorded for all sessions. The latencies to first contact the lever and food cup during the CS for each trial were also automatically recorded. On trials in which contact did not occur, a latency of 10 s was recorded. For each session the lever or food cup probabilities were calculated by determining the number of trials that the lever or food cup response was made, divided by the total number of trials in the session.

TABLE 1 | Repeated measures ANOVAs for Pavlovian lever autoshaping across all tracking groups.

Effect	Degrees of Freedom	Lever							
		Contact		Count		Latency		Probability	
		F	*p*	*F*	*p*	*F*	*p*	*F*	*p*
Session	(17,765)	26.61	<0.001	14.35	<0.001	50.13	<0.001	24.20	<0.001
Tracking Group	(2,45)	17.22	<0.001	27.42	<0.001	12.99	<0.001	13.40	<0.001
Session × Tracking group	(34,765)	1.60	0.017	1.75	0.005	4.55	<0.001	4.91	<0.001

Effect	Degrees of Freedom	Food Cup								PCA	
		Contact		Counts		Latency		Probability		Counts	
		F	*p*	*F*	*p*	*F*	*p*	*F*	*p*	*F*	*p*
Session	(17,765)	0.40	0.99	4.74	<0.001	17.00	<0.001	15.85	<0.001	36.75	<0.001
Tracking Group	(2,45)	22.29	<0.001	33.24	<0.001	33.85	<0.001	31.90	<0.001	52.82	<0.001
Session × Tracking group	(34,765)	2.68	<0.001	5.86	<0.001	5.03	<0.001	4.84	<0.001	4.83	<0.001

We used a Pavlovian Conditioned Approach (PCA) analysis (Meyer et al., 2012) to determine sign-, goal- and intermediate tracking groups. The PCA score quantifies the variation between lever-directed (sign tracking) and food cup-directed (goal tracking) behaviors. Each rat's PCA score is the average of three difference score measures (each ranging from −1.0 to +1.0) including: (1) preference score; (2) latency score; and (3) probability score. The preference score is the duration of lever contacts during the CS minus the duration of food cup contacts during the CS, divided by the sum of these two measures. The latency score is the average latency to make a food cup contact during the CS minus the latency to lever contact during the CS, divided by the duration of the CS (10 s). The probability score is the probability of a lever contact minus the probability of a food cup contact observed across trials in the session. We determined tracking groups by averaging PCA scores during training sessions 4 and 5. Sign-tracking PCA scores range from +0.33 to +1.0, goal-tracking PCA scores range from −0.33 to −1.0, and intermediate group PCA scores range from −0.32 to +0.32.

For the devaluation tests, we examined total behavior, which is the sum of food cup and lever contacts during the 10 s CS period, and we also present these measures separately. We also examined preferred responding—food cup contact for goal-trackers and lever contact for sign-trackers. To account for differences in number of lever and food cup contacts, we examined rats' preferred responding during valued relative to devalued conditions using the following equations: valued preferred responding index = valued preferred responding/(valued + devalued preferred responding) and devalued preferred responding index = devalued preferred responding/(valued + devalued preferred responding). A preferred responding index of 0.5 reflects similar responses during valued and devalued conditions.

We recorded the amount (in grams) of pellets and chow consumed during the hour of satiety prior to all outcome devaluation probe tests and during all the choice consumption tests. For illness-induced devaluation procedures, we recorded the total number of pellets consumed during the CTA procedures and test sessions.

Statistical Analysis

Data were analyzed using SPSS statistical software (IBM v.25) with mixed-design repeated-measures ANOVAs. Significant main effects and interactions ($p < 0.05$) were followed by *post hoc* paired samples or independent *t*-tests when applicable. The between- and within-subject factors and dependent measures within each statistical analysis are described in the corresponding results section.

RESULTS

Experiment 1: Satiety-Induced Devaluation

Pavlovian Lever Autoshaping

We first examined how lever- and food cup- directed behaviors change across training in sign-, goal-, and intermediate tracking rats. The experimental timeline is shown in **Figure 1A**. In **Table 1** we summarize mixed ANOVA (Tracking × Session) main effects and interactions from lever autoshaping training session analyses for each composite measure that makes up the PCA score. In summary, the PCA scores for reinforced lever autoshaping sessions 1–18 are shown for three tracking groups in **Figure 1B**. Notably, we observed a significant main effect of Session ($F_{(17,765)} = 36.75$, $p < 0.001$) and a Tracking by Session interaction for PCA scores (**Figure 1B**; $F_{(34,765)} = 4.84$, $p < 0.001$), indicating that the behavior of sign-, goal-, and intermediate tracking rats is differentially affected by experience in lever autoshaping. When looking specifically in sign-tracking (ST) rats, lever directed behavior emerged during training sessions 1–6 (**Figure 1C**, **Supplementary Table S1**), indicated by a main effect of Session (ST lever; $F_{(5,90)} = 14.18$, $p < 0.001$), and like all other behaviors measured, remained remarkably stable across extended training sessions 7–18 (**Figure 1D**, **Supplementary Table S2**, *F*'s < 1.5, *p*'s > 0.1). Goal-trackers' (GT) food cup behavior increased across training sessions 1–6 (**Figure 1E**, **Supplementary Table S1**), indicated by a main effect of Session (GT food cup; $F_{(5,70)} = 12.06$, $p < 0.001$). As extended training sessions 7–18 progressed, GT rats spent more time engaged with the lever (GT lever, Session main effect; $F_{(11,154)} = 4.55$,

$p < 0.001$; **Figure 1D**), and less time at the food cup (GT food cup, Session main effect; $F_{(11,154)} = 13.20$, $p < 0.001$; **Figure 1F**). This shift is confirmed by analysis in GT rats, including Response (lever, food cup) and Session (7–18) as factors, for which the critical interaction ($F_{(11,154)} = 11.93$, $p < 0.001$) indicates that GT rats' shift towards lever-directed responding and away from food cup responding during extended training (**Supplementary Table S2**). This shift during extended lever autoshaping is also evident in analysis of GT's positive shift in PCA scores during sessions 7–18 (Session: $F_{(11,154)} = 10.24$, $p < 0.001$; **Figure 1B**), and each of the PCA composite measures summarized in **Supplementary Table S2**, including slower latency to first food cup contact (**Supplementary Figure S1A**), faster latency to first lever contact (**Supplementary Figure S1B**), reduced food cup contact probability (**Supplementary Figure S1C**), and increased lever contact probability (**Supplementary Figure S1D**). GT's shift towards sign-tracking is consistent with our previous report (Bacharach et al., 2018). The analyses of approach behavior in intermediate (INT) rats are reported in **Supplementary Materials**.

Devaluation Tests

Next, we investigated the effects of limited and extended lever autoshaping training on satiety-induced outcome devaluation in GT and ST rats. After replicating our prior observation that GT rats shift towards sign-tracking responses with extended training, we set out to test our *a priori* hypothesis that extended training would make GT rats devaluation insensitive. The primary predictions for GT rats are (1) with limited training, GT rats are devaluation sensitive, replicating effects we and others have previously reported (Morrison et al., 2015; Nasser et al., 2015; Patitucci et al., 2016) and (2) with extended training, GT become devaluation insensitive. Based on prior reports of devaluation insensitivity in ST rats, we hypothesized that after both limited and extended training ST rats would be insensitive to devaluation. To directly test these two *a priori* hypotheses, we separately examined satiety-induced outcome devaluation effects in GT and ST rats.

GT Show Devaluation Sensitivity After Limited and Extended Training in Lever Autoshaping

Devaluation performance for GT rats after limited and extended training is shown in **Figures 2A–C**. Due to GT rats' shift in approach from food cup to lever across conditioning, we first examined effects of satiety devaluation on total approach behavior (sum of lever and food cup contacts) using repeated-measures ANOVA with factors of Phase (limited, extended) and Devaluation Condition (valued, devalued). This revealed a main effect of Devaluation ($F_{(1,14)} = 27.96$, $p < 0.001$), expressed as a difference in total approach behavior between the valued and devalued condition during limited ($p = 0.019$) and extended ($p = 0.006$) tests (**Figure 2A**). Based on our consistent observation that GT shift from primarily food-cup behaviors to increasingly more lever directed behavior during extended training (**Figure 1**, **Supplementary Figure S1**; Bacharach et al., 2018), we sought to examine the devaluation sensitivity of each approach response across conditioning. We incorporated Response (lever, food cup) factor into the analysis above maintaining devaluation effect reported above and revealing a marginally significant

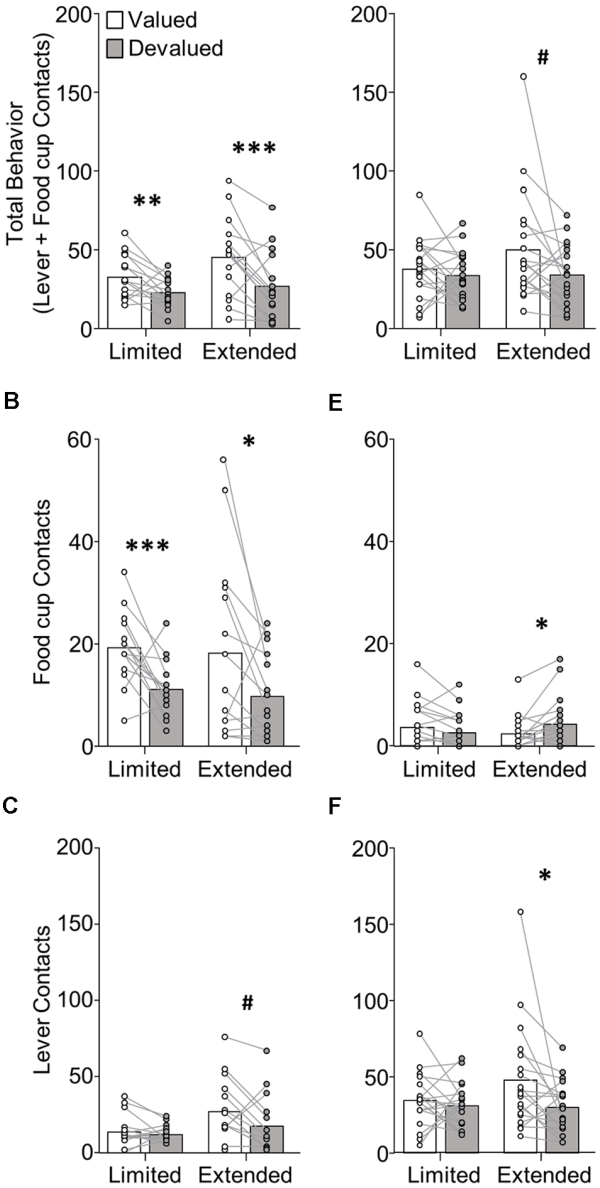

FIGURE 2 | Experiment 1: performance during satiety-induced outcome devaluation probe test. Data show mean and individual data points for performance on devaluation probe test by goal-trackers (left column) and sign-trackers (right column), classified based on PCA scores after limited training. **(A–C)** Goal-trackers' approach under valued (white bars) and devalued (gray bars) conditions during limited and extended satiety-induced outcome devaluation tests for **(A)** total behavior (sum of lever and food cup contacts), **(B)** food cup contacts, and **(C)** lever contacts. **(D–F)** Sign-trackers' approach under valued (white bars) and devalued (gray bars) conditions during limited and extended satiety-induced outcome devaluation tests for **(A)** total behavior (sum of lever and food cup contacts), **(B)** food cup contacts, and **(C)** lever contacts. $^{\#}p = 0.051$, $^{*}p < 0.05$, $^{**}p < 0.025$, $^{***}p < 0.01$.

Phase by Response interaction ($F_{(1,14)}$ = 3.80, p = 0.072). These results suggest that GT rats maintain devaluation sensitivity throughout training. We aimed to confirm that the effects of devaluation were evident in both food cup and the lever approach. Analysis of food cup contacts alone in GT rats revealed main effect of Devaluation ($F_{(1,14)}$ = 20.39, $p < 0.001$), and *post hoc*'s confirmed devaluation sensitivity of food cup contacts during the limited ($t_{(14)}$ = 3.713, p = 0.002) and extended tests ($t_{(14)}$ = 2.305, p = 0.037; **Figure 2B**). Analysis of lever contacts alone in GT rats revealed a marginal main effect of Phase ($F_{(1,14)}$ = 4.28, p = 0.058) but no interaction ($F < 2.1$, $p > 0.1$), with *post hoc*'s confirming marginal devaluation sensitivity of lever approach only after extended training ($t_{(14)}$ = 2.134, p = 0.051; **Figure 2C**). These results suggest that despite a shift in response from food cup to lever directed behavior across conditioning, GT rats use the current value of the outcome to flexibly guide both forms of approach.

ST Show Devaluation Sensitivity Only After Extended Training in Lever Autoshaping

Devaluation performance for ST rats after limited and extended training is shown in **Figures 2D–F**. We examined the effects of satiety devaluation on total approach behavior using repeated-measures ANOVA with factors of Phase (limited, extended) and Devaluation (valued, devalued). This revealed marginal main effects of Devaluation ($F_{(1,18)}$ = 3.92, p = 0.063) and Phase ($F_{(1,18)}$ = 4.15, p = 0.057). *Post hoc* analysis revealed a marginal devaluation sensitivity in ST only after extended training (p = 0.051). We incorporated Response (lever, food cup) factor into the analysis above and found a Response by Devaluation interaction ($F_{(1,18)}$ = 4.61, p = 0.046) and a Phase by Response by Devaluation interaction ($F_{(1,18)}$ = 5.15, p = 0.036), suggesting devaluation sensitivity in ST is carried by a specific response and varies based on the extent of training. *Post hoc* analyses revealed that after extended training ST rats respond more at the lever during valued relative to devalued tests ($t_{(18)}$ = 2.277, p = 0.035; **Figure 2F**), suggesting that lever responding becomes more sensitive to devaluation with extended training. While there is very little food cup responding in ST rats, we observed a devaluation effect in the opposite direction for food cup contacts during the extended test (devalued > valued, p = 0.026; **Figure 2E**), which may account for the marginally significant devaluation sensitivity of ST when examining total approach behavior. Overall, these results suggest ST rats that are insensitive to devaluation after limited training become more sensitive to devaluation after extended Pavlovian training. This emerging devaluation sensitivity in ST rats is specific to lever responding.

Intermediates

The analyses up to this point were based on our *a priori* hypotheses about GT and ST rats. We also analyzed devaluation test data for intermediate rats that approach the food cup and lever at comparable levels (**Supplementary Figure S2**). We present parallel analyses on intermediate rats' devaluation test data in the **Supplemental Materials**. Intermediate data is also included in the next analysis that compares devaluation sensitivity considering tracking group reclassification after extended training.

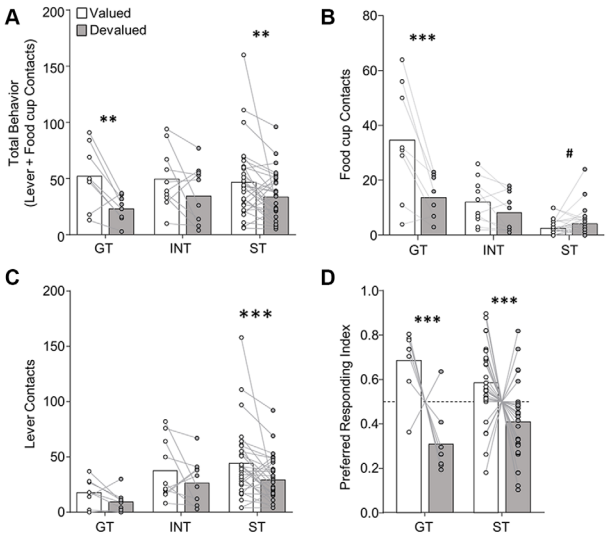

FIGURE 3 | Experiment 1: performance during extended satiety-induced outcome devaluation probe test after reclassification of tracking groups based on PCA scores after extended training. Data show mean and individual data points. **(A)** Approach for reclassified GT, INT and ST under valued (white bars) and devalued (gray bars) conditions during extended satiety-induced outcome devaluation tests for **(A)** total behavior (sum of lever and food cup contacts), **(B)** food cup contacts, and **(C)** lever contacts. **(D)** Preferred responding index during valued relative to devalued conditions for goal-trackers (food cup contact) and sign-trackers (lever contact). Valued preferred responding index = valued preferred responding/(valued + devalued preferred responding). Devalued preferred responding index = devalued preferred responding/(valued + devalued preferred responding). A Preferred responding index value of 0.5 reflects similar responses during valued and devalued conditions. $^{\#}p$ = 0.056, $^{**}p < 0.025$, $^{***}p < 0.01$.

Devaluation Sensitivity After Extended Training Accounting for Tracking Group Shifts

In the interest of comparing our results with that of prior studies, we analyzed the extended devaluation test data after reclassification of tracking group due to the shift in PCA scores that occurred during extended training (**Figure 3**). We calculated PCA scores for session 17, which was the last session of training prior to extended devaluation testing and resulted in 8 GT, 10 INT, and 30 ST. We analyzed the approach behavior during extended devaluation tests using a repeated-measures ANOVA including between-subject factor of Tracking group (GT, INT, ST) and within-subject factors of Devaluation (valued, devalued) and Response (lever, food cup). We observed a main effect of Devaluation ($F_{(1,45)}$ = 15.58, $p < 0.001$), and a Devaluation by Response by Tracking group interaction ($F_{(2,45)}$ = 3.41, $p < 0.05$). *Post hoc* analysis revealed reclassified GT rats were devaluation sensitive on food cup contacts ($t_{(7)}$ = 3.80, $p < 0.01$; **Figure 3B**) and reclassified ST were devaluation sensitive on lever contacts ($t_{(29)}$ = 2.77, $p < 0.01$; **Figure 3C**). When we analyzed the data with only reclassified GT and ST groups (excluding reclassified INT), we observed the same statistical

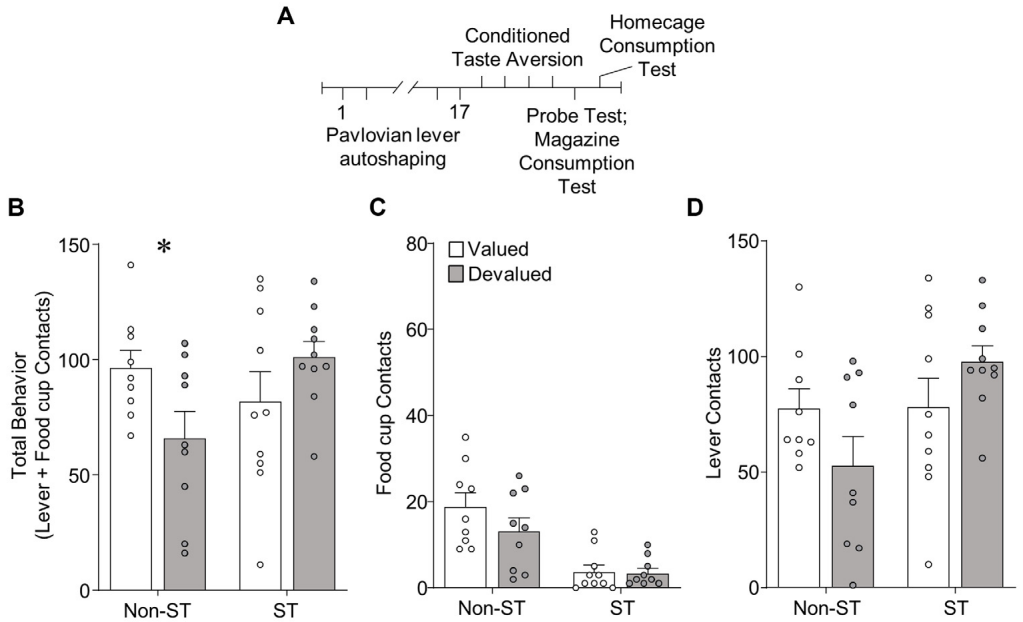

FIGURE 4 | Experiment 2: performance during illness-induced outcome devaluation probe test after extended PLA. **(A)** Experimental timeline. We trained rats on 17 sessions of PLA. We split rats into valued (unpaired) and devalued (paired) groups gave 4 days of conditioned taste aversion (CTA) training in the rats' homecages. After the last day of CTA, we conducted a 10 min probe test that consisted of 10 CS presentations under extinction conditions. Approximately 3 h after the probe test we gave rats 10 min access to 50 training pellets in the magazine of the conditioning chamber. The next day we gave rats 10 min access to 100 training pellets in their homecage to confirm CTA. **(B–D)** Effect of illness-induced devaluation on **(B)** total behavior (sum of lever and food cup contacts), **(C)** food cup contacts, and **(D)** lever contacts for Non-sign-tracking (Non-ST- made up of GT and INT rats) valued and devalued groups, left; and sign-tracking (ST) valued and devalued groups, right. Data are mean ± SEM and show individual data points. $^*p < 0.05$.

outcomes as reported above (same significant main effects and interactions). To eliminate the difference in response levels between GT and ST groups, we examined each rat's preferred response (GT food cup, ST lever) data for the late outcome devaluation test session (see figure legend and methods for preferred response index calculation; a value of 0.5 means rats responded equally during the valued and devalued tests). After extended training, we observed a main effect of Devaluation ($F_{(1,36)} = 17.29$, $p < 0.001$; **Figure 3D**), but no Devaluation by Tracking group interaction ($F < 2.5$, $p > 0.1$), confirming devaluation sensitivity of GT and ST after extended training. Altogether, Experiment 1 results suggest regardless of when tracking group classification occurs, GT rats are devaluation sensitive, and after extended training ST rats become sensitive to satiety-induced outcome devaluation.

Satiety and Devaluation Choice Test

Prior to the devaluation tests sessions, we found no difference in the amount of food consumed between tracking groups during the satiation hour ($F < 0.1$, $p > 0.8$). To confirm the devaluation of the sated food, we gave one cohort of rats a post-satiety choice test. Rats consistently chose to consume the food they were not sated on, as indicated by the main effect of Choice ($F_{(1,23)} = 356.62$, $p < 0.001$). There were no Tracking main effects ($F < 1.0$, $p > 0.4$) or Tracking by Choice interactions ($F < 1.0$, $p > 0.6$), indicating ST and GT rats had a similar preference for the non-sated food during choice test. Because the satiety procedures for devaluation and choice tests were identical, we infer that satiety conditions going into devaluation probe tests were equivalent for both tracking groups.

Experiment 2: Illness-Induced Outcome Devaluation

Pavlovian Lever Autoshaping

The experimental timeline is shown in **Figure 4A**. We gave rats 17 sessions of PLA followed by CTA training to the pellets and devaluation probe and consumption tests. The PCA scores for reinforced lever autoshaping sessions 1–17 are shown in **Supplementary Figure S3A**. Tracking group is based on PCA score classification during extended PLA session 17 to make our results more comparable to previous studies that examined illness-induced outcome devaluation after extended training. Similar to Experiment 1, we observed a significant main effect of Session ($F_{(16,576)} = 41.77$, $p < 0.001$) and a Tracking by Session interaction for PCA scores (**Supplementary Figure S3A**; $F_{(16,576)} = 6.97$, $p < 0.001$). We analyzed lever- and food cup-directed behaviors throughout PLA using repeated-measures ANOVA with a between-subject factor of Tracking group [Non-ST (GT and INT), ST] and within-subject factors of Response (lever, food cup) and Session (1–17; **Supplementary Figures S3B,C**). As expected, we observed a Response by Tracking group interaction ($F_{(1,36)} = 32.23$, $p < 0.001$), a

Response by Session interaction ($F_{(16,576)} = 15.01$, $p < 0.001$), and a Response by Session by Tracking group interaction ($F_{(16,576)} = 4.63$, $p < 0.001$), indicating that behavior of Non-ST (GT and INT) and ST rats is differentially affected by experience in lever autoshaping, similar to Experiment 1.

Devaluation Testing

In Experiment 2, we gave rats the same amount of extended PLA as in Experiment 1, before homecage LiCl-induced CTA procedures [devalued (paired), valued (unpaired)]. We examined approach in a single outcome devaluation test under extinction conditions. Outcome devaluation performance is shown in **Figure 4**. We analyzed devaluation total approach behavior using repeated measures ANOVA including between-subject factors of Tracking group [Non-ST (GT and INT), ST] and Devaluation (valued, devalued). We performed *post hoc* analysis based on a Devaluation by Tracking group interaction ($F_{(1,34)} = 6.22$, $p < 0.05$), which revealed Non-ST (GT and INT) rats were sensitive to devaluation ($t_{(16)} = 2.23$, $p < 0.05$; **Figure 4A**). In contrast, ST rats did not show sensitivity to devaluation on total behavior (p's > 0.1; **Figure 4A**). We present Non-ST and ST food cup and lever data in **Figures 4C,D**, respectively. Incorporating Response as a factor in the analysis revealed the expected main effect of Response ($F_{(1,34)} = 144.17$, $p < 0.001$), and Response by Tracking group interaction ($F_{(1,34)} = 10.05$, $p < 0.01$), which are mainly driven by the group assignments and a greater level of lever compared to food cup contacts. We did not observe a Devaluation by Response by Tracking group interaction ($F < 3.1$, $p > 0.05$), suggesting a specific response did not carry the devaluation difference between Non-ST and ST groups. Altogether, results suggest Non-ST rats' total approach behavior is sensitive to inference-based devaluation after extended training, consistent with our prior study (Nasser et al., 2015). In contrast, ST rats' total approach is devaluation insensitive, consistent with our prior results using inference-based homecage LiCl-induced devaluation (Nasser et al., 2015).

Conditioned Taste Aversion Training and Consumption Tests

To confirm CTA, we analyzed the CTA data using a mixed model repeated measures ANOVA with between-subject factors of Devaluation group (valued, devalued) and Tracking group [Non-ST (GT and INT), ST] and within-subject factor of Trial (1, 2). We found main effects of Devaluation group ($F_{(1,34)} = 38.07$, $p < 0.001$) and Trial ($F_{(1,34)} = 36.24$, $p < 0.001$) and a Trial by Devaluation group interaction ($F_{(1,34)} = 57.14$, $p < 0.001$). Critically, there were no main effects of nor interactions with the Tracking group (F's < 3.8, p's > 0.05; **Supplementary Figure S4A**), suggesting the devalued groups that received pellet-LiCl pairings, developed a CTA to the pellets with no difference between tracking groups.

On the same day of the devaluation probe test, we performed a pellet consumption test in the experimental chamber to confirm aversion to the pellets in the training context. Using an ANOVA with between-subjects factors of Devaluation group (valued, devalued) and Tracking group [Non-ST (GT and INT), ST], we observed the expected main effect of Devaluation ($F_{(1,34)} = 92.43$, $p < 0.001$), but no main effect of Tracking group or interaction (F's < 3.6, p's > 0.05; **Supplementary Figure S4B**). The following day we performed a post-probe homecage consumption test and analyzed consumption data using an ANOVA with between-subject factors of Devaluation (valued, devalued) and Tracking group [Non-ST (GT and INT), ST]. We also observed a main effect of Devaluation ($F_{(1,34)} = 714.86$, $p < 0.001$), but no main effect of Tracking group or interaction (F's < 3.5, p's > 0.1; **Supplementary Figure S4A**). The consumption data indicate successful and strong CTA to the training pellets in the devalued groups that readily transfer to the experimental chambers and, importantly, no differences between tracking groups. Additionally, these results confirm behavioral differences observed during the devaluation probe test reflect differences in inference-based devaluation and not a result of differences in CTA training.

DISCUSSION

Using a within-subject satiety-induced outcome devaluation procedure, we replicated our previous findings that after limited Pavlovian training, GT rats are sensitive to outcome devaluation while ST rats are not (Nasser et al., 2015). This tracking-specific devaluation sensitivity has replicated across several studies, Pavlovian paradigms, and devaluation procedures (Nasser et al., 2015; Patitucci et al., 2016; Smedley and Smith, 2018). As GT rats increased lever-directed and decreased food cup-directed behaviors across extended training, we expected their behavior to become inflexible during outcome devaluation, similar to ST rats. However, GT rats remained devaluation sensitive for both lever- and food cup-directed behaviors after extended training. ST rats' lever-directed behavior became sensitive to satiety-induced outcome devaluation after extended training in PLA. The results of Experiment 1 suggest GT rats remain behaviorally flexible, regardless of the amount of training, while ST rats become flexible with extended training. However, in Experiment 2, while a Non-ST group, made up of GT and intermediates rats, flexibly reduced approach after illness-induced outcome devaluation, ST rats inflexibly responded to lever cues after extended training. The differences in devaluation sensitivity of ST and Non-ST rats in Experiment 2 are consistent with our prior study using illness-induced outcome devaluation after limited training (Nasser et al., 2015).

The tracking-, training-, and devaluation procedure-dependent differences reported here may help to explain the inconsistencies in devaluation sensitivity of sign- and goal-tracking behaviors reported in prior studies. The strong influence of training duration is confirmed by the present within-subject measurement of satiety-induced devaluation sensitivity in ST rats. In Experiment 1, we found the same ST individuals that are insensitive early in training become sensitive to satiety devaluation with extended training. Conversely, we consistently find that ST rats are insensitive to illness-induced devaluation after limited Pavlovian conditioning (Nasser et al.,

2015), and extended PLA training (Experiment 2), consistent with studies from other labs (Morrison et al., 2015). Yet, other studies using illness-induced outcome devaluation find the lever approach to be devaluation sensitive, suggesting other procedural differences may account for contrasting findings (Cleland and Davey, 1982; Derman et al., 2018).

The devaluation sensitivity of GT rats and associated food cup behaviors is consistent with other studies using limited training procedures (<10 sessions). These prior studies used LiCl-induced CTA to devalue outcomes associated with classic Pavlovian cues, including lights, tones, and levers (Holland, 1998; Morrison et al., 2015; Nasser et al., 2015). Consistently, we find GT behavior (food cup approach) is devaluation sensitive across devaluation procedures (satiety and LiCl) and amounts of conditioning. This is entirely consistent with the finding that classic Pavlovian auditory conditioning, which preferentially promotes food-cup behavior, is sensitive to devaluation independent of the number of CS-US pairings (Holland, 1977, 1998). The present study extends these findings, showing that GT rats, defined by their food cup approach, remain sensitive to devaluation with more CS-US pairings, despite a shift away from predominantly food cup-directed and towards lever-directed behaviors. This shift in goal-tracking towards sign-tracking has been reliably observed across labs using different reinforcers (Villaruel and Chaudhri, 2016; Bacharach et al., 2018; Derman et al., 2018). The present study adds an important psychological caveat to the goal-to-sign-tracking behavioral shift, which may appear maladaptive at face value, but remains adaptively sensitive to manipulations of outcome value.

The devaluation insensitivity of ST behavior that we observe after limited training is consistent with several studies that vary in the amount of training prior to outcome devaluation. Insensitivity to devaluation has been observed in ST rats after limited training (<10 training sessions; (Morrison et al., 2015; Nasser et al., 2015) and for lever-directed behaviors after more extended training (>10 training sessions; (Patitucci et al., 2016; Smedley and Smith, 2018).

The emergence of satiety-induced devaluation sensitivity of sign-tracking rats that we observe with extended training is consistent with other studies that also extensively conditioned rats prior to outcome devaluation (>10 training sessions). Notably, two such studies report devaluation sensitivity of lever directed behaviors generally, and specifically in ST rats (Cleland and Davey, 1982; Derman et al., 2018). Extensive training (>25 sessions) of CS-US pairings result in robust devaluation sensitivity of both lever- and food cup-directed behaviors after both illness- and satiety-induced outcome devaluation procedures (Cleland and Davey, 1982). Comparatively less extensive PLA training on two distinct levers (12 sessions of training on each lever contingency for a total of 24 training sessions) also results in robust devaluation sensitivity of lever-directed behaviors (during the cue) and magazine entries (post-cue; Derman et al., 2018). In contrast, after extended training we observe ST rats' lever directed approach becomes devaluation sensitive but is accompanied by a small increase in their non-preferred food cup approach under devalued conditions. We expect the decreased preferred lever approach we observe in ST rats is primarily driven by the current value of the associated outcome. As a result of less lever interaction time, we postulate that the non-preferred food cup approach emerges, which may reflect response competition specifically under devalued conditions. Certainly, this emergence of food cup approach is not sensitive to the current value of the outcome. While we do not observe the emergence of a non-preferred lever approach in GT rats under devalued relative to valued conditions, others have (Morrison et al., 2015). This suggests the emergence of non-preferred responding under devalued conditions is not specific to GT or ST rats and is clearly not sensitive to the current value of the outcome. Notably, the amount of non-preferred responding we observe here after extended training in ST rats represents a very small fraction of overall approach behavior, which is largely driven by the preferred, devaluation sensitive, lever approach. Finally, in Experiment 2, after extended training we observed devaluation sensitivity in GT and intermediate rats (Non-ST), but not in ST rats after illness-induced outcome devaluation. The devaluation sensitive behavior of Non-ST rats was expressed as a decrease in total approach, and neither group showed an emergence of non-preferred responding in the devaluation condition. This difference in the emergence of non-preferred responding for satiety, but not LiCl devaluation suggests potentially divergent psychological processes that warrant further investigation. Altogether, the conflicting observations that sign-tracking and lever-directed behaviors are devaluation sensitive in some studies and insensitive in other studies suggests experience and other procedural differences may be key factors in experimental outcomes (Cleland and Davey, 1982; Patitucci et al., 2016; Derman et al., 2018; Smedley and Smith, 2018).

Notably, such studies have varied considerably in the devaluation approach (satiety, illness), context in which US was devalued (training, homecage, or novel context) and amount of CTA (limited, extensive US-LiCl pairings). Most notably, devaluation sensitivity of lever-directed behaviors is evident when CTA of the US is directly associated with the context in which the rats are trained and tested (Cleland and Davey, 1982; Derman et al., 2018). For CTA in these studies, rats consumed the US in the training context and then received injections of lithium chloride to induce gastric malaise. While the aim of CTA is for the gastric malaise to be associated solely with the US, the aversion induced by the gastric malaise could be generalized to the context itself, resulting in relevant contextual devaluation that influences later testing (Meachum, 1990; Boakes et al., 1997; Rodriguez et al., 2000; Limebeer et al., 2006). If rats are either in the sated state at test (Cleland and Davey, 1982; and Experiment 1 of the present study, but also see Patitucci et al., 2016) or are directly exposed to the training context with CTA (Cleland and Davey, 1982; Derman et al., 2018), then state-dependent or contextual associations may facilitate adaptive suppression of conditioned responding to cues at test (Bouton et al., 2019). There is arguably little inference required at the time of test when using satiety devaluation or CTA in training context procedures, in which devaluation occurs in a temporally contiguous way with exposure to the testing environment. In these cases, rats can use direct experience with the aversion to adaptively reduce

responding to cues. Conversely, if CTA occurs independent of the training context, such as in the homecage or novel context, inference mediated by a representation of devalued outcome is required to adaptively reduce responding to associated cues [(Morrison et al., 2015; Nasser et al., 2015), Experiment 2 of the present study]. Additionally, both the context and amount of CTA (five rounds of US-LiCl pairings in training context in the Derman study) were greater in prior studies than in our Experiment 2 (two rounds of US-LiCl pairings in rats' homecages). Altogether, we expect these contextual and CTA procedural differences contributed to the dissimilar findings between studies.

Here, in Experiment 1, we employed identical satiety devaluation manipulations after limited and extended training, thus controlling for devaluation procedure within-subject, and find that the same ST individuals that are insensitive early in training become sensitive to satiety devaluation with extended training. Our observations that ST rats are sensitive to satiety-, but not illness-, induced outcome devaluation after extended training suggests that ST rats are able to adjust behavior when tested in the devalued state (sated on pellet during testing in the chamber; Experiment 1). Specifically, this indicates ST rats can encode sensory-specific characteristics of the food they are sated on and relate this to the associated stimuli (i.e., lever) to appropriately respond during satiety-induced outcome devaluation, but only after extended PLA training. However, when an inference based on prior, contextually-distinct experience is required (Experiment 2), ST rats are unable to appropriately adjust behavior based on the current value of the outcome.

Instrumental devaluation studies pose a striking dissimilarity to Pavlovian studies regarding devaluation sensitivity after extended training. Instrumental responding, mediated by competing action-outcome and stimulus-response associations, transitions from goal-directed (devaluation sensitive) to habitual (devaluation insensitive) with extended instrumental experience (Adams, 1982; Dickinson et al., 1983; Blundell et al., 2003; Coutureau and Killcross, 2003; Killcross and Coutureau, 2003; Johnson et al., 2009; Parkes and Balleine, 2013). In contrast, Pavlovian behaviors remain sensitive to devaluation, independent of the amount of training (Holland, 1998). While fundamental differences between instrumental and Pavlovian associations likely explain these contrasting findings, the present study suggests individual differences in Pavlovian approach impact the expression of devaluation sensitivity. While we are careful in making parallels to the instrumental devaluation literature, the present study uses a Pavlovian task that results in sign-tracking (i.e., lever pressing), which resembles instrumental responses, but critically is not based on instrumental contingencies. In the instrumental literature, habit is operationally defined as insensitivity of instrumental actions to outcome devaluation, while goal-directed responding reflects the sensitivity of instrumental actions to outcome devaluation. Since rats on the GT end of the tracking continuum are consistently devaluation sensitive under all conditions tested in the current study, one might predict that GT rats would be more goal-directed than ST rats in instrumental settings, perhaps even independent of the amount of instrumental experience. Yet, other factors can impact instrumental devaluation sensitivity, including the amount of reinforcer experience (Adams, 1982), reinforcement schedules (continuous reinforcement, fixed interval/ratio, variable interval/ratio, etc.; Dickinson et al., 1983) and motivational state during training and testing (Balleine, 1992; Dickinson et al., 1995). The extent to which goal-directed vs. habitual responding emerges across conditioning in ST and GT rats requires instrumental devaluation procedures.

The current studies provide a behavioral framework to extend the investigation of individual behavioral and neurobiological differences in devaluation sensitivity, which we find depend on training history and devaluation approach. The individual and timing-dependent differences in devaluation sensitivity suggest potentially distinct and/or shifting neural mechanisms mediating the expression of behavior when outcome value changes. During limited training in PLA cue-evoked striatal dopamine release is evident in ST, but not GT rats, and intra-nucleus accumbens dopamine receptor antagonists reduce sign-, but not goal-tracking behaviors (Flagel et al., 2011; Saunders et al., 2013). Yet, the striatal dopamine release and dopamine-dependence associated with sign-tracking declines with extended training (Clark et al., 2013), at a time that we observe emerging devaluation sensitivity in ST rats. This raises the possibility that, after limited training, striatal dopamine signaling in ST rats masks devaluation sensitivity that is mediated by competing brain mechanisms.

The present study using male rats indicates the importance of considering tracking- and experience-dependent effects in inference-based and state-dependent devaluation. Future studies considering these factors in both sexes will elucidate more precisely defined contributions of dopamine and other brain circuits driving Pavlovian approach and devaluation sensitivity (Pickens et al., 2003; Coutureau et al., 2009; Johnson et al., 2009; Shiflett and Balleine, 2010; Parkes and Balleine, 2013; Zeeb and Winstanley, 2013; Hart et al., 2014; Parkes et al., 2015; Wassum and Izquierdo, 2015; Gourley et al., 2016; Mannella et al., 2016; West and Carelli, 2016; Izquierdo, 2017; Lichtenberg et al., 2017; Fisher et al., 2020). Such efforts are translationally relevant, as human studies report evidence for sign-tracking and individual variability in cue reactivity as well as devaluation sensitivity (Garofalo and di Pellegrino, 2015; Versace et al., 2016; De Tommaso et al., 2017; Pool et al., 2019). Particularly relevant is a recent study dissociating devaluation sensitive and insensitive responses during Pavlovian learning in humans (Pool et al., 2019). Future investigations of psychological and neurobiological differences that are evident prior to drug-experience will further our understanding of how sign- and goal-tracking differences relate to addiction vulnerability (Saunders and Robinson, 2010; Saunders et al., 2013; McClory and Spear, 2014; Versaggi et al., 2016; Pitchers et al., 2017; Valyear et al., 2017).

DATA AVAILABILITY STATEMENT

The raw data supporting the conclusions of this article will be made available by the authors, without undue reservation, to any qualified researcher.

ETHICS STATEMENT

The animal study was reviewed and approved by University of Maryland, School of Medicine Institutional Animal Care and Use Committee.

AUTHOR CONTRIBUTIONS

DC conceived and supervised the project. SK, SB, JC, and DK acquired the data. SK analyzed the data. SK and DC designed the experiments, interpreted the data, and wrote the manuscript. All authors contributed to manuscript revision, read, and approved the submitted version.

FUNDING

This work was supported by a McKnight Memory and Cognitive Disorders Award (McKnight Foundation; DC), a Brain and Behavior Research Foundation NARSAD Young Investigator Grant #24950 (DC), a National Institute on Drug Abuse (NIDA) grant R01DA043533 (DC), and the Department of Anatomy and Neurobiology at the University of Maryland, School of Medicine. The funders had no role in the study design, data collection, and analysis, decision to publish, or preparation of the manuscript.

ACKNOWLEDGMENTS

We thank Anne Tobin for technical assistance and thank the Animal Care Facility for colony maintenance.

SUPPLEMENTARY MATERIAL

The Supplementary Material for this article can be found online at: https://www.frontiersin.org/articles/10.3389/fnbeh.2020.00003/full#supplementary-material.

REFERENCES

Adams, C. D. (1982). Variations in the sensitivity of instrumental responding to reinforcer devaluation. *Q. J. Exp. Psychol.* 34, 77–98. doi: 10.1080/14640748208400878

Bacharach, S. Z., Nasser, H. M., Zlebnik, N. E., Dantrassy, H. M., Kochli, D. E., Gyawali, U., et al. (2018). Cannabinoid receptor-1 signaling contributions to sign-tracking and conditioned reinforcement in rats. *Psychopharmacology* 235, 3031–3043. doi: 10.1007/s00213-018-4993-6

Balleine, B. (1992). Instrumental performance following a shift in primary motivation depends on incentive learning. *J. Exp. Psychol. Anim. Behav. Process.* 18, 236–250. doi: 10.1037/0097-7403.18.3.236

Blundell, P., Hall, G., and Killcross, S. (2003). Preserved sensitivity to outcome value after lesions of the basolateral amygdala. *J. Neurosci.* 23, 7702–7709. doi: 10.1523/jneurosci.23-20-07702.2003

Boakes, R. A. (1977). "Performance on learning to associate a stimulus with positive reinforcement," in *Operant-Pavlovian Interactions*, ed. I. H. D. H. M. B. Hurwitz (Hillsdale, NJ: Erlbaum), 67–101.

Boakes, R. A., Westbrook, R. F., Elliott, M., and Swinbourne, A. L. (1997). Context dependency of conditioned aversions to water and sweet tastes. *J. Exp. Psychol. Anim. Behav. Process.* 23, 56–67. doi: 10.1037/0097-7403.23.1.56

Bouton, M., Allan, S., Tavakkoli, A., Steinfeld, M., and Thrailkill, E. (2019). "Separating goal-directed action from habit: role of the context in which taste aversion learning occurs in creating the reinforcer devaluation effect," in *Society for Neuroscience* (Chicago, IL).

Clark, J. J., Collins, A. L., Sanford, C. A., and Phillips, P. E. M. (2013). Dopamine encoding of Pavlovian incentive stimuli diminishes with extended training. *J. Neurosci.* 33, 3526–3532. doi: 10.1523/JNEUROSCI.5119-12.2013

Cleland, G. C., and Davey, G. C. L. (1982). The effects of satiation on reinforcer devaluation on signal-centered behavior in the rats. *Learn. Motiv.* 13, 343–360. doi: 10.1016/0023-9690(82)90014-5

Coutureau, E., and Killcross, S. (2003). Inactivation of the infralimbic prefrontal cortex reinstates goal-directed responding in overtrained rats. *Behav. Brain Res.* 146, 167–174. doi: 10.1016/j.bbr.2003.09.025

Coutureau, E., Marchand, A. R., and Di Scala, G. (2009). Goal-directed responding is sensitive to lesions to the prelimbic cortex or basolateral nucleus of the amygdala but not to their disconnection. *Behav. Neurosci.* 123, 443–448. doi: 10.1037/a0014818

De Tommaso, M., Mastropasqua, T., and Turatto, M. (2017). The salience of a reward cue can outlast reward devaluation. *Behav. Neurosci.* 131, 226–234. doi: 10.1037/bne0000193

Derman, R. C., Schneider, K., Juarez, S., and Delamater, A. R. (2018). Sign-tracking is an expectancy-mediated behavior that relies on prediction error mechanisms. *Learn. Mem.* 25, 550–563. doi: 10.1101/lm.047365.118

Dickinson, A., Balleine, B., Watt, A., Gonzalez, F., and Boakes, R. A. (1995). Motivational control after extended instrumental training. *Anim. Learn. Behav.* 23, 197–206. doi: 10.3758/bf03199935

Dickinson, A., Nicholas, D. J., and Adams, C. D. (1983). The effect of the instrumental training contingency on susceptibility to reinforcer devaluation. *Q. J. Exp. Psychol.* 35B, 35–51. doi: 10.1080/14640748308400912

Fisher, H., Pajser, A., and Pickens, C. L. (2020). Pre-training inactivation of basolateral amygdala and mediodorsal thalamus, but not orbitofrontal cortex or prelimbic cortex, impairs devaluation in a multiple-response/multiple-reinforcer cued operant task. *Behav. Brain Res.* 378:112159. doi: 10.1016/j.bbr.2019.112159

Flagel, S. B., and Robinson, T. E. (2017). Neurobiological basis of individual variation in stimulus-reward learning. *Curr. Opin. Behav. Sci.* 13, 178–185. doi: 10.1016/j.cobeha.2016.12.004

Flagel, S. B., Clark, J. J., Robinson, T. E., Mayo, L., Czuj, A., Willuhn, I., et al. (2011). A selective role for dopamine in stimulus-reward learning. *Nature* 469, 53–57. doi: 10.1038/nature09588

Flagel, S. B., Watson, S. J., Robinson, T. E., and Akil, H. (2007). Individual differences in the propensity to approach signals vs. goals promote different adaptations in the dopamine system of rats. *Psychopharmacology* 191, 599–607. doi: 10.1007/s00213-006-0535-8

Garofalo, S., and di Pellegrino, G. (2015). Individual differences in the influence of task-irrelevant Pavlovian cues on human behavior. *Front. Behav. Neurosci.* 9:163. doi: 10.3389/fnbeh.2015.00163

Gourley, S. L., Zimmermann, K. S., Allen, A. G., and Taylor, J. R. (2016). The medial orbitofrontal cortex regulates sensitivity to outcome value. *J. Neurosci.* 36, 4600–4613. doi: 10.1523/jneurosci.4253-15.2016

Hart, G., Leung, B. K., and Balleine, B. W. (2014). Dorsal and ventral streams: the distinct role of striatal subregions in the acquisition and performance of goal-directed actions. *Neurobiol. Learn. Mem.* 108, 104–118. doi: 10.1016/j.nlm.2013.11.003

Hearst, E., and Jenkins, H. M. (1974). *Sign-Tracking: The Stimulus-Reinforcer Relation and Directed Action.* Austin, TX: Monograph of the Psychonomic Society.

Holland, P. (1998). Amount of training affects associatively-activated event representation. *Neuropharmacology* 37, 461–469. doi: 10.1016/s0028-3908(98)00038-0

Holland, P. C. (1977). Conditioned stimulus as a determinant of the form of the Pavlovian conditioned response. *J. Exp. Psychol. Anim. Behav. Process.* 3, 77–104. doi: 10.1037/0097-7403.3.1.77

Izquierdo, A. (2017). Functional heterogeneity within rat orbitofrontal cortex in reward learning and decision making. *J. Neurosci.* 37, 10529–10540. doi: 10.1523/jneurosci.1678-17.2017

Johnson, A. W., Gallagher, M., and Holland, P. C. (2009). The basolateral amygdala is critical to the expression of Pavlovian and instrumental outcome-specific reinforcer devaluation effects. *J. Neurosci.* 29, 696–704. doi: 10.1523/jneurosci.3758-08.2009

Killcross, S., and Coutureau, E. (2003). Coordination of actions and habits in the medial prefrontal cortex of rats. *Cereb. Cortex* 13, 400–408. doi: 10.1093/cercor/13.4.400

Lichtenberg, N. T., Pennington, Z. T., Holley, S. M., Greenfield, V. Y., Cepeda, C., Levine, M. S., et al. (2017). Basolateral amygdala to orbitofrontal cortex projections enable cue-triggered reward expectations. *J. Neurosci.* 37, 8374–8384. doi: 10.1523/JNEUROSCI.0486-17.2017

Limebeer, C. L., Hall, G., and Parker, L. A. (2006). Exposure to a lithium-paired context elicits gaping in rats: a model of anticipatory nausea. *Physiol. Behav.* 88, 398–403. doi: 10.1016/j.physbeh.2006.04.014

Mannella, F., Mirolli, M., and Baldassarre, G. (2016). Goal-directed behavior and instrumental devaluation: a neural system-level computational model. *Front. Behav. Neurosci.* 10:181. doi: 10.3389/fnbeh.2016.00181

McClory, A. J., and Spear, L. P. (2014). Effects of ethanol exposure during adolescence or in adulthood on Pavlovian conditioned approach in Sprague–Dawley rats. *Psychopharmacology* 48, 755–763. doi: 10.1016/j.alcohol.2014.05.006

Meachum, C. L. (1990). Overshadowing of a context aversion by a novel incentive in operant conditioning. *Q. J. Exp. Psychol. B* 42, 197–210.

Meyer, P. J., Lovic, V., Saunders, B. T., Yager, L. M., Flagel, S. B., Morrow, J. D., et al. (2012). Quantifying individual variation in the propensity to attribute incentive salience to reward cues. *PLoS One* 7:e38987. doi: 10.1371/journal.pone.0038987

Morrison, S. E., Bamkole, M. A., and Nicola, S. M. (2015). Sign tracking, but not goal tracking, is resistant to outcome devaluation. *Front. Neurosci.* 9:468. doi: 10.3389/fnins.2015.00468

Nasser, H. M., Chen, Y. W., Fiscella, K., and Calu, D. J. (2015). Individual variability in behavioral flexibility predicts sign-tracking tendency. *Front. Behav. Neurosci.* 9:289. doi: 10.3389/fnbeh.2015.00289

Parkes, S. L., and Balleine, B. W. (2013). Incentive memory: evidence the basolateral amygdala encodes and the insular cortex retrieves outcome values to guide choice between goal-directed actions. *J. Neurosci.* 33, 8753–8763. doi: 10.1523/jneurosci.5071-12.2013

Parkes, S. L., Bradfield, L. A., and Balleine, B. W. (2015). Interaction of insular cortex and ventral striatum mediates the effect of incentive memory on choice between goal-directed actions. *J. Neurosci.* 35, 6464–6471. doi: 10.1523/JNEUROSCI.4153-14.2015

Patitucci, E., Nelson, A. J. D., Dwyer, D. M., and Honey, R. C. (2016). The origins of individual differences in how learning is expressed in rats: a general-process perspective. *J. Exp. Psychol. Anim. Learn. Cogn.* 42, 313–324. doi: 10.1037/xan0000116

Pickens, C. L., Saddoris, M. P., Setlow, B., Gallagher, M., Holland, P. C., and Schoenbaum, G. (2003). Different roles for orbitofrontal cortex and basolateral amygdala in a reinforcer devaluation task. *J. Neurosci.* 23, 11078–11084. doi: 10.1523/jneurosci.23-35-11078.2003

Pitchers, K. K., Phillips, K. B., Jones, J. L., Robinson, T. E., and Sarter, M. (2017). Diverse roads to relapse: a discriminative cue signaling cocaine availability is more effective in renewing cocaine seeking in goal trackers than sign trackers and depends on basal forebrain cholinergic activity. *J. Neurosci.* 37, 7198–7208. doi: 10.1523/JNEUROSCI.0990-17.2017

Pool, E. R., Pauli, W. M., Kress, C. S., and O'Doherty, J. P. (2019). Behavioural evidence for parallel outcome-sensitive and outcome-insensitive Pavlovian learning systems in humans. *Nat. Hum. Behav.* 3, 284–296. doi: 10.1038/s41562-018-0527-9

Robinson, T. E., and Flagel, S. B. (2009). Dissociating the predictive and incentive motivational properties of reward-related cues through the study of individual differences. *Biol. Psychiatry* 65, 869–873. doi: 10.1016/j.biopsych.2008.09.006

Rodriguez, M., Lopez, M., Symonds, M., and Hall, G. (2000). Lithium-induced context aversion in rats as a model of anticipatory nausea in humans. *Physiol. Behav.* 71, 571–579. doi: 10.1016/s0031-9384(00)00376-0

Saunders, B. T., and Robinson, T. E. (2010). A cocaine cue acts as an incentive stimulus in some but not others: implications for addiction. *Biol. Psychiatry* 67, 730–736. doi: 10.1016/j.biopsych.2009.11.015

Saunders, B. T., and Robinson, T. E. (2013). Individual variation in resisting temptation: implications for addiction. *Neurosci. Biobehav. Rev.* 37, 1955–1975. doi: 10.1016/j.neubiorev.2013.02.008

Saunders, B. T., Yager, L. M., and Robinson, T. E. (2013). Cue-evoked cocaine "craving": role of dopamine in the accumbens core. *J. Neurosci.* 33, 13989–14000. doi: 10.1523/jneurosci.0450-13.2013

Shiflett, M. W., and Balleine, B. W. (2010). At the limbic-motor interface: disconnection of basolateral amygdala from nucleus accumbens core and shell reveals dissociable components of incentive motivation. *Eur. J. Neurosci.* 32, 1735–1743. doi: 10.1111/j.1460-9568.2010.07439.x

Smedley, E. B., and Smith, K. S. (2018). Evidence of structure and persistence in motivational attraction to serial Pavlovian cues. *Learn. Mem.* 25, 78–89. doi: 10.1101/lm.046599.117

Tomie, A. (1996). Locating reward cue at response manipulandum (CAM) induces symptoms of drug abuse. *Neurosci. Biobehav. Rev.* 20, 505–535. doi: 10.1016/0149-7634(95)00023-2

Valyear, M. D., Villaruel, F. R., and Chaudhri, N. (2017). Alcohol-seeking and relapse: a focus on incentive salience and contextual conditioning. *Behav. Processes* 141, 26–32. doi: 10.1016/j.beproc.2017.04.019

Versace, F., Kypriotakis, G., Basen-Engquist, K., and Schembre, S. M. (2016). Heterogeneity in brain reactivity to pleasant and food cues: evidence of sign-tracking in humans. *Soc. Cogn. Affect. Neurosci.* 11, 604–611. doi: 10.1093/scan/nsv143

Versaggi, C. L., King, C. P., and Meyer, P. J. (2016). The tendency to sign-track predicts cue-induced reinstatement during nicotine self-administration and is enhanced by nicotine but not ethanol. *Psychopharmacology* 233, 2985–2997. doi: 10.1007/s00213-016-4341-7

Villaruel, F. R., and Chaudhri, N. (2016). Individual differences in the attribution of incentive salience to a Pavlovian alcohol cue. *Front. Behav. Neurosci.* 10:238. doi: 10.3389/fnbeh.2016.00238

Wassum, K. M., and Izquierdo, A. (2015). The basolateral amygdala in reward learning and addiction. *Neurosci. Biobehav. Rev.* 57, 271–283. doi: 10.1016/j.neubiorev.2015.08.017

West, E. A., and Carelli, R. M. (2016). Nucleus accumbens core and shell differentially encode reward-associated cues after reinforcer devaluation. *J. Neurosci.* 36, 1128–1139. doi: 10.1523/jneurosci.2976-15.2016

Yager, L. M., and Robinson, T. E. (2013). A classically conditioned cocaine cue acquires greater control over motivated behavior in rats prone to attribute incentive salience to a food cue. *Psychopharmacology* 226, 217–228. doi: 10.1007/s00213-012-2890-y

Yager, L. M., Pitchers, K. K., Flagel, S. B., and Robinson, T. E. (2015). Individual variation in the motivational and neurobiological effects of an opioid cue. *Neuropsychopharmacology* 40, 1269–1277. doi: 10.1038/npp.2014.314

Zeeb, F. D., and Winstanley, C. A. (2013). Functional disconnection of the orbitofrontal cortex and basolateral amygdala impairs acquisition of a rat gambling task and disrupts animals' ability to alter decision-making behavior after reinforcer devaluation. *J. Neurosci.* 33, 6434–6443. doi: 10.1523/jneurosci.3971-12.2013

Conflict of Interest: The authors declare that the research was conducted in the absence of any commercial or financial relationships that could be construed as a potential conflict of interest.

frontiers in Behavioral Neuroscience

ORIGINAL RESEARCH
published: 10 March 2020
doi: 10.3389/fnbeh.2020.00034

Avoidant Coping Style to High Imminence Threat Is Linked to Higher Anxiety-Like Behavior

Shaun K. L. Quah[1,2]*, *Gemma J. Cockcroft*[1,2], *Lauren McIver*[1,2], *Andrea M. Santangelo*[1,2]*† and *Angela C. Roberts*[1,2]†

[1]*Department of Physiology, Development and Neuroscience, University of Cambridge, Cambridge, United Kingdom,*
[2]*Behavioral and Clinical Neuroscience Institute, University of Cambridge, Cambridge, United Kingdom*

Human studies with self-reported measures have suggested a link between an avoidant coping style and high anxiety. Here, using the common marmoset as a model, we characterize the latent factors underlying behavioral responses of these monkeys towards low and high imminence threat and investigate if a predominantly avoidant behavioral response to high imminence threat is associated with greater anxiety-like behavior in a context of low imminence threat. Exploratory factor analysis (EFA) of the human intruder test of low imminence threat revealed a single factor in which a combination of active vigilance and avoidance responses underpinned anxiety-like behavior. In contrast, two negatively-associated factors were revealed in the model snake test reflecting active and avoidant coping to high imminence threat. Subsequent analysis showed that animals with a predominantly avoidant coping style on the model snake test displayed higher anxiety-like behavior on the human intruder test, findings consistent with those described in humans. Together they illustrate the richness of the behavioral repertoire displayed by marmosets in low and high imminence threatening contexts and the additional insight that factor analysis can provide by identifying the latent factors underlying these complex behavioral datasets. They also highlight the translational value of this approach when studying the neural circuits underlying complex anxiety-like states in this primate model.

Keywords: coping, anxiety, fear, threat, stress, emotion

OPEN ACCESS

Edited by:
Fabrizio Sanna,
University of Cagliari, Italy

Reviewed by:
Marilia Barros,
University of Brasilia, Brazil
Jon Cavanaugh,
Dartmouth College, United States

***Correspondence:**
Shaun K. L. Quah
sklq2@cam.ac.uk
Andrea M. Santangelo
as966@cam.ac.uk

† These authors share senior authorship

Specialty section:
This article was submitted to Individual and Social Behaviors, a section of the journal Frontiers in Behavioral Neuroscience

Received: *04 November 2019*
Accepted: *18 February 2020*
Published: *10 March 2020*

Citation:
Quah SKL, Cockcroft GJ, McIver L, Santangelo AM and Roberts AC (2020) Avoidant Coping Style to High Imminence Threat Is Linked to Higher Anxiety-Like Behavior. Front. Behav. Neurosci. 14:34. doi: 10.3389/fnbeh.2020.00034

INTRODUCTION

Anxiety and fear are key components of human emotion and have been described in the NIMH's research domain criteria as adaptive responses to potential threat and acute threat respectively. Anxiety and fear may also be differentiated based on their position on the predatory-threat imminence continuum; with imminence being influenced by temporal, spatial, and probabilistic closeness to the threat, as well as other threat characteristics (Perusini and Fanselow, 2015). Anxiety is hypothesized to drive pre-encounter defensive behaviors when imminence is considered to be low and there is a high level of uncertainty or ambiguity, e.g., increased vigilance for risk assessment (Blanchard et al., 2011). In contrast, fear is hypothesized to drive post-encounter defense behaviors when imminence is considered to be high, e.g., freezing, attack.

Distortion of threat imminence and dysregulated defensive behaviors may form the core symptomatology of anxiety disorders. Individuals with high trait anxiety, a natural disposition to attend to, experience and report negative emotions across many situations, have increased risk of developing anxiety disorders and depression (Weger and Sandi, 2018), and display greater responsivity to threat cues (Indovina et al., 2011). Maladaptive coping patterns to threatening stimuli may play a role in the dysfunctional regulation of emotion observed in patients with anxiety disorders. Specifically, studies of self-report measures in humans have suggested that the tendency to adopt an avoidant coping strategy is linked to anxiety and depressive symptoms during adolescence (Chan, 1995; Herman-Stabl et al., 1995; Seiffge-Krenke and Klessinger, 2000; Gomez and McLaren, 2006), and increased post-trauma PTSD symptom severity (Pineles et al., 2011).

The human literature of coping inventories and questionnaires broadly delineates coping into active and avoidant strategies (Herman-Stabl et al., 1995; Seiffge-Krenke and Klessinger, 2000; Frydenberg and Lewis, 2009; Pineles et al., 2011). Active and avoidant coping refers to cognitive or behavioral activity either towards (active) or away (avoidant) from the threat, sometimes simplified as fight-or-flight. Similarly, animal studies of coping in highly stressful situations categorize responding to the active and avoidant dimensions (Koolhaas et al., 1999). For example, "active/proactive" rats display more aggressive behavior in response to an intruder and spend more time actively burying shock probes, whereas "avoidant/reactive" rats display less aggressive behaviors to an intruder and spend more time being immobile in the defensive burying test (Koolhaas et al., 2010).

To study these complex latent constructs representative of human anxiety and fear in an animal model, first, we should determine whether a similar relationship between coping styles and anxiety is reflected in animals. This requires an approach that can properly represent the construct driving the diverse repertoire of behaviors that animals display across different situations involving low and high imminence threat. Unfortunately, preclinical paradigms often rely on simple unidimensional measures of anxiety-like and fear-like animal behavior that only bear a weak resemblance to human anxious and fear-driven behavior. While these measures may have predictive validity, e.g., rodent's tendency to stay in enclosed spaces in an anxiety-provoking context is sensitive to anxiolytics (Borsini et al., 2002), the use of these measures to represent latent constructs may be an oversimplification. Behaviors such as an animal's tendency to stay in enclosed spaces are likely driven by multiple underlying factors such as an animal's territoriality or propensity for exploration, and not just anxiety *per se*. Indeed, misattributing these observed effects may contribute to the current difficulty in translating findings from animal studies to humans. Thus, a multivariate approach modeling the underlying latent construct driving the observed behaviors is needed.

Such an approach has been used in macaques (Williamson et al., 2003; Fox et al., 2008) and marmosets (Agustín-Pavón et al., 2012; Shiba et al., 2014) in tests measuring responsivity when there is low (human intruder test) and high (model snake test) imminence threat with composite or principal component scores. However, a limitation of using these simple composite scores is that it only simplifies the data and does not determine the latent variables driving the observed changes within the data. Instead, factor analysis is widely utilized in validation studies of psychological tests and has recently been used to uncover the latent variables affecting the behavioral response of rhesus macaques in the human intruder test (Gottlieb and Capitanio, 2013).

Thus, in the present study, we applied an exploratory factor analysis (EFA) to characterize the factors underlying the common marmoset's behavior in response to both low threat imminence (the human intruder test) and high threat imminence (the model snake test) in order to reveal the relationship between coping styles in the high threat imminence context and anxiety-like behavior (in a low threat imminence context) as reported in self-report studies in human.

MATERIALS AND METHODS

Subjects

All animals were bred on-site at the Innes Marmoset Colony (Behavioral and Clinical Neuroscience Institute, BCNI) and when adult, pair-housed predominantly (∼90%) as unrelated male-female pairs (males were vasectomized). Temperature (22 ± 1°C) and humidity (50 ± 1%) conditions were controlled and a dawn/dusk-like 12 h-period was maintained. They were provided with a balanced diet and water *ad libitum*. All procedures were performed in accordance with the project and personal licenses held by the authors under the UK Animals (Scientific Procedures) Act 1986.

The total tested population consists of 184 common marmosets (*Callithrix jacchus*). 171 animals (sex (M/F) = 90/81; age: 2.32 ± 0.62 years) were tested with the human intruder test and 151 common marmosets (sex (M/F) = 77/ 74; age: 2.51 ± 0.68 years) were tested with the model snake test. Of these, 134 (sex (M/F) = 71/63) were tested on both the human intruder test (age: 2.29 ± 0.62 years) and model snake test (age: 2.5 ± 0.68). For animals tested on both tests, the human intruder test was conducted before the model snake test (time between test (months): 2.5 ± 4). Although the order of these tests was not counterbalanced, these two tests used completely different stimulus types and were conducted at least 3 days apart, thus, whilst a potential effect of test order cannot be ruled out, it is unlikely.

All animals received either the human intruder and/or model snake test in early adulthood after having left the family group and been paired with a cagemate of similar age for at least 1 month. The majority of these animals (139 out of 184) formed part of the screening procedure within the colony allowing an animal's emotional reactivity to be assessed prior to entering an experimental protocol. Only thirty-nine of these were not completely naïve, having received anesthesia for restraint purposes only while undergoing MRI scanning during development and early adulthood. The remaining animals (45) were tested on the human intruder and snake tests prior to the introduction of the screening procedure and had received

additional non-related procedures beforehand. Twenty-nine had received a telemetry probe into the descending aorta, and sixteen received a single dose of 5-HT_{2A} receptor radioligand (altanserin) as part of PET scanning. No animal received the human intruder or model snake test within a week of these procedures.

Testing Apparatus

Both tests were performed in the top right-hand quadrant of the animal's home-cage [92 cm (high) × 60 cm (wide) × 98 cm and 73 cm (length of sides)] and were conducted in the presence of conspecifics in adjacent cages. A typical home cage room contains approximately 22–28 animals. Under these conditions, the subject displays a richer repertoire of behaviors in an aversive or ambiguous context than would be seen if the animal was fully isolated. Indeed, unpublished observations from our own laboratory show us that marmosets make little in the way of vocalizations or display active coping behaviors when confronted with an unknown human in isolation and individual differences are less marked. As it is not possible to control for the behavior of neighboring animals in the room, it cannot be ruled out that they may influence the behavior of the subject. But given that up to 184 animals were tested across nine different home cage rooms, it is unlikely that any specific effect of conspecifics on any individual had a significant effect on the overall dataset.

Human Intruder Test

The human intruder test involves measuring the animal's behavioral response to an unfamiliar human, the "human intruder," who stands in front of the animal's home-cage and maintains eye contact with the animal. Since animals bred in the laboratory have prior positive and negative experiences with human encounters, e.g., receiving food treats or being restrained for husbandry or experimental purposes, the unfamiliar "human intruder" acts as a threat with low probabilistic imminence and creates an anxiety-provoking context. Avoidance and vigilance during the task resemble that described for human anxious behavior (reviewed in Grupe and Nitschke, 2013), and behavioral responses to the human intruder are sensitive to anxiolytics (Carey et al., 1992; Santangelo et al., 2016).

The procedure for the human intruder test is based on the method used by Santangelo et al. (2016). Cameras and microphones are routinely present in the room for recording purposes such that all animals are habituated to the presence of recording equipment. Before the testing session begins, a camera and microphone are set up in front of the animal's home-cage. The animal was tested in the top-right quadrant of their home cage (**Supplementary Figure S1**). During testing, the cagemate was separated from the subject and restricted to the left half of the home cage and was obscured from both the human intruder and the subject. After 8 min of being separated, an experimenter (unfamiliar to the animal) wearing a realistic latex human mask (Greyland Film, UK) and standard lab attire stood 40 cm from the cage and maintained eye contact with the subject for 2 min (intruder phase). Recording continued for a further 5 min after the intruder left (recovery phase). Behavior and vocalizations during the intruder phase were scored.

The animal's observable behavior was scored using the program JWatcher V1.0[1]. For the purposes of scoring, the test quadrant was divided into multiple zones represented by different depths and heights (**Figures 1A**, **2A**). While, as described below, the average distance from the threat was used in the model snake test, this measure was not used in the human intruder test because the position of the threat in the model snake test can be reduced to a single point relative to the different positioning of the animal. In contrast, in the human intruder test, the "human intruder" facing the animal covers a larger area and the animal's position relative to the "human intruder" is better represented independently by depth and height instead. Furthermore, both time spent at the front of the cage and the back of the cage were used as measures of approach-avoidance behavior due to studies showing the sensitivity of these measures to anxiolytic and anxiogenic manipulations (Carey et al., 1992).

Human Intruder Test: Behavioral Measures

Time Spent at the Front (TSAF)

Percentage time spent at the front of the cage reflects approach behavior towards the human intruder. For the purposes of scoring, the test quadrant was divided into 3 zones: front, middle, and back. These different zones represent the depth of the zone relative to the "human intruder."

Time Spent at the Back

Percentage of time spent at the back of the cage reflects avoidance behavior away from the human intruder. Scored similarly to "Time spent at the front."

Average Height

Average height of the marmoset in the home-cage throughout the test period in centimeters. Positioning high in the cage and closer to the nestbox may reflect the common marmoset's innate flight response upwards as an arboreal species. For scoring purposes, the test quadrant is divided into five different zones: top of the nestbox, high, middle, low, floor. These different zones represent the height of the zones relative to the bottom of the test quadrant (shown in **Figure 1**).

Locomotion

Percentage of time spent changing locations within the home-cage.

Head and Body Bob

Frequency of the animal making rapid bobs of its head and body from side to side (without changing head angle) while staring at the object of interest and is often followed with egg and tse-egg vocalizations (see descriptions below). Head and body bobs are often observed in the presence of an unfamiliar human and may be an alarm behavior intended to signal potential threats to conspecifics (Carey et al., 1992; Agustín-Pavón et al., 2012).

Model Snake Test

The model snake test involves recording the animal's behavioral response to a rubber snake which acts as an inherent predatory stimulus, provoking an innate fear response (Barros et al., 2002;

[1] http://www.jwatcher.ucla.edu/

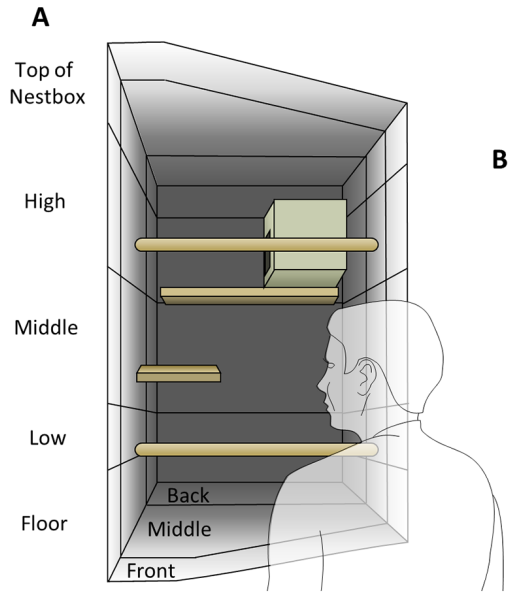

C

Variables	*M*	*SD*	Communalities		Factor loading	Score coefficient
			Initial	Extraction		
Average height	58.69	15.37	.55	.67	**.82***	0.319
Head and body bobs	22.09	22.37	.54	.59	**.77***	0.295
Time spent (back)	31.02	30.07	.52	.47	**.69***	0.110
Tse-egg calls	11.74	14.78	.22	.17	**.42***	0.048
Locomotion	7.90	6.54	.31	.32	**-.57***	-0.100
Time Spent (front)	31.24	25.26	.59	.62	**-.79***	-0.288
Egg calls	9.13	10.03	.19	.11	.33	0.026
Tsik calls	2.73	7.48	.09	.01	-.09	-0.017
Tsik-egg calls	9.65	16.39	.23	.10	.32	0.008

FIGURE 1 | Human Intruder test exploratory factor analysis (EFA). **(A)** Schematic of the top-right quadrant of the home-cage in which the human intruder test takes place, with relevant zones for the measurement of average height, and time spent at the front and back. **(B)** The relative contribution of each behavioral measure loading significantly on the factor representing anxiety-like behavior reflected by the width of the arrow. Red arrows represent positive-loading; blue arrows signify negative-loading. Positive loadings indicate that higher anxiety-like behavior corresponds to an increase in that specific measure, while a negative loading indicates a decrease. **(C)** Table of descriptive statistics, communalities, factor loadings and factor score coefficients for the variables in the human intruder test. *Significant factor loadings (>|0.4|) in bold. Mean (*M*) and standard deviation (SD) of variables from the cohort (*n* = 171).

Cross and Rogers, 2006). Furthermore, as the model snake is placed directly within the homecage, the model snake presents far higher spatial threat imminence compared to the intruder in the human intruder test.

The procedure of the model snake test is based on the methods in Shiba et al. (2014). Before the testing session begins, wireless cameras and a microphone are placed to record the animal's behavior from a top-down view and a frontal view. During a test session, the animal is separated from their cagemate and restricted to the upper right quadrant of their home cage (**Supplementary Figure S1**), while the cagemate was separated by opaque dividers to the left half of the home cage and cannot see into the testing quadrant. The 20-min test session is divided into four 5-min phases: a separation phase, where only the camera and microphone were present; a pre-snake phase, where an empty box without the model snake (a 27 cm tall rubber model of a rearing cobra) is placed in the test quadrant; a snake phase, where the empty box from the previous phase is replaced with a box containing the model snake (a sliding door is removed to expose the model snake once the box is in position); and a post-snake phase, where the empty box from the pre-snake phase is re-introduced into the test quadrant.

Model Snake Test: Behavioral Measures

Average Distance

Average distance of the marmoset from the model snake throughout the test period. For scoring purposes, the test area was divided into seven zones based on their proximity to the model snake (shown in **Figure 2**). Each zone is represented

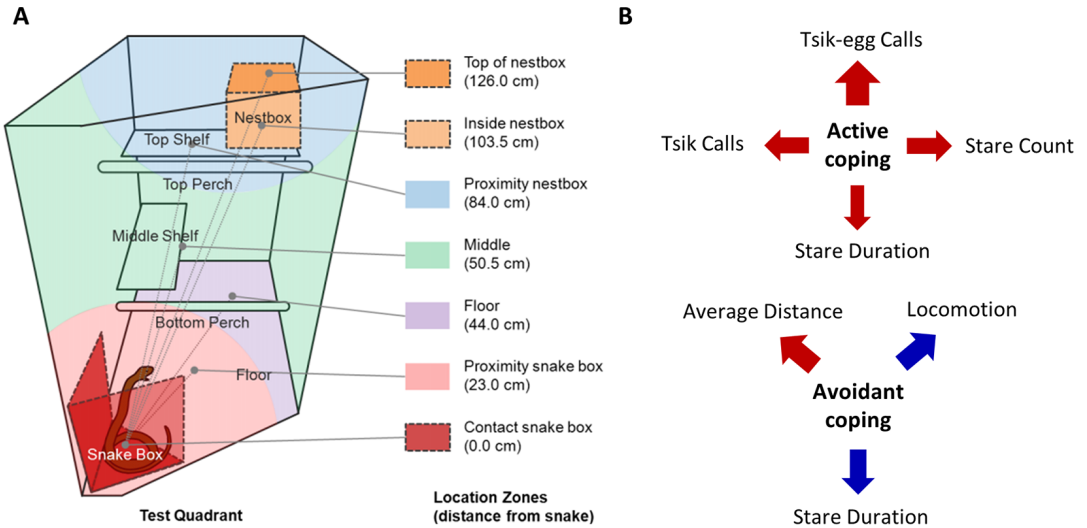

C

			Communalities		Factor loadings		Score coefficient	
Variables	*M*	*SD*	Initial	Extraction	Active	Avoidant	Active	Avoidant
Tsik-egg calls	38.11	47.05	.39	.64	**.81***	.23	0.480	0.150
Tsik calls	23.55	40.00	.31	.35	**.60***	.19	0.177	0.064
Stare count	32.56	10.81	.38	.45	**.60***	-.20	0.257	-0.135
Stare duration	40.12	17.00	.38	.50	**.47***	**-.44***	0.223	-0.275
Locomotion	6.58	3.66	.33	.40	-.09	**-.65***	-0.026	-0.310
Average distance	69.90	16.37	.36	.50	-.02	**.70***	-0.045	0.423
Head-cock	8.41	5.40	.16	.07	.26	-.04	0.061	-0.001
Egg calls	0.93	2.30	.07	.04	.16	-.11	0.033	-0.038

FIGURE 2 | Rubber snake test EFA. **(A)** Schematic from Shiba (2013) of the top-right quadrant of the home-cage with the snake box in the rubber snake test. Zones are depicted in different colors indicating the mean distances those zones represent relative to the rubber snake model. Similar to the human intruder test, the cagemate is separated into the left half of the homecage by dividers (not shown). **(B)** The relative contribution of each behavioral measure in the rubber snake test to the coping factor scores reflected by the width of the arrow. Red arrows represent positive-loading; blue arrows signify negative-loading. Positive loadings indicate that higher coping scores correspond to an increase in that specific measure, while a negative loading indicates a decrease. **(C)** Table of descriptive statistics, communalities, factor loadings and factor score coefficients for the variables in the rubber snake test. *Significant factor loadings (>|0.4|) in bold. Mean (*M*) and SD of variables from the cohort (*n* = 151).

by the distance of the mid-point of that zone from the snake. The average distance is calculated by obtaining the sum of the multiplication of the percentage time spent in each zone with the distance of the respective zones.

Locomotion

Percentage of time spent changing locations around the home-cage.

Stare Duration

Percentage time the animal spent maintaining eye and head orientation directed towards the model snake.

Stare Count

Number of times the animal spends directing its attention towards the snake. Multiple counts indicate looking away and back towards the model snake and reflect an animal repeatedly averting its gaze away from the snake but clearly pre-occupied with the snake.

Head-Cock

Frequency of the animal tilting its head in a smooth motion while maintaining its attention towards the visual target. Head-cocks have been described as an observational behavior when presented with a novel stimulus and occur during visual inspection (Menzel, 1980; Barros et al., 2002).

Vocalizations in the Human Intruder and Model Snake Tests

The animal's vocalizations recorded with a directional microphone to isolate vocalizations from the subject were extracted from the video files using Audacity, an audio editing software (Audacity, v.1.3.13) and subsequently visualized in the form of sonograms using Syrinx, a sound analysis software. The scoring of vocalizations was guided by the video recording to confirm the subject as the source of the vocalizations. Classification of vocalizations was based on identifications from Bezerra and Souto (2008) observation of wild common

marmosets. Although other calls such as phee, twitter, and bark were observed, they occurred very infrequently and only in a small subset of the population which lead to their exclusion from this study.

Egg Calls

A short call with a few harmonics. Maybe uttered singly, in series, or in continuous combination after tse or tsik calls. Egg calls have been associated with vigilance behavior, for instance when an unknown human approaches the group or when the calling marmoset is on the ground with sparse vegetation (Souto et al., 2007). Primarily heard in response to human intruder and seldom heard in response to snake.

Tsik Calls

Tsik calls are uttered as a mobbing call and have been observed being made by captive and wild common marmosets against conspecifics from other social groups, unfamiliar humans, and potential predators (Epple, 1968; Bezerra et al., 2009). Tsik calls have also been observed being made by captive common marmosets in response to the stimulus presentation of a predator (Hook-Costigan and Rogers, 1998; Cross and Rogers, 2006).

Tsik-Egg Calls

Although not clearly characterized in the wild, tsik-egg calls of common marmosets have been associated with isolation in a novel environment and have been shown to be sensitive to anxiogenic drug treatment (Kato et al., 2014).

Tse Calls

Sounds similar to tsik calls but distinguishable *via* sonogram. The lower frequency and end frequency of tse calls are higher than tsik calls. The frequency range in tse calls is also lower than tsik calls (Bezerra and Souto, 2008).

Tse-Egg Calls

A vocalization consisting of a single utterance of tse followed by a single or a series of egg calls. In the wild, tse-egg calls are the primary call type uttered during vigilance behavior (89.2% and 80.4% of total calls during vigilance in adults and juveniles respectively; Bezerra and Souto, 2008).

Exploratory Factor Analysis (EFA)

All statistical analyses were conducted with SPSS (v. 24; IBM Corp.). An EFA with a principal axis factoring extraction method was performed on the data obtained from the human intruder and model snake tests separately. The principal axis factoring extraction method was used as the variables revealed violations of normal distribution (shown in **Supplementary Figures S2, S3**) and principal axis factoring does not assume a multivariate normal distribution.

Pre-factor Extraction Tests

Before factor extraction, the Kaiser-Meyer-Olkin measure of sampling adequacy (MSA) was used to determine the proportion of common variance among the variables that may be driven by underlying factors. The Bartlett's test of sphericity was used to evaluate if there were sufficient correlations between the variables such that the factor analysis is able to model underlying constructs driving these correlations.

Post-factor Extraction

After factor extraction, the communality of a variable is the extent to which that variable correlates with all other variables in the analysis. If the average communality of the variables is more than 0.7 after extraction, the Kaiser's criterion (eigenvalue > 1) should be used to determine the number of factors to extract, otherwise, the scree plot's points of inflection should be referred to instead (Field, 2013). The scree plot shows the eigenvalue, which reflects the amount of variance explained, of each individual factor.

Rotation

If more than 1 factor is extracted, the factors are rotated to improve the interpretability of the resulting factors by maximizing the loadings of each variable to a specific factor and minimizing loading on other factors. A direct oblimin method (oblique rotation) was used to allow for correlations between the factors as there were no theoretical grounds to assume the independence of the factors.

After the factors were extracted and rotated, the factor loadings could be referred to as a measure of each variable's correlation with the extracted factor. Factor loadings are considered significant above $|0.4|$ (Stevens, 1992). To measure the goodness-of-fit for the extracted factor model, a correlation matrix was constructed based on the model and the difference (residuals) between the reproduced correlation matrix and the original correlation matrix computed. The proportion of nonredundant residuals with absolute values greater than 0.05 should be below the recommended value of 50% if the factor model does not have issues of poor fit (Field, 2013). The factor scores were estimated with a regression method, preserving any existing correlation between the factors.

The internal consistency of the factors with significant loading variables was examined using Cronbach's alpha. Cronbach's alpha evaluates how consistently the factor reflects the construct it is measuring (Cronbach, 1951).

Correlation Between Model Snake Test Factor Scores

The resulting factor scores of the model snake test were correlated using Pearson's product-moment correlation coefficient or, if the assumption of normality was severely violated ($p < 0.001$), using Spearman rank correlation coefficient. Data are presented as mean ± SEM, standard error of the mean. Effect sizes of correlations are reflected in the correlation coefficients, r_s (Cohen, 1988, 1992).

RESULTS

EFA Reveals a Single Factor Reflecting Avoidance and Vigilance to Explain Behavior in Response to a Human Intruder

A single factor explained behavior on the human intruder test (**Figure 1A**). Those behaviors that contributed greatest to the factor were the time spent at the front and back of the cage, average height, and head and body bob. Locomotion and tse-egg calls also contributed (**Figure 1B**). Highest scores were associated

with greater avoidance (more time spent at the back of the cage and relatively high up) and increased vigilance (making little movement, performing a greater number of head and body bobs and tse-egg calls).

To derive this factor, initial runs of the EFA included: time spent at the front, time spent at the back, average height, locomotion, head and body bobs, egg calls, tsik call, tsik-egg calls, tse calls, and tse-egg calls. The variable with the lowest MSA that was below the standard of 0.5 defined by Field (2013), tse calls (MSA = 0.42) was removed from the EFA. Subsequently, the KMO MSA for the final model indicated sufficient common variance for the factor analysis, KMO = 0.82, well above the recommended threshold of 0.6 (Kaiser, 1974). Bartlett's test of sphericity was significant ($\chi^2_{(36)} = 460.8$, $p < 0.001$), indicating that correlations between items were sufficiently large for factor analysis. Due to the low level of communalities, reflecting low inter-variable correlations, after extraction (**Figure 1C**), the scree plot was consulted to decide the number of factors to extract, instead of using Kaiser's criterion. The factor coefficient matrix estimated from the final output of the EFA and descriptive statistics of the sample is also shown in **Figure 1C**. Only 1 factor was extracted based on the point of inflection on the scree plot (**Supplementary Figure S4A**). This factor accounted for 39.7% of the total variance. There were 16 (44.0%) nonredundant residuals, reflecting the sufficient fit of the one-factor model.

The factor (as described above) with 6 significant loading items had moderate reliability, Cronbach's alpha = 0.64. Kline (2000) notes that psychological constructs with Cronbach's alpha below 0.7 should be realistically expected. Eliminating individual variables from the factor did not yield substantial increases to the alpha measure.

EFA Reveals Two Negatively Correlated Factors Reflecting Active and Avoidant Coping to Explain Behaviors in Response to a Model Snake

Two factors described behaviors elicited on the model snake test (**Figure 2A**). The first factor included attention towards the snake (long durations spent staring at the model snake and higher frequencies of re-attending to the model snake after looking away) and mobbing calls (tsik-egg and tsik calls). Those scoring high on this factor displayed heightened attentional engagement and increased mobbing calls, altogether reflecting an active coping response. The second factor included distance, locomotion and stare duration. A high score was characterized by an animal maintaining a greater distance from the model snake, remaining relatively stationary and spending less time staring at the snake, reflecting overall behavioral and attentional avoidance of the snake (**Figure 2B**).

To derive these factors, initial runs of the EFA included: average distance, locomotion, stare duration, stare count, head-cocks, egg calls, tsik call, tsik-egg calls, tse calls, and tse-egg calls. Tse calls (MSA = 0.32), the variable with the lowest MSA that was below the criterion of 0.5 defined by Field (2013), were removed from the EFA. Under the same criterion (MSA = 0.46), tse-egg calls were removed in the subsequent run. The KMO MSA for the final model indicated sufficient common variance for the factor analysis, KMO = 0.63, just above the recommended threshold of 0.6 (Kaiser, 1974). Bartlett's test of sphericity was significant ($\chi^2_{(28)} = 233.1$, $p < 0.001$), indicating that correlations between items were sufficiently large for factor analysis. Due to the low level of communalities after extraction (**Figure 2C**), the scree plot was consulted to decide the number of factors to extract instead of using Kaiser's criterion (Field, 2013). The factor loadings, factor score coefficients estimated from the final output of the EFA and descriptive statistics of the sample are also shown in **Figure 2C**. Two factors were extracted based on the point of inflection on the scree plot (**Supplementary Figure S4B**) for 50.3% of the total variance. There were 10 (35.0%) nonredundant residuals, indicating that the two-factor model does not have issues of poor fit.

Factor 1, that reflected active coping behaviors, consisted of 4 significant loading items and had moderate reliability, Cronbach's alpha = 0.61. Factor 2, that reflected avoidant coping behaviors, consisted of 3 significant loading items and had relatively lower reliability, Cronbach's alpha = 0.52. This may be due, in part, to the low number of variables contributing to this factor.

A comparison of the two factors showed that they were negatively correlated with one another. Active coping behavior was significantly negatively correlated (nonlinear) with avoidant coping behavior ($r_s = -0.25$, $p = 0.002$) with a small to medium effect size ($0.1 < |r| < 0.3$; **Figure 3A**), indicating that behaviors corresponding to actively attending to the model snake are negatively associated with avoidant behaviors towards the model snake. The nonparametric Spearman's rank-order correlation was used to determine the relationship between the factors as the factor representing active coping severely violated the assumption of normality ($W_{(151)} = 0.93$, $p < 0.001$, **Supplementary Figure S5**).

Animals Who Display High Avoidance and Low Active Coping to High Imminence Threat Show the Highest Levels of Anxiety-Like Behavior to Low Imminence Threat

Finally, it was determined whether animals with a predominantly avoidant coping style in response to the high imminence threat of the model snake, display higher levels of anxiety-like behavior to the low imminence threat of the human intruder. Accordingly, animals receiving both tests were grouped according to their overall response style to the snake (**Figure 3B**). First, active and avoidant coping factor scores from the model snake test were categorized as high if they were above the median of the population and low if they were below the median (advantages and disadvantages of a median split discussed in Allen, 2017). Subsequently, animals with high avoidant but low active coping scores were grouped as animals with an avoidant coping style ($n = 39$); animals with low avoidant but high active coping scores were grouped as having an active avoidant coping style ($n = 39$), and animals with both high avoidant and high active coping scores were grouped as animals with mixed coping styles ($n = 28$).

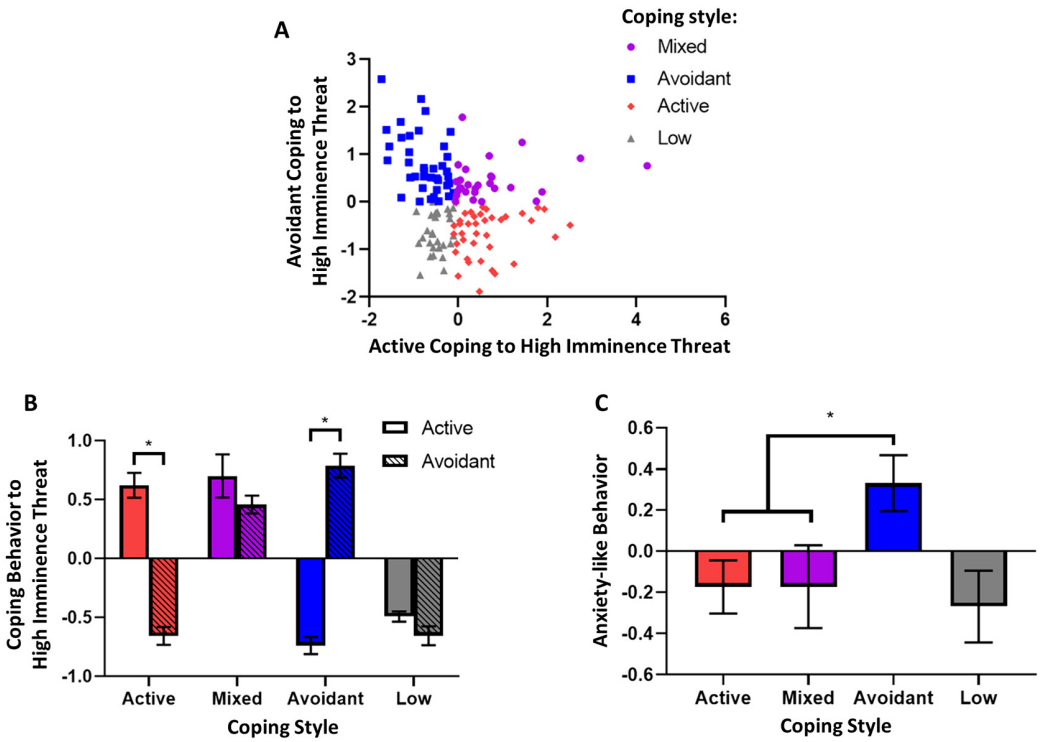

FIGURE 3 | Coping style to high imminence threat and associated anxiety-like behavior. **(A)** Factors representing active and avoidant coping with high imminence threat in the rubber snake test were significantly negatively correlated (Spearman's, $p < 0.005$). **(B)** Animals were grouped based on their coping style to high imminence threat: animals grouped as having active coping styles had significantly higher active coping factor scores compared to avoidant coping scores, while the opposite was true for animals grouped as having avoidant coping styles. For animals grouped as having a mixed coping style, coping scores were both above the mean and not significantly different. Lastly, animals that had low responsivity in the test had coping scores that were both below the mean and not significantly different. **(C)** Animals with an avoidant coping style had higher levels of anxiety-like behavior as measured by the human intruder test factor score. *$p < 0.05$. Error bars represent SEM.

Animals that showed overall low reactivity towards the model snake (both low avoidant and low active coping scores, $n = 28$) did not show a specific coping style and were not included in the subsequent group comparison. The group's distinct distribution of factor scores is shown in **Figure 3B**.

A subsequent analysis comparing these groups' respect to their corresponding behavior towards a human intruder revealed that animals with an avoidant coping style showed greater anxiety-like behavior to the human intruder in comparison to all other groups. Specifically, there was a significant effect of coping style ($F_{(2,103)} = 3.91$, $p = 0.023$) on anxiety-like avoidant/vigilant behavior, and a Dunnett's *post hoc* comparison revealed that animals with a selectively avoidant coping style had higher anxiety-like behavior compared to both animals with a selectively active coping style ($p = 0.027$) and those with a mixed coping style ($p = 0.048$; **Figure 3C**).

DISCUSSION

Although preclinical research with animal models has made substantial contributions to our understanding of emotion regulation in response to the threat, the behavioral substrates underlying these latent constructs remain simply represented and the relationship between these constructs remains poorly understood. Here, in a nonhuman primate, we modeled the factors driving behavior in the context of low imminence (human intruder test) and high imminence (model snake test) threat and established a relationship between these underlying constructs.

In relation to an unknown human, EFA of data from 171 marmosets yielded one underlying factor driving the observed behaviors. We interpret this factor as reflecting the animal's anxious temperament as it includes behavior typically associated with high levels of anxiety-like responses. Specifically, an animal with a high anxiety factor score is characterized by marked avoidance behavior that includes spending more time at positions further away from the human intruder (higher up and at the back of the cage), less time at positions close to the human intruder (the front of the cage) and less time moving around (low locomotion). Moreover, they display marked vigilance behavior including head and body bobs and vigilance calls (tse-egg calls). This pattern is similar to that shown by marmosets in the wild, which predominantly make tse-egg calls when being vigilant of their surroundings, peer into the vegetation while being stationary and make head and body bobs (Bezerra and Souto, 2008). The uncertainty and anticipation model of anxiety posits that behavioral and cognitive avoidance and increased threat

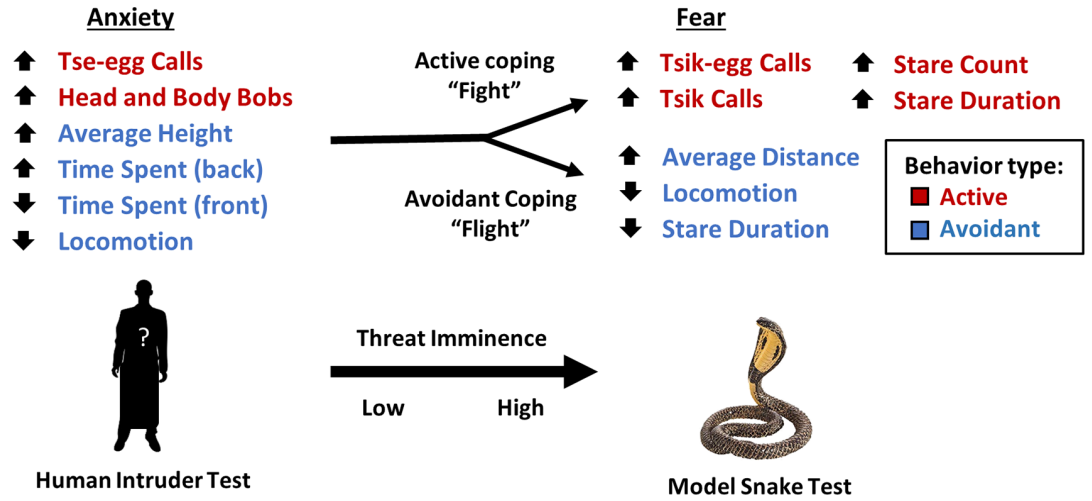

FIGURE 4 | Transition of behaviors in response to low and high imminence threat. As an animal's appraisal of threat transitions from low to high imminence, an animal's behavioral pattern shifts from a combination of both active (red) and avoidant behaviors (blue) to either a "fight" response characterized by active behaviors to confront the threat or a "flight" response characterized by attempts to avoid confrontation with the threat. The direction of arrows for variables indicates the direction of factor loading.

vigilance are among the key psychological processes central to the increased threat expectancies of subclinical and clinical anxiety (Grupe and Nitschke, 2013). Taken together, the putative anxiety factor in the human intruder test reflects classic components of anxiety-like behavior, specifically avoidance and active vigilance (**Figure 4**).

In contrast, the EFA of data from 151 animals confronted by the model snake yielded two underlying factors driving the observed behaviors. The two factors may be interpreted as reflecting the animal's active and avoidant coping response. A higher active coping response (factor 1) includes higher frequencies of mobbing calls (tsik-egg and tsik) in the presence of the predatory stimulus as well as increased attention towards the predatory stimulus, namely longer durations of staring at the model snake and higher levels of re-diverting attention towards the snake (measured by stare count). The mobbing calls serve to alert conspecifics of a potential predator and to drive predators away (Epple, 1968). Tsik calls, in particular, have also been associated with reduced cortisol levels, implicating mobbing behavior in the reduction of physiological stress (Cross and Rogers, 2006). Thus, overall, this active coping factor consists of attentional engagement and vocalizations that may underlie the animal's attempt to confront and overcome the threat (**Figure 4**). In contrast, a higher avoidant coping response (factor 2), including higher average distance, lower locomotion, and lower stare duration serve to avoid contact between the animal and the threat (model snake) and avoid drawing attention to the animal.

While these two factors in the model snake test reflect active and avoidant behaviors separately, the single factor underlying anxiety-like behavior in the human intruder test consists of both active and avoidant behaviors. A potential explanation for this differential pattern of behavior between high and low imminence threat (**Figure 4**) is that high imminence threat necessitates the selection of a specific strategy e.g., active coping vs. avoidance. Evolutionarily, being able to choose between one or other of these two different coping behaviors may allow for higher chances of survival overall, dependent on whether the predator is deterred by active engagement (predators that rely on remaining unnoticed, e.g., snakes) or is not deterred, and therefore the more appropriate course of action would be to avoid and flee (Crofoot, 2012). In contrast, when the threat has low imminence, selecting one option over another is not immediately required and thus the animals show a combination of behaviors more consistent with threat appraisal and risk assessment (Blanchard et al., 2011).

When comparing animal scores on the two factors of the model snake test, it was evident that there was marked individual variation. Noticeably, most animals either showed high scores on the avoidant coping factor but low scores on the active coping factor (avoidant copers), or high scores on the active coping factor but low scores on the avoidant coping factor (active copers). The other animals either had high scores on both the active and avoidant coping factors (mixed copers) or showed low scores on both factors and thus appeared relatively unreactive to the snake overall (low coping behavior). Since 76% were either active or avoidant copers, this suggests that most animals tend to have a predominant coping style. This is consistent with the finding that although most people use both active and avoidant coping strategies in response to stressful situations, individuals tend towards a bias in using one type over the other, reflecting their coping styles (Folkman and Lazarus, 1980).

The finding that avoidant copers in response to the snake showed the greatest responsivity to the ambiguous situation created by the human intruder is consistent with human studies with self-reported measures, and the high comorbidity of avoidant personality disorder and anxiety disorders (Skodol et al., 1995). Furthermore, individuals who changed from an active to avoidant coping style showed an increase in depressive

symptoms, whereas individuals who did the opposite showed a decrease (Herman-Stabl et al., 1995). It is important to note that mixed copers which not only showed high avoidant coping but also highly active coping in response to the snake displayed lower anxiety-like behaviors in response to low imminence threat, similar to active copers, compared to avoidant copers. This highlights the fact that high anxiety-like behavior in the face of uncertainty and ambiguity was linked specifically to the combination of both high avoidant and low active coping when the threat was highly imminent.

Adopting an avoidant coping style can reduce stress acutely by the removal of the individual from the stress-provoking environment, but may lead to prolonged stress in the future as the source of the stress is not overcome (Bardeen, 2015). In addition, natural processes that serve to reduce anxiety and conditioned threat responses such as desensitization or fear extinction are not experienced if the threat is wholly avoided. Consequently, the individual's avoidant coping style is reinforced *via* negative reinforcement and may gain predominance over active coping impulses. Taken together, a predominantly avoidant behavioral pattern to high imminence threat and a lack of active coping behaviors may be maladaptive as it impedes the resolution of threat *via* threat engagement/confrontation, leading to an increased vulnerability to anxiety.

In summary, factors characterizing behaviors in response to low imminence and high imminence threat were identified in the common marmoset on the human intruder and model snake tests respectively. Our findings of distinct factors representing avoidant and active coping support the bimodal theory of defensive behavior under high stress and threatening contexts. Taking an analytical approach to modeling the full repertoire of an animal's behavior revealed a differential pattern of active and avoidant behavioral responses as threat imminence is appraised.

With the factors identified, we demonstrate that a primarily avoidant coping style is associated with higher levels of anxiety-like behavior in response to low imminence threat, implicating a link between a predominantly avoidant coping strategy under high imminence threat and heightened sensitivity to uncertain/ambiguous situations associated with low imminence threat. These findings emphasize the importance of active coping strategies to alleviate stress reactivity and in helping individuals with avoidant coping styles suffering from excessive anxiety and fear. Insights from the paradigms described here promise to guide subsequent work interrogating the brain circuits involved in the control of active and avoidant coping behaviors and should facilitate translation to humans.

DATA AVAILABILITY STATEMENT

The datasets generated for this study are available on the Cambridge research repository Apollo (doi: 10.17863/CAM.49881) and available on request to the corresponding author.

ETHICS STATEMENT

The animal study was reviewed and approved by an Ethical Review Committee from the University of Cambridge and conducted in accordance with the project and personal licenses held by the authors under the UK Animals (Scientific Procedures) Act of 1986.

AUTHOR CONTRIBUTIONS

SQ conducted all analyses and prepared the manuscript. AS and AR contributed to the data and results analyses and to the manuscript, as joint senior authors. GC and LM performed behavioral testing and scoring.

FUNDING

This work was supported by an Medical Research Council (MRC) Programme grant (AR: MR/M023990/1) and performed within the Behavioural and Clinical Neuroscience Institute, University of Cambridge, funded jointly by the Wellcome Trust and MRC. SQ was supported from a scholarship from the Malaysian Public Service Department.

SUPPLEMENTARY MATERIAL

The Supplementary Material for this article can be found online at: https://www.frontiersin.org/articles/10.3389/fnbeh.2020.00034/full#supplementary-material.

REFERENCES

Agustín-Pavón, C., Braesicke, K., Shiba, Y., Santangelo, A. M., Mikheenko, Y., Cockroft, G., et al. (2012). Lesions of ventrolateral prefrontal or anterior orbitofrontal cortex in primates heighten negative emotion. *Biol. Psychiatry* 72, 266–272. doi: 10.1016/j.biopsych.2012.03.007

Allen, M. (ed.) (2017). "Median split of sample," in *The SAGE Encyclopedia of Communication Research Methods*, (Thousand Oaks, CA: SAGE Publications, Inc), 975–976.

Bardeen, J. R. (2015). Short-term pain for long-term gain: the role of experiential avoidance in the relation between anxiety sensitivity and emotional distress. *J. Anxiety Disord.* 30, 113–119. doi: 10.1016/j.janxdis.2014.12.013

Barros, M., Boere, V., Mello, E. L., and Tomaz, C. (2002). Reactions to potential predators in captive-born marmosets (*Callithrix penicillata*). *Int. J. Primatol.* 23, 443–454. doi: 10.1023/A:1013899931878

Bezerra, B. M., Barnett, A. A., Souto, A., and Jones, G. (2009). Predation by the tayra on the common marmoset and the pale-throated three-toed sloth. *J. Ethol.* 27, 91–96. doi: 10.1007/s10164-008-0090-3

Bezerra, B. M., and Souto, A. (2008). Structure and usage of the vocal repertoire of *Callithrix jacchus*. *Int. J. Primatol.* 29, 671–701. doi: 10.1007/s10764-008-9250-0

Blanchard, D. C., Griebel, G., Pobbe, R., and Blanchard, R. J. (2011). Risk assessment as an evolved threat detection and analysis process. *Neurosci. Biobehav. Rev.* 35, 991–998. doi: 10.1016/j.neubiorev.2010.10.016

Borsini, F., Podhorna, J., and Marazziti, D. (2002). Do animal models of anxiety predict anxiolytic-like effects of antidepressants? *Psychopharmacology* 163, 121–141. doi: 10.1007/s00213-002-1155-6

Carey, G. J., Costall, B., Domeney, A. M., Jones, D. N., and Naylor, R. J. (1992). Behavioural effects of anxiogenic agents in the common marmoset. *Pharmacol. Biochem. Behav.* 42, 143–153. doi: 10.1016/0091-3057(92)90458-r

Chan, D. W. (1995). Depressive symptoms and coping strategies among Chinese adolescents in Hong Kong. *J. Youth Adolesc.* 24, 267–279. doi: 10.1007/bf01537596

Cohen, J. (1988). *Statistical Power Analysis for the Behavioral Sciences.* Hillsdale, NJ: L. Erlbaum Associates.

Cohen, J. (1992). *A Power Primer*. Available online at: http://www.bwgriffin.com/workshop/Sampling A Cohen tables.pdf. Accessed August 22, 2018.

Crofoot, M. C. (2012). Why Mob? Reassessing the costs and benefits of primate predator harassment. *Folia Primatol.* 83, 252–273. doi: 10.1159/000343072

Cronbach, L. J. (1951). Coefficient alpha and the internal structure of tests. *Psychometrika* 16, 297–334. doi: 10.1007/BF02310555

Cross, N., and Rogers, L. J. (2006). Mobbing vocalizations as a coping response in the common marmoset. *Horm. Behav.* 49, 237–245. doi: 10.1016/j.yhbeh.2005.07.007

Epple, G. (1968). Comparative studies on vocalization in marmoset monkeys (*Hapalidae*). *Folia Primatol.* 8, 1–40. doi: 10.1159/000155129

Field, A. (2013). *Discovering Statistics Using IBM SPSS Statistics.* London: Sage.

Folkman, S., and Lazarus, R. S. (1980). An analysis of coping in a middle-aged community sample. *J. Health Soc. Behav.* 21, 219–239. doi: 10.2307/2136617

Fox, A. S., Shelton, S. E., Oakes, T. R., Davidson, R. J., and Kalin, N. H. (2008). Trait-like brain activity during adolescence predicts anxious temperament in primates. *PLoS One* 3:e2570. doi: 10.1371/journal.pone.0002570

Frydenberg, E., and Lewis, R. (2009). Relations among well-being, avoidant coping and active coping in a large sample of australian adolescents. *Psychol. Rep.* 104, 745–758. doi: 10.2466/pr0.104.3.745-758

Gomez, R., and McLaren, S. (2006). The association of avoidance coping style and perceived mother and father support with anxiety/depression among late adolescents: applicability of resiliency models. *Pers. Individ. Dif.* 40, 1165–1176. doi: 10.1016/j.paid.2005.11.009

Gottlieb, D. H., and Capitanio, J. P. (2013). Latent variables affecting behavioral response to the human intruder test in infant rhesus macaques (*Macaca mulatta*). *Am. J. Primatol.* 75, 314–323. doi: 10.1002/ajp.22107

Grupe, D. W., and Nitschke, J. B. (2013). Uncertainty and anticipation in anxiety: an integrated neurobiological and psychological perspective. *Nat. Rev. Neurosci.* 14, 488–501. doi: 10.1038/nrn3524

Herman-Stabl, M. A., Stemmler, M., and Petersen, A. C. (1995). Approach and avoidant coping: implications for adolescent mental health. *J. Youth Adolesc.* 24, 649–665. doi: 10.1007/bf01536949

Hook-Costigan, M. A., and Rogers, L. J. (1998). Eye preferences in common marmosets (*Callithrix jacchus*): influence of age, stimulus, and hand preference. *Laterality* 3, 109–130. doi: 10.1080/713754297

Indovina, I., Robbins, T. W., Núñez-Elizalde, A. O., Dunn, B. D., and Bishop, S. J. (2011). Fear-conditioning mechanisms associated with trait vulnerability to anxiety in humans. *Neuron* 69, 563–571. doi: 10.1016/j.neuron.2010.12.034

Kaiser, H. F. (1974). An index of factorial simplicity. *Psychometrika* 39, 31–36. doi: 10.1007/bf02291575

Kato, Y., Gokan, H., Oh-Nishi, A., Suhara, T., Watanabe, S., and Minamimoto, T. (2014). Vocalizations associated with anxiety and fear in the common marmoset (*Callithrix jacchus*). *Behav. Brain Res.* 275, 43–52. doi: 10.1016/j.bbr.2014.08.047

Kline, P. (2000). *The Handbook of Psychological Testing.* New York, NY: Routledge.

Koolhaas, J. M., de Boer, S. F., Coppens, C. M., and Buwalda, B. (2010). Neuroendocrinology of coping styles: towards understanding the biology of individual variation. *Front. Neuroendocrinol.* 31, 307–321. doi: 10.1016/j.yfrne.2010.04.001

Koolhaas, J. M., Korte, S. M., De Boer, S. F., Van Der Vegt, B. J., Van Reenen, C. G., Hopster, H., et al. (1999). Coping styles in animals: current status in behavior and stress- physiology. *Neurosci. Biobehav. Rev.* 23, 925–935. doi: 10.1016/s0149-7634(99)00026-3

Menzel, C. R. (1980). Head-cocking and visual perception in primates. *Anim. Behav.* 28, 151–159. doi: 10.1016/s0003-3472(80)80020-0

Perusini, J. N., and Fanselow, M. S. (2015). Neurobehavioral perspectives on the distinction between fear and anxiety. *Learn. Mem.* 22, 417–425. doi: 10.1101/lm.039180.115

Pineles, S. L., Mostoufi, S. M., Ready, C. B., Street, A. E., Griffin, M. G., and Resick, P. A. (2011). Trauma reactivity, avoidant coping, and PTSD symptoms: a moderating relationship? *J. Abnorm. Psychol.* 120, 240–246. doi: 10.1037/a0022123

Santangelo, A. M., Ito, M., Shiba, Y., Clarke, H. F., Schut, E. H., Cockcroft, G., et al. (2016). Novel primate model of serotonin transporter genetic polymorphisms associated with gene expression, anxiety and sensitivity to antidepressants. *Neuropsychopharmacology* 41, 2366–2376. doi: 10.1038/npp.2016.41

Seiffge-Krenke, I., and Klessinger, N. (2000). Long-term effects of avoidant coping on adolescents' depressive symptoms. *J. Youth Adolesc.* 29, 617–630. doi: 10.1023/a:1026440304695

Shiba, Y. (2013). Characterising trait anxiety in the common marmoset (Callithrix jacchus): Investigations into behavioural, psychophysiological and cognitive phenotypes. *PhD dissertation, University of Cambridge* doi: 10.17863/CAM.28

Shiba, Y., Santangelo, A. M., Braesicke, K., Agustín-Pavón, C., Cockcroft, G., Haggard, M., et al. (2014). Individual differences in behavioral and cardiovascular reactivity to emotive stimuli and their relationship to cognitive flexibility in a primate model of trait anxiety. *Front. Behav. Neurosci.* 8:137. doi: 10.3389/fnbeh.2014.00137

Skodol, A. E., Oldham, J. M., Hyler, S. E., Stein, D. J., Hollander, E., Gallaher, P. E., et al. (1995). Patterns of anxiety and personality disorder comorbidity. *J. Psychiatr. Res.* 29, 361–374. doi: 10.1016/0022-3956(95)00015-w

Souto, A., Bezerra, B., Schiel, N., and Huber, L. (2007). The saltatory search in free-living common marmosets: environmental and age influences. *Int. J. Primatol.* 28, 881–893. doi: 10.1007/s10764-007-9165-1

Stevens, J. P. (1992). *Applied Multivariate Statistics for the Social Sciences.* Hillsdale, NJ: L. Erlbaum Associates.

Weger, M., and Sandi, C. (2018). High anxiety trait: a vulnerable phenotype for stress-induced depression. *Neurosci. Biobehav. Rev.* 87, 27–37. doi: 10.1016/j.neubiorev.2018.01.012

Williamson, D. E., Coleman, K., Bacanu, S. A., Devlin, B. J., Rogers, J., Ryan, N. D., et al. (2003). Heritability of fearful-anxious endophenotypes in infant rhesus macaques: a preliminary report. *Biol. Psychiatry* 53, 284–291. doi: 10.1016/s0006-3223(02)01601-3

Conflict of Interest: The authors declare that the research was conducted in the absence of any commercial or financial relationships that could be construed as a potential conflict of interest.

frontiers in Behavioral Neuroscience

ORIGINAL RESEARCH
published: 26 November 2020
doi: 10.3389/fnbeh.2020.00157

G Protein-Coupled Estrogen Receptor 1 Knockout Deteriorates MK-801-Induced Learning and Memory Impairment in Mice

Chun Zhang[1,2†], Qiang Liu[1†], Chun-Yang Yu[1], Feng Wang[1], Yu Shao[2], Kui-Sheng Sun[1], Tao Sun[1] and Juan Liu[1,2]**

[1]Ningxia Key Laboratory of Cerebrocranial Diseases, Ningxia Medical University, Yinchuan, China, [2]Institute of Basic Medical Sciences, School of Basic Medical Sciences, Ningxia Medical University, Yinchuan, China

OPEN ACCESS

Edited by:
Cesar Venero,
National University of Distance Education (UNED), Spain

Reviewed by:
Annie Andrieux,
CEA Grenoble, France
José Luis Trejo,
Consejo Superior de Investigaciones Científicas (CSIC), Spain

***Correspondence:**
Juan Liu
ryuken0518@163.com
Tao Sun
suntao_nxmu@163.com

[†]These authors have contributed equally to this work

Specialty section:
This article was submitted to Behavioral Endocrinology, a section of the journal Frontiers in Behavioral Neuroscience

Received: 19 April 2020
Accepted: 10 August 2020
Published: 26 November 2020

Citation:
Zhang C, Liu Q, Yu C-Y, Wang F, Shao Y, Sun K-S, Sun T and Liu J (2020) G Protein-Coupled Estrogen Receptor 1 Knockout Deteriorates MK-801-Induced Learning and Memory Impairment in Mice. Front. Behav. Neurosci. 14:157. doi: 10.3389/fnbeh.2020.00157

The role of estrogen receptors in neuroprotection and cognition has been extensively studied in humans over the past 20 years. Recently, studies have shifted their focus to the use of selective estrogen receptor modulators in the treatment of mental illnesses in the central nervous system. We conducted this study to test the behavioral changes shown by G protein-coupled estrogen receptor 1 knockout (GPER1 KO) and wild-type (WT) mice with MK-801-induced schizophrenia (SZ). GPER1 KO and WT mice received intraperitoneal injections of MK-801 for 14 continuous days. Behavioral, learning and memory, and social interaction changes were evaluated by using the IntelliCage system, open-field, three-chamber social interaction, and novel object recognition tests (NORT). The protein expression levels of the NR2B/CaMKII/CREB signaling pathway were tested *via* Western blot analysis. The KO SZ group was more likely to show impaired long-term learning and memory function than the WT SZ group. Learning and memory functions were also impaired in the KO Con group. MK-801 administration to the GPER1-KO and WT groups resulted in memory deficiencies and declining learning capabilities. GPER1 deficiency downregulated the expression levels of proteins related to the NR2B/CaMKII/CREB signaling pathway. Our study suggested that GPER1 played an important role in cognitive, learning, and memory functions in the MK-801-induced mouse model of SZ. The mechanism of this role might partially involve the downregulation of the proteins related to the NR2B/CaMKII/CREB signaling pathway. Further studies should focus on the effect of GPER1 on the pathogenesis of SZ *in vivo* and *in vitro*.

Keywords: schizophrenia, MK-801, behavioral change, intellicage, learning and memory capacity

INTRODUCTION

Schizophrenia (SZ) is a neurological disorder that affects approximately 0.7–1% of the population (Valton et al., 2017; Marder and Cannon, 2019). The symptoms of this disorder include delusions, movement disorders, anhedonia, hallucinations, and cognitive deficits (Marder and Cannon, 2019). SZ is a chronic disease that negatively affects all aspects of a patient's life. Although

most patients with SZ can live in a community, the outcome of this mental disease is generally poor, and some patients with SZ may require chronic institutional care (Borelli and Solari, 2019).

The role of estrogens and estrogen receptors in neuroprotection and cognition has been extensively studied in humans over the past 20 years. Results obtained with rodent models suggest that estrogen treatment can improve memory and cognition functions in various neurological disorders (Bean et al., 2014). For example, a previous study showed that postmenopausal women receiving estrogen therapy may experience improved cognition functions, including verbal memory, oral expression, and information processing (Persad et al., 2009). These findings suggest that estrogens can be used in the clinical therapy of patients with SZ to ameliorate cognitive function. Recent studies have focused on the use of selective estrogen receptor modulators in the treatment of mental illnesses in the central nervous system (Mirkin and Pickar, 2015). Although these modulators may have a positive influence on cognition and memory and exhibit other effects, the related signaling pathways are not fully understood.

G protein-coupled estrogen receptor 1 (GPER1) is a G protein-coupled receptor that was previously known as GPR30 (Funakoshi et al., 2006). GPER1 is expressed in the plasma membranes of neurons in the hippocampus and prefrontal cortex of the brain (Brailoiu et al., 2007; Akama et al., 2013; Almey et al., 2014). In contrast to estrogen receptor α/β, the classic nuclear function of GPER1 is mainly exerted through activation of nongenomic estrogen signaling pathway members, including the second messengers Ca^{2+} and cyclic adenosine monophosphate, and tyrosine kinase receptor. Studies have shown that estrogen may induce synaptic and cognitive functions through the GPER1-mediated signaling pathway (Gaudet et al., 2015; Waters et al., 2015).

The regulatory effects of GPER1 on the N-methyl-d-aspartate receptor (NMDAR) complex and cognition has received little attention. GPER1 may regulate NMDAR expression and function by affecting NMDAR subunit 2B (NR2B) phosphorylation, which affects brain cognitive function. Potentially, GPER1 can phosphorylate NR2B and regulate the NR2B/CaMKII/CREB pathway. In this study, we aimed to determine whether GPER1 deficiency is related to MK-801-induced SZ dysfunction (such as impaired spatial learning, social communication, and executive function) in mice. The reduced expression of the NR2B subunit in SZ has been investigated in previous work (Kristiansen et al., 2010; Yang et al., 2015; Gulchina et al., 2017; Leung and Ma, 2018). Given that GPER1 is a promising therapeutic target in SZ, the present study investigated changes in the behavioral phenotype and NR2B/CaMKII/CREB signaling pathway related to GPER1 in MK-801-induced SZ.

MATERIALS AND METHODS

Mice

GPER1-KO mice that had been knocked out for 17 nucleotides were obtained from Professor Rong Wei Fang (Shanghai Jiaotong University). Wild-type (WT) mice were provided by the Experimental Animal Center of Ningxia Medical University. Mice (7–8 weeks old; male) were randomly divided into experimental groups and then acclimated for 7 days prior to MK-801 intervention. All mice were housed (four mice/cage) in an animal room at 22 ± 2°C with a 12 h light/dark cycle and lights on at 7:30 AM. They had access to water and food *ad libitum*. Only male WT C57BL/6 and GPER1-KO mice were used in the research. This work was conducted in accordance with the Animal Care Committee of Ningxia Medical University (Protocol approval number: 2019-152). Animal suffering was minimized. WT and KO mice that had been induced with MK-801 (0.6 mg/kg/day, Sigma–Aldrich, Czechia) *via* intraperitoneal injection for 14 consecutive days were designated as the experimental groups: WT SZ and KO SZ (n = 14 per group), respectively. WT and KO mice that had been injected with saline (SAL) were designated as controls (WT Con and KO Con, n = 14 per group). IntelliCage research was performed with five C57BL/6 and five GPER1-KO MK-801-treated male mice, as well as five C57BL/6 and five GPER1-KO SAL-treated male mice. The classical behavior studies involved nine mice from each group.

Behavioral Assessment

Classical Behavior Studies

On days of classical behavioral testing, mice were transferred to the behavioral facility 24 h in advance to begin the behavioral assessment for adaptation. All classical behavioral procedures (**Figures 1A**, **2A**) were performed between 06:30 and 11:30 AM (experimental preparation stage: 6:30–7:30 AM and formal experiment stage: 7:30–11:30 AM).

Open Field Test

The mice were tested in a Plexiglass open field (OF) after 14 successive days of MK-801 administration to quantify stereotypical behavior and general locomotor activity. Mice were placed in a square OF arena (50 × 50 × 50 cm) and allowed to move freely for 10 min. The time that each mouse spent in the middle of the OF and total distance moved were recorded by using an automatic video tracking system (Smart version 3.0; Panlab, S.L.U., Barcelona, Spain).

Social Interaction Test

Mice were tested in a sociability testing apparatus 1 day after the OF test. Social communication and social response to new individuals were evaluated by using a three-chamber apparatus. The three-chamber test consisted of three stages. First, a mouse was transferred to the three-chamber polycarbonate facility and allowed to explore freely for 10 min for habituation. Second, the test mouse was transferred gently to the middle area, and the door on both sides was closed. An unfamiliar, age-matched male mouse was placed in a small cage in the upper area. The doors on both sides of the gates were opened, and the test mouse was allowed to explore for 10 min at will. Last, the test mouse was transferred into the middle area. Both gates were closed again, and a second, unfamiliar age-matched male

mouse was placed in the small cage in the lower area. The social capability of mice was expressed by using the preference index (PI).

$$PI_{S1\text{-}Em} = (A - B)/(A + B)$$

$PI_{S1\text{-}Em}$: Social communication capability; A: Time spent in empty cage; B: Time spent with an unfamiliar, age-matched male mouse.

$$PI_{S2\text{-}S1} = (C - B)/(C + B)$$

$PI_{S2\text{-}S1}$: New social individual's capability; B: Time spent with an unfamiliar, age-matched male mouse.

C: Time spent with a second, unfamiliar age-matched male mouse.

Novel Object Recognition Test

Mice were subjected to the novel object recognition test (NORT) at 1 day after the social interaction test. The NORT was used to test the animal's ability to recognize a novel object (position) and preference for novel objects (position; Binyamin et al., 2019) in a familiar environment. The preference for a novel object (position) was expressed as PI as follows: ($Time_{novel\ object(position)}$/($Time_{novel\ object(position)}$+ $Time_{familiar\ object(position)}$; Loh et al., 2015; Dos et al., 2019; Kárpáti et al., 2019; Liu et al., 2019). A mouse that exhibited less than 2 s of the total time exploring objects (position; $Time_{novel\ object(position)}$+ $Time_{familiar\ object(position)}$) was excluded from the analysis. Object recognition testing occurred in two stages, namely, novel object recognition and position recognition. The mice were allowed to explore a field with two identical objects for 5 min during a familiarization trial. This experiment was performed to test the learning and memory of mice for novel objects or positions under free movement. Nonspatial learning and memory capability were evaluated *via* the NORT to verify the effect of GPER1-KO on the recognition and memory functions of SZ mice. After subjecting the mice to 5 min of familiarization and training, the familiar object was replaced with a novel object. The NORT was performed after the mice had rested for 5 min. During the training phase of the novel position recognition test, a mouse was placed in the experimental field. Two identical objects were placed on the same side of the experimental field. During the 5 min training phase, the mouse could identify two objects. One object was placed at the opposite corner of the other object before the test. The novel position recognition test was carried out. The identification time in this experiment was set as 5 min. The PI of the novel object (position) was used to indicate the ability of the mouse to explore the novel object (position).

$$PI = N/(N + F)$$

N: Exploring new objects (positions) time; F: Exploring old object (position) time.

Intellicage

The Intellicage test was performed with mice by using the IntelliCage system, an automated apparatus that monitors the cognitive behavior of multiple mice in a normal living environment (NewBehavior AG[1]). The system contained four intelligent learning condition corners. Each corner had two drinking bottles, and the mouse triggered a sensor chip to open the door by nose-poking and drinking freely. The system automatically recorded the numbers and times the door was opened and the water bottle nozzle was licked. It traced the behavior of the mouse through a transceiver. The IntelliCage system was used to set different experimental procedures to monitor the general activity, spatial learning, and executive function of mice automatically. At 14 days after MK-801 administration, a miniature signal sensor was implanted, and the mice were transferred to an IntelliCage device. During the experiment process, a single administration of MK-801 (0.6 mg/kg) was injected to keep the SZ-like symptoms on days 27 and 34, respectively (**Figures 2A,B**). The general activity, spatial learning, and executive function of mice were detected. The Intellicage system test protocol included five phases: simple adaptation, nose-poke adaptation, place preference learning, reversal learning, and novel object cognition. (1) Free adaptation stage: all mice could enter the cage and obtain water freely, and all corners and doors were open. Before starting the test programs, the mice were allowed to habituate for 1 day in the IntelliCage with free access to food and water. Following habituation, the mice were trained to obtain access to drinking spouts in all four corners after nose-poking. (2) Nose-poke adaptation stage: for 5 days, all doors were closed, and mice had to open the appropriate door through nose-poking to drink. The door remained open for 7 s. The door opened only when mice visited. Therefore, the mice could gain access to water when visiting. The least-preferred corners by each mouse were identified to guide the design of the next module. (3) Place-learning stage: this phase was similar to phase 2, but the mice could only access water from one corner. Spatial location learning was tested to explore the changes in the spatial positioning and recognition memory of mice. The test time was 7 days. The corners for which the mice showed the least preference for nose-poking were set as "correct," and the remaining corners were set as "wrong." Although the experimental mice could poke all corners, the door to the drinking water would open only when the mice poked the "correct" corner. Position-learning capability was evaluated by calculating the error rate of the mice. (4) Reversal learning stage: the identified water corner was replaced by the corner opposite to the one in the place-learning phase. For 7 days, the diagonal corners of the "correct" corners in the spatial position learning of mice were set as the "correct" corners, and the remaining corners were set as the "wrong" corners. The mice may enter all corners at will, and their exploration activities, error rates, and capability to explore new "correct" corners were analyzed. (5) Novel object recognition stage: LED lights in one corner were turned on randomly, and mice could enter and exit all corners and drink water freely. The LED lights in one corner were turned on daily, and the LED lights in different corners were turned in a counter-clockwise direction to monitor the drinking times of mice in the corners where the LED lights were lit. The preference of mice for "new things" were analyzed for 4 days.

[1]http://www.newbehavior.com

Western Blot Analysis

One Week After the Object Recognition Test, Half of the Animals Were Weighed and Decapitated

The mice were sacrificed 1 day after the completion of the classical behavioral tests, and their brains were dissected and isolated. The hippocampus of each mouse was homogenized on ice by using a tissue homogenizer with RIPA buffer. After 15 min of centrifugation at 12,500 rpm and 4°C, the protein concentration was tested *via* the Bradford method. A certain volume of loading buffer was added to each protein sample for denaturation at 100°C for 6 min. After performing SDS–polyacrylamide gel electrophoresis, the targeted proteins were transferred onto PVDF membranes and then blocked with 1% BSA for 1 h. The membranes were incubated with primary antibodies at 4°C overnight (8–12 h), washed with TBST three times, and incubated with secondary antibodies for 1 h at room temperature. Target bands were scanned and analyzed by using the Odyssey Infrared imaging system (Odyssey, LICOR). The following primary antibodies were utilized: mouse anti-NMDAR2B (Abcam, ab181102, 1:500), rabbit anti-phospho-NMDAR2B (Abcam, ab181102, 1:1,000; sites: Tyr1070), mouse anti-CaMKII-α (Cell Signaling Technology, #50049, 1:1,000), rabbit anti-phospho-CaMKII-α (Cell Signaling Technology, #12716, 1:1,000, sites: Thr286), rabbit anti-CREB (Abcam, ab32515, 1:2,000), rabbit anti-phospho-CREB (Abcam, ab32096, 1:1,000, sites: S133), and rabbit anti-β-actin (ZSGB-bio, ZM-0001, 1:1,000).

Data Analysis

Data were analyzed by using SPSS 24.0 software. Unpaired two-tailed *t*-test and two-way ANOVA with Bonferroni or Tukey–Kramer multiple comparison *post hoc* tests were used to determine differences among groups. *P*-values less than 0.05 were considered statistically significant.

Results

Behavioral Studies

OF Test

GPER1 knockdown and MK-801 treatment only slightly influenced stereotypical behaviors ($F_{(1,32)} = 1.563$, $p = 0.22$, two-way ANOVA; **Figure 1B**) and hyperlocomotor activity ($F_{(1,32)} = 0.175$, $p = 0.68$, two-way ANOVA; **Figure 1C**) in the OF test. Meanwhile, our results demonstrated that GPER1-KO mice had higher total distance ($F_{(1,32)} = 28.46$, $p < 0.001$, two-way ANOVA; **Figure 1C**) and spent less time in the central area ($F_{(1,32)} = 17.36$, $p < 0.001$, two-way ANOVA; **Figure 1B**) than WT Con mice. WT SZ mice spent less time in stereotypical behavior ($F_{(1,32)} = 98.75$, $p < 0.001$, two-way ANOVA; **Figure 1B**) and significantly higher locomotion ($F_{(1,32)} = 28.46$, $p < 0.001$, two-way ANOVA; **Figure 1C**) than WT Con mice. *Post hoc* analysis showed that GPER1-KO exacerbated the impairment of hyperlocomotion ($t = 7.873$, $p < 0.001$; **Figure 1C**) and anxiety of mice ($t = 12.96$, $p < 0.001$; **Figure 1B**) with SZ induced by MK-801. Additionally, KO SZ mice showed increased total distance ($t = 5.589$, $p < 0.001$; $t = 12.55$, $p < 0.001$; **Figure 1C**) and spent less time in the central area ($t = 3.677$, $p = 0.002$; $t = 5.956$, $p < 0.001$; **Figure 1B**) than WT SZ and KO Con mice.

Social Interaction Test

In the second phase, KO Con ($F_{(1,32)} = 36.59$, $p < 0.001$, two-way ANOVA; **Figure 1D**) and WT SZ ($F_{(1,32)} = 59.44$, $p < 0.001$, two-way ANOVA; **Figure 1D**) mice showed less preference for the first unfamiliar mouse than WT Con mice. In the third stage, the KO Con group ($F_{(1,32)} = 26.62$, $p < 0.001$, two-way ANOVA; **Figure 1E**) and WT SZ ($F_{(1,32)} = 121.2$, $p < 0.001$, two-way ANOVA; **Figure 1E**) showed less preference for the second unfamiliar mouse than the WT Con group. GPER1 knockdown and MK-801 treatment had no effects on sociability ($F_{(1,32)} = 3.84$, $p = 0.06$, two-way ANOVA; **Figure 1D**) and social novelty recognition ($F_{(1,32)} = 0.62$, $p = 0.44$, two-way ANOVA; **Figure 1E**). Compared with mice in the WT SZ and KO Con groups, those in the KO SZ group had less preference for the first ($t = 5.363$, $p < 0.001$; $t = 6.049$, $p < 0.001$; **Figure 1D**) and second unfamiliar mice ($t = 6.258$, $p < 0.001$; $t = 17.13$, $p < 0.001$; **Figure 1E**). KO SZ mice exhibited abnormal social interaction ability with their conspecifics and novel conspecifics, indicating that GPER1 KO impaired social interaction and novelty recognition in SZ mice.

NORT

The WT SZ group showed a significantly lower preference for novel objects ($F_{(1,32)} = 343.2$, $p < 0.001$, two-way ANOVA; **Figure 1F**) and placement ($F = 122.8$, $p < 0.001$, two-way ANOVA; **Figure 1G**) than the WT Con group. Compared with WT Con mice, KO Con mice had less preference for novel objects ($F_{(1,32)} = 12.24$, $p = 0.001$, two-way ANOVA; **Figure 1F**) and placement ($F = 32.94$, $p < 0.001$, two-way ANOVA; **Figure 1G**). Meanwhile, the ability of KO SZ mice to identify novel objects was lower than that of KO Con group mice ($t = 10.82$ $p < 0.001$; **Figure 1F**). Compared with the WT SZ group, the KO SZ group showed reduced capability to recognize novel placement ($t = 6.265$, $p < 0.001$; **Figure 1G**). There was no interaction of GPER1 knockdown and MK-801 treatment of novel object ($F_{(1,32)} = 1.563$, $p = 0.22$, two-way ANOVA; **Figure 1F**) and novel position ($F_{(1,32)} = 0.175$, $p = 0.68$, two-way ANOVA; **Figure 1G**).

Intellicage Behavioral Experiment

We used the Intellicage system to further investigate the behavioral differences of mice in different groups. The free adaptation phase showed no difference among the four groups in terms of the number of visits and number of nose pokes. There was no statistically significant difference between-group × within-group interaction (**Figures 2C,D**) observed. During the nosepoke adaptation phase, the number of visits significantly differed among the four groups and was lower in GPER1 KO mice ($F_{(1,16)} = 31.62$, $p < 0.001$, two-way ANOVA; **Figure 2E**) and WT SZ group ($F_{(1,16)} = 9.83$, $p = 0.006$, two-way ANOVA; **Figure 2E**) than in WT Con mice. During this phase, the number of visits in the KO Con group was higher than that in the KO SZ group ($t = 2.78$, $p = 0.0652$; **Figure 2E**). WT SZ mice exhibited a higher number of visits than KO SZ mice ($t = 1.021$, $p = 0.8572$; **Figure 2E**). The number of nose pokes showed

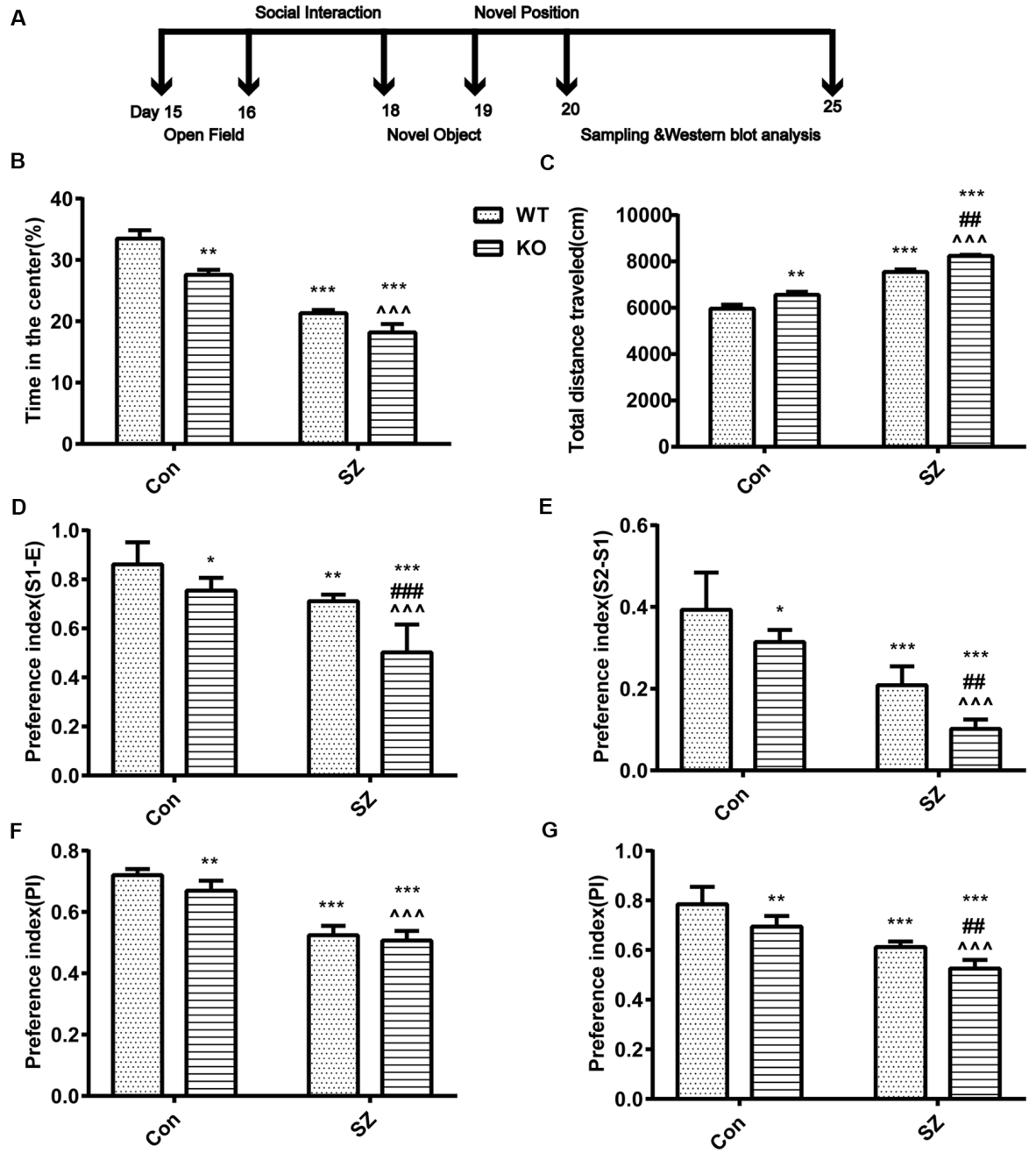

FIGURE 1 | G protein-coupled estrogen receptor 1 (GPER1) deficit increases hyperlocomotion and anxiety-like behavior. **(A)** Classical behavioral experiment design schedule. **(B)** Time spent in the center area among different groups of mice. **(C)** Total distances traveled during the open field test are depicted. **(D,E)** Performance on the social interaction test. Different groups discriminated against the novel individual during the social recognition task. Compared with wild-type (WT) Con mice, knockout (KO) Con mice, and WT schizophrenia (SZ) mice showed less preference for the two unfamiliar mice. Compared with KO Con mice, KO SZ mice showed less preference for the two unfamiliar mice. Compared with WT SZ, KO SZ mice showed less preference for the two unfamiliar mice. **(F)** Novel object preference index (PI). Compared with WT Con mice, KO SZ and KO Con mice spent less time exploring the novel object during the test trial phase. **(G)** Novel placement PI. WT SZ and KO Con mice spent less time exploring novel placement during the test trial phase than WT Con mice. KO SZ mice showed less preference for novel placement than KO Con and WT SZ mice. Data represent the mean ± SD of $n = 9$ mice/group and were analyzed *via* two-way ANOVA followed by *post hoc* test (*$p < 0.05$, **$p < 0.01$, ***$p < 0.001$; $^{\#\#}P < 0.01$, $^{\#\#\#}p < 0.001$; ^^^$p < 0.001$; *WT Con vs. WT SZ, KO Con, KO SZ; $^{\#}$WT SZ vs. KO SZ; ^KO Con vs. KO SZ).

lower degrees of decline in KO Con ($F_{(1,16)} = 5.773$, $p = 0.029$, two-way ANOVA; **Figure 2**F) and WT SZ mice ($F_{(1,16)} = 41.91$, $p < 0.001$, two-way ANOVA; **Figure 2F**) compared with those in WT Con mice. At the same time, the number of nose pokes in the KO SZ group significantly decreased ($t = 2.957$, $p = 0.048$; **Figure 2F**) compared with that in the KO Con group.

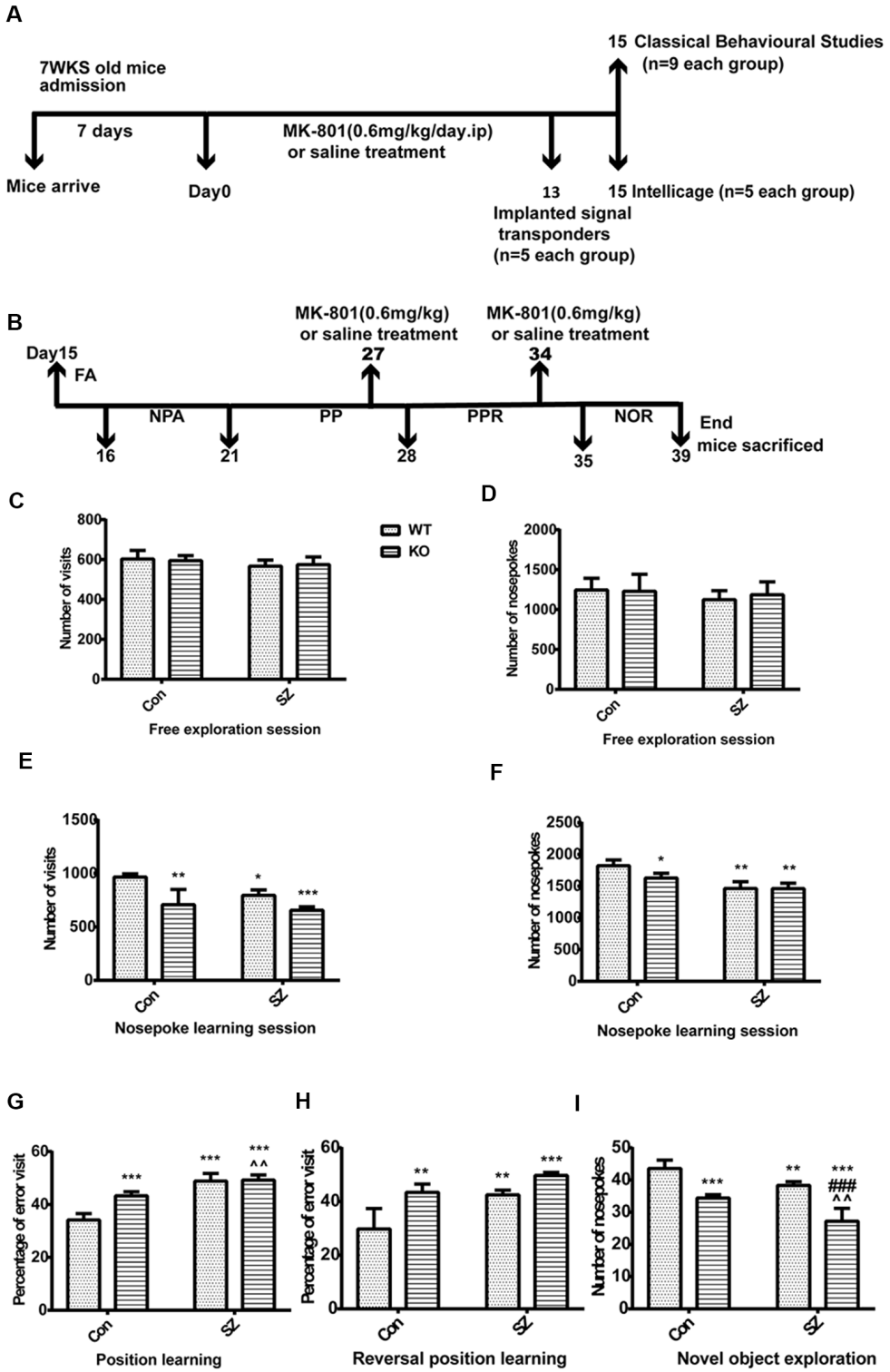

FIGURE 2 | (A) Drug administration and the behavioral experiment protocol in this study. **(B)** Intellicage experiment design schedule for assessing multiple cognitive domains with advantages in the validation and characterization of expected cognitive deficits. FA, free adaptation; NPA, nose-poke adaptation; PP, place preference; PPR, place preference reversal; NOR, novel object recognition. **(C,D)** Free exploratory session. No difference was observed among the four groups in terms of the number of visits and number of nose pokes. **(E,F)** Nosepoke learning session, including the number of visits and nose pokes. Compared with those in the WT Con group, the number of visits decreased and the number of nose pokes remained the same in the other groups. **(G)** Position learning. The WT SZ and KO SZ groups

(*Continued*)

FIGURE 2 | Continued
showed a higher percentage of erroneous visits than the WT Con group. The KO Con group showed a higher percentage of erroneous visits than the WT Con group. **(H)** Reversal position learning. KO SZ, KO Con, and WT SZ mice showed a higher percentage of erroneous visits than WT Con mice. **(I)** Novel object exploration. WT Con mice had a higher number of nose pokes than the other groups. Data represent the mean ± SD of $n = 5$. Data were analyzed *via* two-way ANOVA followed by Bonferroni *post hoc* test (*$p < 0.05$, **$p < 0.01$, ***$p < 0.001$; ###$p < 0.001$; ^^$p < 0.01$; *WT Con vs. WT SZ, KO Con, KO SZ; #WT SZ vs. KO SZ; ^KO Con vs. KO SZ).

GPER1 knockdown and MK-801 treatment significantly affected the number of nose pokes ($F_{(1,16)} = 5.446$, $p = 0.033$, two-way ANOVA; **Figure 2F**). The place learning results showed that the percentage of erroneous visits was higher in the WT SZ group ($F_{(1,16)} = 102.7$, $p < 0.0001$, two-way ANOVA; **Figure 2G**) than in the WT Con group, and KO Con mice exhibited a higher rate of errors in this stage than WT Con mice ($F_{(1,16)} = 21.84$, $p = 0.0003$, two-way ANOVA; **Figure 2G**). A significant effect was seen in the following parameters: genotype × MK-801 interaction in position learning ($F_{(1,16)} = 18.31$, $p = 0.0006$, two-way ANOVA; **Figure 2G**). Meanwhile, KO SZ mice had a higher percentage of erroneous visits than KO Con mice ($t = 4.14$, $p = 0.0038$; **Figure 2G**). In the reversal learning phase, the percentage of erroneous visits in the KO SZ group was higher than that in the WT SZ group ($t = 7.71$, $p < 0.001$; **Figure 2H**). WT Con mice showed a lower percentage of erroneous visits than KO Con mice ($F_{(1,16)} = 30.66$, $p < 0.0001$, two-way ANOVA; **Figure 2H**) and WT SZ mice ($F_{(1,16)} = 25.17$, $p = 0.0001$, two-way ANOVA; **Figure 2H**). There was no interaction of GPER1 knockdown and MK-801 treatment of the reversal learning phase ($F_{(1,16)} = 2.835$, $p = 0.11$, two-way ANOVA; **Figure 2H**). The results from the new object recognition stage showed that the number of nose pokes in the WT SZ ($F_{(1,16)} = 30.91$, $p < 0.0001$, two-way ANOVA; **Figure 2I**) and KO Con groups ($F_{(1,16)} = 81.44$, $p < 0.0001$, two-way ANOVA; **Figure 2I**) was lower than that in the WT Con group. The KO SZ group displayed a lower number of nose pokes than the WT SZ group ($t = 5.951$, $p < 0.001$; **Figure 2I**). Additionally, our results revealed the weak effect of GPER1 knockdown and MK-801 treatment ($F_{(1,16)} = 0.7807$, $p = 0.39$, two-way ANOVA; **Figure 2I**).

Western Blot Analysis

We tested several key proteins of the NR2B/CaMKII/CREB pathway in the hippocampus of GPER1-KO mice to investigate the possible mechanism by which MK-801 induced SZ-like symptoms (**Figure 3A**). GPER1 knockdown and MK-801 treatment significantly influenced the expression levels of the following proteins: CREB ($F_{(1,16)} = 4.761$, $p = 0.0444$, two-way ANOVA; **Figure 3F**), p-CREB ($F_{(1,16)} = 15.11$, $p = 0.0013$, two-way ANOVA; **Figure 3G**), CaMKIIα ($F_{(1,16)} = 5.539$, $p = 0.0317$, two-way ANOVA; **Figure 3D**), p-CaMKIIα ($F_{(1,16)} = 27.08$, $p < 0.0001$, two-way ANOVA; **Figure 3E**), and NR2B-pTyr-1070 ($F_{(1,16)} = 199.3$, $p < 0.0001$, two-way ANOVA; **Figure 3C**). These results suggested that GPER1 deficiency might cause a reduction in the levels of proteins related to the NR2B/CaMKII/CREB signaling pathway in the mouse hippocampus, and MK-801 aggravated this change. Meanwhile, we found there was no interaction of GPER1 knockdown and MK-801 treatment of NR2B expression ($F_{(1,16)} = 2.182$, $p = 0.1591$, two-way ANOVA; **Figure 3B**). Overall, these results proved that the expression levels of NR2B, NR2B-pTyr-1070, CaMKIIa, p-CaMKIIa, CREB, and p-CREB decreased in the presence of SZ symptoms (**Figures 3B–G**). Therefore, the NR2B/CaMKII/CREB signaling pathway in the hippocampus might be involved in the behavioral effects induced by MK-801 in KO SZ mice.

DISCUSSION

SZ is a neuropsychiatric disease with gender differences (Bratek et al., 2016). Female patients with SZ are usually older and have milder symptoms than male patients with SZ. Clinically, estrogen may improve the cognitive impairment caused by SZ. GPER1, a newly identified estrogen receptor, may regulate the rapid nongenetic effect of estrogen. Studies have proven that GPER1 can promote spatial working memory in ovariectomized animals *via* the systemic injection of a GPER1 agonist (Gurvich et al., 2019). GPER1 can regulate anxiety-related emotions, spatial learning, and memory (Hammond et al., 2009; Kastenberger and Schwarzer, 2014; Kim et al., 2016). NMDAR plays a key role in the etiology and drug treatment of SZ (Lee and Zhou, 2019). Numerous studies have confirmed that NMDAR antagonists induce SZ-related behavior (Jeon et al., 2017). Meanwhile, our previous studies (Ding et al., 2017, 2019) and other work (Seillier and Giuffrida, 2009; Jacklin et al., 2012; Karamihalev et al., 2014; Li et al., 2016) found cognition impairment and alterations in anatomical and neurochemical aspects in a mouse subchronic model of SZ induced by the intraperitoneal injection of MK-801 for 14 consecutive days. Given that SZ is a chronic psychiatric disorder, subchronic administration with MK-801 might better represent the enduring cognition deficits of SZ (Karamihalev et al., 2014; Xiu et al., 2014), meaning it may serve as a robust model for the disease. Thus, the subchronic model of SZ was utilized in this study. Moreover, the dose of MK-801 (0.6 mg/kg/day) was utilized in our previous research (Huang et al., 2018; Ding et al., 2019). Based on the hypothesis of this past study, we evaluated the effects of GPER1 deficiency on the hyperlocomotion, stereotypical behaviors, novel object recognition, social interaction, general activity, spatial learning, and the executive capability of the mouse subchronic model of SZ. We also investigated whether GPER1 deficiency is associated with the expression levels of several proteins in the NR2B/CaMKII/CREB signaling pathway in SZ-like mice induced by MK-801. Previous studies found that the male hippocampus expresses all three major estrogen receptors (ER, ER, and GPER1; Hazell et al., 2009; Loh et al., 2015). Meanwhile, no apparent gender differences were observed in the distribution of GPER1/GPR30 in the adult mouse brain (Hazell et al., 2009). GPER1 is an extranuclear estrogen receptor whose functions in the central nervous system are largely unknown. However, it can activate kinase cascades and accelerate calcium flux within cells (Hadjimarkou and Vasudevan, 2018). Studies have demonstrated that GPER1 signaling in the brain is a

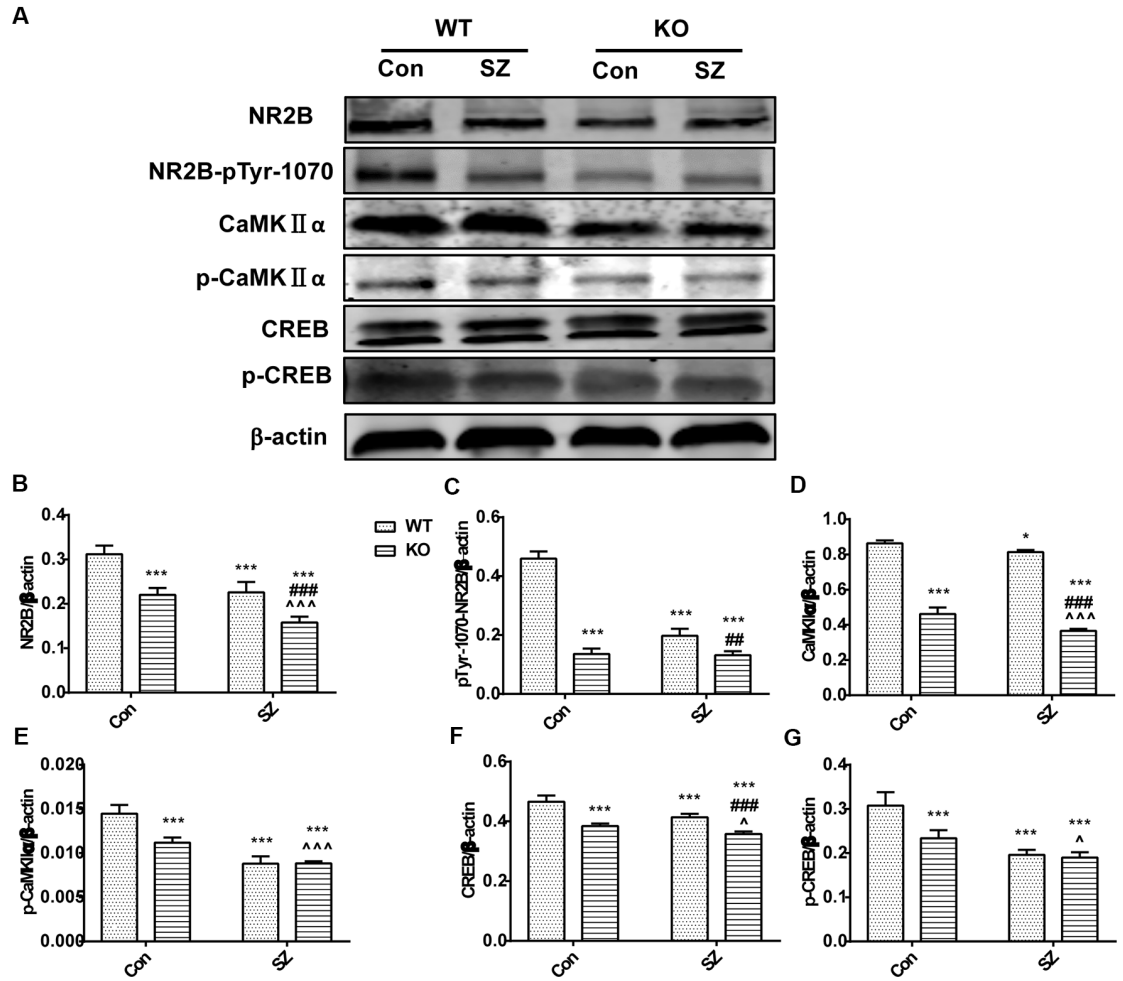

FIGURE 3 | GPER1 deficiency downregulated the NMDAR subunit 2B (NR2B)/CaMKII/CREB signaling cascade in the hippocampus of the mouse models of SZ-like phenotypes. **(A)** Representative immunoblots showing the protein levels of NR2B, pTyr-1070-NR2B, p-CaMKIIα, CaMKIIα, CREB, and phospho-CREB in the hippocampus detected by Western blot analysis. **(B–G)** Histograms showing the quantification of protein band densities that had been normalized to β-actin. Data are presented as mean ± SD of $n = 5$ mice/group. Data were analyzed *via* two-way ANOVA followed by Bonferroni *post hoc* test (*$p < 0.05$, ***$p < 0.001$; ##$p < 0.01$, ###$p < 0.001$; ^$p < 0.05$, ^^^$p < 0.001$; *WT Con vs. WT SZ, KO Con, KO SZ; #WT SZ vs. KO SZ; ^KO Con vs. KO SZ).

response to estrogen, and it performs neuroprotection, cognition, and memory enhancement functions (Vajaria and Vasudevan, 2018). Other studies have reported that GPER1 improves spatial memory and promotes the generation of newborn neurons in the hippocampus; moreover, it may be involved in the release of neurotransmitters (Almey et al., 2015; Briz et al., 2015). Recently, the role of GPER1 in the regulation of mood disorders has been described (Kastenberger and Schwarzer, 2014). Studies on rodents have reported that there is an anti-depressant-like effect of estradiol that is mediated by GPER1, leading to the hypothesis that GPER1 might be an innovative target for the treatment of depression. The serum of patients with generalized anxiety disorder shows increased GPER1 levels, which correlate with the degree of anxiety (Orhan et al., 2018). However, there is no evidence that GPER1 deficiency might aggregate SZ-like behaviors induced by MK-801 *in vivo*. In this study, we performed a classical and intelligent behavioral analysis of mice that received GPER1 knockdown, and our results demonstrated increased hyperlocomotion and stereotypical behaviors, decreased social interaction, impaired novelty exploration, and recognition function, and impaired executive function in GPER1-KO SZ mice compared with their control counterparts. Impairments in learning and memory (Goldman-Rakic, 1994; Stefani and Moghaddam, 2005), hyperlocomotion, and stereotypical behaviors (Morrens et al., 2006; Xiao et al., 2019), and social withdrawal (Kay et al., 1987) are typical SZ symptoms. Our comprehensive behavioral results from learning and memory, social interaction, and executive function tests supported the notion that the administration of MK-801 interfered easily in GPER1-KO mice. Thus, our results suggested that GPER1 knockout aggravated the onset of SZ-like symptoms. We also found that CPER1 deficiency significantly reduced the learning capability and memory of SZ mice. Notably, this study is the first to demonstrate that GPER1 deletion led

to further declines in the learning and memory of mice with MK-801-induced SZ. These results implied that the lack of GPER1 aggravated the cognitive impairment of SZ. Our results were consistent with previous studies on molecular changes in patients with SZ and animal models of the hippocampus (Silvestre de Ferron et al., 2015; Yang et al., 2015; Gulchina et al., 2017; Zhou et al., 2018). Notably, MK-801 significantly reduced the expression of NR2B in the mouse hippocampus. Meanwhile, GPER1 deficiency exacerbated the reduction in NR2B protein levels of SZ mice. We found that the expression of NR2B-pTyr-1070 protein was reduced in SZ mice. In GPER1-KO SZ mice, we found a significant decrease in the NR2B-pTyr-1070 protein expression level. This result indicated that GPER1 was related to the regulation of NR2B phosphorylation possibly in SZ mice. However, the mechanisms by which GPER1 regulates NR2B phosphorylation in the hippocampus of mice with SZ requires further investigation.

As a downstream signal factor of the NR2B subunit, CaMKII participates in a variety of signaling cascade responses and is an important mediation center for learning and memory. CaMKIIα is an extremely abundant protein kinase in brain tissue that participates in multiple signaling cascade reactions to regulate learning and memory. Consistent with previous studies, in this work, we found that the protein expression levels of CaMKIIα, phosphorylated CaMKIIα, CREB (Ren et al., 2014), and phosphorylated CREB decreased in SZ mice. We also saw that the protein expression levels of CaMKIIα, phosphorylated CaMKIIα, CREB, and phosphorylated CREB significantly decreased in GPER1-deficient SZ mice. GPER1 deficiency promoted MK-801-induced SZ in mice, indicating that GPER1 deficiency resulted in NR2B and NR2B-pTyr-1070 hypofunction and NR2B/CaMKII/CREB signaling pathway downregulation in SZ mice. The mechanism underlying the further decline of some cognitive abilities in SZ mice caused by GPER1 deletion might partially occur through the downregulation of the NR2B/CaMKII/CREB signaling pathway. This study is the first to evaluate the relationship between GPER1 and the NR2B/CaMKII/CREB signaling pathway in an animal model of SZ. Thus, GPER1 might phosphorylate NR2B and regulate the NR2B/CaMKII/CREB pathway.

CONCLUSION

Collectively, the results of this study suggest that GPER1 deficiency can attenuate cognitive function in SZ mice. GPER1 deficiency might promote the degradation of the NR2B/CaMKII/CREB signaling pathway by inhibiting NR2B phosphorylation. Therefore, GPER1 activity may be a new target in the treatment of SZ and other symptoms, such as learning and memory impairment. Future studies should focus on the effect of GPER1 on the pathogenesis of SZ *in vivo* and *in vitro*.

DATA AVAILABILITY STATEMENT

The raw data supporting the conclusions of this article will be made available by the authors, without undue reservation.

ETHICS STATEMENT

The animal study was reviewed and approved by Ningxia Medical University Animal Research Ethics Board.

AUTHOR CONTRIBUTIONS

CZ, QL, JL, and TS conceived and designed the experiments. FW and K-SS conducted the experiments and performed the statistic alanalyses. YS and C-YY provided the experimental animals and assisted with the animal breeding. CZ wrote the manuscript. All authors contributed to the article and approved the submitted version.

FUNDING

The study was supported by Ningxia High School first-class Disciplines (West China first-class Disciplines Basic Medical Sciences at Ningxia Medical University; Project No.: NXYLXK2017B07). This work was supported by the Ningxia Hui Autonomous Region 13th Five-Year Plan Major Science and Technology Projects (2016BZ07). This study was supported by the National Natural Science Foundation of China (NSFC, 81660226).

REFERENCES

Akama, K. T., Thompson, L. I., Milner, T. A., and McEwen, B. S. (2013). Post-synaptic density-95 (PSD-95) binding capacity of G-protein-coupled receptor 30 (GPR30), an estrogen receptor that can be identified in hippocampal dendritic spines. *J. Biol. Chem.* 288, 6438–6450. doi: 10.1074/jbc.M112.412478

Almey, A., Cannell, E., Bertram, K., Filardo, E., Milner, T. A., and Brake, W. G. (2014). Medial prefrontal cortical estradiol rapidly alters memory system bias in female rats: ultrastructural analysis reveals membrane-associated estrogen receptors as potential mediators. *Endocrinology* 155, 4422–4432. doi: 10.1210/en.2014-1463

Almey, A., Milner, T. A., and Brake, W. G. (2015). Estrogen receptors in the central nervous system and their implication for dopamine-dependent cognition in females. *Horm. Behav.* 74, 125–138. doi: 10.1016/j.yhbeh.2015.06.010

Bean, L. A., Ianov, L., and Foster, T. C. (2014). Estrogen receptors, the hippocampus and memory. *Neuroscientist* 20, 534–545. doi: 10.1177/1073858413519865

Binyamin, O., Nitzan, K., Frid, K., Ungar, Y., Rosenmann, H., and Gabizon, R. (2019). Brain targeting of 9c,11t-conjugated linoleic acid, a natural calpain inhibitor, preserves memory and reduces Aβ and P25 accumulation in 5×FAD mice. *Sci. Rep.* 9:18437. doi: 10.1038/s41598-019-54971-9

Borelli, C. M., and Solari, H. (2019). Schizophrenia. *JAMA* 322:1322. doi: 10.1001/jama.2019.11073

Brailoiu, E., Dun, S. L., Brailoiu, G. C., Mizuo, K., Sklar, L. A., Oprea, T. I., et al. (2007). Distribution and characterization of estrogen receptor G protein-coupled receptor 30 in the rat central nervous system. *J. Endocrinol.* 193, 311–321. doi: 10.1677/JOE-07-0017

Bratek, A., Krysta, K., Drzyzga, K., Baranska, J., and Kucia, K. (2016). The role of selective estrogen receptor modulators in the treatment of schizophrenia. *Psychiatr. Danub.* 28, 45–48.

Briz, V., Liu, Y., Zhu, G., Bi, X., and Baudry, M. (2015). A novel form of synaptic plasticity in field CA3 of hippocampus requires GPER1 activation and BDNF release. *J. Cell Biol.* 210, 1225–1237. doi: 10.1083/jcb.201504092

Ding, J., Zhou, H. H., Ma, Q. R., He, Z. Y., Ma, J. B., Liu, Y. M., et al. (2017). Expression of NR1 and apoptosis levels in the hippocampal cells of mice treated with MK801. *Mol. Med. Rep.* 16, 8359–8364. doi: 10.3892/mmr.2017.7674

Ding, J., Zhang, C., Zhang, Y. W., Ma, Q. R., Liu, Y. M., Sun, T., et al. (2019). N-methyl-D-aspartate receptor subunit 1 regulates neurogenesis in the hippocampal dentate gyrus of schizophrenia-like mice. *Neural Regen. Res.* 14, 2112–2117. doi: 10.4103/1673-5374.262597

Dos, S. N., Novaes, L. S., Dragunas, G., Rodrigues, J. R., Brandao, W., Camarini, R., et al. (2019). High dose of dexamethasone protects against EAE-induced motor deficits but impairs learning/memory in C57BL/6 mice. *Sci. Rep.* 9:6673. doi: 10.1038/s41598-019-43217-3

Funakoshi, T., Yanai, A., Shinoda, K., Kawano, M. M., and Mizukami, Y. (2006). G protein-coupled receptor 30 is an estrogen receptor in the plasma membrane. *Biochem. Biophys. Res. Commun.* 346, 904–910. doi: 10.1016/j.bbrc.2006.05.191

Gaudet, H. M., Cheng, S. B., Christensen, E. M., and Filardo, E. J. (2015). The G-protein coupled estrogen receptor, GPER: the inside and inside-out story. *Mol. Cell. Endocrinol.* 418, 207–219. doi: 10.1016/j.mce.2015.07.016

Goldman-Rakic, P. S. (1994). Working memory dysfunction in schizophrenia. *J. Neuropsychiatry Clin. Neurosci.* 6, 348–357. doi: 10.1176/jnp.6.4.348

Gulchina, Y., Xu, S. J., Snyder, M. A., Elefant, F., and Gao, W. J. (2017). Epigenetic mechanisms underlying NMDA receptor hypofunction in the prefrontal cortex of juvenile animals in the MAM model for schizophrenia. *J. Neurochem.* 143, 320–333. doi: 10.1111/jnc.14101

Gurvich, C., Hudaib, A., Gavrilidis, E., Worsley, R., Thomas, N., and Kulkarni, J. (2019). Raloxifene as a treatment for cognition in women with schizophrenia: the influence of menopause status. *Psychoneuroendocrinology* 100, 113–119. doi: 10.1016/j.psyneuen.2018.10.001

Hadjimarkou, M. M., and Vasudevan, N. (2018). GPER1/GPR30 in the brain: crosstalk with classical estrogen receptors and implications for behavior. *J. Steroid Biochem. Mol. Biol.* 176, 57–64. doi: 10.1016/j.jsbmb.2017.04.012

Hammond, R., Mauk, R., Ninaci, D., Nelson, D., and Gibbs, R. B. (2009). Chronic treatment with estrogen receptor agonists restores acquisition of a spatial learning task in young ovariectomized rats. *Horm. Behav.* 56, 309–314. doi: 10.1016/j.yhbeh.2009.06.008

Hazell, G. G., Yao, S. T., Roper, J. A., Prossnitz, E. R., O'Carroll, A. M., and Lolait, S. J. (2009). Localisation of GPR30, a novel G protein-coupled oestrogen receptor, suggests multiple functions in rodent brain and peripheral tissues. *J. Endocrinol.* 202, 223–236. doi: 10.1677/JOE-09-0066

Huang, M. W., Lin, Y. J., Chang, C. W., Lei, F. J., Ho, E. P., Liu, R. S., et al. (2018). RGS4 deficit in prefrontal cortex contributes to the behaviors related to schizophrenia *via* system xc(-)-mediated glutamatergic dysfunction in mice. *Theranostics* 8, 4781–4794. doi: 10.7150/thno.25189

Jacklin, D. L., Goel, A., Clementino, K. J., Hall, A. W., Talpos, J. C., and Winters, B. D. (2012). Severe cross-modal object recognition deficits in rats treated sub-chronically with NMDA receptor antagonists are reversed by systemic nicotine: implications for abnormal multisensory integration in schizophrenia. *Neuropsychopharmacology* 37, 2322–2331. doi: 10.1038/npp.2012.84

Jeon, S. J., Kim, E., Lee, J. S., Oh, H. K., Zhang, J., Kwon, Y., et al. (2017). Maslinic acid ameliorates NMDA receptor blockade-induced schizophrenia-like behaviors in mice. *Neuropharmacology* 126, 168–178. doi: 10.1016/j.neuropharm.2017.09.014

Karamihalev, S., Prickaerts, J., and van Goethem, N. P. (2014). Donepezil and the alpha-7 agonist PHA 568487, but not risperidone, ameliorate spatial memory deficits in a subchronic MK-801 mouse model of cognitive impairment in schizophrenia. *Behav. Brain Res.* 272, 248–251. doi: 10.1016/j.bbr.2014.07.017

Kárpáti, A., Yoshikawa, T., Naganuma, F., Matsuzawa, T., Kitano, H., Yamada, Y., et al. (2019). Histamine H1 receptor on astrocytes and neurons controls distinct aspects of mouse behaviour. *Sci. Rep.* 9:16451. doi: 10.1038/s41598-019-52623-6

Kastenberger, I., and Schwarzer, C. (2014). GPER1 (GPR30) knockout mice display reduced anxiety and altered stress response in a sex and paradigm dependent manner. *Horm. Behav.* 66, 628–636. doi: 10.1016/j.yhbeh.2014.09.001

Kay, S. R., Fiszbein, A., and Opler, L. A. (1987). The positive and negative syndrome scale (PANSS) for schizophrenia. *Schizophr. Bull.* 13, 261–276. doi: 10.1093/schbul/13.2.261

Kim, J., Szinte, J. S., Boulware, M. I., and Frick, K. M. (2016). 17β-estradiol and agonism of g-protein-coupled estrogen receptor enhance hippocampal memory *via* different cell-signaling mechanisms. *J. Neurosci.* 36, 3309–3321. doi: 10.1523/JNEUROSCI.0257-15.2016

Kristiansen, L. V., Patel, S. A., Haroutunian, V., and Meador-Woodruff, J. H. (2010). Expression of the NR2B-NMDA receptor subunit and its Tbr-1/CINAP regulatory proteins in postmortem brain suggest altered receptor processing in schizophrenia. *Synapse* 64, 495–502. doi: 10.1002/syn.20754

Lee, G., and Zhou, Y. (2019). NMDAR hypofunction animal models of schizophrenia. *Front. Mol. Neurosci.* 12:185. doi: 10.3389/fnmol.2019.00185

Leung, L. S., and Ma, J. (2018). Medial septum modulates hippocampal gamma activity and prepulse inhibition in an *N*-methyl-d-aspartate receptor antagonist model of schizophrenia. *Schizophr. Res.* 198, 36–44. doi: 10.1016/j.schres.2017.07.053

Li, C., Tang, Y., Yang, J., Zhang, X., Liu, Y., and Tang, A. (2016). Sub-chronic antipsychotic drug administration reverses the expression of neuregulin 1 and ErbB4 in a cultured MK801-induced mouse primary hippocampal neuron or a neurodevelopmental schizophrenia model. *Neurochem. Res.* 41, 2049–2064. doi: 10.1007/s11064-016-1917-x

Liu, P., Li, Y., Yang, W., Liu, D., Ji, X., Chi, T., et al. (2019). Prevention of Huntington's disease-like behavioral deficits in R6/1 mouse by tolfenamic acid is associated with decreases in mutant huntingtin and oxidative stress. *Oxid. Med. Cell. Longev.* 2019:4032428. doi: 10.1155/2019/4032428

Loh, D. H., Jami, S. A., Flores, R. E., Truong, D., Ghiani, C. A., O'Dell, T. J., et al. (2015). Misaligned feeding impairs memories. *eLife* 4:e09460.doi: 10.7554/eLife.09460

Marder, S. R., and Cannon, T. D. (2019). Schizophrenia. *N. Engl. J. Med.* 381, 1753–1761. doi: 10.1056/NEJMra1808803

Mirkin, S., and Pickar, J. H. (2015). Selective estrogen receptor modulators (SERMs): a review of clinical data. *Maturitas* 80, 52–57. doi: 10.1016/j.maturitas.2014.10.010

Morrens, M., Hulstijn, W., Lewi, P. J., De Hert, M., and Sabbe, B. G. (2006). Stereotypy in schizophrenia. *Schizophr. Res.* 84, 397–404. doi: 10.1016/j.schres.2006.01.024

Orhan, F. O., Kurutas, E. B., Doganer, A., Turker, E., Ozcu, S., Gungor, M., et al. (2018). Serum levels of GPER-1 in euthymic bipolar patients. *Neuropsychiatr. Dis. Treat.* 14, 855–862. doi: 10.2147/NDT.S158822

Persad, C. C., Zubieta, J. K., Love, T., Wang, H., Tkaczyk, A., and Smith, Y. R. (2009). Enhanced neuroactivation during verbal memory processing in postmenopausal women receiving short-term hormone therapy. *Fertil. Steril.* 92, 197–204. doi: 10.1016/j.fertnstert.2008.04.040

Ren, X., Rizavi, H. S., Khan, M. A., Bhaumik, R., Dwivedi, Y., and Pandey, G. N. (2014). Alteration of cyclic-AMP response element binding protein in the postmortem brain of subjects with bipolar disorder and schizophrenia. *J. Affect. Disord.* 152–154, 326–333. doi: 10.1016/j.jad.2013.09.033

Seillier, A., and Giuffrida, A. (2009). Evaluation of NMDA receptor models of schizophrenia: divergences in the behavioral effects of sub-chronic PCP and MK-801. *Behav. Brain Res.* 204, 410–415. doi: 10.1016/j.bbr.2009.02.007

Silvestre de Ferron, B., Bennouar, K. E., Kervern, M., Alaux-Cantin, S., Robert, A., Rabiant, K., et al. (2015). Two binges of ethanol a day keep the memory away in adolescent rats: key role for GLUN2B subunit. *Int. J. Neuropsychopharmacol.* 19:pyv087. doi: 10.1093/ijnp/pyv087

Stefani, M. R., and Moghaddam, B. (2005). Systemic and prefrontal cortical NMDA receptor blockade differentially affect discrimination learning and set-shift ability in rats. *Behav. Neurosci.* 119, 420–428. doi: 10.1037/0735-7044.119.2.420

Vajaria, R., and Vasudevan, N. (2018). Is the membrane estrogen receptor, GPER1, a promiscuous receptor that modulates nuclear estrogen receptor-mediated functions in the brain? *Horm. Behav.* 104, 165–172. doi: 10.1016/j.yhbeh.2018.06.012

Valton, V., Romaniuk, L., Douglas, S. J., Lawrie, S., and Series, P. (2017). Comprehensive review: computational modelling of schizophrenia. *Neurosci. Biobehav. Rev.* 83, 631–646. doi: 10.1016/j.neubiorev.2017.08.022

Waters, E. M., Thompson, L. I., Patel, P., Gonzales, A. D., Ye, H. Z., Filardo, E. J., et al. (2015). G-protein-coupled estrogen receptor 1 is anatomically positioned to modulate synaptic plasticity in the mouse hippocampus. *J. Neurosci.* 35, 2384–2397. doi: 10.1523/JNEUROSCI.1298-14.2015

Xiao, X., Xu, X., Li, F., Xie, G., and Zhang, T. (2019). Anti-inflammatory treatment with β-asarone improves impairments in social interaction and cognition in MK-801 treated mice. *Brain Res. Bull.* 150, 150–159. doi: 10.1016/j.brainresbull.2019.05.017

Xiu, Y., Kong, X. R., Zhang, L., Qiu, X., Chao, F. L., Peng, C., et al. (2014). White matter injuries induced by MK-801 in a mouse model of schizophrenia based on NMDA antagonism. *Anat. Rec.* 297, 1498–1507. doi: 10.1002/ar.22942

Yang, Y., Li, W., Zhang, H., Yang, G., Wang, X., Ding, M., et al. (2015). Association study of N-Methyl-D-aspartate receptor subunit 2B (GRIN2B) polymorphisms and schizophrenia symptoms in the han chinese population. *PLoS One* 10:e125925. doi: 10.1371/journal.pone.0125925

Zhou, D., Lv, D., Wang, Z., Zhang, Y., Chen, Z., and Wang, C. (2018). GLYX-13 ameliorates schizophrenia-like phenotype induced by MK-801 in mice: role of hippocampal NR2B and DISC1. *Front. Mol. Neurosci.* 11:121. doi: 10.3389/fnmol.2018.00121

Conflict of Interest: The authors declare that the research was conducted in the absence of any commercial or financial relationships that could be construed as a potential conflict of interest.

Advantages of publishing in Frontiers

OPEN ACCESS
Articles are free to read for greatest visibility and readership

FAST PUBLICATION
Around 90 days from submission to decision

HIGH QUALITY PEER-REVIEW
Rigorous, collaborative, and constructive peer-review

TRANSPARENT PEER-REVIEW
Editors and reviewers acknowledged by name on published articles

Frontiers
Avenue du Tribunal-Fédéral 34
1005 Lausanne | Switzerland

Visit us: www.frontiersin.org
Contact us: frontiersin.org/about/contact

REPRODUCIBILITY OF RESEARCH
Support open data and methods to enhance research reproducibility

DIGITAL PUBLISHING
Articles designed for optimal readership across devices

FOLLOW US
@frontiersin

IMPACT METRICS
Advanced article metrics track visibility across digital media

EXTENSIVE PROMOTION
Marketing and promotion of impactful research

LOOP RESEARCH NETWORK
Our network increases your article's readership